INSIGHTS INTO FUTURE ELECTRIC MOBILITY

by

I-Yun Lisa Hsieh

B.S. in Chemical Engineering, National Taiwan University

B.B.A. in Finance, National Taiwan University

Submitted to the Department of Chemical Engineering

in partial fulfillment of the requirements for the degree of

Doctor of Philosophy in Chemical Engineering

at the

MASSACHUSETTS INSTITUTE OF TECHNOLOGY

May 2020

Author_____

Department of Chemical Engineering

May 8, 2020

Certified by_____

William H. Green

Hoyt C. Hottel Professor of Chemical Engineering

Thesis Supervisor

Accepted by_____

Patrick S. Doyle

Robert T. Haslam (1911) Professor of Chemical Engineering

Chairman, Department Committee on Graduate Students

Insights into Future Electric Mobility

by

I-Yun Lisa Hsieh

Submitted to the Department of Chemical Engineering

on May 8, 2020, in partial fulfillment of the requirements for the degree of

Doctor of Philosophy in Chemical Engineering

Abstract

Growing global awareness of the environmental impacts of combustion is accelerating electric vehicles (EVs) adoption. However, future sustainable mobility cannot be achieved without substantial changes in vehicle technology, consumer behavior, infrastructure systems, and policy. Great impacts and uncertainties are anticipated during the transition towards electric mobility. This thesis examines key areas of interest such as battery techno-economic characteristics, EV recharging ecosystem, dynamics behind the market evolution, the prospects and challenges for the transition to electrification, and the impacts of evolving EV policies.

For example, given that the battery prices have been dropping rapidly in the past several years, a recurring question is how much lower battery prices can be expected to go. Greater production volumes and improvements in manufacturing efficiency will drive down costs, but the prices will eventually stabilize as they get closer to the cost of the materials they are made of. A 2-stage learning curve model is developed to investigate how the essential materials, especially expensive elements (lithium, nickel and cobalt) used in current battery technologies, will constrain the declining trajectory of production costs and set practical lower bounds on battery prices. Another big uncertainty surrounding EVs is whether they could really create a cleaner planet. EVs avoid tailpipe emissions of CO2 and air pollutants from fossil fuel combustion but may lead to greater emissions from the upstream stage of electricity generation, especially in the world's largest EV market, China, where coal-fired power generation has been the backbone of the electricity supply. The current lifecycle emissions comparison for vehicles with different

powertrains is presented and how China's sustainable mobility policy will affect future climate change, air quality, and public health is also explored.

This thesis provides information that will help stakeholders anticipate and navigate some of the changes that lie ahead owing to a policy-driven shift from liquid fuels to electrification. The evaluation focuses mostly on private passenger vehicle sector, which in part reflects a recognition that this is the segment that is likely to be responding most proactively to the developments in advanced powertrains, alternative fuels, and environmental policies.

Thesis Supervisor: William H. Green
Title: Hoyt C. Hottel Professor in Chemical Engineering

Acknowledgement

First and foremost, I would like to express my sincere appreciation to Professor William H. Green for his supervision and the insights at every stage of this work. He has been supportive and has given me a lot of freedom to explore my research work, making me more confident in my abilities to push boundaries. His gracious personality and advising style are examples that I will always remember and seek to emulate. My thesis committee members—Professors Robert C. Armstrong, Steven Barrett, and Sergey Paltsev—have brought complementary and helpful perspectives into our annual meetings. This interdisciplinary work is only possible due to their involvement and generous supports.

I would like to acknowledge the financial support of the MIT Energy Initiative's Mobility of the Future Study and Taiwan's Think Global Education Trust Scholarship. It is from their support that I am able to spend the time to investigate the complex mobility systems.

I feel very fortunate to be part of the Mobility of the Future Study: for me, the most attractive part is that the project involves more than one discipline of science, so I can not only hone my existing skills but also learn a lot from researchers I would never have a chance to interact with by staying in my department. Because I am the only graduate student from the Chemical Engineering Department in the team, I can work independently to address problems when coming up. Therefore, I would also like to thank Randy Field for his admirable leadership and persistence in pulling everything together, no matter how hard it is. I would like to extend my thanks to other members of the Mobility Study team, including John Heywood, Christopher Knittel, Chintan Vaishnav, Jinhua Zhao, Emre Gençer, Joanna Moody, Abbas Ghandi, Ashley Nunes, Paul Kishimoto, Jennifer Morris, Raymond Speth, Ian Miller, Rakesh Sridhar, and Dustin Weigl.

It is a real pleasure to get to know Menghsuan Sam Pan, who has contributed to several chapters of this work. I thank him for his friendship as well as technical supports. I also thank my friends at MIT, both in my class and from Taiwan, for their company and their encouragement, helping me overcome all the difficulties in my Ph.D. life.

I am also grateful to be part of the Green Research Group. Although I do not have a chance to collaborate with the other members in the group, I still want to thank all of them for being so friendly and keeping such a great research atmosphere.

I cannot express how grateful I am to my wonderful Taipei support team—especially Dad Jindar Hsieh, Mom Amy Lee, Sisters Elaine Hsieh and Shirley Hsieh—for their love and continuous confidence in everything I do. Finally, I want to express my special gratitude to my husband, Johnson Wen, for always being there for me right from the first day we met. We have shared so many beautiful moments together since kindergarten, from Taiwan to the USA; his support and unflinching care always bring me energy and inner peace.

Contents

List of Figures

List of Tables

Chapter 1. Introduction

Vehicles burning gasoline produce both carbon dioxide and other chemicals that are precursors of air pollutants such as particular matter and ozone. The former contributes to global climate change, while the latter degrades the local human health. Growing global awareness of the negative environmental impacts of combustion is accelerating electric vehicles (EVs) adoption; EVs include plug-in hybrid electric vehicles (PHEVs) and pure battery electric vehicles (BEVs). There are great uncertainties about the future of EVs, and this thesis aims to gain insights into factors that have driven the recent developments in electric mobility, the dynamics behind the market evolution, the prospects and challenges during the transition towards electrification, and the impacts of evolving EV policies.

1.1 Background

1.1.1 Benefits to electric vehicles

Multiple societal benefits are believed to be delivered during transition to electric mobility, including:

- Better energy efficiency: EVs convert over 77% of the electrical energy, from input energy to power at wheels (kinetic energy). On the other hand, conventional internal combustion engine vehicles (ICEVs) using gasoline are only 12%-30% percent efficient [1]. Thus, EVs provide substantial energy efficiency improvement potential for road transportation.
- Increased national energy security: Electricity is a domestic energy source. By shifting from liquid fuels to electrification, petroleum imports would be reduced for many countries.
- Reduced greenhouse gas emissions: One of the main reasons for EV deployment is the concern over global warming. If accompanied by decarbonization of electricity generation, EVs will feature prominently in climate change mitigation pathways that limit global warming to within 2 °C.
- Reduced toxic pollutants: EVs emit zero tailpipe pollutants and thus greatly reduce the negative impacts of transportation needs on air quality and public health, especially in urban areas.
- Industrial development stimulation: EV battery innovation and technology help promote domestic industry and economic growth by creating more employment.

1.1.2 Electric vehicle market

Electric mobility continues to expand, with more than 5 million EVs sold worldwide by the end of 2018 [2]. Over the past few years, more than a dozen countries and 20 city governments have pledged to phase out conventional ICEVs to meet their climate and air quality goals. For example, Norway, Denmark, Iceland, and Sweden are targeting 2030 or even sooner, while the UK and France are aiming for 2035 and 2040 [3]. Although EVs sales are increasing across most of the counties, they are still disproportionately concentrated in a small number of markets. As shown in Figure 1.1, the People's Republic of China (hereafter China) is leading the world in EV sales, followed by Europe and the United States. But in terms of EV penetration rate, Norway is the world's leader—with a sales market share of 46% in 2018.

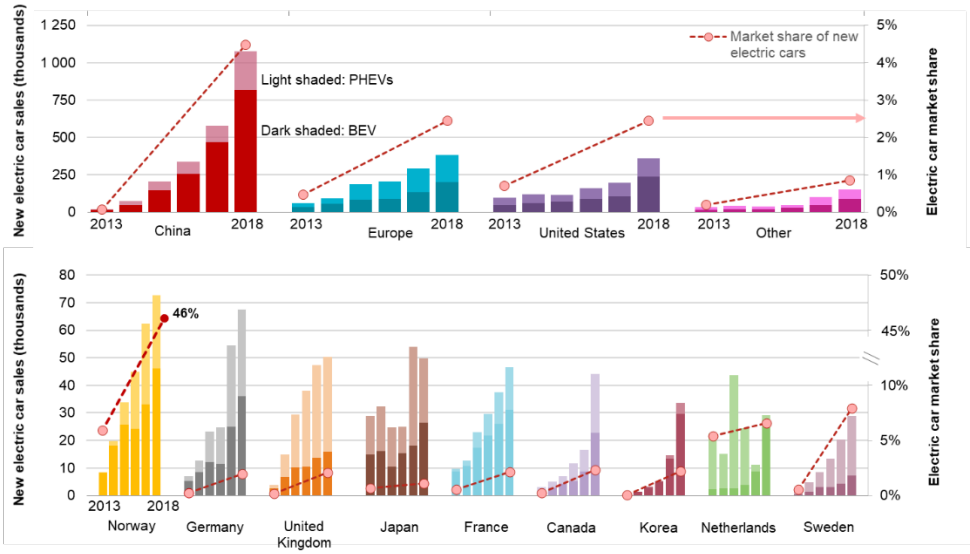

Figure 1.1. Global electric vehicle sales and market share, 2013-2018, reported by International Energy Agency [2].

1.1.3 Barriers to electric vehicle adoption

Although vehicle electrification offers a wide range of societal benefits, widespread EV adoption is still impeded by several barriers—price, range anxiety, and home charging availability [4]. Firstly, the higher EV price (relative to comparable ICEVs) is often cited as the primary hurdle to EV deployment [5]; this price discrepancy will be shrinking as advances in battery technology and economies of scale reduce the battery production cost. Secondly, range anxiety is the fear that a vehicle has insufficient range to reach its destination or a convenient charging station. At present,

the relatively low driving range and long charging time for EVs contribute to this worry, posing a hurdle for consumer adoption. The last big barrier is the location of charging stations. Home charging is typically the most convenient and lowest-cost means of fueling an EV. If home charging (or even destination charging) is not available, EV owners have to rely on public chargers and could incur high charging fees at public charging stations. Lacking access to home charging may be an inherent obstacle to the penetration of EVs.

1.1.4 Policies to promote EV deployment

Today, both economics and convenience benefit the continuation of ICEVs, and thereby government intervention is critical to stimulate the transition to electric mobility. Leading countries pursue a variety of strategies to support the development and uptake of EVs. Financial incentives—including rebates, tax exemptions, and tax credits— are a major tool for decreasing the upfront costs of EVs. In the U.S., EVs purchased after 2010 are eligible for a federal tax credit of up to $7,500; the credit amount is based on the battery capacity and gross vehicle weight rating. The tax credit is available until a manufacturer sells 200,000 EVs, at which point the credit begins to phase out over time for vehicles sold by that company; Tesla achieved the threshold multiple quarters before any other automaker, General Motors achieved second, and Nissan is likely to be the next [6]. In Europe, France, and Norway offer the most EV incentives [7]. France offers a generous purchase subsidy of up to €6,000 to EV buyers, plus up to €5,000 for older diesel and petrol vehicles scrappage bonus. The Norwegian government has offered EV incentives since the 1990s and today, such as exemption from 25% value-added tax (VAT) on purchase. China is taking more aggressive actions to make EV more cost-competitive; EVs are exempted from purchase taxes from 2014 to 2020, plus receiving generous price subsidies from both national and local governments from 2010. The subsidy program is renewed every two or three years, decreasing the subsidies and raising the eligibility threshold; this implies that the government believes that EV costs will be reduced with a higher level of commercialization. China plans to phase out the subsidy entirely by 2020 [8].

In the EV-leading cities or regions, fiscal incentives are often coupled with regulatory measures—including EV mandates, fuel economy standards (i.e., embedding incentives for low tailpipe emission), and ICEV demand management. In the U.S., nine states (including Connecticut, Maine, Maryland, Massachusetts, New Jersey, New York, Oregon, Rhode Island, and Vermont)

have adopted California's zero-emissions vehicle (ZEV) program, requiring automakers to produce zero-emissions vehicles [9]. In Canada, British Columbia has introduced the ZEV Act [10]; Québec has adopted a ZEV mandate program that is very similar to the California program [11]. China's dual-credit policy, sometimes called NEV mandate, is implemented at a national level and can be viewed as combining some features of the Corporate Average Fuel Economy (CAFE) standards in the U.S. and California ZEV program [12]. Furthermore, some megacities in China have implemented car ownership restriction policy, mostly exempting EVs from this quota, to solve the serious urban air pollution problems [13].

1.1.5 Mobility system growth and policies in China

Great impacts and uncertainties are anticipated during the global transition to electric mobility. Although Norway is the world's most enthusiastic consumers embracing EVs per head of population, the sheer scale of China makes understanding its market dynamics very critical. Being one of the fast-growing major economies, China has seen the largest increases in vehicle sales between 2005 and 2017, overtaking the U.S. and becoming the largest auto market since 2008 [14]. This strong growth in the development of the automotive industry, however, has resulted in a variety of negative externalities that are not directly borne by vehicle owners, such as national energy security concerns, global warming, and air pollution. To achieve environmentally sustainable ground transportation, the Chinese government is promoting new energy vehicles via aggressive policies. Generous purchase subsidies and aggressive policies such as EVs being exempted from quota policies are driving up the local sales of EVs, helping China to lead global EV adoption since 2015. The dual-credit scheme mandate has been enacted recently to encourage improved fuel-efficiency, and more importantly, electrification technologies in the passenger vehicle market. The dual-credit policy is envisioned to compensate for the phase-out of the subsidy program after 2020 by forcing increased battery-powered vehicle sales.

1.2 Thesis overview

This thesis seeks to understand the interactions between car purchasing power, battery techno-economic characteristics, EV recharging ecosystem, and government policy for shaping the future landscape of electric mobility in China; these tasks are complicated by the scope, scale, and speed of change. The aim is to provide information that will help stakeholders anticipate and navigate some of the changes that lie ahead, owing to a policy-driven shift from liquid fuels to electrification.

In this thesis, I focus my evaluation mostly on the private passenger vehicle sector, which in part reflects a recognition that this is the segment that is likely to be most strongly and rapidly affected by fast-moving developments in advanced powertrains, alternative fuels, and environmental policies.

To measure policy effectiveness requires a model constructing a counterfactual for the outcomes in the absence of the policy intervention. First, in Chapter 2, I develop a model projecting future economically-driven demand for private car ownership in China at the national level based on growth in car purchasing power. Early-stage motorization data in China do not contain much information about the eventual saturation level of ownership. A range of future forecasts in transport demands that are conditioned on observed reality was developed, producing a characterization that can help policymakers or transport infrastructure project managers create flexible designs that are robust to eventualities. Second, in Chapter 3, I present a careful and well-documented projection of future battery prices for passenger battery electric vehicles (BEVs). Given that the battery prices have been dropping rapidly in the past several years, a recurring question is how quickly battery prices can be expected to drop to the target of $100/kWh and how much lower battery prices can be expected to go. I discuss how the essential materials, especially expensive elements used in current battery technologies, will constrain the declining trajectory of production costs and set practical lower bounds on battery prices. This practical limit would delay the occurrence of the transition to e-mobility at an attractive real cost, especially if the raw material shortages lead to spikes in mineral prices. The findings provide policymakers a realistic view of how much support (e.g., through mandates, subsidies, gasoline taxes) BEV technology will need to take a major role in the transportation sector.

Third, in Chapters 4 and 5 together, I quantify some of the major implications of the dual-credit policy on the whole society—including motorization trends, battery market, consumer-centric total cost of ownership, and transition cost to society. These are all of great interest to policymakers, the public, and business leaders, and thus it is vital to have an accurate projection that takes the evolving policies into account and is supported with rigorous techno-economic analyses. Fourth, in Chapter 6, with an aim to enhance the economics of the electrified taxi fleet network, I analyze the outlook of battery swapping business model by comparing it to other strategies for BEV charging. By using real-world financial data taken from an operating electrified

taxi fleet in Beijing, this chapter provides a theoretical and practical reference for cities moving toward electric taxi ecosystems and sustainability. Finally, considering that China is the global largest vehicle market (both for ICEV and EV), it is of timely importance to conduct a systematic and comprehensive evaluation of carbon emissions, air quality, and public health benefits under the current policy mix; Chapter 7 presents my contribution to this area. The major novelties of Chapter 7 are in the bottom-up model development and cross-scale information integration. The established framework captures how policy alters the vehicle ownership demand and its corresponding environmental externalities across spatial scales (from provincial to national) and time horizons (from 2017 to 2030).

Chapter 2. Counterfactual prediction in vehicle demand: Incorporating multiple uncertainties into projections of Chinese private car sales and stock

Much of the material in this chapter has been published in Hsieh, I-Yun Lisa, Paul Natsuo Kishimoto, and William H. Green. "Incorporating multiple uncertainties into projections of Chinese private car sales and stock." Transportation Research Record 2672.47 (2018): 182-193. Paul Kishimoto verified the analytical methods and collaborated in the formulation of the arguments in the text.

Abstract

China is in a fast-growing stage of mobility development, and its increasing demand for private cars comes with growing energy consumption and pollutant emissions. Uncertainty in Chinese parameterization of car ownership models makes forecasting these trends a challenge. We develop an application of the Monte Carlo method, conditioned on historical data, to sample parameters for a model projecting aspects of private car diffusion, such as the mix of new and replacement sales. This chapter projects economically driven private car ownership demand at the national level absent government interventions (i.e., no-policy counterfactual projections; policy includes city-level car ownership restriction policy and national-level EV mandates). Our model includes changes in per-capita disposable income—both the mean and level of inequality—and a measure of car affordability.

By incorporating multiple uncertainties, we show a distribution of possible future outcomes: a low stock of 280 million (1st decile); median of 430 million; and high of 620 million vehicles (9th decile) in 2050. This illustrates the limitations of attempts to model vehicle markets at the national level, by showing how uncertainties in fundamental descriptors of growth lead to a broad range of possible outcomes. While uncertainty in projected per-capita ownership grows continually, the share of first-time purchases in sales is most uncertain in the near term and then narrows as the market saturates. Replacement purchases increasingly capture the sales market from

2025. Our results suggest that stakeholders have a narrow window of opportunity to regulate the fuel economy, pollution and other attributes of vehicles sold to first-time buyers. These may, in turn, shape consumers' experience and expectations of car ownership, affecting their additional and replacement purchases.

2.1 Introduction

Being one of the fast-growing major economies, China has seen the largest increases in passenger vehicle sales between 2005 and 2015, overtaking the U.S. and becoming the largest auto market since 2008 [15]. However, if compared to the history of U.S. motorization, per-capita car ownership in China is just passing the level in the U.S. as of 1922 [16]. The strong growth in development of the automotive industry is closely associated with the economic boom in China. On the other hand, this growth has resulted in an increase in demand for fuel, and caused more pollutant and carbon dioxide emissions associated with petroleum combustion, as well as worsened traffic congestion problems in urban regions—all of which are urgent challenges for China's government.

Establishing the range of possible future outcomes allows stakeholders to decide how robust their strategies are to uncertainty, and to determine the risk of following status quo approaches. In addition to design of policies to limit the environmental impacts of transport, governments must choose to size infrastructure (roadways, parking facilities, etc.) to accommodate expected traffic volumes. Automakers must construct durable assets such as assembly plants and make supply chain investments to meet demand competitively in a future market of a certain size. The criteria for robustness differ according to an organization's tolerance for risk, and type of decision or policy under consideration; but in all cases information about distributions of future outcomes is essential. The evolution of the auto market, especially private car market, is of interest to numerous agencies. Hamilton et al. [17] distinguishes four stages in the growth of the automobile industry: first, experiment with invention; second, luxury uses and markets; then planned price reduction and expansion of markets; and finally, price stabilization and competition in design and salesmanship. The size of China's car market is growing robustly, and the critical feature of the future growth potential of car markets has been approached and forecasted by many researchers. Different car ownership models have been applied for various purpose and different interests, as reviewed by de Jong et al. [18]. It is suggested that the preferred model type for car stock forecasting depends on the research objectives and data availability. For those countries only having limited data, like China, some of the sophisticated methodologies may not be applied. A widely used method for application to developing countries is to express car density as a logistic function of either time [19], per-capita GDP [20] or per-capita income [21], because they have the

lowest data requirements, and rising incomes are widely considered to be the key factor in allowing increased car ownership.

By fitting Gompertz functions to data on per-capita vehicle ownership and per-capita GDP, Wu, Zhao, and Ou [20] showed that car stock level in China has followed an S-shaped curve like most other motorizing countries, and projected that the inflection point would appear around the year 2030. Instead of relying on a single economic variable, Huo and Wang [22] built up a China-specific fleet model in more detail, simulating private car ownership on an income-level basis and taking into account explicitly the influence of car price on vehicle ownership, in order to investigate the energy demand and environmental impacts of the rising number of vehicles in China. They separated car sales into two categories: new-growth purchases (i.e., first-time car purchases and additional purchases) driven by increased income, and replacement purchases, which households use to replace retired or scrapped vehicles. The approach in Huo and Wang [22] serves as a key example for the current chapter. However, we include uncertainty in the vehicle adoption trajectory, thereby addressing a key parameter and source of uncertainty in outcomes omitted in prior research. We describe an approach that allows exploration of the probability distribution of the saturation level of car ownership at high purchasing power, and allows comparison of effects of uncertain parameters, including disposable income, Gini index, and car price. We show results by conducting Monte Carlo simulation, and discuss the sensitivity to major parameters. We conclude by stating some implications for policy makers and city planners.

2.2 Methodology and data

2.2.1 Car stock and sales

With the survey of Chinese urban families with different income levels owing cars, conducted by China's Statistical Bureau, it is confirmed that it is more likely for people with higher income to own cars. Compared to income alone, per-capita income coupled with car price, called car purchasing power, was shown to have much better correlation with car ownership in China [22]. Especially for emerging economies like China's, car purchasing power is a more suitable independent variable to be used to model car ownership than income level alone, because the automotive industry is expanding as car prices decrease in the early stage of motorization.

Let A represent an affordability index, or purchasing power, which is the ratio of disposable income to car price index. We arbitrarily choose the car price index in 2003 (p2003) to be 1 and

use the United Nations medium-variant population projection as our baseline [23]. The total private car stock ($\hat{V}_i$) can be calculated by integrating across the entire population's range of incomes, x, the product of the income distribution density, I, and the propensity, g, that an individual with that affordability index owns a car, as shown in (2.1).

$$\hat{V}_i = P_i \int_{\frac{x}{p_i}=0}^{\infty} I_i\left(\frac{x}{p_i}\right) g\left(\frac{x}{p_i}\right) d(\frac{x}{p_i}) = P_i \int_{A=0}^{\infty} I_i(A) g(A) dA \tag{2.1}$$

where

$\hat{V}$ = Total private car stock in year *i*

P_i = Population in year *i* [persons]

x = Income of the incremental individual [RMB2007/year]

I_i = Income distribution function for year *i*

p_i = Car price index in year *i*

$A = \frac{x}{p_i}$ = Car affordability index

g = Deterministic relation between private car ownership (%) and affordability index

We decompose car sales, S, into two segments: new-growth purchases, S^N, associated with increases in ownership due to rising income, and replacements, S^R, for scrapped cars. New-growth purchases, calculated as (2), represent the spread of ownership to a larger portion of the population as incomes rise.

$$S_i^N = \hat{V}_i - \hat{V}_{i-1} = P_i \int_{A=0}^{\infty} I_i(A) g(A) dA - P_{i-1} \int_{A=0}^{\infty} I_{i-1}(A) g(A) dA \tag{2.2}$$

Even if per-capita ownership does not rise, households must buy replacements for old vehicles that are scrapped or retired. We call these replacement purchases, and calculate them as (2.3).

$$S_i^R = \sum_{j=1}^{i} S_{i-j}(SR(j-1) - SR(j)) \tag{2.3}$$

where

$S_{i-j} = S_{i-j}^N + S_{i-j}^R$ total number of new cars purchased in year *i-j* (2.4)

$SR(y) = \exp(-\left(\frac{y}{T}\right)^b))$ survival ratio [dimensionless] (2.5)

y = Age of vehicle [years]

T = Average vehicle life span = 14.46 years

b = Scrappage intensity = 4.7

The vehicle survival rate, $SR(y)$, describes the decreasing share of vehicles of a certain age remaining in use as the vehicle age grows. Hao et al. [24] collected data from a field study and employed the Weibull distribution to simulate it, as shown in (2.5). Because China has no official scrappage statistics and no compulsory scrappage standards for private cars, we adopt their values for T and b (shown above) in our analysis and assume that the pattern will remain the same in the future.

The careful reader will note certain differences in equations (2.1) and (2.2) compared with those given in reference [25]. In (2.1), we use $I_i(A)g(A)$ instead of $I_i(x)g(A)$. This is necessary such that the integral properly represents the expectation of g over a population of individuals with car affordability index distributed as A. In (2.2), the cited paper has something akin to ${S_i^N}_i = P_i \int_{M_{i-1}}^{M_i} \int_x^{\infty} I_i{}'(x) g(x, p_i) dx dM$, where M is the population mean income. This again mixes functions of x and A; and additionally uses a derivative of the income distribution, $I_i{}'(x)$. In the absence of model source code, the meaning is ambiguous; a derivative of $I(\cdot)$ with respect to x or A is negative at certain points, leading to negative projected sales in some future years, and we find that a derivative with respect to M (or μ) yields results that do not match observations. We instead use the method of finite differences described above.

2.2.2 The car ownership function, $g(x, p_i)$

Parameter uncertainty in Gompertz functions

It is recognized that a primary driving force for the growth of private car ownership is income level [26]. The statistics relating to Chinese consumer price index [27,28] show that the car price in China decreased rapidly in the past decade, driven by excess capacity and competition in the rapid-growing automotive market. Based on the theory of four stages in the growth of the car industry [17], car price stabilizes after the stage of the planned price reduction and expansion of markets, as shown in Figure 2.1(a). Compared to the early motorization stage in the U.S. [29], the theory suggests that both countries would have similar price trends.

A special case of the logistic function, the Gompertz curve allows for different curvatures at extreme values of the economic factors [30]. We use a formulation (2.6) that represents the probability that an individual owns a car as a function of A.

$$g(x, p_i) = g(A) = \gamma \exp(\alpha \exp(\beta A)) \tag{2.6}$$

where

g = Probability to own a private car

A = Car affordability index

γ = Probability of owning a private car at very high income

$0 > \alpha, \beta$ = Shape parameters

In order to illustrate the limitation of point estimates, we use data from the 2008, 2009, and 2010 China urban household surveys [31]. (Note that prior to 2010, only Shanghai limited car ownership using a license plate quota system, but in recent years a growing number of cities have adopted such policies. To avoid obscuring the underlying relationship, we omit data from 2011 onwards.) Figure 3.2 shows values of g ranging from 20% to 80% or higher produce fits that are all apparently close matches to the data. A common response in the literature is to arbitrarily choose g from another country with saturated ownership, or some plausible low or high bounding values for a few scenarios.

Economic development and car ownership in China are both behind those of motorized countries, and thus as a whole the country is still below the inflection point of g. Thus, the survey data tell us little about the eventual probability of possessing a car when people have higher income levels, even though the results show that people with higher car purchasing power are more likely to own cars, as expected. Due to the uncertainties arising from unclear future economic context and unpredictable consumer preference, the value of single-point estimates is limited.

Monte Carlo simulation of the distribution of γ, α, and β

Following [32], our updated algorithm to estimate the parameters of Gompertz function by incorporating uncertainty is as follows. The unknown parameters are γ, α, and β while the state variable is only $r = \gamma$, because the latter two parameters can be further determined by linear regression at a given g. As the data are available for per-capita disposable income at national level, car price index, population, and private car stock numbers during 2007 to 2015, we then define the root-sum-of-square (RSS) residual between back-cast private car stock ($\widehat{V_i}$) by (2.1) and actual historical data (V_i) as (2.7).

$$RSS = \sqrt{\sum_{i=2007}^{2015} (\widehat{V_i}(r) - V_i)^2} \tag{2.7}$$

Monte Carlo simulation with 400 iterations is applied to estimate the possible outcomes of the saturation level of possibility (γ) forecasts. γ is constrained to the range between the 23% (the observed per-capita car ownership for the highest income household in 2012 (16)) and 100%. A discrete probability density function for $\gamma \in (23,100)$ is constructed by randomly sampling 50 points across the range and calculating their associated $RSS(\gamma)$, subtracting from max(RSS) and then normalizing so that the density is lowest where the residual is greatest. From the resulting distribution of r for each iteration, a single sample is drawn and accepted as the γ in that run, followed by estimating the other two parameters, α and β, from linear-regression model as (2.8), which is converted from (2.6) by log-linearization. As shown in (2.8), $ln\ (-\alpha)$ and β are linearly related and are regressed as a least-squares fit for time series data in each iteration.

$$\ln\left(ln\frac{\gamma}{g(A)}\right) = \ln(-\alpha) + \beta A \tag{2.8}$$

The income distribution, I

Various probability distribution functions have been studied in research on income disparity. By comparing observations to mathematical models, researchers can determine the distribution function with the best fit. Some scholars prefer the log-normal distribution; for example, Steyn [33] examined the inhabitants in the Orange Free State rural areas of the Union of South Africa, and showed that the logarithmic normal model is quite a good model. On the other hand, McDonald and Ransom [34] stated that the log-normal distribution performed the worst while considering the log-normal, gamma, beta, and Singh-Maddala functions as descriptive models for the distribution of family income for 1960 and 1969–1975 in the U.S.

Data availability has been a major obstacle for research in many fields in China, including research on income inequality. Chen et al. [35] investigated 20 sets of grouped data on family income between 2005 and 2012 in China, and demonstrated that the fitting of the log-logistic distribution is better, while the log-normal distribution function underestimates the income of the high-income group due to its thinner right tail. Following [35], we approximate a continuous income distribution for China with (2.9).

$$f(x;a,b) = {bx^{b-1}}\Big/{a^b(1+(\tfrac{x}{a})^b)^2} \tag{2.9}$$

where

x = per-capita disposable income [RMB2007/year]

a, b = scale and shape parameters of the distribution

Note that if x is log-logistically distributed, then A has also a log-logistic distribution but with different scale parameter (2.10).

$$X \sim f(x; a, b) \Rightarrow A = \frac{X}{p} \sim f\left(\frac{x}{p}; \frac{a}{p}, b\right) \tag{2.10}$$

Given historical data and projections of the mean disposable income (M) and Gini index (G), we then solve the equations, shown as (2.11) and (2.12), analytically by computer mathematical software to simulate the income distribution in a given year.

$$G = \frac{1}{b} \tag{2.10}$$

$$M = \frac{a\pi}{b\sin(\pi/b)} \tag{2.11}$$

For future income, we use projections from China's 13th Five-Year Plan and the OECD, and assume that M will increase at the same rate as GDP after 2020 [36]. Note that these projections were made before the coronavirus disease (COVID-19) epidemic, so they might be optimistic. Figure 2.1(b) shows the future projection of M. Hu, Luo, and Yang [37] adopted the grey forecasting model, commonly applied in academic fields such as electrical engineering, mechanical engineering, and agriculture, to predict the Gini index in China until 2022. With the given difference between the official Gini index (0.465) in 2016 and Hu, Luo, and Yang's predicted value (0.479), we first correct those from 2017–2022, and then adopt the same rate of change in subsequent years to give the future Gini index projections, shown in Figure 2.1(c). Figure 2.1(d) depicts the resulting income distributions in China for some years, i, between 2007 to 2050 based on our derived projected function parameters; in computing projections, we use a distinct $I_i(A)\ \forall\ i$.

2.3 Results and analysis

2.2.1 Parameter space for α, β, and γ

Figure 2.3 illustrates the parameter space for the Gompertz function at 400 samples of γ with the associated probability distribution from Monte Carlo simulation and regression. Note that for a randomly-selected g, our regression procedure for a, b constrains these parameters to a narrow range that matches historical data, unlike [32] which treated all three as a state vector and applied Gibbs sampling, drawing each of three parameters in sequence from a joint distribution.

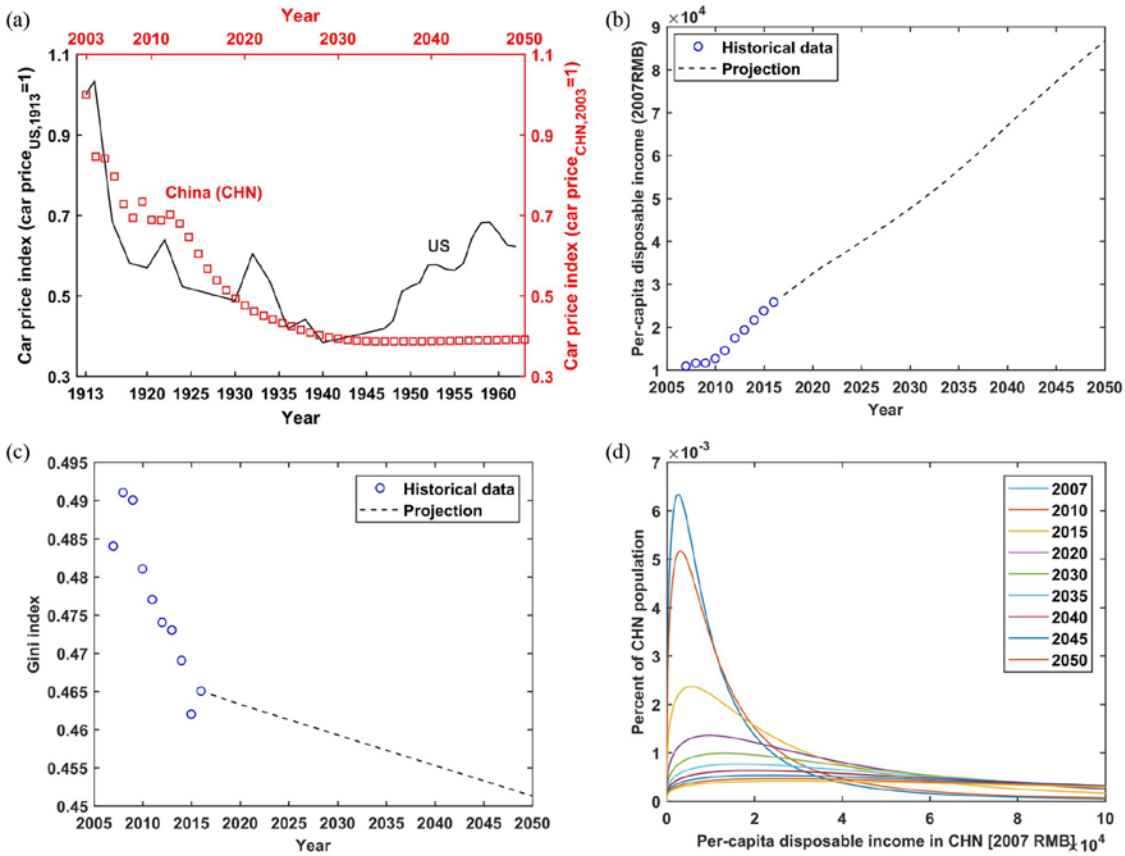

Figure 2.1. Major parameters and functions in car stock model: (a) Car price index in China (historical data 2003–2016 and future projection to 2050) and the historical data in U.S. (1913–1962); (b) Per-capita disposable income (2007 RMB), 2007–2050; (c) Gini index, 2007–2050; and (d) Income distribution with the log-logistic assumption, 2007–2050.

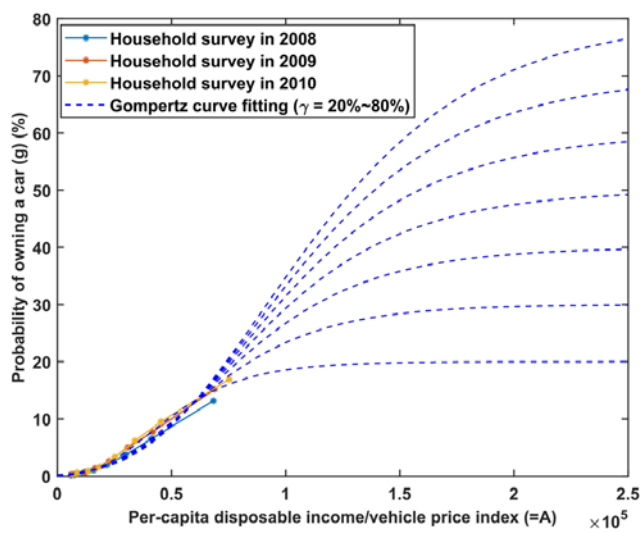

Figure 3.2. Private car ownership and car affordability index in China, $g(x, p_i)$, with assumed γ between 20% and 80%.

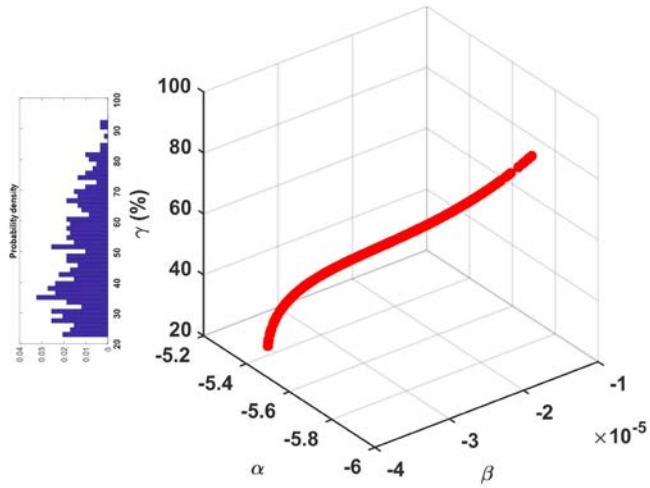

Figure 4.3. Parameter space for α, β, and γ with the probability density distribution of γ.

2.2.2 Private car stock

Figure 5.4 presents the outcomes of the private car stock and ownership in China projected by our stock model for all 400 samples, with 1st decile, mean and 9th decile shown by black lines, and the probability distribution of the outcomes in 2030 and 2050. We also show the projection results, for comparison, from Huo and Wang [25] for stock, and from TASRI (Tsinghua Automotive Strategy Research Institute [38]) for ownership. Note that our model is forecasting private cars, rather than all vehicles as in TASRI. The model shows a range of possible future private car stock in China: 430 million (low of 280 million at 1st decile; high of 620 million at 9th decile) in 2050. Table 2.1 gives a summary of the parameter values for 1st decile, median, 9th decile and the expectations with standard deviations, with the associated projected private car stock numbers and per-capita car ownership. As shown in Table 2.1, uncertainty is larger in estimating the parameter γ compared to the other two, which implies that predicting the probability of private car ownership in China is challenging, as discussed above ("*Parameter uncertainty in Gompertz functions*").

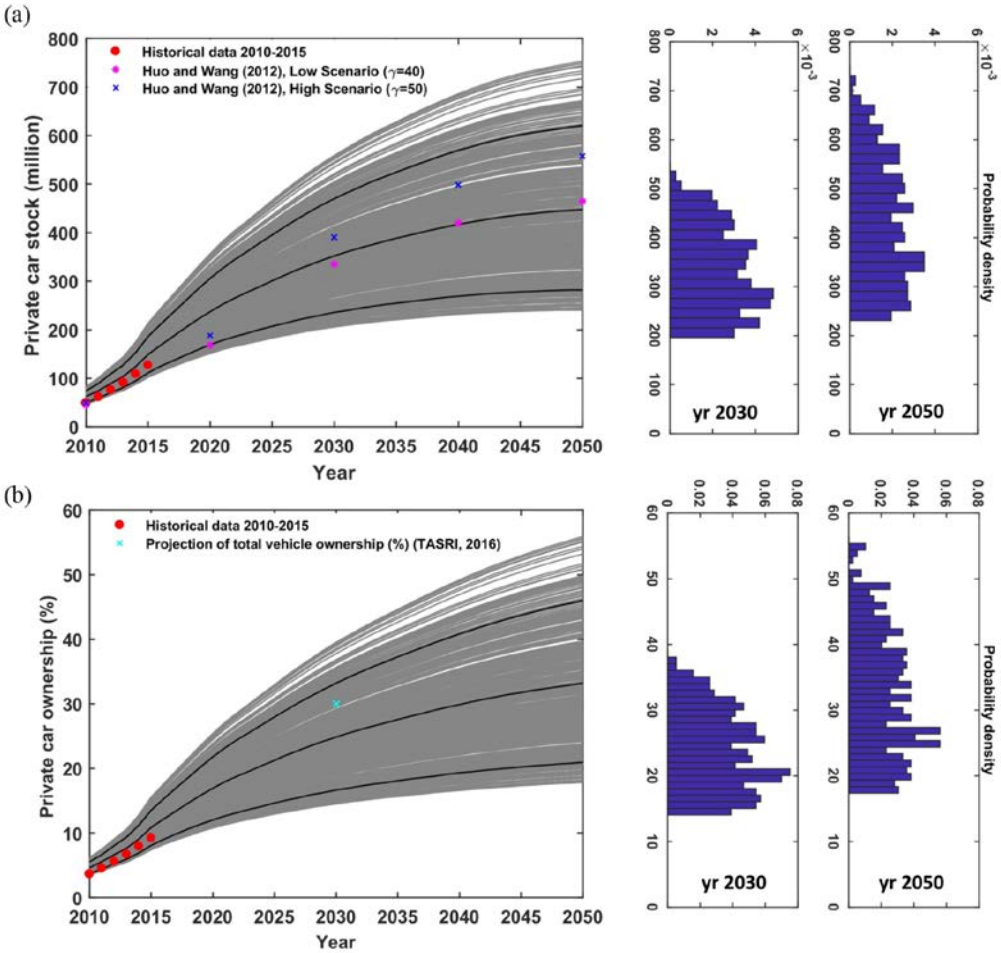

Figure 5.4. Possible outcomes from Monte Carlo simulation: (a) 2010–2050 private car ownership with the probability distribution in 2030 and 2050; and (b) 2010–2050 private car stock with the probability distribution in 2030 and 2050.

Table 2.1. Parameter Values and the Associated Projected Values for Private Car Stock

Parameter	1st decile	Median	9th decile
γ (%)	28.206	48.090	74.538
α	−5.307	−5.491	−5.796
β	3.18×10^{-5}	2.38×10^{-5}	2.00×10^{-5}
Stock $\hat{V}_{2030}$ (million)	235.62	342.75	470.14
Stock $\hat{V}_{2050}$ (million)	282.26	434.21	620.32
Vehicle per 100 capita$_{2030}$	16.634	24.213	33.213
Vehicle per 100 capita$_{2050}$	20.938	32.210	46.016

2.2.3 Private car sales

Figure 6.5 draws out, for every sample, the results of private car sales in China, with 1st decile, mean and 9th decile shown in black lines, and the associated shares of replacement purchase in dark red lines, and the probability distribution of the both outcomes toward 2050. It is noted that higher car sales correspond to a lower share of replacement purchases; that is, the order of the black quantile lines is reversed for the two outcomes. The predicted distribution of the private car sales in China will be centered at 30 million from 2030 to 2050 (low of 19 million at 1st decile; high of 44 million at 9th decile). While scenario analysis, which brackets uncertain outcomes of interest, is one response to improve the value of single-point estimates, our upgraded methodology provides a more detailed characterization of the uncertainty in transport projections.

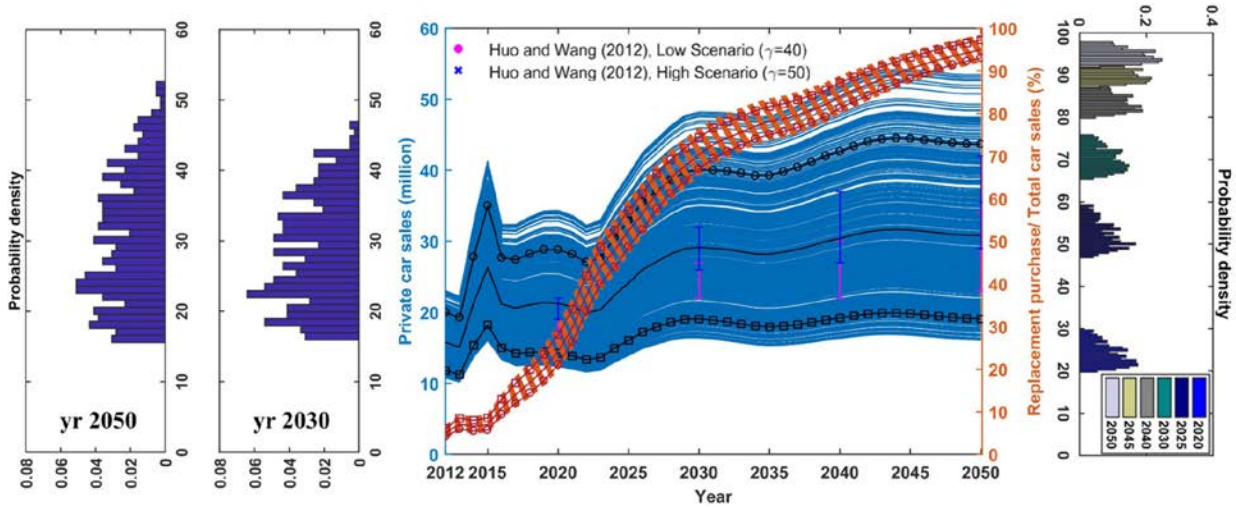

Figure 6.5. Possible outcomes from Monte Carlo simulation: (a) 2010–2050 private car ownership with the probability distribution.

Table 2.2 summarizes the expected value of private car sales numbers and replacement purchases share with the associated standard deviations by our model. As stated ("2.2 Methodology and data"), private car sales are divided into two groups due to their purchasing motivations: new-growth purchase and replacement purchase. The split between these two groups characterizes the maturity of the auto market [22]. As shown in Figure 2.5, current car sales in China are mainly driven by first-time car purchases—i.e., the share of replacement purchases is still low. Our results show that replacement purchases will dominate the sales market from 2025, which is a feature of maturity. However, the replacement purchase share is still lower than 100%

in 2050, implying that the car market in China will not be fully mature by 2050. Unlike the uncertainty in projections of private car stock/ownership and car sales, which grow continually into the future, the distribution of the replacement purchases share narrows toward the saturated (~2050) market state. We discuss the implications below (see "Discussion").

Table 2.2. Private Car Sales Projections from Car Sales Model

$E[\cdot] \pm \sigma$	Car sales (million)	Replacement purchases share (%)
2020	21.27 ± 5.39	24.16 ± 2.56
2025	24.17 ± 6.24	52.49 ± 3.17
2030	29.16 ± 7.78	70.38 ± 2.70
2040	30.40 ± 8.68	83.97 ± 2.18
2050	30.80 ± 9.13	94.95 ± 1.54

Another way to characterize the maturity of a car market is using the ratio (r) of the private car sales to the change in private car stock as an indicator. Note that "one minus the inverse of the ratio" is the proportion of the new cars sold to replace the old models which have been scrapped. Therefore, the ratio should be close to 1 in an emerging car market, as the new-growth purchases dominate sales. As a check on our model projections, we compare this indicator with data from the early stage of motorization in the U.S. [39], as shown in Figure 2.6. According to our model, two lines (black line represents the numerator while blue dash line represents the denominator of the ratio) are close to one another in initial years but will separate gradually as the auto market in China becomes more mature, which is the same as the observed pattern in the U.S. in the 20th century.

However, care should be taken when drawing parallels between China and the United States: while some trends may be similar, the adoption of personal vehicles in China nowadays happens in a much different context compared to the one in the United States a hundred years ago. The preferences, technology options, costs, earnings, urban situation, and policy environment faced by 21st-century Chinese households differ in important ways from those of 20th-century Westerners; our projections highlight the uncertainty these distinctions create in the trajectory of motorization.

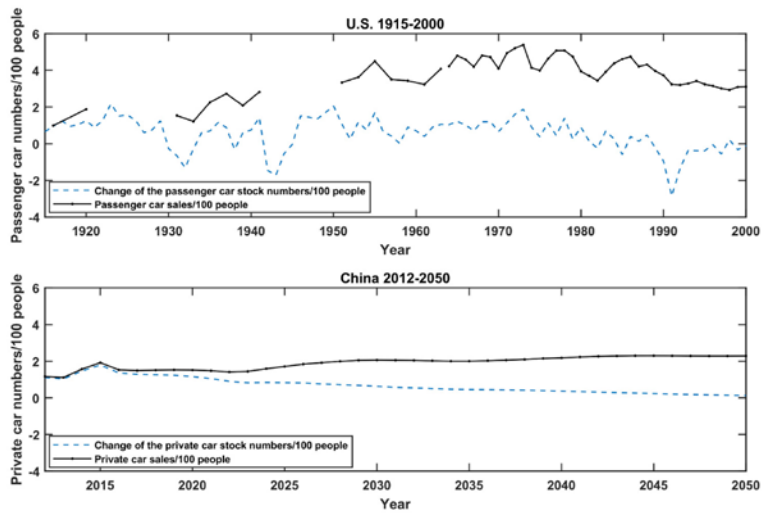

Figure 7.6. Comparison of our model results for China 2010–2050 with the motorization-stage in U.S. 1915–2000.

2.2.4 Sensitivity analysis

The projections presented above rely on historical data, household sample surveys, and exogenous projections of the independent variables. We conduct sensitivity analysis to help assess how much the model output values are conditioned by the latter. The major parameters here are car price (p_i), mean per-capita disposable income (M), Gini index (G_i), and the ultimate saturation level (γ). As uncertainty in g has been investigated by Monte Carlo simulation, the influences of the other three parameters (p_i, G_i, and x) are studied, and we adopt the expectation value of γ as a base case. For brevity, we focus only on sensitivity of this central value to assumptions; however, the method we describe makes it straightforward to study sensitivity of the spread and shape of the distributions of projected outcomes, as well.

There is disagreement in the literature over the estimation of China's household income [40] and the precise past and present values of the Gini index [35]; future forecasts contain additional uncertainty. In Figure 2.7, we show projections from other agencies (HSBC [41], Standard Chartered [42], and Morgan Stanley [43]) for income level and literature (Wang et al. [44]) for Gini index, and our sensitivity trajectories that result in values that are $(100 + n)\%$ of the projected values in 2050, where $n \in (-40, -30, \ldots, 30, 40)$.

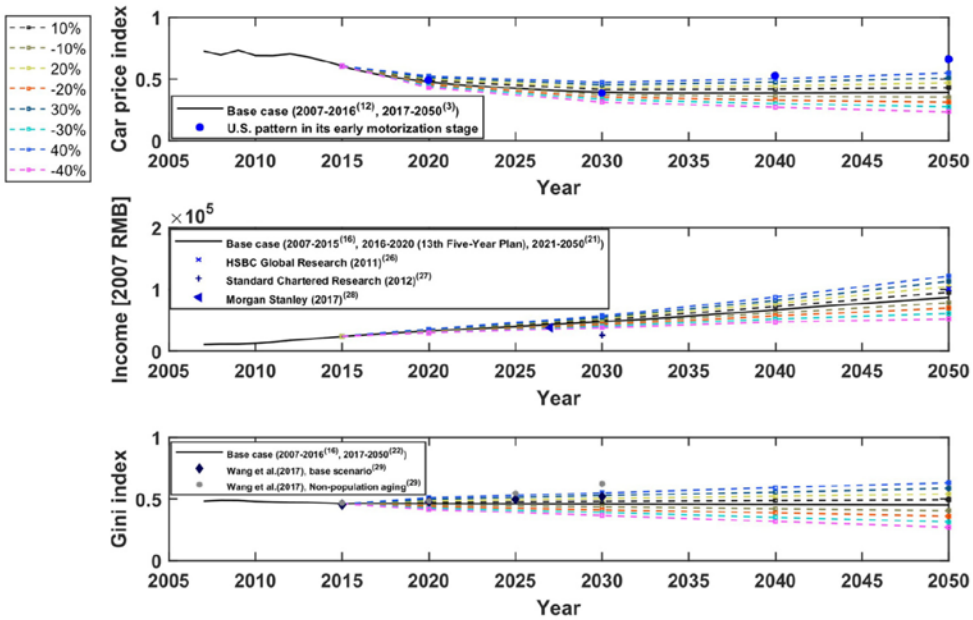

Figure 8.7. Trajectory of the major parameters varied in the sensitivity analysis.

Figure 2.8 presents how the change in car ownership as the major parameters change. As expected, car ownership increases when car purchasing power increases, due to either an increase in per-capita disposable income level or a decrease in car price index. Note that car ownership is most sensitive to car price in near-term future (2020); whereas it is nearly equally sensitive to income level along the future period.

The Gini index has a negative relationship with car ownership in near and mid-term future (2020 and 2030): as Gini index (level of income inequality) increases, the mass of income distribution shifts to the left, and thus the majority of the society becomes poorer while almost all income is held by a small fraction of very wealthy households. In this case, per-capita car ownership is lower, because a larger fraction of the population cannot afford car ownership at all. By contrast, when China's economy and car market become developed and mature, income inequality has little effects on private car ownership. While the sensitivity of car ownership to car price shown in Figure 2.8 is consistent with [25], the sensitivity results with respect to per-capita disposable income and Gini index are different. Our study shows the similar sensitivity to income level toward 2050, whereas the magnitude of the changes decreases as time passes in [25]; in the current results, the sensitivity of car ownership to Gini index is not always monotonically decreasing. This result is due to the different probability distribution functions chosen to simulate

the income distribution in China and the different calculation mechanisms for car stock, as described above ("2.2.1. Car stock & sales"). For example, the log-normal distribution used in [25] somewhat underestimates the income of the highest-income households, and thus may further underestimate the sensitivity to income level in the long-term projections as more people become wealthy.

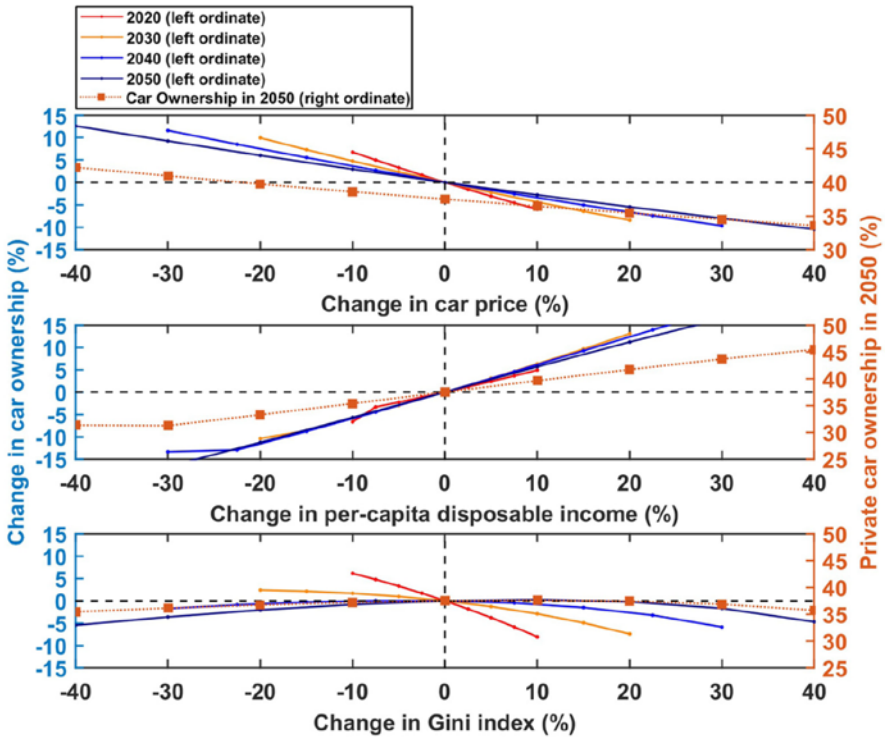

Figure 9.8. Sensitivity of private car ownership with respect to major parameters (solid line) and the corresponding ownership level in 2050 (dotted line).

2.4 Discussion

Our analysis simulates the possible outcomes of China's growth in private car ownership and sales by characterizing the distribution of the adoption trajectory. Figure 2.4 shows that our model captures the pattern of growth, although the expected value slightly overestimates historical car ownership and stock. As mentioned ("*Parameter uncertainty in Gompertz functions*"), we are modeling the development of car market without many government interventions. However, besides household incomes, car price, and income inequality, policy also affects transport-related consumption. To reduce private vehicle travel and create more livable and sustainable cities, an

increasing number of the largest cities in China have sharply restricted new vehicle registration by implementing quota policies [45]. While Shanghai was a proactive adopter of license auctioning (starting in 1994), other cities did not impose their own quotas until 2011 or later, when the motorization was already in rapid progress. Such caps on vehicle purchases may increase the deviation of our projections from observations in the future; however, the likely distribution of our projections can aid in the design of robust transportation policy that relies on forecasts of demand. Previous research has shown that the preferences of existing vehicle owners are, to some extent, anchored—they may prefer to get a vehicle that is similar to the one they are replacing, or already own [46]; or they may even prefer to upgrade their cars in size and horsepower [47]. Manufacturers both encourage and follow these preferences. We show (Figure 6.5) that the percentage of replacement sales can be expected to be large in the new car sales market around 2025. Therefore, in the near-term where new sales are a large share of the market, the government has significant opportunities to guide the type, size, fuel economy and pollution characteristics of vehicles sold. These will in turn condition households' experience and expectations of vehicle ownership, and thereby affect their future replacement and additional purchases.

According to the 13th Five-Year Plan (2016–2020), China proposed to become "a moderately prosperous society in all respects" [48]. The government is aiming to double per capita income by 2020 from 2010 levels, and to improve the fairness of income distribution through expanded public services. If these objectives are achieved, Figure 2.8 reveals that the private car ownership rate in China will be higher in 2020 as the economy is more equal (i.e. the Gini index is lower). Proper transport demand management (TDM) strategies are required to reduce private vehicle travel, curb car congestion, and to make sustainable transport a reality—and our results show that they are even more urgent if the government is successful in pursuing its goal of reducing inequality.

2.5 Extension

The regional distribution of China's current vehicle market reflects the regional heterogeneity in GDP contribution across the country and the different regional urbanization level. China's six largest civil vehicle owning provinces—Shandong, Guangdong, Jiangsu, Zhejiang, Hebei, and Henan—represented around 47% of the total vehicle fleet at the end of 2015. In particular, in terms of the contribution for incremental growth, these six provinces accounted for

nearly 50% every year in the past ten years [31]. This pattern shows that the coastal regions have dominated the national market.

In order to incorporate the significant regional differences in the level of economic development and vehicle ownership, and produce more precise projections with possibly narrower distributions, the national-level methodology shown in this chapter could be applied at the regional or provincial level. To do this, the car ownership function, g, would be sampled separately and survival ratio, SR(y), is estimated differently for provincial-level cities and other sub-national regions, and the exogenous variables could be drawn from province-level projections.

Finally, with the car stock and car sales models at either the national or regional levels, this chapter allows examination of uncertainty in the future trends of life cycle energy demand and emissions from private car use in China.

2.6 Conclusion

Undoubtedly, China's car stock will continue to grow, driven by the growing economy. However, due to the short history and the country being in a fast-growing stage of transport system expansion, national observations contain little information about the eventual saturation level. Here, we improved on existing methods by incorporating adoption uncertainties and considering multiple key influencing factors, demonstrating a novel treatment of uncertainty in transport forecasting in China. A range of future forecasts in transport demands that are conditioned on observed reality was developed, producing a characterization that can help policy makers or transport infrastructure project managers create flexible designs that are robust to eventualities. On the other hand, the use of single-point estimates could lead to a 'flaw of averages', by obscuring irreducible future uncertainty [49].

We found that the distribution of car stock/ownership is wider in 2050 than 2030; on the other hand, the distribution of the share of new-growth purchases is higher in the near term than in a saturated market, with replacement sales expected to dominate the car sales market after the next decade. Finally, our sensitivity analysis results suggest that the car ownership will increase further in 2020 as the society becomes less unequal; and more so if this trend goes faster than the literature suggests. We also discussed how our method and estimates have important implications

for regulators and planners, and could be a basis for regionally-disaggregated projections with similar advantages.

Chapter 3. Outlook for vehicle batteries: Practical limits on battery price reduction

Much of the material in this chapter has been published in Hsieh, I-Yun Lisa, Menghsuan Sam Pan, Yet-Ming Chiang, and William H. Green. "Learning only buys you so much: practical limits on battery price reduction." Applied Energy 239 (2019): 218-224. Menghsuan Sam Pan collaborated in the model derivation, contributed to the analysis of the results, and to the formulation of the arguments in the text. Yet-Ming Chiang was involved in planning and supervising the work.

Abstract

Wide deployment of electric vehicles (EVs) would greatly facilitate global de-carbonization, but achieving the emission targets depends on future battery prices. Conventional learning curves for manufacturing costs, used in many battery projections, unrealistically predict battery prices will fall below $100/kWh by 2030, pushing EVs to hit price parity with internal combustion engine vehicles (ICEVs) in the absence of incentives. However, in reality, essential materials costs set practical lower bounds on battery prices.

Our 2-stage learning curve model projects the active material costs and NMC-based lithium-ion battery pack price with mineral and material costs as the respective price floors. The improved model predicts NMC battery prices will fall only to about $124/kWh by 2030 – much cheaper than today, but still too expensive to truly compete with ICEVs, due primarily to the high prices of cobalt, nickel, and lithium. Our results suggest that stabilizing raw materials prices and/or stimulating R&D activities on alternative battery chemistries will be important to achieve environmentally sustainable EV-based ground transportation at an attractive price.

3.1 Introduction

Growing global awareness of the environmental impact of combustion is accelerating the adoption of electric vehicles (EVs), but high EV purchase prices prevent their widespread market penetration. The U.S. DOE has set a battery price target of $125/kWh by 2022 for clean transportation applications [50], suggesting that significantly lowering battery price (pack prices were $200-$300/kWh in 2016 and 2017) is a necessity to make EVs economically attractive [51]. High battery price is considered to be an important barrier to EV profitability for automakers, and $100/kWh has been estimated as a threshold for an EV to be truly cost-comparable to an internal combustion engine vehicle (ICEV) [52]. Currently, EV production is mainly driven by government subsidies and mandates. The new "dual-credit scheme" mandate in China is expected to drastically increase EV adoption and correspondingly increase battery production volumes. According to the learning curve concept, as cumulative installed capacity increases, battery production costs per kWh are expected to decline as a power law owing to improved designs/manufacturing techniques and economies of scale. However, battery prices depend on both materials and manufacturing costs. Essential materials, especially expensive elements (lithium, nickel and cobalt), used in current battery technologies, will eventually constrain the declining trajectory of production cost and set practical lower bounds on battery prices.

Cobalt price, in particular, has soared over the past few years, mainly due to the projected increase in EV battery production, but also due to political factors in the world's largest cobalt producer -- Democratic Republic of Congo (DRC) [4]. Even though mining companies like Glencore and ERG are exploring and developing new cobalt operations and productions, it is expected that the world cobalt supply will not keep up with the growing demand driven by EV mandates. To secure raw materials that are critical for EV batteries, GEM, a major Chinese supplier of battery chemicals, recently announced a deal with Glencore to purchase roughly one-third of its cobalt production in the next three years [53]. Further downstream, Volkswagen has recently placed $24.6 billion in battery orders with CATL, a major customer of GEM, to deliver most of the batteries for Volkswagen EVs sold to the Chinese domestic market [54]. These announcements highlight the fact that large-scale EV adoption depends on reliable supplies of battery materials and that the costs of these materials are significant.

3.2 Methodology

3.2.1 Collection of battery price data

Existing literature sometimes uses price and cost interchangeably: price paid to a battery pack supplier is a cost to the automaker purchasing the battery pack. Here, we use the term 'price' throughout this work. The systematic review in Nykvist and Nilsson [55] serves as a key source for this chapter, and we select only sources for battery packs using NMC cathodes in the references. We further incorporate new price estimates released after Nykvist and Nilsson [55] was published, but exclude those before 2010 due to the large uncertainty in earlier price evaluations and the lack of data on total global EV battery capacity installed at that time. Price estimates are adjusted for inflation to US$ (2017) based on consumer price index data [56]. A total of 46 data points are tabulated in Table A1 (Appendix A).

3.2.2 Two-Stage Learning Curve Model

Based on the battery supply chain structure (see Figure A1), we developed a two-stage learning curve model to capture the practical limits to battery cost reduction. In the first-stage learning (material synthesis; MS), mineral costs (MinC) are considered as a floor for active materials costs (MatC); in the second-stage learning (battery pack production; BP), the active materials costs from the first-stage calculation are taken as a floor for battery pack price (BPP). The model can be found in Eq. (3.1) and Eq. (3.2).

$$\text{Stage 1: } \mathrm{MatC_t} = (\mathrm{MatC_0} - \mathrm{MinC_0})\left(\frac{\mathrm{V_{MS,t}}}{\mathrm{V_{MS,0}}}\right)^{\mathrm{b_{MS}}} + \mathrm{MinC_t} \quad (3.1)$$

$$\text{Stage 2: } \mathrm{BPP_t} = (\mathrm{BPP_0} - \mathrm{MatC_0})\left(\frac{\mathrm{V_{BP,t}}}{\mathrm{V_{BP,0}}}\right)^{\mathrm{b_{BP}}} + \mathrm{MatC_t} \quad (3.2)$$

By performing linear regression of the production cost and cumulative installed capacities (V_{MS} and V_{BP}), we derive learning rates (LR) for the identified two stages:

$$\text{Stage 1: } \mathrm{LR_{MS}} = 1 - 2^{\mathrm{b_{MS}}} \quad (3.3)$$

$$\text{Stage 2: } \mathrm{LR_{BP}} = 1 - 2^{\mathrm{b_{BP}}} \quad (3.4)$$

Details of the model parameterization are shown in Appendix A.II. Uncertainties are reported using 95% confidence intervals based on the average (μ) and standard deviation (σ) of derived learning rates, given as μ±2σ.

3.2.3 Passing from Stage 1 to Stage 2 in the Model

While there are numerous different compositions of NMCs, our study focuses on four specific compositions: NMC111, NMC532, NMC622, and NMC811 (where the numbers indicate the molar ratio of Ni, Mn and Co within the cathode compounds). Increasing nickel content for higher energy density is a clear trend to satisfy the need for longer range in EV applications. This also reduces the amount of expensive cobalt required. Element requirements for a unit of energy differs across various compositions, and thus the effects of elemental prices on $/kWh active material costs are different. Therefore, different NMC variants provide the lowest material costs at different times as mineral prices fluctuate. The projected floor price for battery pack price was constructed by using the composition of NMC with the lowest projected material cost each year.

3.2.4 Chemical Cost of Storage and Chemical Specific Energy

Chemical cost represents a floor on the cost of the complete battery, while the chemical specific energy gives an upper bound on battery specific energy. The chemical cost and chemical specific energy for representative electrochemical couples (including electrolyte) are computed using the unit costs of the electrochemically active materials (including cathode and anode) and electrolyte, and practical capacity of active materials. Chemical specific energy is defined as the amount of energy stored in a given mass of active materials and electrolyte. Both commercially available and potential future rechargeable battery chemistries are included. Numerical values and details of the calculations are shown in Appendix A.IV.

3.3 Results and Discussion

3.3.1 Two-Stage Learning Curve Model

One limitation of the conventional one-stage learning curve is that it implicitly suggests that cost reductions can go on forever until the cost approaches to zero. However, materials costs set a floor, which was usually ignored in the past studies of EV battery price projections using a learning curve. The mathematical model of the 2-stage learning curve is described in Eq. (3.1), Eq. (3.2), and the Appendix (A.II). Our analysis focuses on NMC-based LIBs, which are widely adopted by electric vehicle manufacturers. NMC-based LIB pack price estimates between 2010 and 2016, tabulated

in Table A1, are collected from Nykvist and Nilsson [55] as well as other more recent sources. Annual battery capacity installed in EVs has grown by around 133% annually from 2010, and reached 34.5 GWh/y in 2017, with accumulated capacity of 85 GWh since the introduction of a new generation of EV batteries in 2008 [57]. The learning rate, shown in Figure 3.1, for active materials synthesis (LR_{MS}=3.5%) is obtained by the first-stage linear regression with the mineral cost as a floor. The second-stage fitting then depicts the learning curve of EV battery pack manufacturing (LR_{BP}=16.5±4.5%, considering uncertainty in battery price estimates) with active materials cost as a floor. Our model predicts a stronger learning effect on EV battery pack price compared to the study performed by Nykvist and Nilsson [55], but in line with more recent studies [58,59]. This suggests that our 2-stage learning curve model captures the practical limit on cost reduction and structure of the battery supply chain without sacrificing learning rate estimations. The price floors determined by materials costs play an insignificant role in historical battery prices "learning" as the materials costs accounts for only marginal amount of the total battery prices. However, as discussed below, when battery prices continue to fall in the future, the materials costs become much more important, and set practical lower bounds on battery prices.

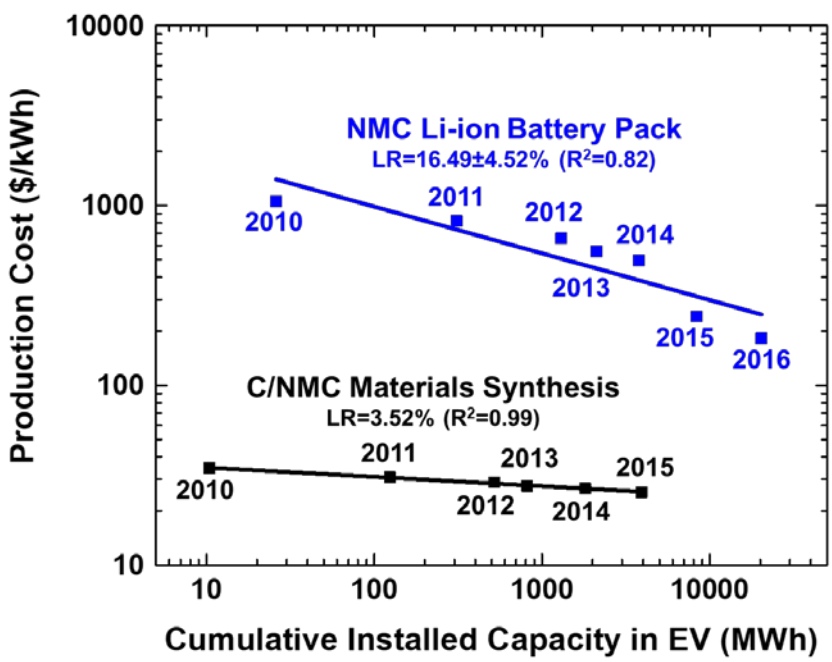

Figure 3.1. Two-stage learning curve model: materials synthesis and battery pack production. Learning rate (LR) is calculated by linear regression of the log of production costs and the log of estimated cumulative capacity installed, as shown in equation (3.1) and

equation (3.2). Production costs during material synthesis and battery pack production are obtained by subtracting mineral costs from active materials costs, and the active materials costs from battery pack prices, respectively, see details in Appendix A. II. NMC111 is chosen as representative for the learning rate of C/NMC material synthesis.

3.3.2 Future Projection for EV Battery Pack Prices

To project the future trajectory for battery prices, battery production volume and elemental costs are evaluated. Driven by strong government support, sales of new energy vehicles (NEV, including pure battery electric cars (BEVs), plug-in hybrids (PHEVs) and fuel cell models) in China rapidly grew in the past few years [60]. China has been the leading nation in total EV (BEV plus PHEV) sales since 2015, accounting for approximately 50% of EVs sold worldwide in 2017, and reaching over four times the BEV sales volume of the U.S in 2017 [61]. The introduction of the dual-credit system in 2017 [62] further shows China's commitment to speeding up clean vehicle development and its ambitions to boost local NEV adoption. Because China dominates the EV market, it is chosen as a main driving force for global future EV market penetration. EV market penetration in China is described by fitting a Gompertz function, as shown in Figure 3.2, to the historical sales market share, taken from Global EV Outlook 2017 [63], and the future targets set by China's government (7% in 2020, 15% in 20205, and 40% in 2030) [64]. By incorporating a China-specific passenger car ownership and sales model [65] with the derived EV penetration curve, we obtain the predicted electric passenger car sales in China between 2018 and 2030. The shifting from less expensive $LiFePO_4$ (LFP) to higher specific energy NMC in China is also considered here [66]. The detailed assumptions and methodology for battery production volumes are included in Appendix A.III.I, and the estimated equivalent installed capacity in China and in the world toward 2030 is shown in Figure 3.2.

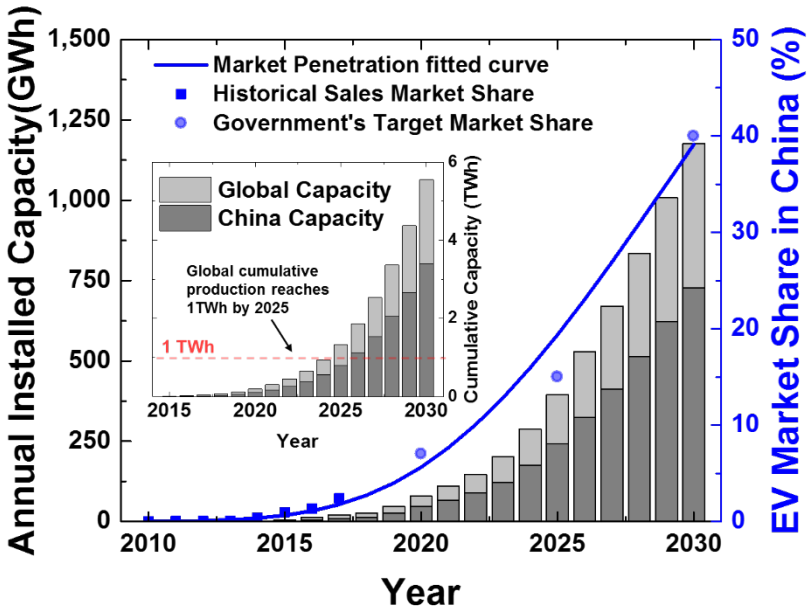

Figure 3.2. Projected annual NMC batteries installed capacity based on the EV sales market share in China; the inset shows the projected cumulative installed capacity, both in China and global market. Projected EV market penetration in China from fitting a Gompertz function to the historical EV sales market share and the government's targets for 2020, 2025 and 2030. Global EV production is estimated by assuming that China keeps dominating the EVs sales toward 2030.

Lithium and cobalt are experiencing price fluctuations as automakers and high-tech companies rush to lock down the supplies of critical battery materials. Lithium's price has steadily increased by about $1.9/kg/y annually for the past 7 years [67]. Cobalt's price on the London Metal Exchange (LME) surpassed $90,000/tonne in March 2018, up from $25,000/tonne in early 2016 [68]. To obtain a reasonable cobalt price projection as a base case scenario, we exclude price surges that resulted from specific political events and linearly extrapolate the resulting moderately growing cobalt price trajectory in 2017, shown in Figure A3. Given the volatility of cobalt prices, active materials costs across multiple compositions in the NMC class could have various positive or negative slopes as cobalt's price increases or decreases, depicted in Figure A4. The model then takes the lowest active materials cost curve as a price floor for battery price projections. Our projections generally show a shift toward Ni-rich compounds with higher specific capacity and less use of the expensive cobalt in the future. Appendix A.III details the cobalt price extrapolation

and NMC composition selection by the model as the determining the floor price, followed by the battery price projections under various scenarios.

Figure 3.3 depicts the projected battery pack price reductions over time along with active materials costs and mineral costs as EV technologies diffuse through the market. The downward inflection in mineral costs around 2022 corresponds to the widespread adoption of NMC811 replacing other NMC compositions. Note that the active materials costs *increase* over time; this is because the growth in mineral costs outweighs the cost benefits of greater learning in materials synthesis processes. However, strong learning effects in battery manufacturing nonetheless continue to drive total battery pack price reductions over time, approaching ~$124/kWh in 2030 in the base case, and ranging between $93/kWh to $140/kWh depending on price projections for lithium, cobalt, and nickel. The lower bound can only be reached by assuming fixed 2016 prices for the minerals, quite unlikely since the cobalt price has more than tripled since 2016. The base case value reported here is slightly lower than the bottom-up projections of NMC-based Li-ion battery pack price (~$130/kWh for Graphite/NMC622 couple) given by the US Dept of Energy Vehicle Technologies Office [69], this is because Graphite/NMC811 couple (with less usage of expensive cobalt) is expected to dominate the 2030 EVs battery market. Figure 3.4 investigates the effects of mineral price fluctuations on battery pack price forecasts in 2030, showing that the cobalt commodity market greatly affects the projected battery pack price, and thus the adoption rate of EVs. The lowest and the highest price projections toward 2030 in Figure 3.3 and 3.4 are discussed in detail in Appendix A.III.IV as scenario 1 and 2. Overall, the unknown price trajectory of minerals leads to an uncertainty of ±$25/kWh in the battery pack price in 2030.

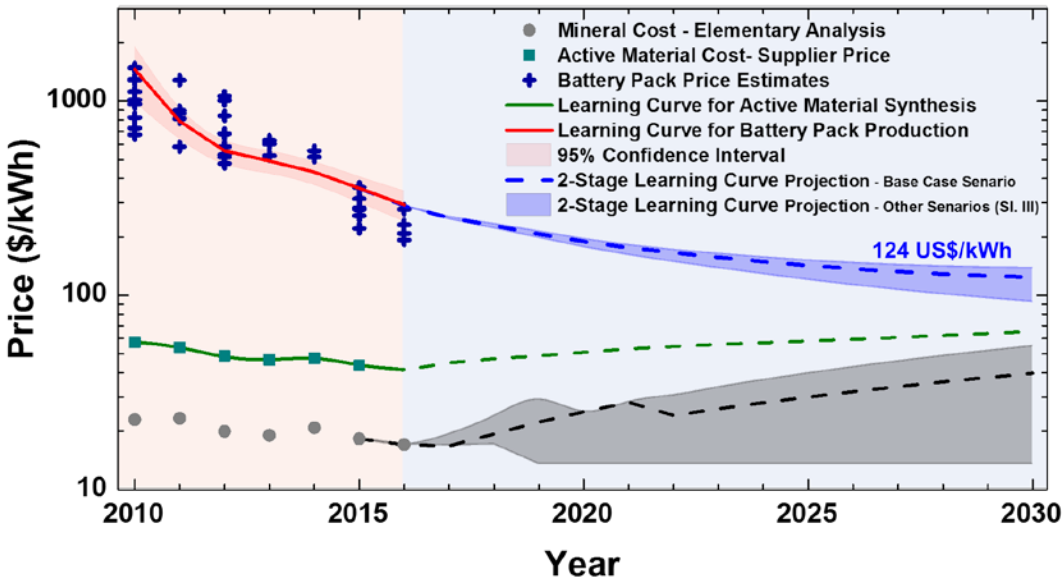

Figure 3.3. Past and projected price trajectory of NMC Li-ion battery pack from our 2-stage learning curve model. Base case scenario is shown in blue dash line, which approaches $124/kWh in 2030, while the light-blue shaded region represents the price range resulted from different projections of elemental costs (shown in grey shaded region). The lower bound and the upper bound of the light-blue shaded region are described as scenario 1 and scenario 2 in Appendix A. III-4.

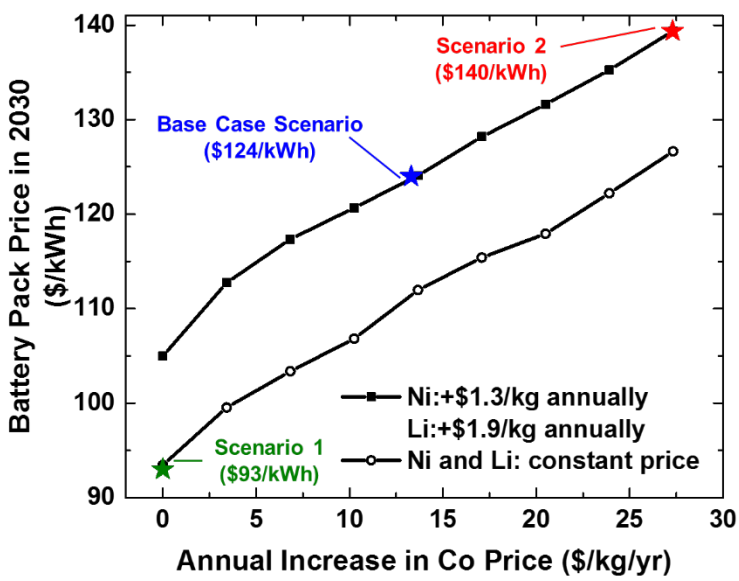

Figure 3.4. The effect of cobalt price fluctuations on predicted battery pack price in 2030. The base case scenario assumes that the price of cobalt will increase moderately by

$13.3/kg per year after 2016; Scenario 1 infers that cobalt price keeps constant after 2016 while Scenario 2 supposes that cobalt price will annually increase by $27.3/kg.

3.3.3 Comparison with Existing Models

Plugging in the global EV production volumes implied by the aggressive EV targets set by China and other countries, the published "learning curve-based" models for EV battery pack price predict that battery pack price would fall asymptotically towards zero, falling below $100/kWh before or around 2030. Figure 3.5 plots the base case scenario of our 2-stage learning analysis (blue line) which accounts for the fact that mineral costs set a floor on the price, in comparison with projections made by previous publications (circles) as well as the price projections by existing "learning curve-based" models (dashed lines) using the price data tabulated in Table A1 and capacity volume presented in Figure 3.2. The conventional learning curve, also described in Appendix A.III.I, predicts a $77/kWh battery pack price in 2030, which is 38% lower than our base case scenario. Nykvist and Nilsson [55] estimated a 8% annual price reduction probable in the future, which implies that battery pack prices would be $102/kWh in 2030 and $94/kWh in 2031. Schmidt et al. [58] predicted battery price will be around $150/kWh when the cumulative installed capacity reaches 1 TWh with no timeline specified. With our assumption of China's EV market serving as a major driving force, the global cumulative production of 1 TWh would be achieved by 2025, and that year our 2-stage learning curve model predicts a price of $143/kWh, a value consistent with that of Schmidt et al. However, if starting from $150/kWh in 2025, the experience curve model presented by Schmidt et al. would predict battery prices to drop to $106/kWh in 2030 with our production volume projection. Kittner et al. [59] estimated much lower EV battery pack price in 2015 and forecasted the price would go down to $124/kWh in 2020, just 2 years from now. By applying their two-factor learning curve model to our production volume forecasts, and following their assumption on patent activity, the battery price would fall to $33/kWh in 2030, even below our projection for active materials cost. Berckmans et al. [70] developed a process-based cost model decoupling battery costs into 4 individual learning curves (each going to zero) and predicted NMC battery pack prices of $75/kWh in 2030. Adopting their reported model parameters for 2015 with our projected production volume results in a much lower forecast of $46/kWh in 2030, less than our projected materials cost as well. In Figure 3.5, we also

include the projection from Bloomberg New Energy Finance (BNEF) that LIB pack prices would fall to $73/kWh in 2030 [71].

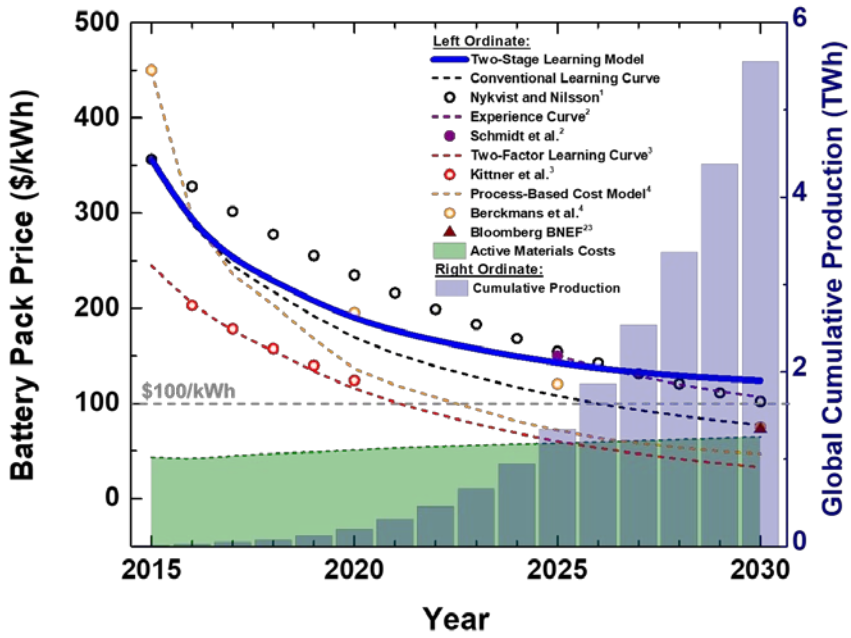

Figure 3.5. Comparison of battery pack price projections among various existing models. Blue line represents the projection from two-stage learning curve model presented in this study (base case scenario); black dash line is the conventional learning curve which is widely applied in previous studies; red and orange dash lines come from applying two-factor learning curve model proposed by Kittner et al. and process-based cost model developed by Berckmans et al. respectively to the projected production volume. $100/kWh is considered the point where EV can compete with ICEV without subsidy. Active materials cost (base case scenario) is also shown in the figure (shaded green region) to emphasize its growing contribution to battery pack price. Our analysis suggests NMC battery pack prices are unlikely to drop as low as $100/kWh, disagreeing with models which ignore material costs.

According to our 2-stage learning curve model, the battery price reduction will significantly slow down around 2025-30. This is due to the growing contribution of active material costs. The projected battery pack price breakdowns over time in the base case scenario are shown in Figure 3.6, these emphasize the significant role that the active materials cost plays. The active

materials cost corresponded to only 12% of the total battery price in 2015 (Fig 3.6(a)), making the projections from our model and the previous “learning curve-based” models close to each other in the short term. However, as active materials contribute more (about half of battery pack price in 2030 in our base case), the projected trajectories deviate as our model recognizes the practical limits on cost reductions missed in the models published previously. By comparing Figure 3.6(b) and Figure 3.6(c), NMC-based LIB essential elements (cobalt, nickel and lithium) and material synthesis cost are increasingly important in battery pack price contribution toward the future. In our base case scenario, total mineral costs and active materials synthesis costs comprise up to 32% and 21% of total battery pack price in 2030, starting from 5% and 7% in 2015, respectively. The former is driven by the increasing mineral prices, while material synthesis, a well-established technology, has a much lower learning rate of 3.5% when compared to that of EV battery pack production. The summation of these two costs determines a price floor of active materials costs for NMC-based LIB packs. As shown in Figure 3.5, some of the existing models would predict battery pack prices in 2030 approaching or even below this floor price, which is highly unlikely. These models in prior works omitted considerations of battery market supply-chain structure and price floor governed by the materials cost in battery price projections. This results in an unrealistic underestimation (by up to 73%) of future battery pack price for NMC-based LIBs.

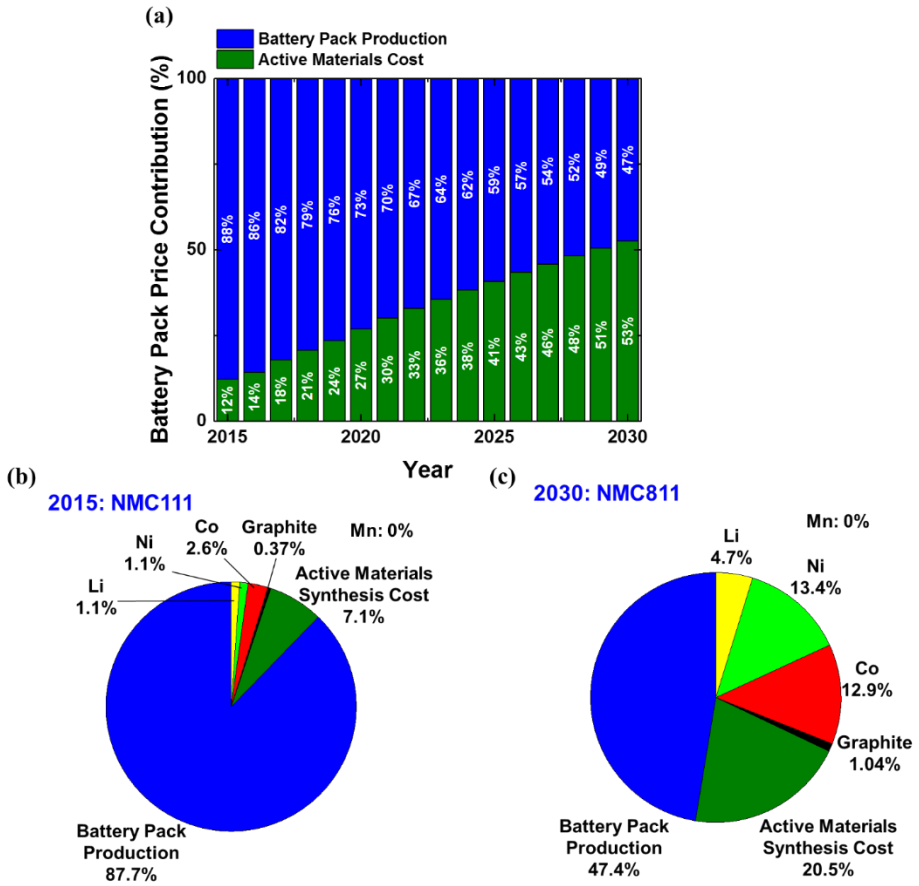

Figure 3.6. Battery pack price breakdowns using two-stage learning curve model (this work) in the base case scenario: (a) 2015-2030 battery pack price contribution over time of battery pack production and active materials cost; (b) and (c) 2015/ 2030 battery pack price breakdowns among elemental prices, active materials synthesis cost and battery pack production when NMC111/ NMC811 provides lowest synthesis cost for battery pack producers, respectively. Note that in both (b) and (c), the contribution of Mn is negligible.

3.3.4 Promising Electrochemical Couples for EV Battery

Our battery pack price projection suggests that the current dominant NMC-based LIBs are unlikely to achieve the price targets required for widespread EV adoption. To achieve these targets, batteries made of less expensive minerals will be required. Therefore, we evaluate current techno-economic performances of emerging battery chemistries proposed for EV application. Adapting the methodology of Li et al. [72], chemical cost of storage and chemical specific energy for 24 representative and promising electrochemical couples for EV applications are calculated and

shown in Figure 3.7. “Chemical”, here, includes cathode-active material, anode-active material, and electrolyte. Closed symbols represent commercially available batteries, while open symbols are chemistries under development. The numerical results in Figure 3.7, calculation methods, and reference sources are shown in Table A3 and in Appendix A.IV. Commercial LIBs, denoted as closed black squares in Figure 3.7, currently dominate the battery market. China’s EV battery producers, who previously focused on less expensive $LiFePO_4$ (LFP) for their cathode active material, are now also shifting towards higher specific energy $LiNi_xMn_yCo_{1-x-y}O_2$ (NMC) [66]. Two main materials approaches are identified to reduce the chemical costs and enhance the energy density of LIBs. Ni-rich NMC provides higher specific capacity by enhancing the ratio of extractable Li, illustrated in Figure A12, and thus higher specific energy. Currently, LIB using NMC811 ($57.2/kWh) incurs a higher chemical cost than that of NMC111 ($53.6/kWh), NMC532 ($56.1/kWh), or NMC622 ($52.8/kWh) due to lower technology maturity, but this is expected to reverse with continued development. Such shift toward Ni-rich NMC is also captured in our 2-stage learning curve as discussed earlier. LIBs with NMC111, NMC532, and NMC622 are already commercial realities, while NMC811 will join them in the near future. On the other hand, Li-rich intercalation compounds such as $0.3Li_2MnO_3$-$0.7LiMn_{0.5}Ni_{0.5}O_2$ (LRMO-LNMO) enhance the specific capacity by increasing the number of Li per transition metal atom. Another potential pathway receiving significant attention is the lithium metal battery, which replaces a graphite anode with Li metal foil (assuming 50% Li utilization here). Other widely recognized candidates for EVs including Na-ion, multivalent-based, and Li-sulfur batteries are also included in Figure 3.7. Most notably, the Li-S battery, utilizing a conversion cathode capable of storing multiple electrons per host atom, can provide >1,500 Wh/kg_{c+e} at a very low chemical cost of $14/kWh, but currently suffers severe capacity fading. It should be noted that the chemistries presented here are in various stages of maturity, so many of their costs are expected to decrease, while the specific capacities are expected to increase as exemplified by the history of $LiCoO_2$, shown in Figure A13.

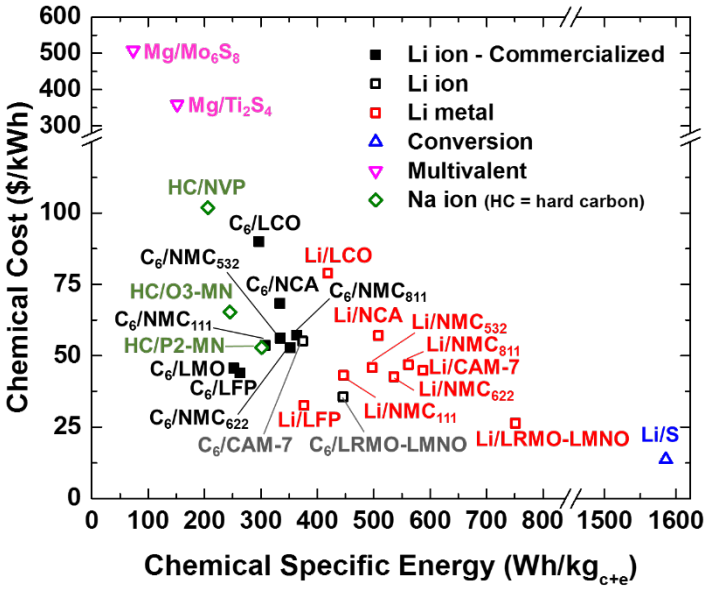

Figure 3.7. Chemical cost of storage ($/kWh) and chemical specific energy (Wh/kg$_{c+e}$) at present for representative electrochemical couples for EV applications, categorized into 6 groups. "Chemical" is defined to be made of cathode-active materials, anode-active materials, and electrolytes in typical combinations. Solid symbols represent commercialized chemistries.

3.4 Conclusions

This chapter tackles the limits of the conventional learning curve and upgrades it by incorporating floor costs set by materials into our 2-stage learning curve model. Figure 3.5 points out that existing models based on a learning curve without consideration of the floor set by materials costs predict an unrealistically low lithium-ion battery pack prices <$100/kWh, suggesting that EV will soon become economically competitive with conventional vehicles. On the other hand, our 2-stage learning curve model, taking into account supply chain structure and materials costs, shows that continued maturation of the existing NMC-based lithium-ion battery technology platform alone is unlikely to reach the $100/kWh price target. Our results show that omitting the materials costs of batteries could lead to an incorrect assessment of whether EV incentives should be extended and how soon the transition to e-mobility will occur.

While NMC battery prices are dropping rapidly now, this process will slow in the medium-term (~10 years) as materials will make up an ever increasing fraction of the total battery price.

Out to and beyond 2030, it is improbable that EVs using lithium-ion NMC batteries will dominate the world vehicle market unless they are supported by significant government interventions such as high fuel taxes, subsidies, or mandates. Instead, accelerating battery chemistry innovations and stabilizing raw materials supply, amongst other actions, will be necessary before widespread electrification of transportation becomes attractive in most markets without EV-related financial incentives or high gasoline taxes. Our base case scenario shows that 2030 global cobalt demand from EVs batteries (NMC811) will reach approximately 80% of the world's total 2016 cobalt mine production [21], which suggests that automakers may need to move to different battery chemistries even less reliant on cobalt to avoid raw materials shortages and price spikes. A report given by Vehicle Technologies Office, DOE (Ref. 301) and Figure 3.7 in this chapter highlight some of the potential alternative battery chemistries, such as lithium-metal, lithium-sulfur, magnesium-ion batteries, and so on, that could further lower battery pack prices for EV applications.

Chapter 4. The dual-credit policy: Implications for private motorization rate and battery market

Abstract

China has recently enacted the dual-credit mandate to replace the existing subsidies as a continued effort to electrify its ground transportation sector. This chapter quantifies the impacts of such policy transition on private motorization rate and battery market. Throughout the next decade, affordability remains the determinant for vehicle purchases; forcing broader adoption of pricier battery-powered cars without subsidies will inevitably diminish the market growth. Under the mandate, China's electric vehicle sales will continue to grow through 2030 despite the temporary car market contraction. Cumulative private electric vehicle sales are projected to reach 66 million by 2030 (with 37% sales market share); this will drive the battery demand from China's private car sector to expand rapidly and accumulate ~420 GWh (2 million tonnes) of spent lithium-ion batteries. This significant increase in battery demand will exacerbate pressure on the global supply for lithium and cobalt. The cobalt demand from China's private vehicle sector in 2030 alone would be almost half of the total global cobalt production in 2017; up to 16% of this 2030 demand could be satisfied by battery recycling. A recycling-based battery supply chain is needed to alleviate the concerns of supply shortages and to achieve a circular economy.

4.1 Introduction

Being a major and fast-growing economy, China has led world growth in demand for private car ownership over the past decades, surpassing the United States to become the biggest automotive market in 2008 (OICA, 2017). However, on a per capita basis, China's car ownership is still relatively low and just passing a level of ~13% (i.e., 13 cars per 100 people) that the U.S. achieved in 1923, in contrast with ~80% in the U.S. today [16]. In the absence of any constraint or effective countermeasures, private motorized transport will continue to increase as purchasing power further grows.

China's economic boom has promoted the development of its automotive industry and allowed more than 100 million citizens to experience the convenience of personal mobility. However, growing private vehicle travel—primarily powered by internal combustion engines (ICEs) in the modern transportation systems—has caused more pollutant and greenhouse gas emissions, as well as increased China's dependency on oil imports. To reduce these negative externalities, the Chinese government has put forth policies to encourage the adoption of alternative fuels vehicles—plug-in electric vehicles (EVs) in particular; EVs include pure battery vehicles (BEVs) and plug-in hybrid vehicles (PHEVs). The generous subsidies toward the purchases of EVs of the past several years have pumped up sales; about half the world's EVs were sold in China in 2017 [61]. When the subsidy program is removed after 2020, the new dual-credit scheme mandate, enacted recently, is expected to continue the strong growth in the local EV market [12].

From now to 2030, private vehicle sales volume in China is mostly controlled by affordability—per-capita income divided by car price [73], and thus mandating wider adoption of cleaner but more expensive EVs will inevitably shrink the car market in the absence of subsidies. Moreover, the new mandate will force increased battery-powered vehicle sales, correspondingly leading to a growing demand for lithium-ion batteries (LIBs) as well. The increased significance of LIBs—largely driven by China's strong EV demand—is believed to pose several challenges throughout the world in the upcoming decade:

(1) Global supply shortages of critical elements, especially cobalt, lithium, and perhaps also nickel [74,75]. Disruptions in the supply chain of raw materials may cause materials cost to surge and thus, diminish the benefits from learning effects in battery price reductions. This already occurred in late 2018 when the price of cobalt surged to more than US$90,000/ton [76], more than

4 times the price 15 months earlier due in part to increasing demand and in part to political instability in the largest cobalt producer—Democratic Republic of Congo (DRC). Although the cobalt price has since dropped, the worries of supply shortages and raw materials price volatility still remain.

(2) Potential environmental and health risks caused by the improper disposal of spent LIBs (Heelan, et al. 2016). Most of the LIBs produced in the past decade have been for use in portable electronics, and few of them are recycled—the vast majority of batteries are discarded along with the devices that contain them. The battery-recycling rate in Australia, for example, is just 2% (King, Boxall and Bhatt 2018). Over the next three decades, the automotive sector is expected to be the fastest-growing source of spent LIBs, mainly due to the movement toward vehicle electrification. Since LIBs contain toxic substances, environmental concerns arise if large volumes of spent LIBs go to landfills. In landfills, LIBs may catch fire and lithium can leach into groundwater, creating a new source of hazardous waste. To help alleviate these concerns, recycling spent LIBs is being considered as a promising approach [77]. However, the battery recycling industry lags behind the continuing LIB development and uses by the automotive industry.

The vehicle market in China is already changing in response to rising incomes, emerging battery technologies, and EV policies. Significant impacts are anticipated during the transition to electrification, and this chapter aims to quantify some policy implications for the private passenger vehicle (also called private car in this study for brevity) market and the EV-driven battery market. With a focus on China—the largest market for both EVs and ICEVs in the foreseeable future—we first explore how the car price and the private motorization rate will change when vehicle emission standards get more stringent and as more expensive EVs penetrate the auto market. We then project the annual private EV sales and the corresponding battery raw material demand, examining the concerns of global supply shortages for battery minerals. We also estimate the potential market size of spent batteries when installed EV batteries reach their retirement age throughout the next decade. We conclude with key findings and implications for policymakers. The time horizon for this chapter is between 2020 and 2030; during this time period, Nickel-Manganese-Cobalt (NMC) Li-ion batteries are expected to dominate the passenger vehicle market.

4.2. China Private Car Ownership and Sales Model

As shown in Chapter 2, we have built a national-level fleet model projecting China's private car market based on the evolution of car affordability index (***A***), defined in Equation (1) [73].

$$A_i = x_i / p_i \tag{4.1}$$

where x_i is the per-capita disposable income in year *i* and p_i is the car price index in year *i*. Car price index was defined to be the average new car price in year *i* relative to that in year 2003 (i.e., $p_{2003} = 1$). Driven by excess capacity and price competition, the car price in China decreased rapidly since 2003 (approximately 50%), which is similar to the price trend happened in the early motorization stage (from 1913 to 1930) in the U.S. [16]. The fleet model showed that the number of vehicles in China will continue to be fairly sensitive to affordability from now to about 2030: 10% decrease in the car price index or 10% increase in the disposable income would increase the car ownership level by 5% [73]. However, Chapter 2 did not account for China's rapidly evolving EV policies, which will lead to more expensive battery-powered vehicles replacing ICEVs in the sales mix after 2020, and thus, increase the average car price. Hence, the car price index and the projected car sales in China require reevaluation in the light of the new mandate.

To project the future average new car price index, we need to determine 1) the car sales market share by different types of vehicle technologies and 2) the relative price of EV to ICEV. The governing equation is shown in Equation (2).

$$p_i = p_{ICEV,i} \times \left(MS_{ICEV,i} \times 1 + MS_{PHEV,i} \times \frac{p_{PHEV,i}}{p_{ICEV,i}} + MS_{BEV,i} \times \frac{p_{BEV,i}}{p_{ICEV,i}} \right) / \, 100\% \tag{4.2}$$

p_i is the average new car price index in year *i* (*i* starts from year 2020 to 2030); $p_{v,i}$ is the price index of vehicle type *v* in year *i* (*v* = *ICEV*, *PHEV*, and *BEV*); $MS_{v,i}$ is the sales market share (%) of vehicle type *v* in year *i*; $\frac{P_{PEV,i}}{P_{ICEV,i}}$ is the ratio of EV price to ICEV price in year *i* (*EV* = *PHEV* and *BEV*). The EV market share projection is discussed in Chapter 4.2.1 and the methods for estimating the relative price of EV to ICEV are detailed in Chapter 4.2.2; the resulting car price indexes of different vehicle types are presented in Table 4.1.

4.2.1 EV Market Share

The EV market penetration projection is quite uncertain since it is still an emerging technology and highly affected by evolving government policies. Based on the historical EV sales market share [2], the government's new energy vehicle technology roadmap (Li, 2016), and the new energy vehicle industry development plan [79], we simulate China's private EV adoption rate using a Gompertz function. We estimate that EVs could account for 21% and 37%[1] of the total private passenger vehicle market share in 2025 and 2030, respectively. The fitted curve, shown as the black line in Figure 4.1, is taken as the EV market penetration in this study. Moreover, since the government policies are more selective to encourage BEVs [8], we further assume that the ratio of PHEVs to BEVs sold in China continues to stay constant at the 2018 level—about 3/10 [2]. Figure 4.1 shows the resulting market shares for the different types of new vehicle sales between 2020 and 2030. Sensitivity analysis is performed to address the uncertainty in these EV penetration assumptions (Appendix B).

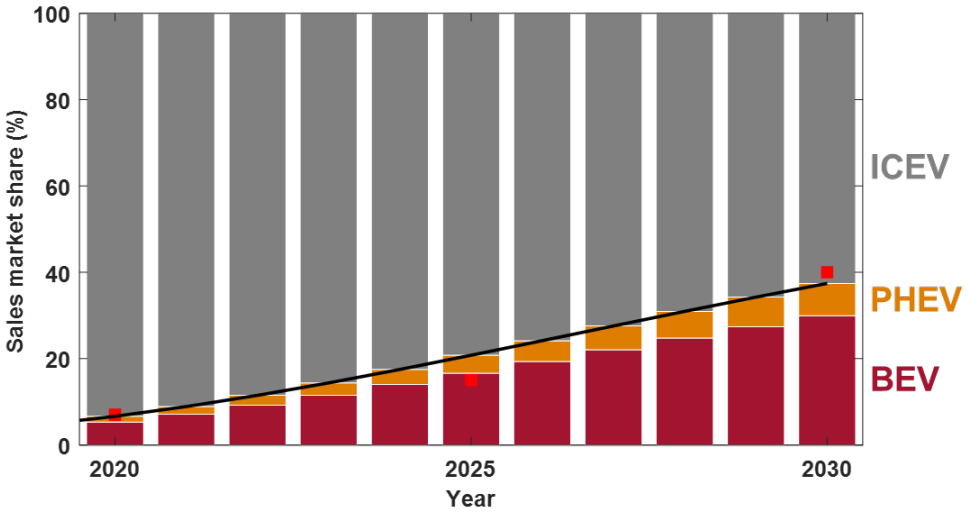

Figure 4.1. Sales market share of ICEV, PHEV, and BEV in China assumed in this study; the government targets are indicated in red square and the fitted curve for EV market penetration is presented in black line.

[1] Our projected value of 2030 EV sales market share (37%) is similar to Liang et al.'s estimation (38%) [80].

4.2.2 Relative Price of EV to ICEV

Reference Vehicle Models

Car price analysis is based on the average of the best-selling 5-seat compact vehicle models in 2017 in China. Key parameters for the reference ICEV, PHEV, and BEV are described here[2], while the detailed vehicle specifications of the selected vehicles are listed in Chapter 5.

- ICEV: a gasoline-powered car with a curb weight of 1,280 kg, equipped with a 1.5 L and 85 kW engine. Its on-road fuel consumption is 7.6 L/100 km and the driving range is 685 km.
- PHEV: a hybrid electric car with a curb weight of 1,623 kg, equipped with a 1.5 L and 78 kW engine and a 11.9 kWh NMC Li-ion battery. It provides 64 km of all-electric range and additional 615 km of gasoline-powered range.
- BEV: a battery-powered car with a curb weight of 1,619 kg, equipped with a 50.5 kWh NMC Li-ion battery. It has an all-electric range of 352 km.

The prices of the reference ICEV, PHEV, and BEV with the model year 2017 are 136,700, 173,800, and 223,500 Yuan, respectively.

Battery Pack Price Projection

Widespread market penetration of EVs is impeded in part by the high vehicle purchase price, mostly due to high battery price. Battery pack price, a large part of the manufacturer's suggested retail price (MSRP) in a BEV, is expected to drop significantly in the near future as battery production volume increases. As shown in Chapter 3, we proposed that the battery pack price should follow a 2-stage learning curve approaching a price floor dominated by the active materials costs, while the active materials costs themselves approach a price floor determined by the mineral costs. The results indicated a 3.5% learning rate for the materials synthesis stage and a 16.5% learning rate (±4.5%) for the battery production stage [81]. Realizing the practical limits set by materials costs on battery price reductions, the model suggested that the continued maturation of the existing NMC-based lithium-ion batteries (LIBs) is unlikely to get as low as $100/kWh (~ 630 Yuan/kWh assuming the exchange rate of USD/Yuan is 6.32) by 2030. Battery pack price of $100/kWh is widely considered as the level at which BEVs become economically competitive

[2] Reference vehicle specifications are the averages over the best-selling vehicle models.

with ICEVs in the absence of incentives [52]. Figure 4.2 shows the declining trajectories of EV battery pack prices used in this study based on the 2-stage learning curve model results. PHEV battery pack costs are assumed to be $65/kWh higher than BEV pack costs in 2015 ($356/kWh) due to their higher power density [82], and have the same learning rate as BEV batteries. We further assume that the battery prices in year *i* determine the powertrain costs of EVs with model year *i+1*. Sensitivity analysis is performed to address the uncertainty in future battery pack price projection (Appendix B).

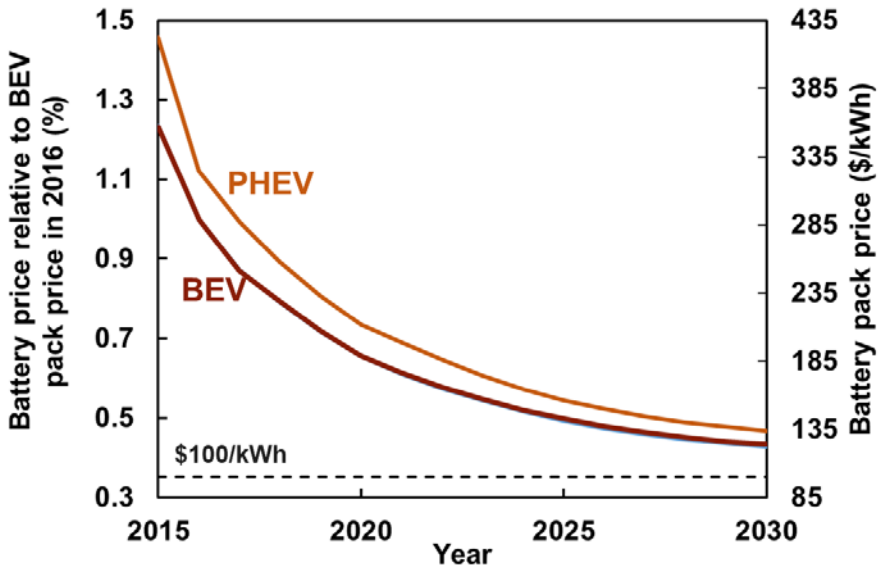

Figure 4.2. Projected NMC Li-ion battery prices for BEV and PHEV relative to 2016 BEV battery pack price (i.e., $289/kWh) from 2-stage learning curve model [81]

Relative Vehicle Price Projection

Future vehicle prices are hard to project. Here we assume that average profit margin (i.e., retail price divided by manufacturing cost) per car stays constant from 2020 to 2030[3]. From the available literature on the underlying technology costs [83,84], we estimate the manufacturing cost structures for the reference vehicles with the model year 2017, as indicated in Figure 4.3. The base car, defined as the car without a propulsion system, is assumed to be the same across different vehicle technologies; all the cost components are normalized by the base car which is thus 1

[3] The profit margins (as a percentage of sales price) of the reference vehicles with the model year 2017 are found to be nearly uniform across different types of vehicle technologies (Hsieh and Green (submitted)).

(shown in the dark blue segment). Direct powertrain cost for ICEV, including combustion engine (CE) parts, ICE auxiliary, transmission, exhaust system, and engine control unit/ sensors, was shown to sum to 20% of the entire compact car cost. The BEV's powertrain excluding the battery pack was estimated to be 16% less expensive than the counterpart ICEV's full powertrain. For a PHEV, the battery pack is smaller but still needs to provide a high level of power, i.e., a higher rated energy-to-rated power ratio, and thus resulting in a higher cost of energy storage (see Figure 2). In addition to an electric motor and high-energy battery, a PHEV is also equipped with a combustion engine (smaller and less costly than that of ICEV), exhaust system, and conventional transmission. After 2020, ICEV cost of production is assumed to stay constant owing to the tighter emissions standards (e.g., standards China 6a and China 6b will be implemented nationwide in 2020 and 2023, respectively [85]) and the increasing maturity of the Chinese automotive industry [86], while EV costs are expected to continue decreasing toward 2030 as the battery pack price drops. The governing equations for the relative EV prices are shown in Equation (4.3) and Equation (4.4) where *BPP* denotes battery pack price and *i* starts from year 2020 (see Table 4.1 for the resulting car price index).

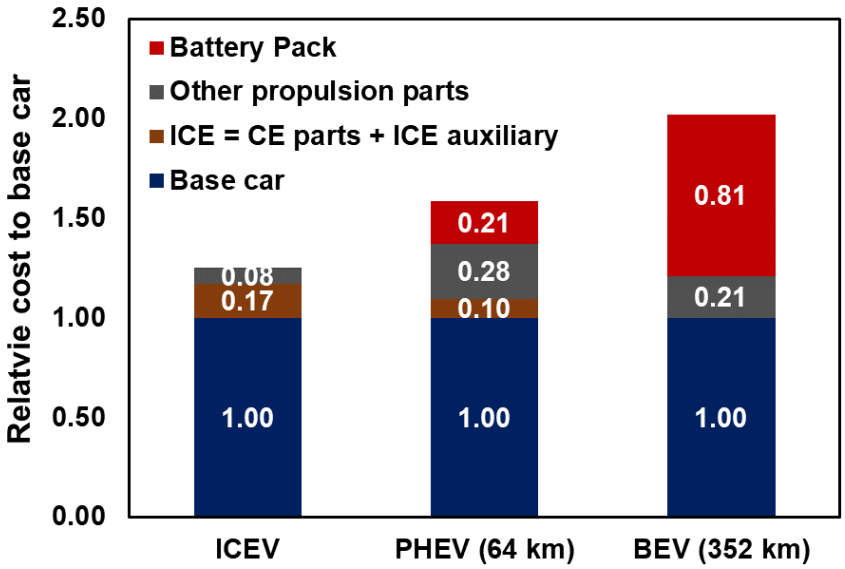

Figure 4.3. Breakdown of the relative manufacturing costs compared to the base car (i.e., a car without propulsion system) across ICEV, PHEV, and BEV with the model year 2017

$$p_{PHEV,i}/p_{ICEV,i} = \left(1 + 0.1 + 0.28 + 0.21 \times \frac{BPP_{PHEV,i-1}}{BPP_{PHEV,2016}}\right) \Big/ (1 + 0.17 + 0.08) \tag{4.3}$$

$$p_{BEV,i}/p_{ICEV,i} = \left(1 + 0.21 + 0.81 \times \frac{BPP_{BEV,i-1}}{BPP_{BEV,2016}}\right) \Big/ (1 + 0.17 + 0.08) \tag{4.4}$$

Table 4.1. Projected price indexes of ICEV, PHEV, and BEV in China (p_{2003} = 1)

Year (i)	**ICEV** ($p_{ICEV,i}$)	**PHEV** ($p_{PHEV,i}$)	**BEV** ($p_{BEV,i}$)
2020	0.505[a]	0.621	0.724
2025	0.505	0.604	0.659
2030	0.505	0.598	0.632

[a] Based on the assumption that the ICEV price in China up until 2020 would follow a similar price trend as seen in the U.S. between 1910 and 1930 [73].

4.2.3 Car Price Index Projection

Combining the EV market share (Chapter 4.2.1) and the relative vehicle price (Chapter 4.2.2), we project the average car price index from 2020 to 2030 using Equation (4.2). Figure 4.4 presents both the previous [73] and updated car price index projections; as discussed in Chapter 4.2.2, this chapter updates the car price assumption to reflect the impacts of vehicle electrification and tighter emission standards. Before 2020, we expect that the average new car price would keep dropping but at a slower rate compared to the previous projection, shown in dash line, in which no EV adoption is assumed. After 2020, the car price index is anticipated to start increasing owing to the constant ICEV production costs and the growing market share of more expensive EVs.

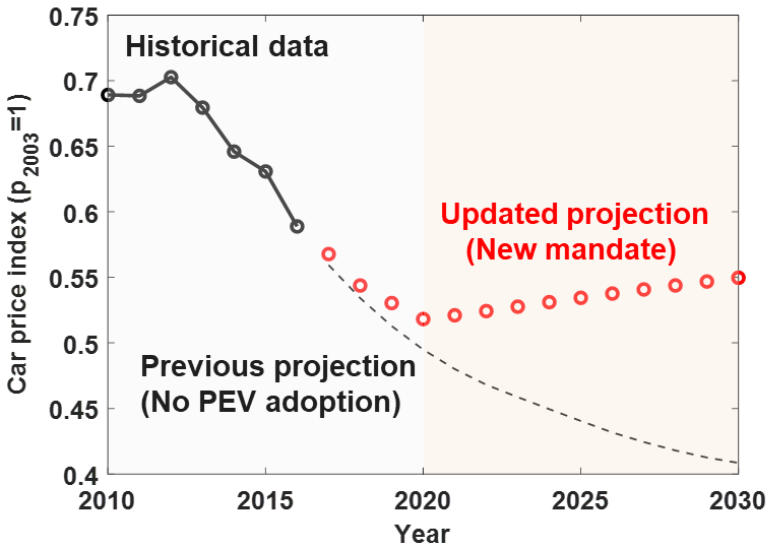

Figure 4.4. Past and projected car price index in China considering the impacts of more EV market penetration; the updated projection is shown in red circles and the previous projection [73] is shown in dashed line. The timeline of interest of this chapter is from 2020 to 2030.

4.2.4 Vehicle Sales Market

Car sales were decomposed into new-growth purchases (associated with increases in car ownership due to rising income) and replacement (for scrapped cars); the split between these two segments determines the maturity level of the auto market: in a mature car market, most car purchases are replacing retired vehicles.

New-growth purchase in year *i* is determined by the growth of car stock between year *i* and year *i-1* as car affordability index (*A*) increases. The update in car price index is described in Chapter 4.2.3; for the other key model input—per-capita disposable income, we assume that it would increase at the same rates as GDP from 2015 to 2030. The assumed compound annual growth rates are 7.00% for 2016-2020, 5.36% for 2021-2025, and 4.60% for 2026-2030 [87]. Both the "NO EV adoption" counterfactual (Chapter 2) and updated car affordability index projections are presented in Figure 4.5.

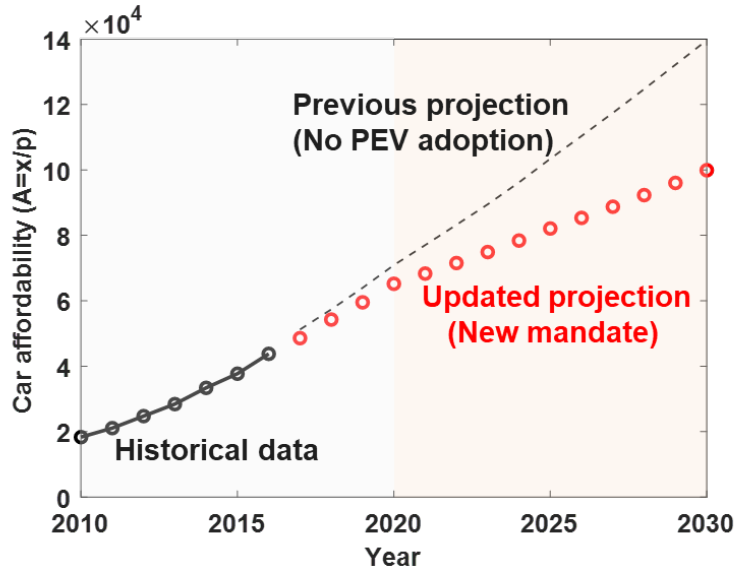

Figure 4.5. Past and projected car affordability index in China; the updated projection is shown in red circles and the "No EV adoption" counterfactual projection (Chapter 2) is shown in dashed line. The timeline of interest of this chapter is from 2020 to 2030.

Replacement purchase, on the other hand, is determined by the private vehicle scrappage pattern. We update the passenger vehicle survival function by fitting a two-parameter logistic model (shown in Equation (4.5)) to the data points between survival ratio of vehicles ($\boldsymbol{SR_V}$) and the vehicle age ($\boldsymbol{y}$) that were recently published [88].

$$SR(y) = 1/[1 + \exp(b \cdot \left(\frac{y}{L_{50}} - 1\right))] \tag{4.5}$$

where $\boldsymbol{L_{50}}$ is the vehicle age when 50% of the vehicles are retired (=11.5 years) and $\boldsymbol{b}$ is the shape factor related to the scrappage intensity (=6.62), i.e. how spread out the scrapping distribution is. Figure 4.6 presents the fitted vehicle survival pattern in China. Due to the limited data, we assume the scrappage patterns of EVs are the same as that of ICEVs; however, care should be taken when drawing parallels between these two different vehicle technologies. The scrappage patterns of the EVs and battery are inherently uncertain—depending on charging behaviors and driving conditions.

4.3. Electric vehicle Battery market analysis

4.3.1 Electric vehicle battery demand

China's private EV market is expected to be one of the fastest-growing sources of lithium-ion battery (LIB) demand over the next decade, mainly due to the strong government support toward vehicle electrification. Battery demand (or installed battery capacity) within the automobile industry comes from two main sources: one is the new EV sales that are driven by the ongoing purchase subsidies and the new EV mandates, and the other one is the battery replacements for existing EVs due to the lifespan mismatch between EVs and EV batteries.

For the evolution of a EV's battery capacity (expressed in terms of kilowatt-hours; kWh), we make several assumptions, as discussed below, in accordance with the new dual-credit rules [89]. It was reported that the average battery installations per PHEV and per BEV in China in 2016 were about 14 kWh and 32 kWh per car, respectively [90]. Since the credits for PHEVs with the electric range greater than or equal to 50 km are unchanged (i.e., the basic credit of PHEV is fixed at 2; the electric range of 50 km can typically be achieved by a PHEV with 10 kWh battery capacity), we expect automakers would have few incentives to increase the battery size, and thus, assume that the average installed capacity per PHEV will stay at a similar level as that in 2016—15 kWh between 2017 and 2030. On the other hand, many BEVs sold in China in the past had a much smaller range compared to the rest of the world, where the average battery capacity per BEV was about 45 kWh in 2016. However, China's recent subsidy programs and the new dual-credit scheme rewards long-range BEV models [12]. Thus, we expect the average installed capacity per BEV to keep increasing toward the future. Based on the rules, the maximum basic credit of BEV is 5, corresponding to the electric range of greater than or equal to 350 km. Moreover, from the fuel economy performance data of various BEV models [91], we determine that the driving range of 350 km can be achieved by a 45 kWh battery. So we assume that the battery capacity in BEVs in China would linearly increase from 32 kWh in 2016 to 45 kWh in 2020. After 2020, we assume the battery capacity per BEV will further linearly increase to 75 kWh by 2030 to satisfy the demands for larger vehicles and longer driving ranges [92]. It is noted that our calculation considers the ongoing shift from less expensive $LiFePO_4$ (LFP) to higher specific energy NMC in China. NMC-based LIB contributed to 45%, 58%, and 74% of total China's new private EV battery installation in 2015, 2016, and 2017, respectively [90,93]. Further, we assume that Li-ion NMC

battery would account for 80% in 2018, 90% in 2019, and then eventually capture the whole battery market of new private EV sales after 2020, until 2030.

In addition to the battery demand from annual new EV sales, there is an additional demand for LIBs from battery replacement owing to the lifespan mismatch between EV and EV battery. We simulate the scrappage patterns of EV battery ($\boldsymbol{SR_B}$) using Equation (4.5), assuming that the median lifetime of EV battery is 8 years (i.e., $L_{50} = 8$), which is a standard battery lifetime warranty offered by electric car manufacturers, and the scrappage intensity is same as the vehicle (i.e., b = 6.62). Figure 4.6(a) shows the corresponding survival ratio functions of both vehicle and EV battery in China's private car sector applied in this study. From the two different scrappage patterns, we derive the probability that battery replacement occurs before the vehicle is retired[4], as presented in Equation (4.6)[5]. Figure 4.6(b) depicts the obtained probability for battery replacement demand; note that the probability distribution does not sum to 1, which is due to the fact that not everyone needs to replace the battery before scrapping the car.

$$P_i(BR, VS) = P_{BR|VS,i}(BR|VS)SR_V(i) = [\big(1 - SR_B(i)\big) - \big(1 - SR_B(i-1)\big)] \times SR_V(i) \quad (6)$$

where

$P_{BR|VS,i}$ = Probability that battery replacement (***BR***) occurs at year *i* given that the vehicle survives (***VS***) until year *i*

$SR_V(i)$ = Probability that the vehicle survives until year *i*

$P_i(BR, VS)$ = Probability that battery replacement occurs at year *i* <u>and</u> the vehicle survives (***VS***) until year *i*

[4] Here we are only interested in the case where battery replacement occurs before vehicle is scrapped; we ignore the probability that battery is replaced twice before the vehicle is retired.

[5] Assuming battery replacement (that occurs first) and the vehicle survival are independent, we can derive $P_{BR|VS,i}(BR|VS)SR_V(i) = P_{BR,i}(BR)SR_V(i)$.

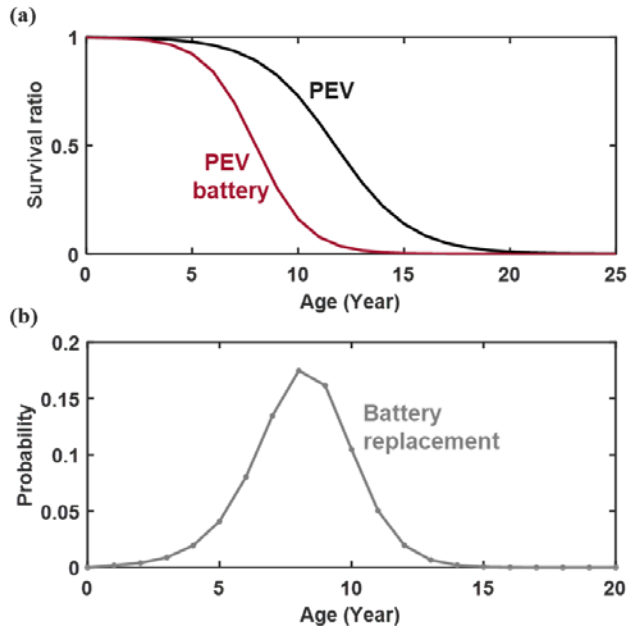

Figure 4.6. (a) Survival ratio functions of plug-in electric vehicle (EV) and EV battery in China; (b) the derived probability of battery replacement occurring due to the lifespan mismatch between EV and EV battery.

4.3.2 Spent electric vehicle battery

If China meets its government's vehicle electrification targets, the resulting EV boom will lead to a considerable increase in the volume of spent batteries when EVs and EV batteries reach their retirement age. We calculate the volume of spent battery (***SpentB***) in year *i* coming from vehicle retirement (***VR***) using Equation (4.7) and coming from battery replacement (***BR***) using Equation (4.8); the sum of these two segments is the total retired EV batteries in year *i* (Equation (4.9)). $\boldsymbol{r_{NMC}}$ is the market share of Li-ion NMC battery in the private EV battery market; as discussed previously, $\boldsymbol{r_{NMC}}$ is assumed to be 1 for vehicles sold after 2020.

$$SpentB_{i,VR} = \sum_{j=1}^{i}(r_{NMC,i-j} \times S_{PEV,i-j} \times Bcap_{PEV,i-j})(SR_V(j-1) - SR_V(j)) \quad (4.7)$$

$$SpentB_{i,BR} = \sum_{j=1}^{i}(r_{NMC,i-j} \times S_{PEV,i-j} \times Bcap_{PEV,i-j})P_j(BR, VS) \quad (4.8)$$

$$SpentB_i = SpentB_{i,VR} + SpentB_{i,BR} \quad (4.9)$$

where *i* starts from year 2016 (*i* = 1 is 2016); $S_{PEV,i-j}$ is the total EV sales in year $i-j$ (starting from year 2015); $Bcap_{PEV,i-j}$ is the average battery capacity per EV sold in year $i-j$; SR_V is the

survival rate of vehicles (Equation (4.3) and Figure 4.6(a)); $P_j(BR, VS)$ is the probability that battery replacement occurs at year *j* before the vehicle is retired (Equation (4.6) and Figure 4.6(b)).

4.4. Results and discussion

4.4.1 Changes in China's Private Car Market

Impacts of promoting clean battery-powered vehicles on China's national private car market are quantified and shown in Figure 4.7 (see Figure 4.4 and Figure 4.5 for the corresponding car price index and car affordability projections). Since car ownership level in China is far behind well-motorized countries, a key uncertainty in the projections is to estimate the eventual probability of owning a car when people have high purchasing power, which was investigated in our previous study [73]. In Figure 4.7, we only show the mean values of the projection for illustrative purposes; the systematic uncertainty will mostly cancel out when estimating the difference between the scenario with the new mandates and the scenario without significant EV adoption.

We find that rising car price resulting from the deployment of more sustainable (but more expensive) mobility would significantly diminish the domestic demand growth for private motorization. Private car sales are expected to be reduced by an average of 30% (~ 5.9 million cars) per year from 2021-2030, resulting in a difference in China's private car stock of 18% (~ 69.3 million cars) by 2030 compared to the counterfactual "no EV adoption" case. This observation is in line with the fleet model's sensitivity results [73], showing that car ownership is quite sensitive to car price in near and mid-term future when the car market is still developing. As depicted in Figure 4.7, the private vehicle market will temporarily shrink in 2021 due to the removal of EV subsides. However, the growing economy and purchasing power will continue to drive up the demand for private car ownership; from the end of 2021 to 2030, the private car sales are still expected to grow with a compound annual rate of 5%, and the number of car sales would exceed that of 2020 as early as 2025. Table 4.2 summarizes the expected private car ownership (i.e., cars per 100 people), car stock, car sales, and replacement purchases share (as a percentage of total car sales), together with the modeled standard deviations, by our updated model. It is noted that while the current car sales in China are mainly driven by new-growth purchases, replacement purchases will dominate the sales market starting about 2021 (i.e., the share of replacement purchases becomes greater than 50%), as the Chinese car market matures; this feature of car market matureness is found to occur four years earlier than what we expected in our previous study that

did not consider the evolving EV policies. However, first-time car buyers will still make up about 25% of car purchases in China in 2030, so the market size will still have some sensitivity to affordability.

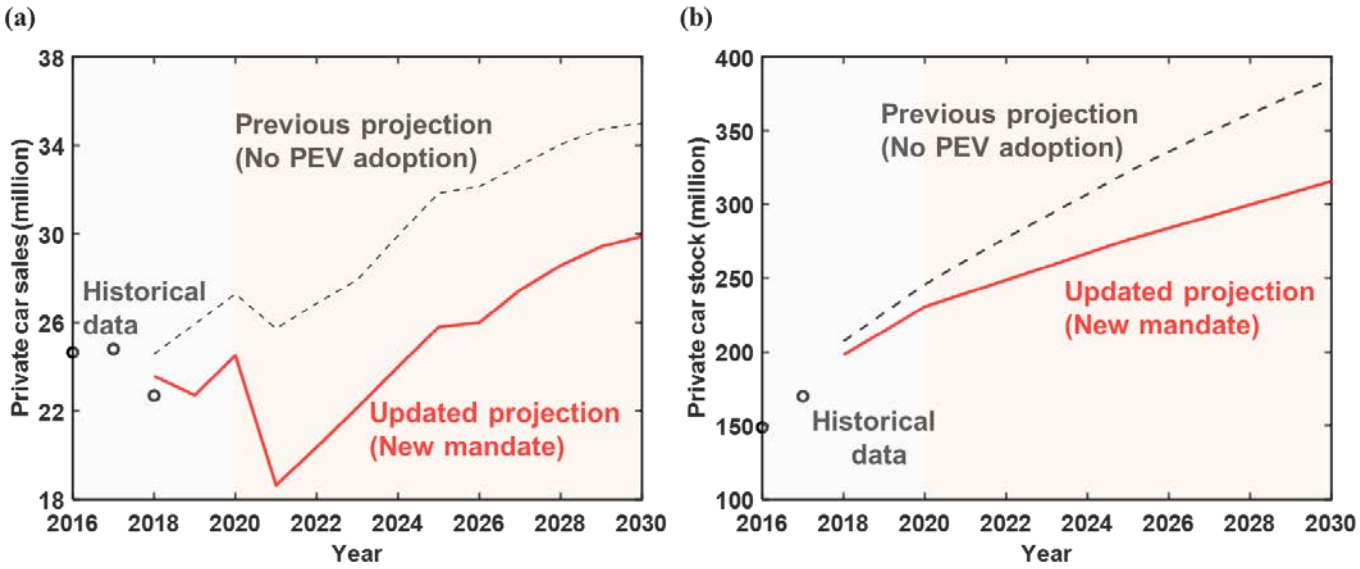

Figure 4.7. Comparisons of projected national (a) private car sales and (b) private car stock in China between no EVs adoption and with new EV mandate scenarios

Table 4.2. Private vehicle stock and sales projections in China (in the form of expected value ± standard deviation) from the updated model considering the new EV mandate

Year	Car ownership (%)	Car stock (million)	Car sales (million)	Replacement purchase share (%)
2020	16.5 ± 3.4	230.7 ± 48.2	24.5 ± 4.5	33.9 ± 6.1
2025	19.5 ± 4.3	276.1 ± 61.2	25.8 ± 3.0	65.0 ± 6.4
2030	22.3 ± 5.2	315.7 ± 73.4	29.9 ± 4.7	74.1 ± 4.4

4.4.2 Private Plug-in Electric Vehicle Market

Given the projected annual private car sales (Figure 4.7(a)) and EV market penetration (Figure 4.1), we derive the yearly private EV sales ($S_{EV,j}$) in China. As shown in Figure 4.8, the new mandate is expected to keep the growth momentum in local EV market, compensating for the removal of subsidies. EV sales will continue to grow throughout 2030 even though the whole private car market would shrink temporarily for a few years in 2021. These government supports are expected to boost the annual EV sales to reach 5 million in 2025 and 11 million in 2030, bringing the total cumulative private EVs sold to nearly 66 million units in China by 2030.

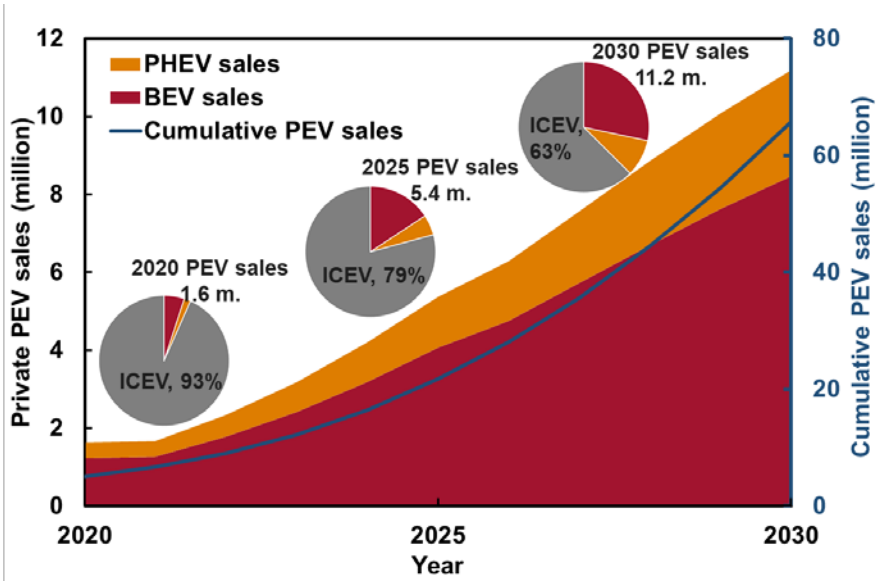

Figure 4.8. Projected annual (left ordinate) and cumulative (right ordinate) private EV sales between 2020 and 2030

4.4.3 Battery Market in Private Vehicle Sector

The shift from ICEVs to EVs will result in large demand growth for lithium-ion batteries (LIBs), raising pressure on the availability of relevant resources. In this section, we quantify the battery demand driven by private vehicle electrification and the expected spent battery market when these batteries hit retirement age.

Battery Demand

From now out to 2030, NMC-based LIBs are expected to dominate the private EV battery market, and consequently, our evaluation of battery (demand/recycling) market size focuses on the NMC platform. The bars in Figure 4.9 indicate the projected annual installed capacity, assuming BEVs would hold increasing kWh of energy (thus achieving longer ranges per charge) toward 2030 (see Chapter 4.3.1 for more detailed assumptions). The lifespan mismatch between EV and EV battery, as shown in Figure 4.6, leads to the additional demands for LIBs, i.e., battery replacement, on top of the volume from annual new EV sales. The annual battery installations in China's private car sector is expected to expand at a rapid compound annual growth rate of 30.2% in the ten-year period, from 62 GWh in 2020 to 873 GWh in 2030. This high growth rate comes from three mutually reinforcing factors: growth in EV sale (Figure 4.8), increase in the average installed capacity per BEV, and the expansion in battery replacement demand as EV stock increases. Growing LIBs demand has driven the essential mineral prices (including lithium, nickel, and cobalt) up over the past three years, fueling fears of a shortage – most notably of lithium and cobalt [94]. Despite a clear trend toward higher nickel loadings to boost the energy densities for more extended range, the EV LIB community will still have to continue using cobalt (though with less cobalt content) for materials stability in the foreseeable future [95]. Based on Figure 4.9, we further compute the corresponding demand (in the unit of tonnes per year) for key battery elements—lithium, nickel, and cobalt, investigating the potential challenges associated with the secure raw materials supply.

We recognize mining capacity will expand in response to the expected growing LIB demand. However, to examine the potential bottlenecks in the supplies of raw materials, we select the 2017 global production volume as a proxy, comparing the projected battery demands for essential metals to their global mining productions in 2017 [96]. These analysis results are illustrated in the black areas in Figure 4.10, which informs stakeholders the magnitude of the required expansion in production. The upper bound of the nickel and lower bounds of lithium and cobalt weights are obtained by assuming all the batteries are NMC811 (high nickel and low cobalt content; the numbers denote the molar ratio of nickel, manganese, and cobalt within the cathode), while the lower bound of nickel and upper bounds of lithium and cobalt weights are derived from the opposite case that all batteries are NMC111. Among the three materials, nickel is used much

more widely in other industries; about 75% of all primary nickel consumption in 2017 went to the stainless steel industry, while the battery industry only accounted for 3.7% [97]. On the other hand, more than 50% of global lithium and cobalt[6] consumption were used in batteries [98–100]. These statistics suggest that even with China's strong shift to EVs, pressure on global nickel supply will be modest, but lithium and cobalt supplies would be largely impacted.

Our analysis (Figure 4.9) offers some consensus, showing that 1) global nickel supply is unlikely to be a limiting factor for wider battery production; 2) both lithium and cobalt production volumes have to be largely expanded. For lithium supply, more resource explorations and mining activities have occurred recently in response to the growing demand for battery applications [101]. The supply concerns of lithium are focusing more on whether the lithium production can be speeded up in the immediate future, rather than the material quantity itself thanks to the supply diversity in terms of geographical distribution and extraction technology [102,103]. Compared to lithium, cobalt is more likely to disrupt large-scale battery production. More than 60% of world cobalt mine production occurs in the politically unstable Democratic Republic of Congo (DRC), meaning that the political situation in that region will have a significant influence on the price and the supply security of cobalt. Figure 4.10 suggests that if new EV purchases in the rest of the world match China, and cobalt mine production does not increase[7], cobalt demand for EVs alone (even if all LIBs are NMC811) could approach and even exceed global cobalt production. Besides expanding the production capacity and lessening the amount of cobalt used in batteries, the potential supply risks arising due to geo-political barriers could be ameliorated with battery recycling.

Spent Battery

Along with the strong movement toward vehicle electrification, a massive volume of spent LIBs will be returned to the Chinese market for recycling. As shown in the red line with right ordinate in Figure 4.8, the expected spent NMC-based LIBs volume, merely from the private EV market, will start from around 0.6 GWh in 2020, increase to 18 GWh in 2025, reach 138 GWh in 2030, and grow by another factor of 3 by 2040. Assuming the specific energy of 200Wh/kg for LIBs

[6] Global demand for cobalt in 2017 was about 104,000 tonnes, and 38% of which was for consumer batteries and 15% of which was for EV battery.

[7] Inspired by the high (but highly fluctuating) cobalt price, global cobalt production has increased by about 20% since 2017 [104].

[105], about 2 million tonnes of spent LIBs will be retired from China's private car sector through 2030.

Spent battery metals as a weight percentage of global mining production in 2017 are shown in the red areas in Figure 4.10. It is clear that recycled supply will not be a sufficient source of battery materials in the time horizon considered in the study because the current battery installations are much smaller than the expected great demand due to the rapid growth of the electric vehicle market. However, LIB recycling might be an inevitable need for automotive-battery manufacturers to satisfy electric vehicle demand. In the near term, cobalt supply from mining should meet the demand for LIBs in EV industry; however, in the long term, besides further reducing the required amount of expensive cobalt, supply from battery recycling will help meet the accelerating cobalt demand driven by widespread EV adoption. Cobalt demand from China's private EV batteries alone would reach at least 46% of the world's 2017 cobalt mine production by 2030; about 16% of that demand could be met from recycling rather than mining[8]. Though lithium is mostly recyclable, the recycled lithium cannot reach battery-grade quality with the available recycling technology on an industrial scale at the moment [107]. Instead of acting as a battery resource, the recycled lithium is currently used for non-automotive purposes like lubricating greases or sold to the construction industry [77,108]; such downgraded purity constrains the contribution of LIB recycling to near-term future lithium availability. Currently, the most widely used commercial battery recycling technology is pyrometallurgical process. With this technology, the transition metals can be recovered effectively—such as cobalt, nickel, iron, and copper, but not lithium and aluminum [109]. However, the recovery of battery-grade lithium carbonate is expected to become commercially achievable in the future. Researchers have recently started developing recycling methods to not only recover valuable elements from spent batteries, but regenerate the spent materials—including lithium—into pristine-state cathodes [110,111].

The large number of spent batteries becoming available suggests that a substantial business opportunity exists for LIBs recycling. Because cathode materials are the most expensive battery component, we investigate the potential market for LIB recycling based on key cathode elements. Assuming that all the spent battery capacity shown in Figure 4.9 is either NMC111 or NMC811, we project that a China industry for recycling batteries from privately owned electric vehicles

[8] The recovering efficiency is assumed to be 92% for cobalt [106].

could process almost 20 billion Yuan worth of metals per year by 2030 (Figure 4.11(a)); the uncertainty is from various NMC compositions, ranging from NMC111 (upper bound with a dash line) to NMC811 (lower bound with a solid line). Assumptions about commodity market prices for this analysis are summarized in the inset of Figure 4.11(a) (lithium and manganese data taken from the USGS mineral commodity summaries report 2018 [96]; nickel and cobalt prices retrieved from the London metal exchange, January 2019 [76]). Figure 4.11(b) and (c) break down the potential market values, derived from two NMC composition trajectories, by essential cathode metals. It is noted that cobalt is currently getting more supply press, but with a shift toward nickel-rich compounds (NMC811), most (>80%) of the mineral values come from nickel and lithium (Figure 4.11(c)). Furthermore, even though lithium only contributes a small fraction of battery weight compared to nickel and cobalt, the recent increase (by more than 60% from 2016 to 2017) in the lithium carbonate price makes lithium one of the most important contributors to the intrinsic value of LIB recycling business. We note that these numbers likely understate the actual business opportunity for battery recycling since our analysis considers only the most expensive cathode materials in their mineral values. But if the spent NMC can be recycled to produce pristine-state cathode materials, as mentioned earlier, the value of the recycling products would far exceed their mineral values. Moreover, other metals used in battery manufacture, such as copper foils used as the current collector for anode and aluminum foil for the cathode, are also valuable for recycling [112]. In addition, it is likely that some of the manufactured assemblies in a battery could be reused, so they have a higher value than the raw materials used to make them. This suggests that landfilling the majority of spent LIBs instead of recycling would not only create environmental problems but also miss a significant economic opportunity.

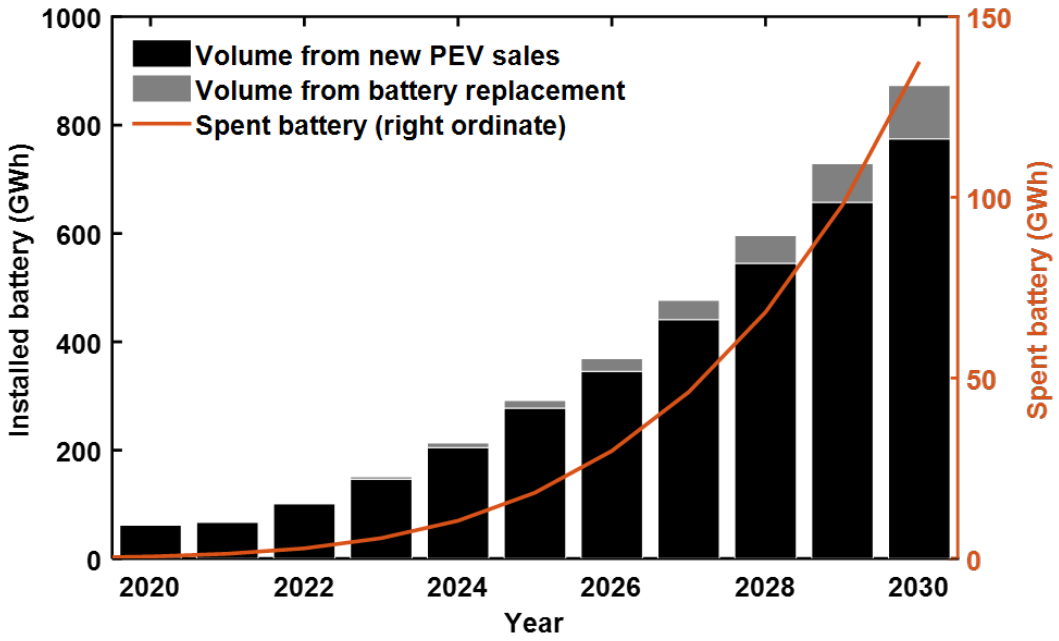

Figure 4.9. Projected annual Li-ion NMC batteries installed capacity (left ordinate) and spent batteries volume (right ordinate) (in terms of GWh) in China's private car sector, 2020-2030

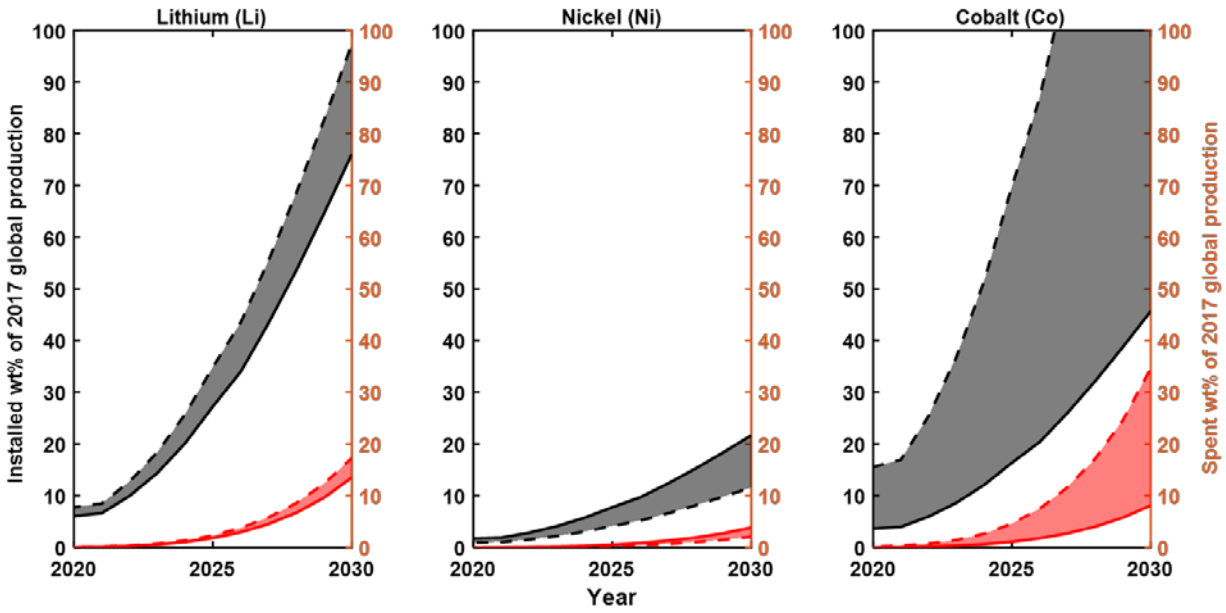

Figure 4.10. Projected annual installed weight (black, left ordinate) and spent batteries weight (red, right ordinate) of lithium, nickel and cobalt in China's private car sector as a

percentage of global mine production in 2017; the uncertainty is from the various NMC compositions, ranging from NMC111 (shown in the dashed lines) to NMC811 (shown in the solid lines).

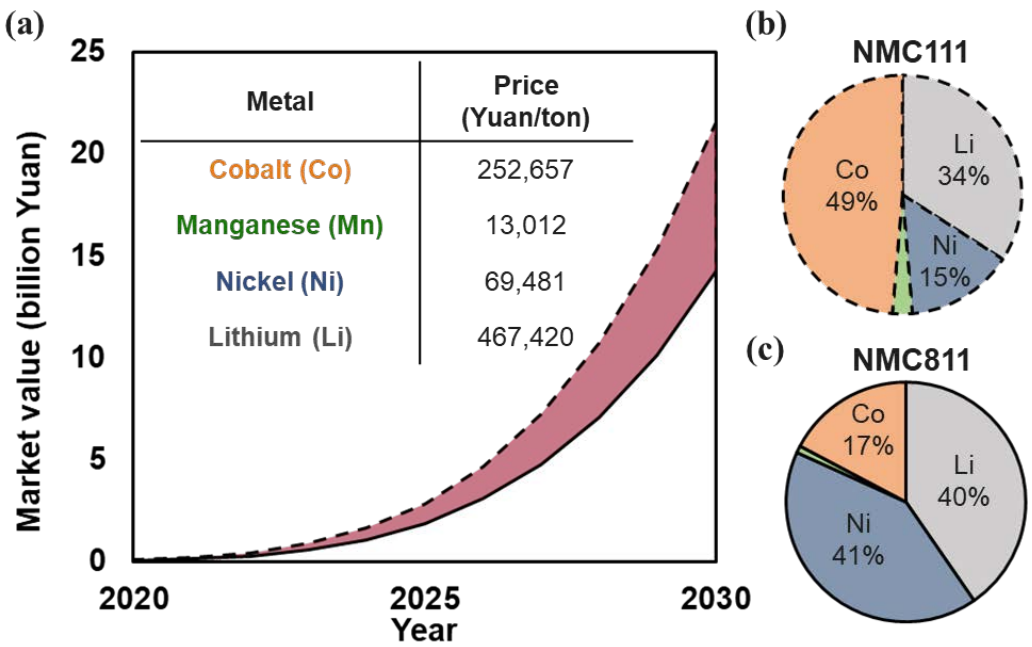

Figure 4.11. (a) The potential market value of battery recycling in China's private car sector considering only the value of the 4 cathode essential elements; the upper bound (dashed line) assumes all spent batteries are NMC111, and the other assumes all spent batteries are NMC811; the assumed metal prices applied in the analysis are tabulated in the inset; (b) and (c) Pie charts break down the values by cathode metals; Co in orange, Mn in green, Ni in blue, and Li in gray.

4.5. Conclusion and policy implications

China is leading the world in local plug-in electric vehicle (EV) deployment, mostly credited to the strong government supports. The recent enactment of the dual-credit system mandate is expected to increase EV adoption in China and correspondingly increase battery production dramatically. Greater production volume will drive the battery costs down owing to improved manufacturing efficiency; however, the ultimate production cost reduction will be constrained by the essential battery materials (lithium, nickel, and cobalt), making it unlikely that the price target

of $100/kWh for widespread EV adoption will be achieved by 2030. Due to this practical limit on battery prices, EVs are expected to remain more costly than the counterpart internal combustion engine vehicles (ICEVs) through 2030.

Over the next decade when car ownership in China is still sensitive to affordability (income divided by car price), forcing broader vehicle electrification while phasing out subsidies will noticeably decrease the growth rate of the Chinese private car market. The average new car price is expected to keep dropping—but at a much slower rate compared to the historical trend—until 2021, and then it would start evolving in the reverse direction as more expensive EVs penetrate the market and emission standards tighten. The rising car price will diminish the consumers' car affordability, resulting in a decline in the stock by 18% (~ 69 million cars) in 2030 compared to the counterfactual "no EV adoption" projections. The results suggest that the private car stock of China would reach nearly 280 million and over 315 million in 2025 and 2030, respectively. Driven by the mandate, the annual private EV sales in China are projected to keep growing and reach over 11 million (cumulatively 66 million units) by 2030 despite the anticipated temporary contraction in the private car market when the new dual-credit rules come into effect. With the analysis of the relative car price of EVs to ICEV as well as the considerations of the evolving EV policies, this study provides up-to-date insights on China's private vehicle market size.

This EV expansion will accumulate around 420 GWh (~ 2 million tonnes) of spent NMC-based LIBs in need of recycling throughout the next decade. The core ingredients in cathode materials are finite and thus valuable, most notably cobalt. The cobalt demand merely from China's private EV sector in 2030 will make up at least 46% of the 2017 annual global cobalt mine production, suggesting that battery recycling may be needed to reduce the risk of supply shortages and mineral price spikes. While cobalt supply is currently more stressed, with newer battery formulations most of the mineral cost is for nickel and lithium. Nickel supply is not likely to be significantly impacted because LIBs only account for a small portion of nickel use. Lithium, on the other hand, should receive greater attention, especially on its recycling technology where high-quality lithium recovery is not yet commercially achievable. If the recycling rate is low, China would not only create a number of environmental problems but also miss a significant economic opportunity. Thus, the policymakers should help integrate the entire industry chain among automakers, battery producers, used-car dealers, and scrap companies in battery recycling systems

to achieve a more sustainable and circular society. With a recycling-based LIBs supply chain established, not only millions of tonnes of batteries will be saved from entering the waste stream and characterized as hazardous, but also the supply pressures on critical materials will be mitigated.

Chapter 5. The dual-credit policy: Implications for total cost of ownership and cost to society

Abstract

China is driving the transition away from internal combustion engine vehicles (ICEVs) to plug-in electric vehicles (EVs) to address its pressing energy security and environmental pollution problems. The recent enactment of the dual-credit scheme mandate will compensate for the phase-out of the subsidy program, while ostensibly shifting the burden of filling in the cost gap between EVs and ICEVs from the government to the automakers (though in practice to car buyers). We estimate that creating an inflection point for EV demand via the mandate will put substantial transition costs on the society—on average on the order of 100 billion Yuan per year from 2021 to 2030, consuming about 0.1% of China's growing GDP each year, an economic cost of achieving the energy security and air pollution benefits. The consumer-centric total cost of ownership (TCO) is investigated using the local data: thanks to the generous subsidies, China's subsidized EVs are in TCO parity with counterpart ICEVs from 2016 to 2020. It is uncertain how the cost gap will be covered when the subsidies are removed. However, automakers are expected to use internal subsidies to lower EV prices and raise ICEV prices as needed to achieve the mandated percentage of sales.

5.1 Introduction

Over the past decades, China's massive economic growth has driven demand for private car ownership, improving mobility but causing more pollutant and greenhouse gas emissions associated with combustion and increasing the country's dependence on imported petroleum. To mitigate these problems, the Chinese government is promoting new energy vehicles via aggressive policies, giving priority to plug-in electric vehicles (EVs); EVs include pure battery vehicles (BEVs) and plug-in hybrid vehicles (PHEVs).

China's central and local governments are currently providing generous subsidies toward the purchases of EVs, boosting national sales to account for nearly half the world's EV market in 2017 [61]. However, paying subsidies is expensive for the government, and thus the authorities have decided to phase out EV subsidies at the end of 2020. Instead, the government will be relying on the dual-credit scheme mandate to achieve its goal of high electrification of transportation by forcing increased battery-powered vehicle production volumes. The dual-credit policy, enacted recently, was shown to be able to pump up the annual EV sales in China to over 2 million units by 2020 if the policy is strictly complied with [12]. The incremental cost of EVs over counterpart internal combustion engine vehicles (ICEVs), which is recognized as one of the major barriers to electromobility, will be imposing significant transition costs on society during the shift from ICEVs to EVs. With a specific focus on China – the largest market for both EVs and ICEVs – this Chapter is offered as a contribution towards assessing the costs to society during the transition towards electric transportation. In this study, societal costs are defined as the "direct" cost incurred to society due to the car's purchase and uses themselves; the external costs caused by the ownership of the car—such as greenhouse gas emissions and air pollutants—are not within the study's scope (but were addressed in De Clerck et al. (2018)).

Since consumer decisions are mainly driven by the private cost (excluding vehicle externality costs), this chapter also evaluates the lifetime private cost to individuals by employing the total cost of ownership (TCO) method. A comprehensive review of the TCO method can be found in Letmathe and Suares (2017). Existing literature has developed a mature TCO analysis framework with a range of region-specific studies, but few research has been done regarding TCO of EVs versus ICEVs in China's context. Hao et al. (2014) estimated the impacts of China's EV subsidy scheme on consumer's TCO, focusing on the subsidy duration from 2010 to 2015. Zhang et al. (2017) applied TCO approach to determine the effectiveness of China's EV financial policy

in 2014. Yet, none of the existing studies systematically related the emerging battery technologies and the evolving EV policies to the temporal variation in TCO. To the best of our knowledge, this Chapter is the first to study the mixed impacts—including decreasing battery pack price, phase-out of EV subsidies, vehicle ownership restriction policy, and the introduction of EV mandates—on consumer's vehicle ownership costs, providing the latest insights on TCO competitiveness of EVs relative to ICEVs in China.

Great impacts are anticipated during the transition to electrification, and this Chapter aims to quantify such policy implications for societal and consumer costs. Profit margins have a big impact on the future TCO of EVs (van Velzen et al., 2019) and thus should be taken into careful consideration. We select the vehicle models that are popular in China and are comparable to each other in terms of vehicle specifications. Some low-volume vehicle models sell at very different prices than the popular models, probably because the automaker is taking a very different profit margin on those models. We cautiously avoid those models having unusual retail prices to reduce the distortion in vehicle price estimates. We compute the transition cost to society due to the price gap between EVs and ICEVs and demonstrate that this is non-negligible and should be considered when researchers quantify the total cost to society associated with vehicle electrification. We also investigate the consumer ownership cost competitiveness of EVs, exploring how it would change in conjunction with the policy evolution. We test the robustness of our projections for the years 2020, 2025 and 2030 using Monte Carlo simulations. The time horizon for this study is between now and 2030; during this time period, lithium-ion nickel-manganese-cobalt (Li-ion NMC) batteries are expected to dominate the EV market.

5.2 Methodology and data

5.2.1 Selected Passenger Vehicle Models

The leading auto market players in China are different from the rest of the world: in 2018, local Chinese brands accounted for 92% of EVs sold [116][9], and the Chevy Bolt, the world's first true mass-market BEV with a range well above 200 miles (322 km) on a single charge, is not currently sold in China. In the past, many EVs sold in China had a much smaller range, but China's recent subsidy programs and the new dual-credit scheme system favor pure battery electric sedans with a more extended range (greater than 250 km) [12]. These government policies have driven the

[9] Even joint venture brands are growing their sales market share, under "Made in China 2025" industrial plan, the government wants local Chinese brands to have an 80% market share of EVs sold in China [117].

ongoing shift from less expensive $LiFePO_4$ (LFP) to higher specific energy NMC in China's private car sector. Therefore, we choose those NMC battery-powered compact cars with a driving range greater than 300 km as our representative BEVs—BJEV EU400, Geely NEV EV450, and Changan Eado EV 300, and the counterpart PHEVs (Trumpchi GA3S PHEV, Geely NEV PHEV, and Changan Eado PHEV) are also equipped with a NMC Li-ion battery as one of their power sources. It is noted that other popular BEV models like BJEV EC series, Zhidou D2, and Chery EQ are not considered here because they are categorized as micro/small vehicles rather than compact cars. BYD Qin EVs are not included in our analysis because they are powered by an LFP battery. For the representative ICEVs, we choose seven of the top 10 best-selling compact gasoline cars that have comparable vehicle characteristics to the selected EVs. We estimate the reference vehicle specifications based on the average of these selected cars with the model year 2017, as presented in Table 5.1.

The reasons why we exclude the comparable ICEVs made by Chinese car brands—BAIC Senova D50, Geely Emgrand, and Changan Eado—from our model selections are because 1) these local car companies are not the best sellers in the ICEV sector; 2) their current price structures are probably distorted: the retail price ratios of the local automakers' EVs to ICEVs are found to be much higher than the manufacturing cost ratios of EVs to ICEVs. The manufacturing cost of a compact BEV with a driving range of 322 km was estimated to be 75% higher than the counterpart ICEV[10]. However, the retail price of BJEV EU400 (BEV) is about 130% more expensive than the counterpart BAIC Senova D50 (ICEV) and the Geely NEV EV450 (BEV) is about 140% more expensive than the counterpart Geely Emgrand (ICEV). These very high retail price ratios of EVs to ICEVs are caused by unusually low ICEV prices. We speculate the Chinese automakers might be offering lower prices for their ICEVs than the market leaders to grab market share. Therefore, to avoid giving any biased estimations, we do not select these local brand ICEVs in the analysis.

[10] Chevy Bolt (BEV)—the world's first true mass-market BEV with a range well above 200 miles (322 km; 60 kWh Li-ion NMC battery) on a single charge—was estimated to be about 75% more costly than the counterpart VW Golf (ICEV) [83].

Table 5.1. Specifications of the reference compact passenger vehicles with the model year 2017; all the numbers are from the average of the selected vehicles.

Vehicle Technology	ICEV	PHEV	BEV
Selected Models	FAW-VW: Golf, Sagitar, Bora; SAIC-VW Lavida; SAIC-GM Buick: Hideo, Verano; GAC-Toyota Camry	Trumpchi GA3S Geely NEV Changan Eado	BJEV EU400 Geely NEV EV450 Changan Eado EV300
MSRP (Yuan)	136,700	173,800	223,500
Fuel Consumption	7.6 L/100 km	Gasoline = 6.0 L/100km Battery = 18.6 kWh/100km	14.4 kWh/100 km
Vehicle Platform	4573*1787*1463 (mm) Curb Weight=1,280 kg	4600*1790*1530 (mm) Curb Weight=1,623 kg	4618*1801*1517 (mm) Curb Weight=1,619 kg
Engine Power	1.5 L, 84 kW Engine	1.5 L, 78 kW Engine + 108 kW Electric Motor	103 kW Electric Motor
Energy Storage	52 L Fuel Tank	37 L Fuel Tank + 11.9 kWh NMC Battery	50.5 kWh NMC Battery
Performance	Range = 685 km Max Speed = 185 km/h	Range = 64 km electric + 615 km gasoline Max Speed=180 km/h	Range = 352 km Max Speed=140 km/h

5.2.2 Total Cost of Ownership (TCO)

The total cost of ownership (***TCO***) refers to the costs incurred during the car ownership period, which entails several different cost categories: vehicle purchase cost, fuel cost, and non-fuel operation and maintenance cost. The TCO per kilometer calculation approach applied in this study is shown in the following formulas; noted that all the upfront costs are amortized across all of the kilometers to get the levelized costs of driving.

$$\boldsymbol{TCO\ per\ km} = \frac{\boldsymbol{PC \times CRF + FC + O\&MC}}{\boldsymbol{VKT}} \tag{5.1}$$

where

$$\boldsymbol{PC = VP + VPT + VRF - FinInc} \tag{5.2a}$$

$$\boldsymbol{FC = \frac{1}{FE} \times FP \times VKT} \tag{5.3}$$

$$\boldsymbol{O\&MC = IC + MC + VUT + BR \times PVF \times CRF - TaxInc} \tag{5.4}$$

$$\boldsymbol{PVF = \frac{1}{(1+r)^n}} \tag{5.5}$$

$$\boldsymbol{CRF = \frac{r(1+r)^N}{[(1+r)^N - 1]}} \tag{5.6}$$

r is the discount rate, ***N*** is the vehicle lifespan, and ***n*** is the battery lifespan; ***PC*** is the vehicle purchase cost incurred at time zero, which is made up of vehicle price (***VP***), vehicle purchase tax (***VPT***), vehicle registration fee (***VRF***), and financial incentives such as purchase subsidies (***FinInc***); ***FC*** is the fuel cost incurred every year, determined by the fuel economy (***FE***; unit of km/L), fuel price (***FP***) and annual vehicle kilometers traveled (***VKT***); ***O&M*** is the annual non-fuel operation & maintenance costs, including insurance cost (***IC***), maintenance cost (***MC***), annual vehicle use tax (***VUT***), battery replacement cost (***BR***) (which is <u>only</u> incurred in year ***n***), and tax incentives (***TaxInc***); ***PVF*** is the present value factor to discount the future battery replacement cost (***BR***) incurred in year ***n*** to time zero; ***CRF*** is the capital recovery factor that is used to distribute the upfront costs (including ***PC*** and the present value of ***BR***) to all the kilometers driven. Vehicle residual value is not considered here for simplicity, and also because the recent studies showed that expected resale value did not feature prominently among the critical factors for purchasing a new passenger car [118].

We build up a China-specific consumer-centric TCO model and analyze the ownership cost competitiveness of EVs by taking the tax/ subsidy scheme in Beijing as representative of China average. We project temporal variations in TCO out to 2030 to examine the economic viability of an unsubsidized EV after 2020 when all the subsidies are scheduled to be phased out. The potential impact of the city-level vehicle ownership restriction policy on TCO is also explored in addition to the financial incentives.

Vehicle Price without VAT

When we estimate the future vehicle price trajectory, we exclude the value-added tax (***VAT***) from the retail price (i.e., MSRP shown in Table 5.1 includes the VAT rate of 17%) so that we can separate price changes caused by production cost reductions from that caused by VAT cuts.

We identify the pre-VAT price structure of the selected vehicle models by applying a "Top-Down" approach, as shown in Figure 5.1(a), given that the battery pack prices are $324/kWh and $289/kWh for PHEVs and BEVs with the model year 2017 (as discussed below; Table 5.2), respectively. The top-down (i.e., based on manufacturing suggested retail prices, MSRP) approach gives a price ratio of 1.27 and 1.63 for a PHEV and a BEV relative to an ICEV. The price difference between EVs and ICEVs is mainly due to the expensive battery pack costs and possibly because of the higher R&D and investment in new factories for EV than ICEV. Compared to the vehicle cost ratio obtained from a "Bottom-Up" approach (i.e., based on vehicle component manufacturing cost; Figure 5.1(b) from Chapter 4), we find that the profit margins (as a percentage of sales price) of the reference cars are nearly uniform across different types of vehicle technologies.

Assuming that the ICEV pre-VAT price in China before 2020 would follow a similar vehicle price trend as seen in the U.S. between 1910 and 1930 [73], the reference ICEV price would decrease by 11% from 2017 to 2020[11]. Automakers' pricing strategies are hard to project, and here we assume that profit per car would stay constant throughout 2030. For simplicity's sake, all the price segments except for battery pack are assumed to remain the same from 2020 to 2030. The price of the battery pack, which is a large cost item in a EV, is expected to drop more significantly during the time horizon of this study, so this price variation is taken into account when projecting the future vehicle prices. The governing equations for estimating the future reference vehicle prices are shown in Equation (5.7) - (5.9) where *BPP* denotes battery pack price (see Table 5.2), $preVAT\ VP_{v,i}$ is the price of reference vehicle type *v* excluding VAT in year *i* (*v* = *ICEV*, *PHEV*, and *BEV*), and *i* starts from year 2020.

[11] Based on the historical data, the ICEV price in China had dropped by ~45% from 2003 to 2017 [73]

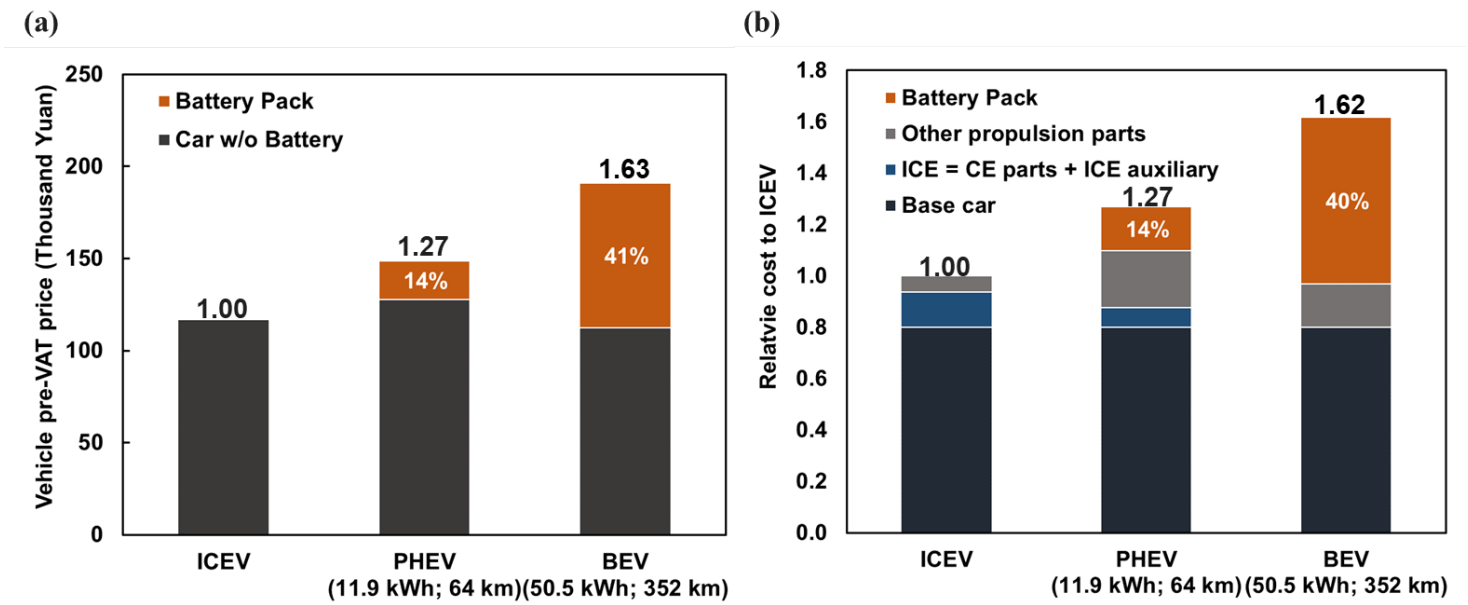

Figure 5.1. (a) Pre-VAT prices of the reference ICEV and EV with the model year 2017; (b) manufacturing costs of the reference EVs relative to ICEV cost with the model year 2017 (from Chapter 4). For the reference cars in 2017, the EV/ICEV price ratio was almost the same as the manufacturing cost ratio.

$$preVAT\ VP_{ICEV,i} = \frac{136{,}700}{(1+17\%)} \times (1 - 11\%) = 104{,}000 \tag{5.7}$$

$$preVAT\ VP_{PHEV,i} = preVAT\ VP_{ICEV,i} \times 1.27 \times (14\% \times \frac{BPP_{PHEV,i-1}}{BPP_{PHEV,2016}} + 86\% \times 1) \tag{5.8}$$

$$preVAT\ VP_{BEV,i} = preVAT\ VP_{ICEV,i} \times 1.63 \times (40\% \times \frac{BPP_{BEV,i-1}}{BPP_{BEV,2016}} + 60\% \times 1) \tag{5.9}$$

Battery Price Projection

Chapter 3 [81] suggested that the continued maturation of the existing NMC-based lithium-ion batteries (LIBs) is unlikely to reach the price target of $100/kWh (where BEV could be economically competitive with ICEV in the absence of incentives [52]) over the next decade. Table 5.2 shows the battery pack price trajectories of EVs used in this study, which are derived from the projections of Hsieh et al., (2019). The exchange rate for USD/Yuan is set to be 6.32. PHEV batteries have a higher Yuan/kWh cost than BEV batteries due to their higher power density [119]. We assume that the battery prices in year *i-1* determine the powertrain costs of EVs with model year *i*.

Table 5.2. Projected price (Yuan/kWh) trajectories of NMC Li-ion battery pack for BEV and PHEV from 2-stage learning curve model [81]

Model Year (i)	PHEV ($BPP_{PHEV,i-1}$)	BEV ($BPP_{BEV,i-1}$)
2017	1,825	2,043
2020	1,310	1,474
2025	944	1,046
2030	797	871

Purchase Cost (PC)

The primary purchase cost is from vehicle price (***VP***); in 2017, the price of BEVs in China equipped with Li-ion NMC batteries price was about 1.6 as much as the counterpart ICEVs (see Figure 1). The vehicle purchase tax (***VPT***) rate in China is 10% of pre-VAT (value-added tax) vehicle price (i.e., ***VPT*** = 10% × ***preVAT VP*** = 10% × ***VP***/(1+***VAT***)), and EVs are exempted from ***VPT*** until 2020. China's ***VAT*** rates for the manufacturing sectors were cut from 17% to 16% in 2018 and then further lowered to 13% in 2019 [120]; we assume that the ***VAT*** rates will remain 13% from 2019 to 2030.

The registration fee (***VRF***) in Beijing is about 500 Yuan. To lower the upfront vehicle purchase costs of EVs, the Chinese government is currently providing generous financial incentives (***FinInc***). The consumer subsidy program has been renewed and modified every two to three years, favoring long-range BEVs. Figure 5.2 indicates the subsidies that the reference BEV (range of 352 km) and PHEV (electric range of 64 km) receive during 2015-2020, showing that the subsidy program is more selective to promote BEVs. According to the current government policy, all financial incentives for EVs in China will be phased out at the end of 2020.

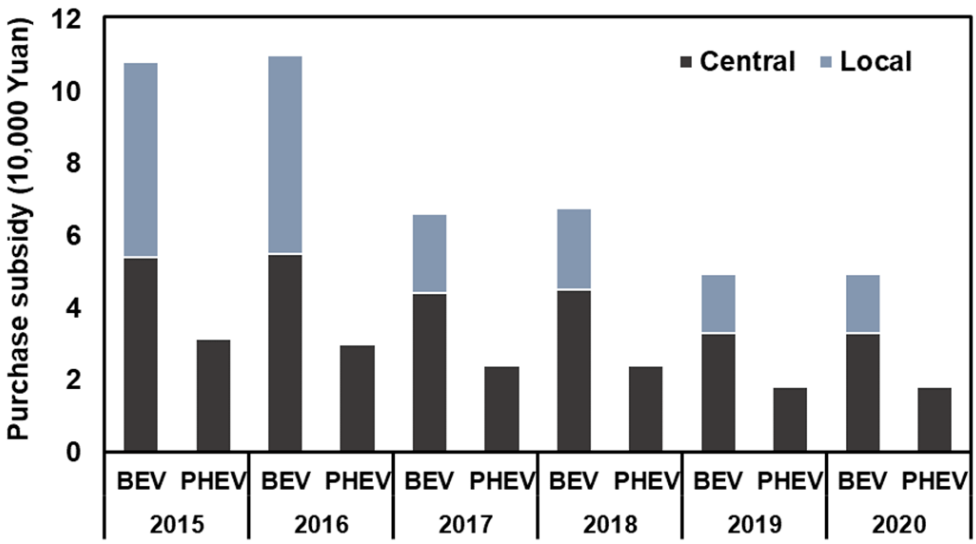

Figure 5.2. Purchase subsidy available for a BEV (R=352 km) and a PHEV (R=64 km) from 2015 to 2020 from the Chinese central government and Beijing local government; after 2020 all subsidies are to be ended.

Operating Cost

Operating costs, including fuel cost (***FC***) and non-fuel O&M cost (***O&MC***), vary significantly depending on driving patterns, travel habits, charging frequency, and vehicle lifespan. For example, the cost of electricity is highly variable: while the residential electricity rate is about 0.47 Yuan/kWh for home charging (when VAT is 13%), the rate for public charging stations is more than double due to the service fee (about 0.5 Yuan/kWh) imposed by public charging operators. Another example is that if the EV ownership period is less than 8 years and the car is not heavily used, then the owners do not need to worry about battery replacement costs because a standard battery warranty coverage is for 150,000 km or 8 years, whichever comes first. Here all the battery replacement costs incurred after 2030 are assumed to be the same as 2030; this is because the replacements are very likely to (or might have to) retain the same battery specifications and pack design as the retired ones, meaning that even if disruptive battery chemistries are commercialized after 2030, the battery replacement costs will remain around the same as in 2030 for several years. The vehicle kilometer traveled per year (***VKT***) in China was shown to decrease over a period when the car ownership increases rapidly [121]. While the annual VKT had decreased by about 30% from 2005 to 2015 [122], we expect that the VKT level will gradually stabilize after 2020 as the

auto market is maturing in China. For the base case in this study, we assume that the national average passenger VKT in China is 12,500 km throughout 2030, which is the average value of the high and low projections given by Huo et al. (2012). The discount rate (***r***) is assumed to be 5%, which is about the same as the current Chinese central bank's interest rate for long-term (i.e., more than five years) loans [123]. The average passenger vehicle lifespan in China is about 12 years [88] while the EV battery is assumed to last for 8 years (i.e., $\boldsymbol{n} = 8$, which is a standard battery lifetime warranty offered by electric car manufacturers). Based on the empirical studies on Shanghai [124], we assume 76% of kilometers traveled by PHEV are powered by a battery. About future fuel price (***FP***), we assume that EVs owners would do 85% of their charging at home and 15% charging at public stations—resulting in an average electricity rate of 0.66 Yuan/kWh with VAT of 13%. The retail gasoline price (including all types of taxes[12]) is assumed to stay constant at 7.48 Yuan/L.

The key non-fuel O&M costs for representative vehicles are summarized in Table 5.3. Annual insurance cost is based on Beijing insurance quote (including compulsory accident liability insurance, vehicle damage insurance, third-party liability insurance, deductible-exempt insurance with deductible amount of 10,000 Yuan) with vehicle model year 2017 [125]; the incremental insurance costs of EVs over ICEVs are found to be proportional to the differences of the vehicle MSRP (i.e., $\Delta \boldsymbol{IC} = 0.0131 \times \Delta \boldsymbol{MSRP}$), suggesting that the insurance costs for future EVs purchases will be less due to the decreasing battery prices and thus the decreasing MSRP. Maintenance cost is derived from multiple sources [124,126,127], showing that BEV holds a significant cost advantage in maintenance thanks to its much simpler propulsion system compared to the counterpart ICEV regarding mechanical complexity. In addition to the purchase grants, tax incentives (***TaxInc***) are also provided to promote more green consumption in China: energy-saving vehicles (including ICEVs with the engine not greater than 1.6L and PHEVs) are eligible for a reduction in vehicle use tax (***VUT***) by half, and BEVs are entirely exempted from the use tax (see the last row in Table 5.3 for the tax incentives provided to the selected vehicles in 2018). We assume that these tax incentives will also be removed at the end of 2020, along with the phase-out of the EV purchase subsidies.

[12] The retail gasoline price in China includes multiple taxes—VAT, sales tax, urban maintenance and construction tax, education surcharges, local education surcharges, corporate income tax (and imported oil tax). These gasoline taxes would account for about 38% of the retail gas price (7.48 Yuan/L) when VAT is 13%.

Table 5.3. Non-fuel operating and maintenance costs for the selected passenger vehicles in 2018; tax incentives are assumed to be removed at the end of 2020.

Vehicle Technology	ICEV	PHEV	BEV
Annual Insurance Cost (Yuan/year)	4,180	4,665	5,314
Maintenance Cost (Yuan/10,000 km)	900	720	220
Vehicle Use Tax (VUT) (Yuan/year)	420	420	300
Tax incentives for VUT (Yuan/year)	210	210	300

Impact of vehicle ownership restriction policy on TCO

To curb the fast-growing vehicle population, some China's megacities (including Beijing, Shanghai, Guangzhou, Shenzhen, Tianjin, and Hangzhou) are adopting car ownership restrictions, and EVs are often exempted from these city's vehicle license plate control systems [128]. Shanghai was an early adopter of license auctioning and the bid-weighted average price for an ICEV plate was about 92,850 Yuan in the end of 2017 [129]. Beijing was the second city adopting a car ownership restriction policy, opting for a lottery system; the odds of winning an ICEV plate was about 0.04% (bjhjyd.gov.cn, 2020). Compared to ICEVs, the license plates for EVs in Beijing are distributed on a first-come, first-serve basis. Based on the price difference between a car with a license plate and a counterpart car without a license plate in the used car market, the license plate value in Beijing was estimated to be 130,000 Yuan [13]. Guangzhou, Shenzhen, Tianjin, and Hangzhou adopted hybrid policies, allowing residents to opt in to either an auction or a lottery for ICEV plates.

For the cities having vehicle ownership restriction policy, the TCO per kilometer is also computed from Equation (1), but the purchase cost for ICEV is slightly different from Equation (5.2a)—containing one more cost contributor "ICEV license plate ($\boldsymbol{LP_{ICEV}}$)" (Equation (5.2b)). We take the license plate value in Beijing as representative for those megacities with car ownership restrictions.

$$\boldsymbol{PC = VP + VPT + VRF + LP_{ICEV} - FinInc} \tag{2b}$$

5.2.3 Transition Cost to Society (TrCS)

Transition cost to society (***TrCS***) is identified as part of the societal costs on the way to electromobility owing to the incremental costs of EVs over ICEVs. In this analysis, the system boundary of cost to society (***CS***) is limited to the car's purchase and uses themselves, including fuel/electricity consumption, insurance, maintenance, and battery replacement; all the other less direct societal impacts imposed by the vehicle ownership and uses (e.g., environmental, health, balance of trade, national security, employment) are outside this study's scope. ***TrCS*** is obtained from multiplying EV sales (S_{EV}) in year *j* by the incremental cost to society of EV over ICEV (see Equation (5.10)). When we assess the incremental ***CS*** due to the switch from an ICEV to a EV, all the taxes- and incentives-related terms in Equation (5.2) - (5.4) are excluded since they are just a redistribution within China instead of a cost to society as a whole. Taxes excluded from the ***TrCS*** calculation are ***gas tax*** (about 41% in 2017, 40% in 2018 and 38% between 2019 and 2030 of the retail gasoline price) and all the ***VAT*** embedded in the vehicle price, electricity price, insurance and maintenance costs (17% in 2017, 16% in 2018 and 13% from 2019 to 2030).

Unlike the ***TCO*** model that amortizes the upfront costs across all the kilometers to obtain the consumer levelized cost of driving, the ***TrCS*** model discounts all the future costs to their present values to compute the lump sum societal cost difference (i.e., CS_{EV}- CS_{ICEV}) for a EV sold in a specific year *j*, as shown in Equation (5.10) – (5.11). Note that battery replacement cost (***BR***) is only incurred in the 8th year (*i* = 8) (Equation (5.14)).

$$\boldsymbol{TrCS_j = S_{PEV,j}(CS_{PEV,j} - CS_{ICEV,j})} \tag{5.10}$$

where

$$\boldsymbol{CS = VP' + \sum_{i=1}^{N} \frac{(FE \times FP' \times VKT)_i + (IC' + MC' + BR')_i}{(1+r)^i}}$$

$$\boldsymbol{= \frac{VP}{(1+VAT)} + \sum_{i=1}^{N} \frac{(FE \times FP' \times VKT)_i + \left(\frac{IC+MC+BR}{1+VAT}\right)_i}{(1+r)^i}} \tag{5.11}$$

$$\boldsymbol{FP'_{gas} = FP_{gas} \times (1 - gas\ tax)} \tag{5.12}$$

$$\boldsymbol{FP'_{electricity} = FP_{electricity}/(1 + VAT)} \tag{5.13}$$

$$\boldsymbol{BR = 0}\ \ when\ i \neq 8 \tag{5.14}$$

5.2.4 Uncertainty Analysis

Table 5.4 indicates the key governing parameters in our ***TCO*** and ***CS*** analyses, with the possible ranges identified for the future projections. We examine the uncertainties to these assumptions. Ranges for EV battery prices are taken from our previous study that considered the impacts of materials cost [81]. The uncertainty of electricity price is large: while the lower bound represents the residential electricity rate (i.e., 100% home charging), the upper bound of electricity price is the rate for EV owners doing all the charging during the peak hour at the public charging stations in Beijing [131]. We conduct a Monte Carlo analysis with 1,000 simulations to test the robustness of the results (2020, 2025, and 2030), assuming that all the uncertainties in the parameters are uniformly distributed and the vehicle lifespan is fixed at 12 years.

Table 5.4. Governing parameters and the associated uncertainties in the TCO and CS analyses

Parameters		Base Value	Range	Unit
Gasoline Price		7.48	6 ~ 8	**Yuan/L**
Electricity Price (including VAT of 13%)		0.66	0.47 ~ 1.74	**Yuan/kWh**
Discount Rate		5	4 ~ 6	**%**
Vehicle Distance Driven		12.5	10 ~ 15	**Thousand km/year**
PHEV Battery-Driven Percentage		76	60 ~ 90	**%**
BEV Battery Price in MY	**2020**	1,310	1,249 ~ 1,354	**Yuan/kWh**
	2025	944	811 ~ 999	
	2030	797	610 ~ 886	
PHEV Battery Price in MY	**2020**	1,474	1,414 ~ 1,512	**Yuan/kWh**
	2025	1,046	911 ~ 1,094	
	2030	871	682 ~ 953	

5.3 Results and discussion

5.3.1 Transition Cost to Society

High battery pack prices make electrified transportation with EVs more expensive than travel by ICEVs. Here we calculate the total cost to society of the transition from ICEVs to EVs implied by the dual-credit scheme mandate. We first compute the cost to society difference between EV and ICEV (i.e., $\boldsymbol{CS_{EV} - CS_{ICEV}}$) from 2021 to 2030, and then estimate the yearly transition cost to the society ($\boldsymbol{TrCS_j}$) based on the EV sales in that year ($\boldsymbol{S_{EV,\,j}}$) using Equation (5.10); the results are shown in Figure 5.3.

As the battery pack prices drop, the delta cost to society (ΔCS) for a switch from one ICEV to a EV will be shrinking. We find that a PHEV is likely to achieve CS parity with an ICEV faster than a BEV; a BEV using a large battery pack will stay more than 20,000 Yuan more costly to society than an ICEV even out to 2030 (Figure 5.3(a)). The new mandate, on the one hand, is expected to drive the local EV sales from 1.7 million per year in 2021 to 11.2 million per year by 2030 (with 37% sales market share) (Chapter 4); but on the other hand, this would impose substantial transition costs upon the whole society. Since the annual number of EVs sold will increase more rapidly than the decreasing rates of ΔCS, the yearly transition cost to society is expected to keep growing toward 2030—from 59 billion Yuan per year in 2021 to 228 billion Yuan per year in 2030 (bars shown in Figure 5.3(b)). This transition cost to society associated with the mandate would be – on average – on the order of 100 billion Yuan per year from 2021 to 2030, consuming about 0.1% of the projected annual GDP in China[13] each year (Figure 5.3(c)), equivalent to about 2% of the total size of the transport sector of China's GDP[14].

This transition cost should be taken into account when researchers are attempting to quantify the total cost to society associated with vehicle electrification. It is noted that cities having ICEV license restrictions (e.g., Beijing, Shanghai, Shenzhen, Tianjin, Hangzhou, and Guangzhou) will have higher EVs adoption rates than the others [134]; depending on how EVs and ICEVs are priced across China and how gasoline tax revenues are shared, those cities might contribute either more or less to the total transition cost than other parts of China. Regardless, it is expected that

[13] China's GDP is assumed to grow with the compound annual growth rates of 7.00% in 2016-2020, 5.36% in 2021-2025, and 4.60% in 2026-2030 [87].

[14] From 2012 to 2018, the sector of "transport, storage and post" had contributed 4.5% of China's GDP per year [133].

people in all regions of China will feel the transition cost by having less access to cars, so decreased mobility and fewer trips.

This sizable societal investment can be compared with the projected benefits: first, the large battery production volumes will help drive down battery prices, thus closing the cost gaps between EVs and ICEVs; second, electrifying private mobility would lead to substantial societal benefits in the long run due to reduced emissions leading to lower health costs and increased quality of life and life expectancy in urban areas; third, this transition has additional potential long-term societal benefits to China in terms of the balance of trade and national security due to reduced reliance on imported petroleum. Both the costs and the benefits associated with this mandate are substantial, and so deserve careful consideration.

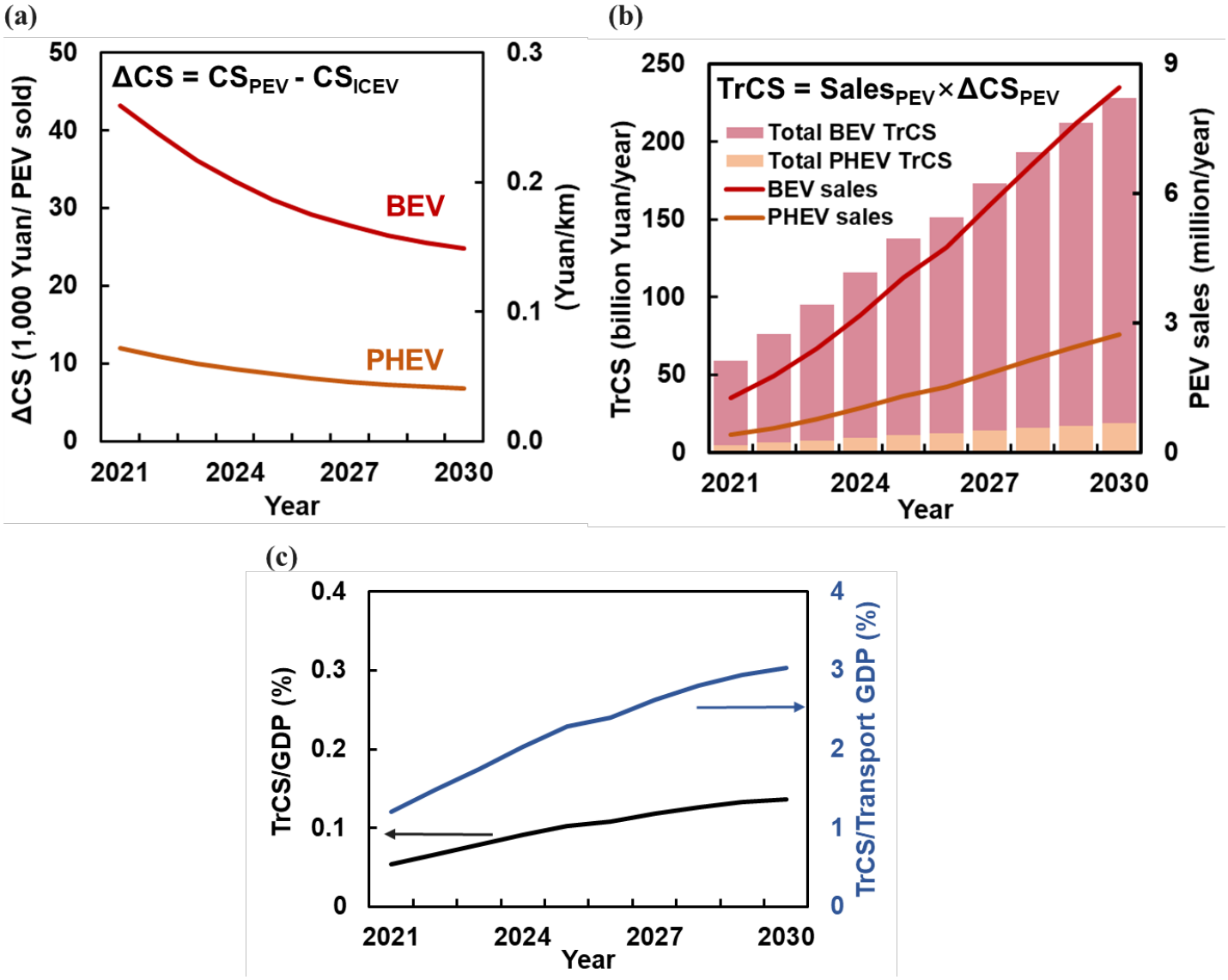

Figure 5.3. (a) The delta cost to society (ΔCS) for a switch from ICEV to EV; both the 12-year (with 12,500 km driven/year) lump sum CS differences (left ordinate) and the corresponding per km CS differences (right ordinate) are presented; (b) the yearly transition cost to the society (left ordinate) for forcing the targeted EV market penetration (right ordinate) by 2030; EV sales are from Chapter 4; (c) the transition cost's contribution to the Chinese growing economy (left ordinate) or to its transport sector composition (right ordinate).

5.3.2 Ownership Cost to Consumer

Consumer decisions are determined by personal cost rather than societal cost; taxes, subsidies, mandates, and regulations could significantly alter the actual ownership costs. Thus, we evaluate total ownership costs borne by the consumers for per-kilometer driving, exploring how the local tax/ subsidy scheme and car ownership restriction policy would affect the relative ownership cost competitiveness across different vehicle technologies from now out to 2030. It is noted that the results shown in Chapter 5.3.1 and Chapter 5.3.2 assume a home-dominant charging behavior where EV owners have access to home charging and prefer to do most charging at home. The uncertainty in drivers' charging patterns—home charging versus public charging—is addressed in Chapter 5.3.3.

Current Status in China (2018)

First, we investigate the differences in levelized TCO considering the government financial incentives (including purchase subsidies and tax breaks/ exemptions) and ICEV license plate quota policy across ICEV, PHEV, and BEV in China, using the reference vehicles' parameters. While the solid bars in Figure 5.4 represent the results of 12-year levelized TCO, the error bars are from the uncertainty in the vehicle lifespan ranging from 8 to 15 years.

The current financial incentives for a PHEV/ BEV purchased (with subsidy) in Beijing amount to 54,435/ 118,785 Yuan reductions in lifetime 12-year (i.e., 150,000 km) TCO, equivalent to 0.36/ 0.79 Yuan reductions per kilometer traveled respectively, making PHEVs and BEVs more economically attractive than conventional gasoline cars. The ICEV license plate quota policy, on the other hand, would impose an additional cost of 1.17 Yuan per kilometer traveled on ICEV purchase, causing ICEVs to be much more costly than subsidized EVs in China's megacities.

However, in the absence of financial incentives and quota policy, the current 12-year TCO of PHEVs/ BEVs is 3%/ 24% higher than that of ICEVs; this reemphasizes that government subsidies or mandates are essential for EV take-off at today's economics.

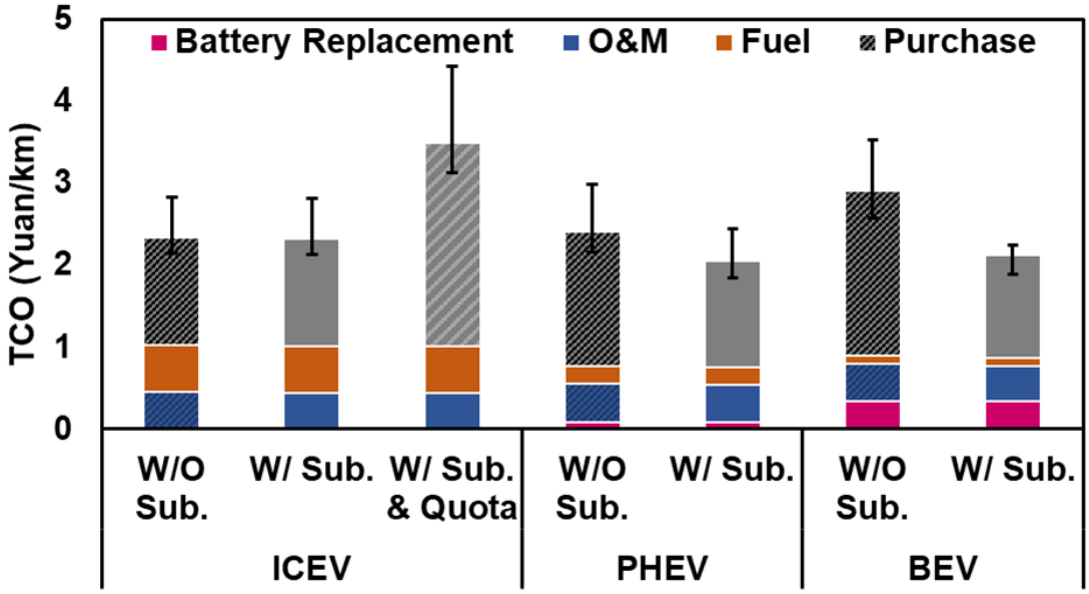

Figure 5.4. TCO component breakdown with and without the government subsidies and ICEV license plate quota policy in 2018 across three different vehicle technologies in China (Beijing); the upper error bound is assuming the vehicle lifespan is 8 years, while the lower error bound assumes 15 years.

Figure 5.5 compares the subsidized per-km TCO results (i.e., W/ Sub. in Figure 5.4) across various vehicle lifespans: 8, 12, and 15 years. Current subsidies are shown to be sufficient to make the TCO of EVs lower than that of ICEVs with all 3 vehicle lifespans in China. However, most consumers still prefer ICEVs nowadays, suggesting that other barriers beyond cost (of ownership) have to be overcome as well to achieve mass EV adoption; barriers include limited access to charging infrastructure, range anxiety, and consumer familiarity. Figure 5.5 also points out that no matter which propulsion system a vehicle is equipped with, the longer period a car is owned and used, the cheaper per-km TCO would be, even considering the battery replacement cost. For vehicle lifespans greater than 8 years, consumers should be aware that battery replacement costs would be very likely to incur since the battery age is beyond the warranty coverage (i.e., 8 years). However, compared to the per-km TCO with the vehicle lifespan more than 8 years, the expensive

battery replacement costs would be offset by the increased total vehicle distance driven. While the battery pack prices are about 1,590 Yuan/kWh for BEVs (MY 2018) and 1,814 Yuan/kWh for PHEVs (MY 2018), they are expected to drop to around 900 Yuan/kWh and 994 Yuan/kWh, respectively, in the next 8 years when they achieve their retirement age [81].

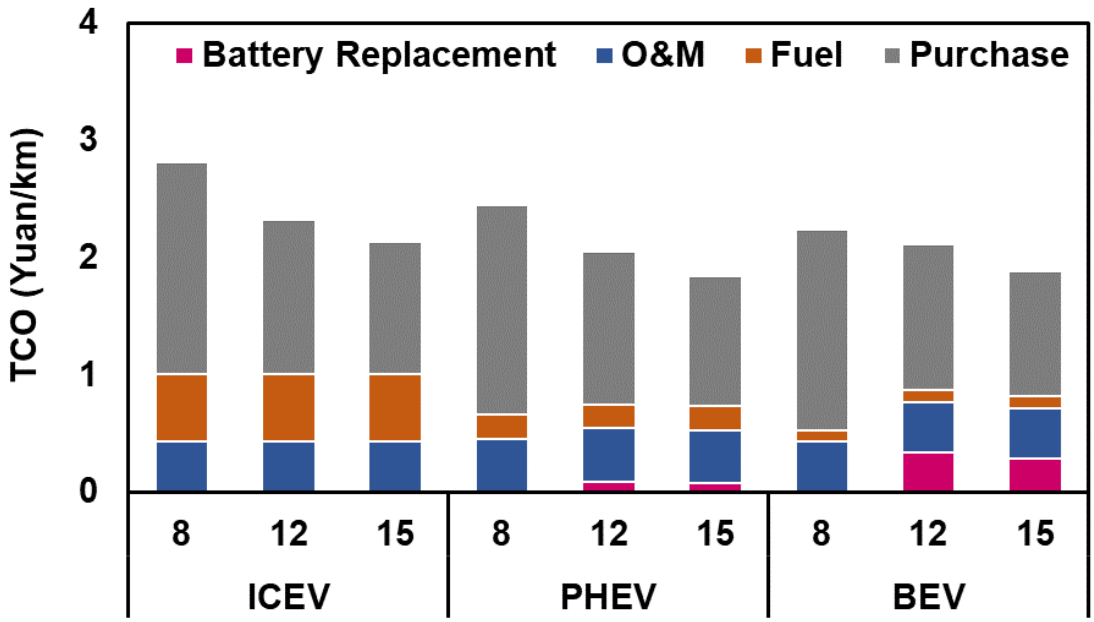

Figure 5.5. TCO component breakdown including 2018 government subsidies for vehicle lifespans of 8, 12, and 15 years across three different vehicle technologies in China (Beijing); battery replacement is not expected to incur when the vehicle lifespan is 8 years. "Fuel" includes electricity.

TCO Trajectory toward 2030

Based on the battery price (Table 5.2) and the subsidy (Figure 5.2)/ ICEV license plate quota policy scheme in Beijing, the temporal 12-year TCO variations during 2015 to 2030 in China are computed. The TCO ratios between EVs and ICEVs are shown in Figure 5.6, and several observations and findings are worth highlighting:

2015-2020

- The battery pack of a BEV is larger than a PHEV (i.e., 50.5 kWh for a BEV and 11.9 kWh for a PHEV in this analysis), and thus the purchase cost reduction owing to the large decrease in battery prices in 2016 is more notable in a BEV.

- The substantial cuts in BEV subsidy in 2017 and 2019 result in the two rises in TCO ratio of BEV to ICEV.
- Since the government is closing the cost gaps through subsidies and differences in taxes collected, China's TCO ratio of EV to ICEV is about 10% less than 1 (i.e., TCO parity is achieved) in the period of 2016 to 2020. The government has been heavily subsidized the EV industry, making EV more profitable in China than in some other countries.
- For China's megacities with car ownership restrictions, the special treatments on licensing (i.e., with EV exemption) and financial subsidies make EVs much more cost-attractive than the counterpart ICEVs; these have catalyzed the sales of EVs in these megacities. The six megacities in China that currently have car ownership restriction policies (Beijing, Shanghai, Guangzhou, Shenzhen, Tianjin, and Hangzhou) have contributed about 50% of national annual EV sales in 2017 and 2018 [135].

2021-2030

- The plan to entirely phase out all the subsidies by the end of 2020 will lead to a big jump in TCO ratios in 2021. If the automakers keep the same price structure as today, the TCO of a BEV in the absence of incentives and quota policy will no longer achieve parity with an ICEV even out to 2030. On the other hand, TCO parity is expected to remain achieved for PHEV even with no subsidies and no quota policy.
- It is reasonable to expect that consumer-centric TCO (including subsidies, taxes, different automakers profits on different types of vehicles) for BEV and ICEV will have to be comparable (i.e., TCO ratio close to 1 or even less than 1) for broader vehicle electrification by 2030 in accord with the government targets.
- It is uncertain how the cost differentials will be covered when some of the current EV subsidies in China are replaced by mandates. Based on the experience in the USA with CAFE (Corporate Average Fuel Economy) standards[15], car manufacturers are likely to raise the price of ICEVs while lowering the price of EVs to persuade consumers to purchase the required fraction of EVs. This change in the vehicle pricing strategy will address the consumer cost differential, and shift much of the societal cost of vehicle electrification onto Chinese purchasers of ICEVs. Nevertheless, we expect that a big fraction of the transition

[15] CAFE standards would impose a constraint on automakers' profit maximization problem that creates an implicit subsidy for fuel-efficient vehicles and an implicit tax for fuel-inefficient vehicles [136].

cost will continue to be borne by the government due to the reductions in gasoline tax revenues, and the automakers may bear part of the cost differentials in the form of reduced profit margins during the transition period.

- Under car ownership restriction policy with EV exemption, EVs will remain their cost competitiveness advantages even after the phase-out of the subsidies. However, there remains uncertainty surrounding the long-term implications of the quota policy. Fearing the impact of additional city-level ownership restrictions on China's domestic car manufacturing industry—particularly with vehicle sales falling in 2018 for the first time since the 1990s—China's national government announced a new policy to temporarily stop local government from implementing new restrictions on car purchases [137]; however, Beijing city government has yet to take any action to respond to this national mandate.

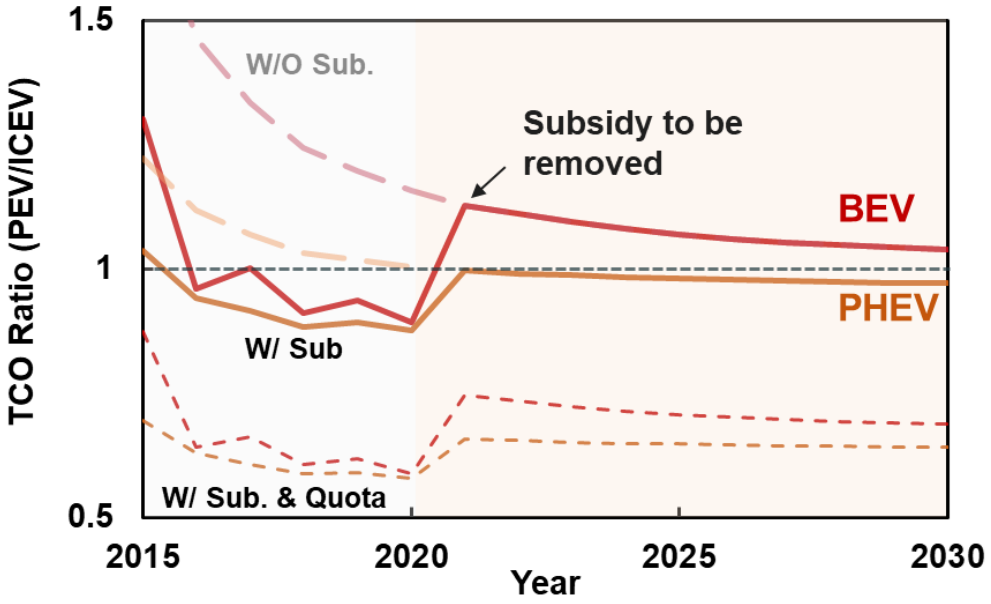

Figure 5.6. TCO trajectories of EVs relative to ICEVs in China by 2030. Data up to 2018 are historical; 2019-2030 are the results of assuming the automakers keep the same price structure as today. After 2020 when the subsidies are removed, TCO parity will remain achieved for PHEV but not for BEV even out to 2030 (in most of China's regions where ICEV license plate quota policy does not exist). However, the mandate targets will not be achieved if the TCO of BEVs is higher than TCO of ICEVs. Instead, we expect automakers will raise ICEV price and lower BEV price to keep the TCO ratio less than 1. On the other

hand, in some China's megacities with car ownership restrictions, EVs will remain much more cost-attractive even after the removal of subsidies.

5.3.3 Uncertainty Analysis

To examine the ***TrCS*** and ***TCO*** result robustness, we perform a Monte Carlo simulation varying the key model inputs, assuming that these parameters are uniformly distributed within the ranges identified in Table 5.5. Figure 5.7 and Figure 5.8 show the uncertainties about the projected ratios of cost to society (i.e., $\boldsymbol{CS_{EV}/CS_{ICEV}}$) and of cost to consumers[16] (i.e., $\boldsymbol{TCO_{EV}/TCO_{ICEV}}$) in 2020, 2025, and 2030. Each box describes lower quartile, median and upper quartile values; most extreme values (whiskers) are within 1.5 times the inter-quartile ranges from the ends of the box; outliers are displayed in red + sign; the base case results (presented in Chapter 5.3.1 and Chapter 5.3.2) are marked in circles. The uncertainty range of BEV is always larger than for PHEV, which is due to the fact that larger battery capacity in BEV magnifies all the uncertainties in future fuel (electricity) costs and battery prices. Besides, the base case results (i.e., circles in the figures) are all in the lower half of variance; this is mainly because in the base case EV owners are assumed to do 85% of their charging at home, therefore having much lower electricity costs (about 0.66 Yuan/kWh) than for public charging stations (mostly between 1.6 Yuan/kWh and 1.8 Yuan/kWh).

Cost to society (Figure 5.7):

Almost all the simulation outcomes of CS ratio of EV to ICEV are greater than 1, highlighting the fact that a shift away from fossil fuels to battery-powered vehicles will impose costs throughout the entire society, and which should be taken into account when assessing the true transition cost. For box-to-box comparison, BEVs are always higher than that for PHEVs, suggesting that a switch to a BEV will impose heavier transition cost than a shift to PHEV; this is mainly because of the larger (thus more costly) battery packs in BEVs.

BEV direct costs to the Chinese society are always more than ICEV even in 2030. On the other hand, PHEVs have fewer direct costs to society than BEVs and are more likely to be on a par with ICEVs by 2030, making PHEV a promising form of transportation to achieve a less-costly transition from liquid fuels to electrification.

Cost to consumer (Figure 8):

[16] For brevity, we focus only on uncertainty of TCO with no quota policy to the model assumptions.

In 2020 when the subsidies still exist, TCO parity will keep being achieved between EVs and ICEVs. Moreover, with the help of China's subsidies that favor BEV more than PHEV, the TCO for BEV (even having higher consumer purchase prices) is comparable to that for PHEV, meaning that there are no differences between these two types of EVs from the perspective of consumer's cost of driving in 2020.

Most of the outcomes of TCO ratio of BEV to ICEV are larger than 1, pointing out that when the subsidies are removed, BEVs are not likely to achieve TCO parity with ICEVs by 2030 (unless carmakers discount the price of BEVs relative to ICEVs). This implies that for BEV take-off over the next decade, either the government has to extend BEVs subsidies or the automakers need to adjust their pricing structures by internal subsidies. On the other hand, PHEVs are very likely to remain less costly than ICEVs to consumers in terms of TCO.

It should be noted that even without vehicle pricing strategies changed, there is still a possibility that BEVs reach TCO parity with ICEVs; this might happen when gasoline price and annual distance driven are in higher ends of their uncertainty ranges, while electricity price, discount rate, and battery prices are in lower ends.

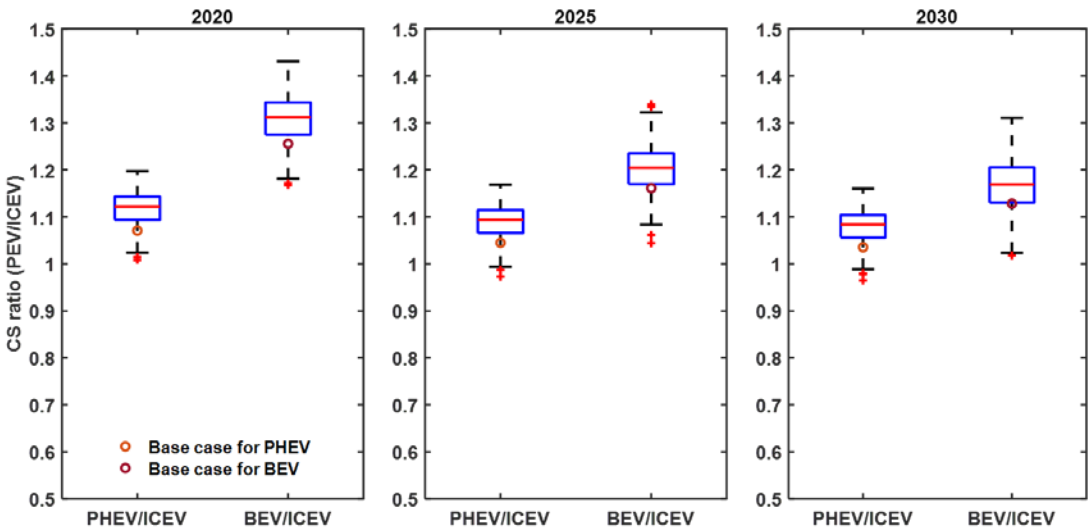

Figure 5.7. Variations in the projected ratios of cost to society (CS) of EVs to ICEVs in China in 2020, 2025, and 2030. Since many more EVs will be sold in 2030 than 2020, the total transition cost to society (TrCS) will be higher then (see Figure 5.3(b)).

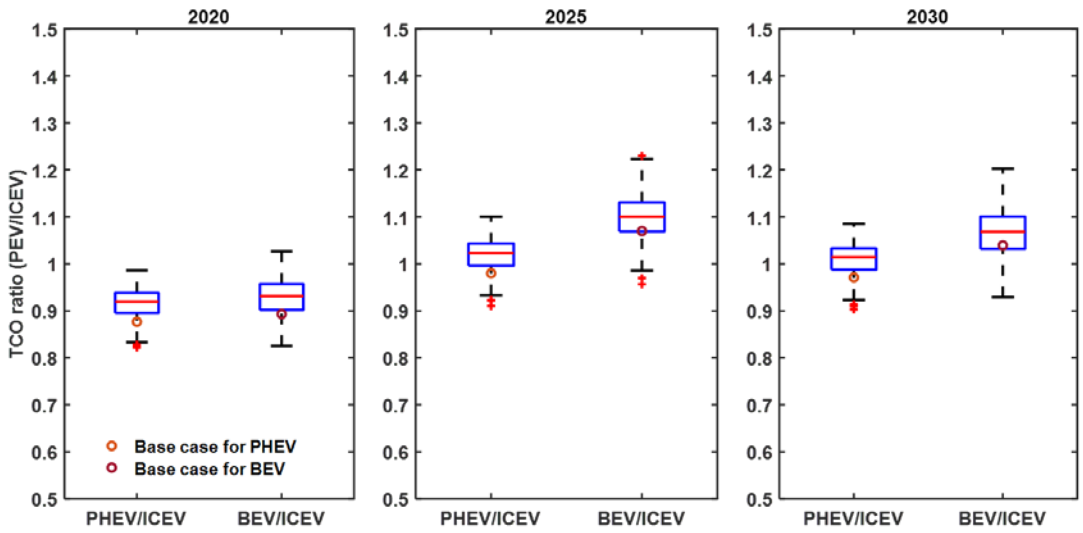

Figure 5.8. Variations in the projected ratios of the 12-year total cost of ownership (TCO) to consumers between EVs and ICEVs in China (Beijing) in 2020, 2025, and 2030; subsidies are included in 2020 numbers. We expect automakers to adjust prices to eliminate the TCO differential in order to achieve the mandated sales mix.

5.4. Conclusion and policy implications

While battery prices have been dropping rapidly over the past decade, the essential battery materials (lithium, nickel, and cobalt) will eventually constrain the declining trajectory of battery production cost and set lower bounds on battery prices. This practical limit would undoubtedly delay the occurrence of the transition to electromobility at an attractive cost, especially if the elemental price spiked resulted from a raw material shortage. We select China as a market of particular interest owing to its leadership position in plug-in electric vehicle (EV) deployment, mostly credited to the aggressive government policies. The recent enactment of dual-credit system mandate is expected to compensate for the phase-out of the subsidy program, increasing EV adoption in China dramatically, ostensibly by transferring the burden of subsidizing the EV industry from the government to the automakers (but in reality to the car buyers).

We compute the transition cost to China of switching from internal combustion engine vehicles (ICEVs) to EVs and find that PHEVs could provide a less costly transition from liquid fuels to electrification, while BEV direct costs to the Chinese society will always be more than

ICEV even in 2030. Moreover, we show that creating an inflection point for EV demand via the mandate will put substantial transition costs on the entire society: from ~60 billion Yuan for 2 million EVs sold per year in 2021 to ~230 billion Yuan for 11 million EVs sold per year in 2030, which is about 0.1% of the growing China's GDP annually—equivalent to 2% of the nationwide expenditure on transport sector every year in China. This sizable societal investment should be compared to the social benefits of vehicle electrification – e.g., electrified mobility may reduce local air pollution and CO_2 emissions with health and climate benefits, and it may also enhance national security owing to reduced dependence on imported petroleum.

However, mass-market consumer's decisions are not driven by the social cost, but primarily by the private cost. To spur mass adoption of EVs, the industry must go beyond the early adopters and become appealing to the majority of consumers who care more about price and convenience than environmental policy. Thus, this study also considers the consumer-centric total cost of ownership (TCO), i.e., the lifetime cost to a customer of purchasing and operating a car including taxes, subsidies, fuel, maintenance, insurance, and battery replacement costs for EVs. We examine the cost attractiveness of EVs by depicting their localized TCO trajectories relative to ICEVs out to 2030. Supported by various subsidy programs, China's EVs have been heavily subsidized by the government during the period of 2016-2020, making them more TCO attractive than ICEVs. However, after subsidies are eliminated at the end of 2020, while PHEVs could remain cost-competitive, this TCO parity will no longer be reached for BEVs, probably even out to 2030, if the automakers keep the same price structure as today. The phase-out of the EV subsidies and the introduction of the dual-credit system mandate will force the automakers to adjust their pricing strategy. Based on the experience in the USA with CAFE (Corporate Average Fuel Economy) standards, carmakers are very likely to raise the price of ICEVs and lower the price of BEVs to make the consumer TCO lower for BEVs, to achieve the mandated targets. On the other hand, for the megacities with car ownership restrictions, the "valuable" ICEV license plates make EVs much more cost-attractive than ICEVs even with no subsidy, boosting the local EV sales.

Although TCO-based methodology is applied throughout this study to investigate the impacts of achieving China's aggressive goals for electric transport, several limitations are recognized. First, gasoline prices will be fluctuating rather than staying constant. Second, TCO is not the only factor affecting the new technology adoption; other barriers include limited access to

charging infrastructure and consumer familiarity. Third, the effects of policies cannot efficiently be computed by static single-point estimations. For example, the electrified mobility will probably reduce emissions of greenhouse gases and air pollutants, leading to valuable health and climate benefits that are not captured in this direct-cost analysis. Furthermore, the calculation ignores the secondary effects due to reduced petroleum imports and increased electricity generation, and costs of building more recharging infrastructure. Thus, further investigation based on this study is required to improve the policy impact evaluations of private vehicle electrification.

Chapter 6. Battery swapping deployment: Recharging systems and business operations to improve the economics of electrified taxi fleets

Much of the material in this chapter has been published in Hsieh, I-Yun Lisa, Ashley Nunes, Menghsuan Sam Pan, and William H. Green. "Recharging systems and business operations to improve the economics of electrified taxi fleets." Sustainable Cities and Society (2020): 102119. Ashely Nunes collaborated in the formulation of the arguments in the text. Menghsuan Sam Pan contributed to the analysis of the results.

Abstract

While vehicle electrification offers great benefits to society, mass-market adoption of battery electric vehicles remains a challenge owing to the long recharging times and limited recharging infrastructure. High opportunity costs tied to long recharging times are particularly problematic for commercial fleet operators. With an aim to improve the economics of electrified taxi fleets, this Chapter presents a framework for techno-economic analysis, examining the cost competitiveness of various recharging business models (i.e., combined ecosystems of recharging systems and taxi operations).

When considering the achievable throughput of the recharging systems, we find that—on a per-kilometer basis—1) battery swapping emerges as a cost-effective option although it requires higher upfront investments for the battery inventory requirement; 2) increasing vehicle fleet size enhances the economic viability of double-shift taxi electrification. We expect that an electrified taxi fleet relying on the *right* recharging systems/operations could achieve cost parity with a gasoline-powered taxis system by 2022. Between now and then, the electrification of high-use vehicles requires government support; policies discussed include purchase subsidies and revenue-neutral gas tax imposition. By using real-world financial data taken from an operating electrified taxi fleet in Beijing, this Chapter provides a theoretical and practical reference for cities moving toward electric taxi ecosystems and sustainability.

6.1 Introduction

While internal combustion engine-powered vehicles (ICEVs) are the preeminent mover of goods and services, they also remain a major source of hazardous air pollutants [138]. The ensuing public health outcomes are particularly worrisome for China, where motorization rates are soaring [139]. Although battery electric vehicles (BEVs) offer an opportunity to reduce the impact of these negative externalities, widespread market penetration of this technology remains a challenge owing in large part to longer-than-average energy replenishment times [140]. Currently, most BEVs are recharged using Level 2 chargers, where a BEV is plugged into external energy supply and left for several hours [141]; this in comparison to the few minutes taken to refuel a gasoline-powered vehicle.

Long BEV charging times are particularly problematic for multi-shift taxis and similarly operated mobility-on-demand fleets. Because minimizing vehicle downtime is crucial to maximizing profit, fleet owners show preference for ICEVs over electric ones. The consequences of this preference are not insignificant. Compared to personal light-duty vehicles, taxis – owing to traveling greater distances – consume more fossil fuels making them disproportionally larger contributors to air pollution [142]. In Beijing, for example, an average taxi emits nearly 10 times as much as a private car [143]. As part of a drive to cut air pollution, the Beijing municipal government has announced its plan to replace all 67,000 conventional taxis in the city with BEVs (Hanley 2017). This changeover will take place over time with a mandate that all newly added and replaced taxis in the city must be battery-powered. While this plan shows the city's ambitions to improve air quality with BEVs, the proliferation of the technology still requires efficient recharging infrastructure.

Charging concerns remain an obstacle for fleets even with fast charging; current fast charging speeds cannot compete with gasoline refueling and are thought to reduce the battery's lifespan [144]. Battery swapping, on the other hand, could be a viable option to solve the charging conundrum. This technique entails rapidly replacing – rather than slowly charging – depleted batteries with charge-ready substitutes. As the company Better Place demonstrated earlier (George, 2013), with specially designed BEVs and appropriate infrastructure, such 'swaps' can be achieved in a few minutes [145], making this technology appealing to a dense closed system like the taxi industry where downtime minimization is crucial to business viability. In 2016, the world's largest

network of battery swapping stations commenced operation in Beijing, China [146]. BAIC BJEV (a new energy subsidiary of Beijing Automotive Group) established the alliance, cooperating with Sinopec Beijing (an oil and gas company) to commercialize battery swapping services. BAIC BJEV started implementing the idea in a taxi fleet, building up a solid prototype in the close-collaboration network as the first step before trying to expand a capital-intensive battery swapping network. As the supporting infrastructure comes to maturity, BAIC BJEV plans to expand its swapping business to car-sharing, car-hailing, and ultimately to private vehicle markets [147].

Published literature on battery swapping focuses on operation scheduling and infrastructure planning [148–151], while research on electric taxis centers more on aspects of charging stations optimization [152,153], service pricing [154,155], environmental benefit compared to gasoline taxis [156,157], and charging behaviors [158,159]. However, few economic evaluations have been conducted that compare fleet operating costs across various energy replenishment modes—BEV fleet with charging or battery swapping and ICEV fleet with gasoline refueling. A BEV taxi system was claimed to have higher gross cost in the battery swapping mode than in the charging one owing to the higher fixed equipment/construction cost [160]; but, this statement may not hold true if the achievable throughput of infrastructure is considered.

Consequently, this Chapter examines - for the first time to our knowledge - the cost competitiveness of swappable battery technology against BEV charging activities, accounting for the throughput of the fleet network. With an aim to accelerate the urban transformation toward sustainability, this Chapter identifies cost-effective options for emission-free taxi service networks. We conduct a techno-economic analysis to investigate the extent to which battery swapping addresses the recharging time concerns surrounding the adoption of BEVs by fleet operators, using the real-world financial data in Beijing. We also propose an alternative business operation that double-shift electric taxis could run with to deliver the same number of passenger trips as gasoline taxis. We explore whether any of the proposed BEV recharging business models can achieve cost parity with existing ICEV based system, and how the outcomes change if improving battery technology and the government supports/interventions are considered. We conclude by stating some implications for policymakers seeking to facilitate the transition to electric mobility.

6.2 Methodology and data

We begin this section by first defining the business models that are explored in this study. Secondly, we identify the cost components considered in the combined ecosystem of taxi operations and the recharging systems. Lastly, we present the framework for per-kilometer cost evaluation.

6.2.1 Business models

BEV fleet with conventional Level 2 charging

In this scenario, the taxi fleet relies on a network of Level 2 chargers. The Level 2 chargers have an assumed rate of 7 kW[17] and, as discussed below, this delivers about 44 km driving range per hour of charging. Unless otherwise stated, we assume that with this and other business models, the driver stays with the taxi during recharging, similar to how current taxi fleets using gasoline-powered vehicles operate. For taxis that run single 12-hour shift per day, although most of the Level 2 charging can be done while the driver is not working, they still need to temporarily halt operations for a few hours mid-day for partial energy replenishment to deliver the same number of passenger trips in their daily shift. For taxis with double shifts (i.e., two 12-hour shifts), a much larger taxi fleet is needed to meet customer demand since each taxi spends a lot of time off the road recharging.

BEV fleet with Level 2 charging with extra vehicles

In this scenario, the fleet avoids long idle time associated with Level 2 charging by having a sufficient number of charged and readily available vehicles. The driver can go to a charging depot and switch to a fully charged vehicle when the taxi runs low on charge. This strategy is important for taxi drivers who operate in multiple shifts and always need to be on the road generating revenue. Currently, double-shift ICE-powered taxis in Beijing operate an average of 570 km per day to meet consumer demand[18]. If the double-shift taxi business is relying on Level 2 charging, the time needed to recharge for 570 km is 13.2 hours. In this business model, the taxi company

[17] In Beijing, 7 kW is the most common Level 2 charging rate in public charging stations [161].

[18] From the fact that 60% of Beijing taxis run single shift and the rest 40% work double shifts [162], we infer that the average operating hours a day is 16.8 hours. Assuming a taxi travels 400 km daily [162], the distance driven per active hour of taxi time is estimated to be 23.8 km/hr (=400 km/16.8 hr). This suggests that the daily distance driven is about 285 km for single-shift taxis and 570 km for double-shift taxis.

purchases several extra vehicles, and always has a rotation of vehicles being charged. Therefore, the idle time (or opportunity costs) associated with Level 2 charging times is minimized. To keep the same number of double-shift taxis on the road generating revenue, the fleet needs to be 1.55 times as large as a conventional double-shift taxi fleet (0.55 = 13.2 hours/24 hours).

Note that we do not consider single-shift taxis with extra vehicles case for simplicity and also for the following reasons. Firstly, current Beijing single-shift taxis are always single driver with one vehicle; only that one driver is authorized to drive each taxi. It would be convenient for the driver to have a second taxi to avoid the need to stop mid-day to recharge, but the capital expense for the additional vehicle, which would have very low utilization[19] makes this option infeasible. Secondly, the extra vehicle would be shared among several drivers, but only be on the road for 12 hours/day. This is out of consideration because if vehicle sharing is already part of the fleet arrangement, this sub-optimal operation (as opposed to double-shift taxis with extra vehicles) is not economically justifiable.

BEV fleet with conventional fast charging

In this scenario, the fleet relies upon a network of fast chargers. The fast chargers are assumed to charge a BEV from 20% to 80% in 22.5 minutes; another 30 minutes is required to charge from 80% to 100%.

BEV fleet with fast charging with extra vehicles

Similar to the scenario of Level 2 charging with extra vehicles, we only consider double-shift taxis in this case. The fleet avoids idle time associated with fast charging by having a sufficient number of charged and readily available vehicles. The time that must be spent recharging each day, in order to travel 570 km/day, using a fast charger is about 2.4 hours. So to keep the same number of double-shift taxis on the road double-shift fleet needs to be 1.1 times larger than a conventional double-shift fleet (0.1 = 2.4 hours/24 hours).

[19] Assuming that a fully-charged taxi can go 208 km (=260 km×(100%-20%)) before it needs another charge, an extra vehicle for single-shift taxis would only have to provide 77 km (=285-260 km) to satisfy the consumer travel demand (note that an average distance traveled per day for single-shift taxis is 285 km).

BEV fleet with battery swapping

In this scenario, the fleet relies upon battery swapping stations to replace depleted batteries with fully-charged batteries within a few minutes (about the same time required to refuel a gasoline vehicle). Battery recharging rate and battery stock quantity determine the maximum number of fully charged batteries a swapping station can provide each day. Based on the commercialized battery swapping services in Beijing, battery swapping stations are assumed to have 28 swappable batteries in stock and host 28 chargers [163], each with 1/3 C rate (i.e., three hours for a full charge), used to charge the swapped-out batteries with remaining 20% state of charge[20]; this implies that each swapping station, ideally, can provide about 280 swaps per day, about one fully charged battery every five minutes.

ICEV fleet with gasoline refueling

This is a business-as-usual scenario in which the taxi fleet uses ICE-powered vehicles and replenishes the vehicle energy within a few minutes via gasoline refueling.

6.2.2 Cost components

We examine the value proposition of various business models through the lens of applicable expenditures. These include vehicle procurement, battery, extra battery, electricity, recharging system, land, maintenance, labor, opportunity, and gasoline refueling costs, each of which are fully described in this section. Table 5.1 shows a list of governing parameters applied in our investment appraisal for the taxi business; the exchange rate for USD/Yuan is set to be 6.32. BAIC BJEV EU260 is chosen as the representative BEV taxi due to its capability to be delivered either for battery swap mode or BEV charging modes [166].

1) *Vehicle procurement cost* is the upfront cost to purchase a base car (i.e., BEV without battery). The battery cost is separately taken into account in its own category.
2) *Battery cost* accounts for battery usage for delivering kilometers and is determined by the battery's cycle life, degradation, production volume, and mechanical complexity. Cycle life is the number of complete charge/discharge cycles a battery can support before its capacity falls

[20] Zou et al. (2016) showed that the majority of the electric taxis drivers in Beijing charge their cars when the available driving range drops to about 55 km. Thus, we assume that battery's state of charge at the start of charging events is 20% (~55 km/260 km) and end up with 100% across all the business models in this study.

below 80% of the charge envisioned by the manufacturer. Today, a standard BEV battery warranty covers 150,000 km. Presumably, the warranty is quite conservative; most BEV batteries will actually last significantly longer. We assume that the warranty includes a factor of 2 safety factor, so an average battery is assumed to last about 300,000 km with Level 2 charging before it needs to be replaced (sensitivity analysis is performed to address the uncertainty in this safety factor assumption; see Chapter 5.3.1). For the business case using the swapping technique, we assumed its lifetime is the same as that of Level 2 charging; this is because, according to the swap station designers, swappable batteries are charged in the optimal condition (i.e., constant humidity and constant temperature), and thus the battery life can be maximized (Aulton.com 2019). However, if the battery is routinely charged using a fast charger, its lifetime would be degraded by 20% to 30% [144]. We assume that average battery with fast charging lasts for 225,000 km (i.e., degradation by 25%) before it needs to be replaced.

Due to the lower production volume and higher mechanical complexity, a swappable battery pack cost was reported to be $383/kWh in a BEV with the model year (MY) 2017 [163], being ~$95/kWh more expensive than more widely produced non-swappable batteries[21]. Battery prices are expected to drop significantly over the next decade as production volumes increase [81]. This incremental cost of $95/kWh is also expected to decrease as the battery swapping scale increases in the future.

3) *Extra battery cost* is the capital investments for the batteries in the extra vehicles and for the battery inventory in the swapping stations.
4) *Electricity cost* quantifies the electrical expenditures associated with charging batteries. The current commercial electricity price during the normal time period (aka. non-peak and non-off peak) in Beijing is used in our analysis ($0.135/kWh) and charging efficiency is assumed to be the same across different BEV recharging options.
5) *Recharging system cost* monetizes the costs (excluding land) associated with building a recharging system. These costs include building construction, charging mechanism procurement and associated installation. The cost of running power lines to the charging station is not included; it is assumed this is covered by the electricity cost. The cost of a fast charger

[21] We use a lithium-ion battery pack price of $288/kWh in 2016 to represent the non-swappable battery cost in a BEV with MY 2017 [81].

is about 20 times as much as a Level 2 charger (Wang 2016). The recharging system costs of battery swapping stations do not include the expensive battery inventory requirement (28 swappable batteries are assumed in this study) (Zhou 2016), which is considered in the extra battery cost category.

6) *Land cost* quantifies expenditures for the land used for rechargers. For BEV charging alternatives (i.e., Level 2 and fast charging), the land/vehicle ratio is similar to that of a parking garage [165]. Battery swapping stations require larger space for higher swappable battery housing requirement – an inventory of 28 swappable batteries and 28 chargers [163]. However, since each vehicle spends only a few minutes at the swapping station, the land requirement per vehicle in the fleet is much less than the other recharging options. A swapping station's land/vehicle supported ratio[22] is about half as much as a fast charger and only one-tenth as much as needed for a fleet using Level 2 chargers.
7) *Maintenance cost* is the cost associated with maintaining the charging/swapping station. The annual maintenance costs are assumed to be 10% of recharging system costs [167,168].
8) *Labor cost* is the drivers' revenue when operating on the roads. In Beijing, taxi drivers pay taxi companies a monthly fee to "rent" the vehicles. The operating revenue (before deducting the costs) for a taxi in Beijing was shown to be 34.5 ¢/km, and about 62% of which is for taxi driver[23] while the rest 38% is for taxi companies [162]. Therefore, this study uses 21.4 ¢/km as a per-km labor cost to taxi companies for operating taxis on the roads. Note that the labor cost while recharging is taken into account separately, in the opportunity cost category, as discussed below.
9) *Opportunity cost* is the operating revenue lost by a taxi company owing to the idle time that taxis and drivers spent on recharging/refueling. These costs exclude fluctuations in consumer demand based on time of day and days of the week.
10) *Gasoline refueling cost* represents the business-as-usual gasoline taxi energy replenishment cost, which is computed using the retail gasoline price in Beijing.

[22] Land/vehicle supported ratio is defined as the land use per vehicle actively charging; parameters are shown in Table 1.

[23] Note that the taxi drivers *net* earnings in Beijing are the revenues minus the sum of the monthly rent fee to the taxi company, the operating fuel costs, and the vehicle maintenance costs.

Table 6.1. Governing parameters used in the study and the sources

Parameter	Value	Source
BEV Model (BAIC BJEV EU260)		
MSRP ($)	32,600	[166]
Fuel Economy (kWh/100 km)	15.9	
Battery Capacity (kWh)	41.4	
Driving Range per Full Charge (km)	260	
ICEV Model (BAIC Senova D50)		
MSRP ($)	15,340	[166]
Fuel Economy (on-road) (L/100 km)	7.5	
Driving Range per Full Refuel (km)	670	
Retail Gasoline Price ($/L)	1.14	[169]
Refueling Time for 536 km (gas tank from 20% to 100%) (Minutes)	4	Assumption
Taxis in Beijing		
Fleet-Average Daily Distance Driven (km)	400	[162]
Distance Driven per Active Hour of Taxi Time (km/hours)	23.8	[162]; footnote 2
Vehicle Lifespan (Year)	6	[170]
Annual Productivity (Days)	350	[171]
Operating Revenue (¢/km)	34.5	[162]
Labor Cost (¢/km)	21.4	
Discount Rate for Cost of Capital (%)	5	[123]; Chinese central bank's interest rate for long-term (i.e., more than five years) loans.
Recharging Vehicle Attributes		
Changes in State of Charge (%)	20 - 100	[159]; footnote 4
Range per charge (km)	208	Assumption
Recharging System Attributes[24]		
Level 2 Charging Rate (kW)	7	[161]
Fast Charging Rate (kW)	45	
Swap Station Battery Inventory (#)	28	[163]
Swap Station Battery Charging Rate (kW)	14	Assumption

[24] Uncertainties in the recharging system attributes (i.e., land use and system cost) are assumed to be uniformly distributed over the range; a Monte Carlo cost model is run with 1,000 runs for each of the business cases and the resulting mean values are presented in Results & Discussion (Chapter 6.3).

Recharging Time with Level 2 for 208 km (Hours)	4.8	Estimation based on the parameters shown in Recharging Vehicle/System Attributes
Recharging Time with Fast Charge for 208 km (Minutes)	52.5	
Recharging Time with Swapping for 208 km (Minutes)	5.1	
BEV Charging Land Use (m^2/plug)	25 - 40	[161,165]
Level 2 Charging System Cost ($/plug)	820 - 1,300	
Fast Charging System Cost ($/plug)	16,300 - 24,200	
Swap Station Land Use (m^2/station)	150 - 200	[163]
Swap Station Cost ($/station)	997,400	
Battery Inventory Cost ($/station)	443,970	
Recharging System Lifespan (Years)	8	Assumption
Unit Land Use Cost ($/$m^2$)	3,530	[172]
Land Use Lifespan (Years)	40	
Electricity Cost ($/kWh)	0.135	(Beijing Municipal CDR, 2018)
Battery Parameters		
Non-swappable Battery Cost (Car Model Year 2017) ($/kWh)	288	[81]
Swappable Battery Cost (Car Model Year 2017) ($/kWh)	383	[163]
Level 2 Battery Cycle Life (Cycles)	1,155	Assumption based on the battery warranty.
Fast Charge Battery Cycle Life (Cycles)	865	[144]; 25% lower than that of Level 2 charging
Swappable Battery Cycle Life (Cycles)	1,155	[174]; swappable battery lifespan is maximized because being charged in an optimal condition.

6.2.3 Conversion into per-kilometer costs

To assess the cost-effectiveness across the business models, each cost component is transformed to be on a per-kilometer (per-km) basis by applying conversion factors. Conversion factors vary depending on the cost component and the achievable throughput of the recharging systems. To combine upfront investments and operating costs into a single number, we distributed all costs over all kilometers by using a 5% discount rate to determine the cumulative costs per kilometer. The calculation framework is demonstrated in Table 6.2, and the governing equations are shown in Appendix C. Each vehicle/trip served corresponds to a driving range of 208 km. For the cost

components of recharging facility (including recharging system, land, maintenance, and battery inventory in swapping stations), an annual number of vehicles served is determined by 1) recharging times and 2) utilization factor that captures the real-world efficiency discounts related to infrastructure utilization. On the other hand, for the cost components of vehicle (including vehicle procurement and batteries in the extra vehicles), annual number of trips served is determined by 1) recharging time, 2) active hour of taxi time per charge (i.e., operating hours for 208 km), and 3) utilization factor that describes how intensively a vehicle is used. Recharging times with Level 2 charger, fast charger, and battery swapping for 208 km are indicated in Table 6.1. An active taxi drives 208 km in 8.74 hours on average (= 208 (km)/ distance driven per active hour of taxi time (km/hours) = 208/ 23.8). Utilization factors are different between single-shift and double-shift taxis, as explained below (see Appendix C.I for more details):

- Vehicle: utilization factor for a vehicle is determined by the vehicle usage intensity; single-shift taxis would have lower vehicle utilization factor and so higher per-km vehicle procurement cost compared to double-shift taxis.
- Recharging facility: utilization would be very poor in single-shift BEV fleet relying on the conventional Level 2 charging. We expect that there would be one Level 2 charger for each single-shift taxi, but that charger would only be used for 4.8 hours at night (reaching full charge, 208 km of useful driving distance) plus another 1.8 hours mid-day (for 77 km), so the utilization factor would be only 27%.

  On the other hand, recharging behaviors of single-shift taxis working with fast chargers are uncertain; one would think that all the single-shift taxis would like to charge at the end of the day or early in the morning, but there will not be enough plugs at those peak hours. The ideal case would be fast chargers being uniformly used during the workday (i.e., 12 hours active hours plus recharging times for 285 km), and thus the utilization rate of fast chargers would be 55% at best. For single-shift BEV taxis relying on battery swapping, we expect that they will not use swap stations in the middle of the night. In the case that all BEV taxis use swap stations uniformly during the workday, the utilization would be about 50% at best. Because of real-world recharging scheduling problems and downtime for maintenance, the infrastructure utilization rate needs to be discounted further. Assuming there is an efficiency discount of 30% in reality even for an ideal recharging system, for single-shift taxis we estimate the utilization rate for recharging facilities could only achieve 39% and 35% in the

conventional fast charging and battery swapping modes, respectively. In contrast, utilization factors (or utilization rates) for recharging facilities would be much higher for a double-shift BEV fleet: we assume 90% for conventional BEV charging modes, and 80% for BEV charging with extra vehicles and battery swapping modes[25].

Table 6.2. A framework to transform cost components into per-kilometer (per-km) costs; labor cost data is provided on a per-km basis, so no conversion factor is needed. Equations for per-km cost evaluations are detailed in Appendix C.I.

Cost Component	Conversion Factor
Recharging System, Maintenance, Land, Extra Battery (for swappable battery inventory)	Annual number of vehicles served ~ *f* (recharging time, utilization factor for recharging facility)
Vehicle Procurement, Extra Battery (for extra vehicles)	Annual number of trips served ~ *f* (recharging time, active hours of taxi time, utilization factor for vehicle usage)
Battery	~ *f* (per-kWh battery cost, battery cycle life)
Electricity	~ *f* (battery capacity, driving range)
Opportunity	~ *f* (distance driven per active hour of taxi time, recharging time)
Gasoline Refueling	~ *f* (fuel economy)

6.3. Results & Discussion

6.3.1 Cost competitiveness comparison

Figure 6.1 presents the costs on a per-km basis across various BEV recharging modes for taxis with single and double 12-hour shifts, and compares these with the existing gasoline taxi system. The aggregation represents the total costs per kilometer incurred by taxi operators to run a fleet. It

[25] The recharging facility would be more heavily utilized when the time duration for each charge is longer (and thus the required number of coordinated BEV charging activities is fewer per day per plug).

is noted that we do not aim to include all cost components of the taxi business but rather, major expenditures. The key observations are highlighted as follows:

Cost breakdown

Firstly, labor cost is the most significant cost contributor, accounting for up to 68% of the total per-km costs in China's taxi business; we expect that the cost contribution from labor would be even higher in other well-developed countries. Secondly, per-km battery costs for the fast charging business models are higher than the Level 2 charging cases due to the higher degradation rate and thus shorter battery cycle life. However, per-km battery costs are comparable between fast charging and battery swapping even though battery lifespan in the latter is longer than the former; this is because the swappable batteries are more expensive per-kWh than mass-market non-swappable batteries. Thirdly, electricity costs on a per-km basis are the same among all scenarios, results from the assumption that electricity costs per kWh and charging efficiency are homogeneous across all the BEV recharging modes. However in reality, the electricity costs for fast chargers may be higher than the others due to the lower charging efficiencies (i.e., higher losses) from fast charging and potential demand charges [175].

And fourthly, per-km vehicle procurement (i.e., BEV without battery) costs are the same across different recharging modes for single-shift taxis because those BEVs—regardless of recharging options—are all able to deliver 285 km per day. However, these costs are various depending on the recharging options for double-shift taxis; vehicles relying on battery swapping can deliver higher number of trips per year than those using fast/ Level 2 chargers, causing per-km vehicle procurement cost in the swapping option to be the least, followed by the fast charging cases and then the Level 2 charging cases. We observe that per-km vehicle procurement costs are the same between conventional BEV charging scenarios and BEV charging with extra vehicles scenarios; this is due to the fact that the increased vehicle fleet size would not only increase the upfront costs but also increase the vehicle usage utilization rate (see Appendix C.I for more details). Finally, opportunity costs associated with the recharging times are nonnegligible when the taxis are relying upon conventional BEV charging (without extra vehicles), especially for those running double shifts per day. Note that the impacts of fluctuations in consumer demand on per-km opportunity cost are ignored due to data availability. But in reality, we can expect that the operating revenue lost due to the recharging time should be higher during periods of high demand in the day.

Total cost

For single 12-hour shift taxis (Figure 6.1(a)), most of the BEV recharging activities can be done when the drivers are not working. But since a taxi can only go 208 km for each charge, and single-shift taxis drive farther than that each day, the driver has to stop mid-day to get another (partial) charge. The idling time (or opportunity costs) for recharging[26] in the middle of a shift makes the conventional Level 2 charging mode at least 21% more expensive than the alternative BEV business models, so it is not economically attractive. On the other hand, the conventional fast charging and battery swapping options are found to be cost comparable to each other at present (the difference is within 3%), but single-shift BEV fleet relying upon fast chargers is expected to reach cost parity with ICE sooner (as discussed below).

For double-shift taxis (Figure 6.1(b)), conventional Level 2 charging with drivers idling during the time it takes to fully recharge the BEVs would not work. To meet customer demand, the taxi company could increase the size of the vehicle fleet. Although imposing higher upfront capital costs for the extra vehicles than the conventional Level 2 case, the Level 2 with extra vehicles scenario dramatically improves the cost-effectiveness of double-shift BEV taxis by mitigating the idle time associated with slow charging, and even makes this business model a more attractive option than conventional fast charging, despite the latter boasting an 82% shorter charging time. However, these aforementioned scenarios (i.e., conventional Level 2, Level 2 with extra vehicles, and conventional fast) are all significantly more costly (by 11% - 64%) than the existing ICE-powered double-shift taxis. To make BEV taxi ecosystems more appealing to fleet owners running with multiple shifts, more efficient recharging alternatives are needed. Obtained results reveal that the fast charging with extra vehicles and the battery swapping scenarios are the two most economical business models among all the electrified energy replenishment options.

An important finding here is that battery swapping emerges as one of the least costly options on a per-km basis for both single-shift and double-shift taxis, although it imposes high aggregate upfront costs for its battery inventory requirement. Its fiscal attractiveness is mainly due

[26] Single-shift taxis are expected to spend shorter recharging times on partial (instead of full) charge for another 77 km (=285-208 km) in middle of their daily shift. The opportunity costs of charging that 77 km are amortized across 285 km when we calculate per-km opportunity cost for single-shift taxis.

to a swapping station's ability to serve 10 times as many BEVs as a fast charger and 56 times as many BEVs as a Level 2 charger. Despite the BEV taxis ecosystem still being more costly than the business-as-usual ICEV fleet at the moment, these incremental costs will be shrinking as the battery costs drop in the future. We assume that the cost difference between swappable battery and non-swappable battery (i.e., $95/kWh in 2017) would follow the same learning rate that was found in non-swappable battery production [81], decreasing over time when the scale of battery swapping increases. Based on BAIC BJEV's timeline for their swapping service deployment[27], we estimate that when the non-swappable battery cost for car MY 2022 is $176/kWh [81], the swappable battery cost will be around $220/kWh. These cost improvements in batteries will drive the BEV taxi ecosystem recharged by either battery swapping (for double-shift taxis) or fast chargers (conventional fast for single-shift and fast with extra vehicles for double-shift taxis) to achieve cost competitiveness with the existing ICE-powered system in Beijing in 2022.

[27] There was about two-year time delay between BAIC BJEV's first stage—100 swapping stations and 4,000 vehicles being in operation—in Optimus Prime Plan and their actual battery swapping service implementation [176,177]. Hence, we expect and assume that the second stage—1,000 swapping stations and 100,000 vehicles—will not be completely fulfilled until 2022 (two years later from the planned schedule). This production expansion is estimated to reduce the cost difference between swappable batteries and non-swappable batteries to $44/kWh.

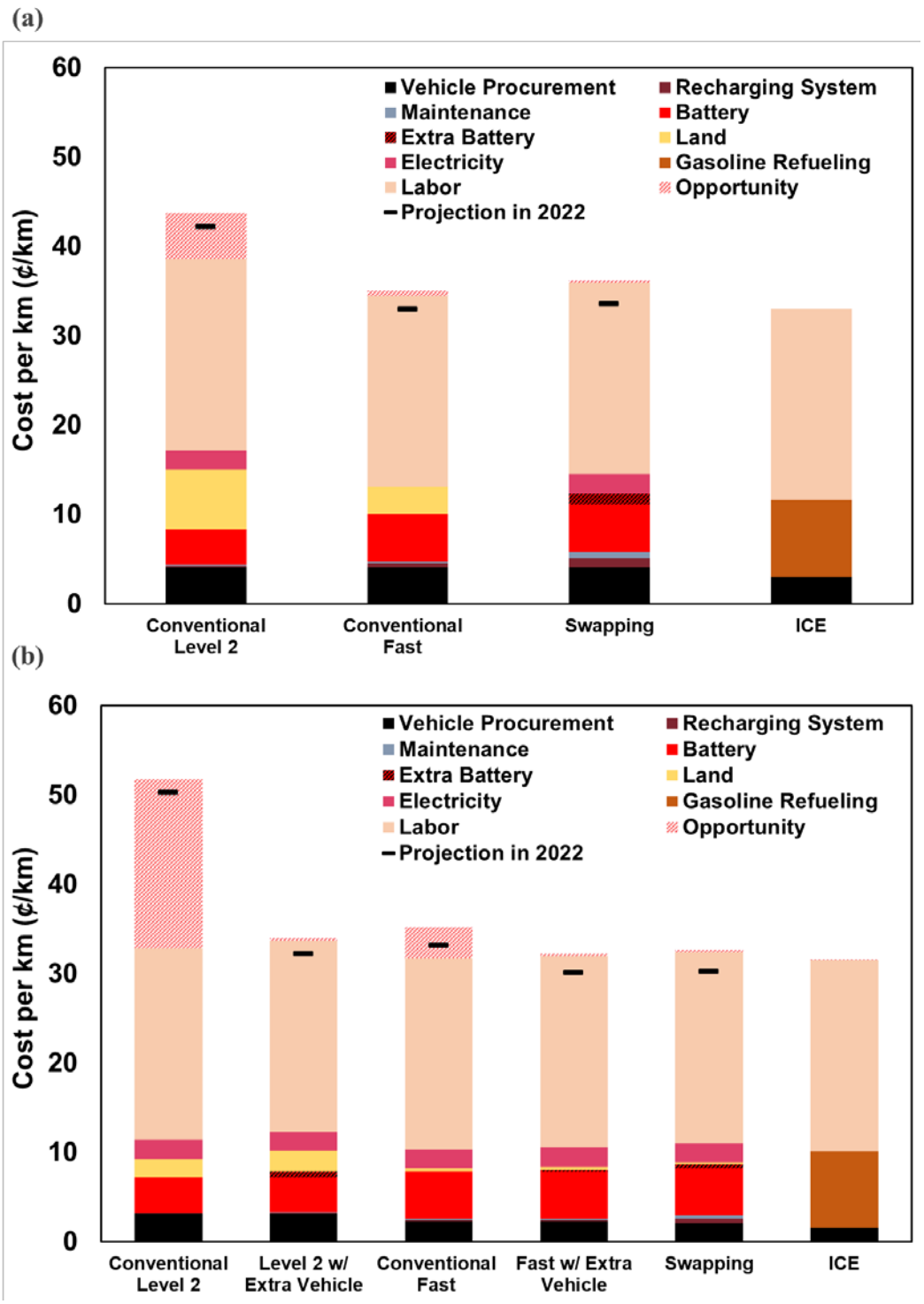

Figure 6.1. Cost breakdown per kilometer of different recharging/refueling options for (a) single-shift taxis and (b) double-shift taxis using the financial numbers in Beijing. For electric taxis with double shifts to meet consumer demand, a larger vehicle fleet is needed if

they rely on conventional BEV charging, since a significant fraction of the taxis will be out of service (recharging).

Sensitivity analysis

The total cost comparisons presented above (Figure 6.1) rely on a number of parameters (Table 6.1). We use a tornado diagram (Figure 6.2) to illustrate how the cost ratios (i.e., BEV taxi ecosystems relative to ICE-powered taxi system) are conditioned by the assumptions. The major parameters here are battery cost, battery cycle life, equipment life, electricity cost, gasoline price, annual maintenance cost, and discount rate. For brevity, we focus only on the sensitivity of per-km costs for double-shift taxis (excluding conventional Level 2 charging option that is not feasible) to the assumptions. The sensitivity range for each variable is based on the low and high values provided in Appendix C.II. The governing parametric values from Table 6.1 are used to calculate the base of the tornado diagram (grey vertical lines in Figure 6.2).

Figure 6.2 shows that the three variables with the largest impact on the per-km cost ratios are gasoline price, battery cycle life, and battery cost. It is noted that higher gasoline prices and longer battery cycle life correspond to a lower cost ratio. The sensitivity analysis reveals several findings. Firstly, the cost competitiveness of per-km cost for ICEV and BEV taxis is highly dependent on location. This is because gasoline price varies widely across countries. Compared to the U.S. (with gasoline price of $0.77/L), many countries levy substantially higher fuel taxes for multiple reasons—including energy security, local air pollution, climate change, and government revenue. BEV taxis are found to be already financially more attractive than ICEV taxis in countries with very high gasoline tax such as Norway (with gasoline price of $2.28/L). Secondly, even doubling battery cycle life (i.e., doublling safety factor for battery warranty—from 2 to 4) or reducing battery cost by half, BEV taxi ecosystem could not achieve cost parity with ICEV taxi system unless with the business models of either battery swapping or fast with extra vehicles. Thirdly, electricity price is also an important factor even having less influence on the per-km cost ratio than the top three variables. Low electricity prices could make an electrified taxi fleet relying on the right recharging systems/operations on par with their gasoline-powered counterparts.

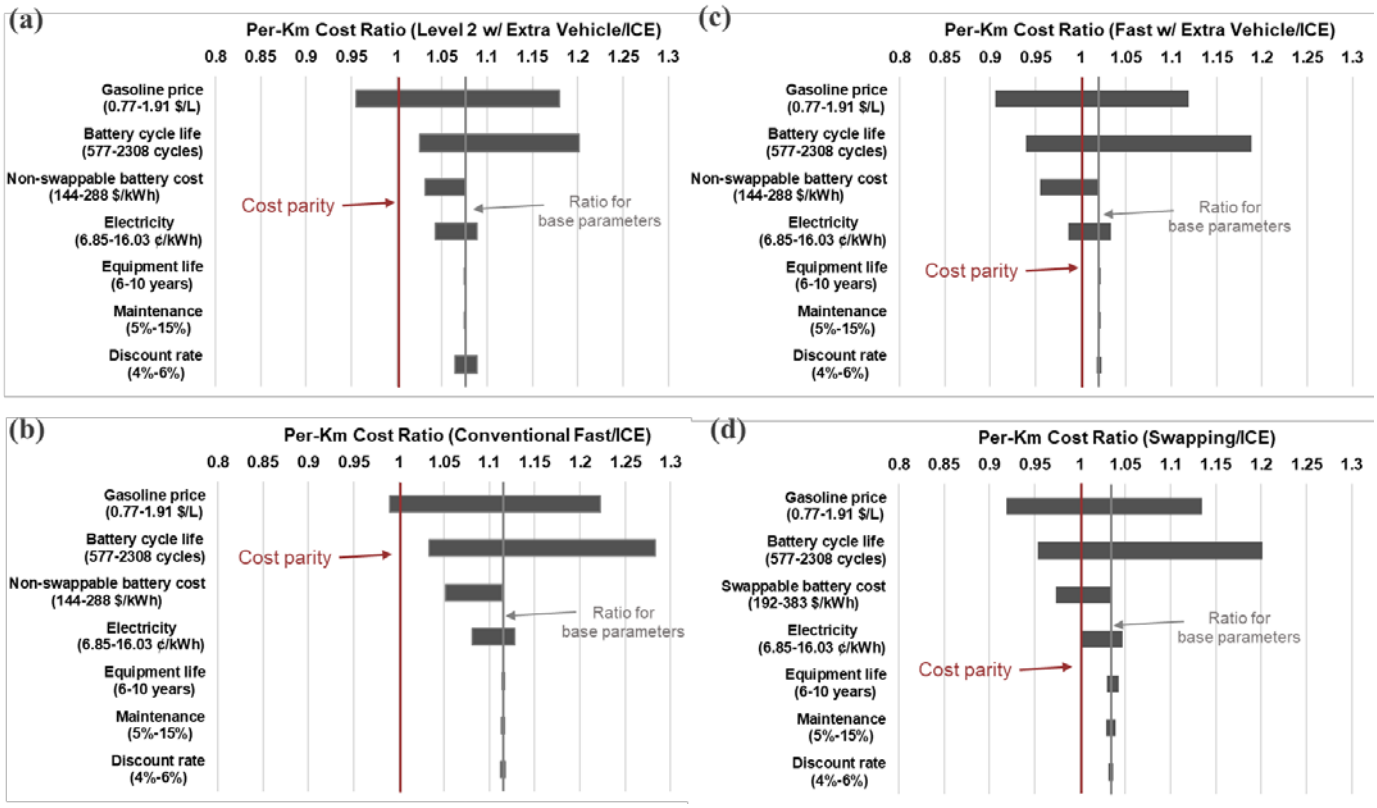

Figure 6.2. Sensitivity of per-kilometer cost ratios of double-shift BEV taxi ecosystem relying on (a) Level 2 charging with extra vehicle; (b) conventional fast charging; (c) fast charging with extra vehicle and (d) battery swapping relative to ICE-powered taxi system with respect to major parameters.

6.3.2 Policy analysis and implication

Currently, BEV taxi ecosystems – independent of recharging options – are more expensive than existing ICE-powered systems. Yet, gasoline consumption is associated with numerous negative externalities: reduced energy security, increased greenhouse gas emissions and diminished quality of life and public health due to local air pollution. To achieve environmentally sustainable ground transportation, local governments are taking a variety of actions to accelerate the adoption and use of electrified vehicles. In several cities all or a portion of the taxi fleet has been mandated to be electrified; this with present-day economics typically reduces net revenue by the taxi fleet or requires an increase in fares paid by passengers, though as shown above this economic impact is expected to become much smaller or vanish entirely in the next decade. In this section, we discuss

some government policies that could be utilized to close the cost gaps between the proposed BEV fleet alternatives and the existing ICEV fleet system.

Purchase subsidy

Procurement subsidies are the most common policy employed by national governments – particularly in China – to incentivize widespread BEV adoption. In 2017, the central and Beijing municipal subsidies for electric taxi operators totaled up to about $18,370 per vehicle[28], the use of which puts BEV taxi purchase costs on par with their gasoline-powered counterparts [178]. Thanks to the government's financial assistance, a subsidized electrified fleet is already per-km cost comparable to ICEV fleet, if they rely upon fast chargers (conventional fast for single-shift and fast with extra vehicles for double-shift taxis) or battery swapping techniques (for double-shift taxis). Although Level 2 with extra vehicles business model particularly benefits from BEV purchase subsidies because of its largely increased size of the vehicle fleet, it still cannot become economically favorable. The magnitude of this benefit varies according to BEV recharging options, as summarized in Appendix C.III. However, paying subsidies puts strains on government budgets and is not a sustainable expenditure policy for achieving the goal of high electrification of transportation.

Gas tax

Instead of paying subsidies, an alternative policy instrument that could be implemented to stimulate BEV adoption by fleet owners is raising a gas tax to fund BEV recharging infrastructure in a revenue-neutral manner. It was demonstrated that people would be more likely to accept a gas tax increase if they understood that the extra revenue would be used for energy efficiency [179]. While raising a gas tax would affect the whole car market (not specific to the taxi industry), this will have a much more significant effect on taxis than private cars because taxis consume much more fuel. We estimate that a 10% increase in retail gasoline price or 22% increase in gasoline tax (i.e., $0.11/L increase) would increase the cost/km of an ICEV taxi fleet by 3%; the gas tax needed

[28] The first-stage subsidy for general BEV purchase is linked to the driving range (e.g., about $10,450 for range greater than 250 km in Beijing, 2017). On top of that, there was a second stage of financial incentives for electric taxis in 2017 to cover the remaining cost gap between BEVs and counterpart ICEVs, which was up to $7,916 (=50,000 Yuan).

to close the cost gap between ICEV and BEV fleet is discussed below (Figure 3). Raising a gas tax (which internalizes the negative externalities of gasoline consumption) diminishes the current cost advantage hold by ICEV fleet and also generates extra revenue that the government can direct toward promoting an electrified transportation system. Government support that scales up battery production volume, is key to driving the cost of batteries down, making them more economically competitive.

While shifting to the electric fleet ecosystem would impose a heavy burden on taxi business owners during the transition period, the per-km cost differences between BEV taxi (with the most economical recharging options) and ICEV taxi are marginal and will drop further as the battery production increases. Figure 6.3 depicts the additional gas tax (relative to China's gas tax level of about 50¢/L [180]) needed to cover the incremental cost incurred due to the fleet electrification, given the various conditions of battery cost. Although BEV taxi fleet relying upon fast chargers (conventional fast for a single shift; fast with extra vehicles for double shifts) requires minimum extra gas tax imposition compared to the other options in 2017, we find that per-km cost of battery swapping will improve at an even faster rate when the battery costs drop. We compute that when the non-swappable battery cost decreases to $250/kWh (/$220/kWh) or the swappable battery cost drops to $310/kWh (/$180/kWh), double-shift (/single-shift) BEV taxi ecosystems relying on fast charging with extra vehicles (/conventional fast) or battery swapping will achieve cost parity with the existing ICEV taxi system. On the other hand, electric taxis recharged by conventional Level 2 or conventional fast chargers without extra vehicles are very unlikely to become economically favorable to fleet owners in the next decade unless being strongly supported by a high gasoline tax[29]; this finding highlights the importance of supporting the right business models in order to accelerate the fleet transition to electric drive.

[29] Our previous study predicted that the non-swappable battery pack price would fall to about $124/kWh by 2030 [81]. By incorporating the battery price projections with the gas tax analysis, we find that double-shift BEV fleet relying on Level 2 charging with extra vehicles will be cost-competitive with ICEV in 2030. However, double-shift (/single-shift) BEV fleet relying on conventional fast (/conventional Level 2) will still need a 16% (/223%) increase in the gas tax to reach cost parity with an ICEV taxi fleet.

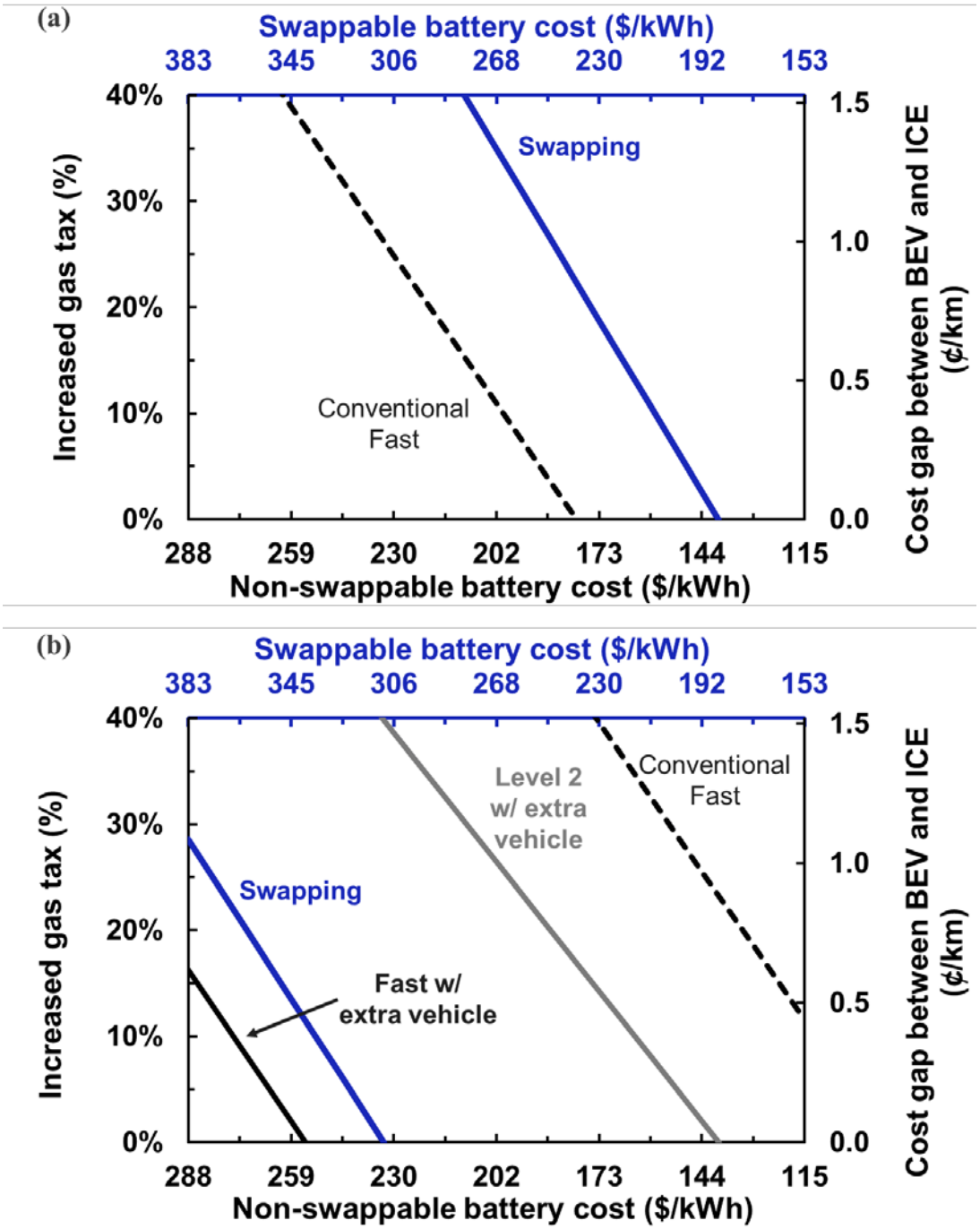

Figure 6.3. Increased gas tax needed (left ordinate; relative to 50 ¢/L) to close the cost gaps (right ordinate) between the existing ICEV taxi system and BEV taxi ecosystems with (a) a single shift or (b) double shifts per day at different levels of battery costs (x-axes). Each increment in the x-axes represents a 10% decrease in battery costs relative to the base year 2017 level (i.e., $288/kWh for a non-swappable battery and $383/kWh for a swappable

battery). This policy analysis emphasizes the importance of choosing the right recharging business models for the electrified fleet.

6.4. Conclusion

Although vehicle electrification offers a wide range of societal benefits, high opportunity costs tied to the charging times remains an impediment to widespread electric fleet adoption. These costs are not insignificant, raising concerns about the technology's commercial viability. This chapter demonstrates the potential for alternative BEV recharging modes to assuage these concerns.

We propose alternative business models—e.g., BEV charging with extra vehicles— that enable double-shift taxis to keep operating on the road generating revenue by having a sufficient extra number of charged and readily available replacements. Adoption of this strategy imposes higher capital costs, but helps avoid the high opportunity costs associated with Level 2 charging, dramatically improving the performance of the Level 2 charged fleet ecosystem. This, combined with the improved battery lifespan, ultimately makes Level 2 charging with extra vehicles mode a more attractive option than conventional fast charging. A BEV fleet with these aforementioned business models is still much more expensive (by 11% - 64%) than the existing gasoline-powered taxi system. For BEV taxis to compete on price and performance with ICEV taxis, we find that a more economical recharging option—either fast charging with extra vehicles or battery swapping—is needed for taxis with multiple shifts per day. Although the battery swapping scenario requires higher upfront investments, it emerges as a cost-effective alternative on a per-kilometer basis; this is mainly because of the ability of swap stations to serve a higher number of BEVs than a Level 2/ fast charger. Indeed, battery swapping at this moment does not seem suitable to the market for privately owned vehicles owing to the big concern of cross-brand compatibility and battery ownership, but our analysis shows that it is already economically competitive in large dense closed systems.

Electrified taxi ecosystems are currently strongly supported by government subsidies and even driven by mandates in a few Chinese cities—such as Beijing, Taiyuan, and Shenzhen [181]. Yet as battery technology becomes more mature in the future, the incremental costs of BEV over ICEV will be shrinking owing to the dropping battery costs. We ascertain that cost parity will be achieved by 2022 for BEV taxi fleets relying upon either battery swapping (for double shifts) or

fast chargers (conventional fast for a single shift; fast with extra vehicles for double shifts). Considering the fact that paying subsidies is an unsustainable government policy and enforcing mandates might not be suitable to many other cities, we investigate an alternative policy lever—raising the gasoline tax to support the recharging alternatives—that could incentivize BEV use in the fleet industry. We demonstrate that with the right BEV recharging business models, the government could cover the cost gaps by modestly raising the gas tax. Moreover, the need for mandates or increased gas tax to support BEV taxi adoption will diminish in the coming years as battery costs drop rapidly.

In the future transportation sector, a major evolution will be the movement toward electric mobility, along with a growing BEV ridesharing market and (eventually) BEV autonomous vehicles being introduced to urban fleets. These transformations require efficient (or even fully automated) recharging mechanisms so that electric cars can always be on the roads satisfying people's travel demand. Furthermore, providing affordable tailpipe emission-free taxi/rideshare services would make cities healthier for residents and help reduce greenhouse gas emissions, making the whole society more sustainable and livable. This Chapter, using the real-world financial data in Beijing, demonstrates that a network relying on either fast charging with extra vehicles or battery swapping is essential to accelerate the electrification of high-use vehicles, providing the reference for urban transformations toward a sustainable future.

Chapter 7. How clean are electric vehicles? Impacts of sustainable mobility policy on oil demand, CO2 emissions, air quality, and public health in China

7.1 Introduction

Growing global awareness of the environmental impacts of combustion is accelerating electric vehicles (EVs) adoption; over 50% of the global EVs sales – a total of 1.98 million – in 2018 were in China [2]. China's fast-growing personal vehicle ownership has imposed negative externalities on society, such as national energy security concerns, global climate change, and air pollution. To achieve environmentally sustainable ground transportation, the Chinese government is promoting new energy vehicles via a variety of policies. Generous fiscal subsidies and tax incentives have helped EVs achieve ownership cost parity with counterpart internal combustion engine vehicles (ICEVs) in China in the period of 2016-2020 [182]. City-level car ownership restrictions with EVs exemption have further boosted the local EV demand in Beijing, Shanghai, Guangzhou, Shenzhen, Tianjin, and Hangzhou [13,128]; these megacities contributed about 50% of the national annual EV sales over the past few years [135]. While gradually phasing out the nationwide EV subsidies, the government has recently enacted the dual-credit policy (i.e., The Passenger Cars Corporate Average Fuel Consumption and New Energy Vehicle Credit Regulation; also called EV mandates) to force more fuel-efficiency and electrification technologies adoption in the passenger vehicle market [12].

Vehicle electrification offers clear national energy security benefits but unclear climate and air quality benefits, especially in China where coal-fired power generation has been the backbone of the electricity supply. EVs avoid tailpipe emissions of CO2 and air pollutants from fossil fuel combustion but may lead to greater emissions from the upstream stage of electricity generation. To tackle this issue, life cycle analysis is commonly adopted to compare lifecycle environmental impacts per distance driven among different types of vehicle technologies [183–186]. Several studies have incorporated bottom-up fleet models to assess the lifecycle energy demand and CO2 emissions from China's road transport, including both at the national level [187–189] and regional/provincial level [190–193]. However, all these studies focused on the policy impacts

mainly on national security and climate change mitigation. A few studies have extended the bottom-up fleet-wide assessment to air pollutant emissions.

As a result of the increasing public concern for better air quality, there have been some comparative studies investigating lifecycle air pollutant emissions between EVs and ICEVs in China [194–198]. Still, the trends of aggregate air pollutant emissions under various fuel-efficiency and EV policies have not yet been extensively studied. Liang et al. [80] quantified the air quality and health impacts from fleet electrification in China, focusing on the mixed impacts of the decrease in vehicle tailpipe emissions and the increase in power plant emission during the shift from liquid fuels to electrification. However, ignoring the changes in the upstream emissions (also called well-to-tank emissions) from gasoline production may introduce significant bias in their calculations; this is because China's gasoline refinery is burning coal as the major process fuel, and in the absence of strict emission control standards, gasoline refining process is producing substantial emissions [198].

Great impacts are anticipated during the transition towards sustainable mobility in China. Considering that China is the global largest vehicle market (both for ICEV and EV), it is of timely importance to conduct a systematic and comprehensive evaluation of carbon emissions, air quality, and public health benefits under the current policy mix. The major novelties of this work are in the bottom-up model development and cross-scale information integration (Supplementary information D.I). The established framework captures how policy alters the vehicle ownership demand and its corresponding environmental externalities across spatial scales (from provincial to national) and time horizons (from 2017 to 2030). Given that few studies have addressed emissions from vehicle manufacturing process, this chapter, first, evaluates how the lifecycle emissions of counterpart vehicles with different powertrains (including ICEV, hybrid electric vehicle (HEV), plug-in hybrid electric vehicle (PHEV), and pure battery electric vehicle (BEV)) are varied across provinces. Second, more importantly, we explore the impacts of the sustainable mobility policy on the vehicle market, oil demand, climate change, air quality, and public health in China, considering geographical and socioeconomic differences.

In this study, we focus our evaluation on private passenger vehicle sector, which in part reflects a recognition that this is the segment that is likely to be most strongly and rapidly affected by fast-moving developments in advanced powertrains, alternative fuels, and environmental

policies. The future national-level private car population throughout 2030 is taken from our previous study [132], examining the impacts of policies promoting more energy-saving vehicles as well as electric vehicles deployment on private passenger vehicle market and EV adoption. Main policies considered in this chapter include the dual-credit policy (or EV mandates), city-level car ownership restriction policy (or quota policy), vehicle tailpipe emission standards, and power plant ultra-low emission standards. For brevity, throughout this chapter, we call these policies "*EV policies*." The main objective of this work is to study the environmental benefits of the EV policies in 2030. To assess the policy impacts, we design one scenario called "*NO EV POLICY COUNTERFACTUAL*" – representing a future in which nearly 100% of private vehicles are powered by gasoline (i.e., conventional ICEVs), with the national private car stock of 385 million. All policies promoting the development of EV and energy-saving ICEVs/HEVs are frozen; vehicle emission standards and fuel consumption rates stay the same after 2020. By contrast, "*CURRENT POLICY SCENARIO (CPS)*" is designed as a plausible EV penetration pattern with full implementation of current EV policies – representing a future in which vehicle market growth would be diminished owing to the EV policies, and the national EV sales in 2030 would achieve 37% market share. Projecting future EV sales at the province level is uncertain. In the CPS case, we expect that the markets having higher EV cumulative sales today, stronger EV policies (including EV purchase subsidies and green license plate for EVs), a greater variety of EV models, and more charging infrastructure will all reinforce those provinces' leadership position in the EV sales performance by 2030. In other words, we assume that the provinces that are currently leading the national EVs sales will continue to dominate through 2030 in the CPS case. So far, a limited number of provinces account for a majority of EV sales in China—Tianjin, Beijing, Zhejiang, Hubei, Shanghai, Sichuan, and Henan collectively contribute to about 50% of the current EV cumulative sales [88]. We derive the future provincial EV sales based on "open market index of new energy vehicle", which was proposed to describe the differences in EV brand/model variety and level of EV market penetration across provinces in China [199] (details are given in Supplementary information D.III). The uncertainties in future EV penetration rate and geographical patterns of EV population growth are addressed by developing two additional scenarios—one is with double EV adoption rate relative to CPS (i.e., 74% EV sales market share in 2030); the other one is similar to CPS but with homogeneous EV penetration pattern across China (i.e., all provinces are having the 37% EV sales market share in 2030).

7.2 Methodology and data

7.2.1 Lifecycle emissions comparison

The comparison of per-km lifecycle emissions is based on the reference compact 5-seat passenger vehicles, which were derived by taking the average of the selected best-selling comparable cars with the model year 2017 in our previous study [182]. The technical parameters of the reference vehicles are provided in Supplementary information D.II.

We assume a nominal lifetime distance traveled of 150,000 kilometers for all powertrains. However, for EVs, battery lifetime could differ from vehicle lifetime; in this comparison, we assume battery replacement happens once during the vehicle ownership period. Emissions from vehicle maintenance and end-of-life disposal are negligible compared to emissions from vehicle production and operation and thus are neglected in this analysis.

7.2.2 Private vehicle fleet market

The car stock and sales model at the national level [73] is briefly described below, and the impacts of the dual-credit policy on national fleet size projection were shown in our previous study [132]. For fleet size projection, this study disaggregates the existing national-level model by provinces for a more detailed level of granularity (Supplementary information D.IV.I), develops a gravity-based migration model to capture the future people flows across provinces (Supplementary information D.IV.I), but also incorporates the impacts of city-level car ownership restriction policy on China's provincial car fleet (Supplementary information D.IV.II).

The model calculates the total private car stock in year i ($\hat{V}_i$) by integrating across the entire range of car affordability index (A), the product of the income distribution density (I) and the propensity that an individual with that purchasing power owns a car (g):

$$\hat{V}_i = P_i \int_{A=0}^{\infty} I_i(A) g(A) dA \tag{1}$$

Where A = car affordability index, which is per-capita disposable income level (x) divided by car price index (p). P_i = population in year i. I_i = income distribution function for year i, simulated using the log-logistic function with a given Gini index and mean per-capita disposable income. The projected compound annual growth rate of per-capita disposable income at the provincial level is assumed to be the same as the per-capita GDP growth rate from the China Regional Energy Model (C-REM) [87]; due to limited data availability, provincial Gini index is assumed to be

constant from 2016 to 2030. $g(A)$ = Gompertz function describing the probability of owning a car as a function of affordability index. Fitting the Gompertz function (i.e., $g(A) = \gamma \exp(-\alpha\, exp(-\beta A))$) requires the estimation of three shape parameters— α, β, and γ—from historic data on household car ownership as a function of car affordability (Supplementary information D.IV.I).

Car sales were decomposed into new-growth purchases (associated with increases in car ownership due to rising income; also called first-time purchases) and replacement (for scrapped cars); the split between these two segments determines the maturity level of the auto market: in a mature car market, most car purchases are replacing retired vehicles.

7.2.3 Vehicle use intensity

Vehicle use intensity (always expressed as vehicle kilometer traveled (VKT) in China) is one of the key parameters determining the emissions of the vehicle fleet. Our understanding of China's VKT is very limited owing to the lack of data. In the absence of officially released data, we estimate vehicle use intensity based on the trends of car ownership level at the provincial level (Supplementary information D.V). We find that the annual VKT in provinces/ province-level cities having higher per-capita ownership levels (usually with higher economic development) is lower than the others. This phenomenon could be explained by several aspects: firstly, multicar households are more and more common as the household income grows, causing VKT per vehicle to decrease assuming that their demand for vehicle use does not change substantially (or at least car use does not increase linearly with the number of vehicles in the household); secondly, multiple traffic control measures have been enforced in major cities across China; thirdly, public transportation has been promoted in big cities having severe traffic congestion.

7.2.4 Emission factors

This study calculates the impacts on oil consumption and emissions (including CO_2, CO, VOC, NO_x, SO_2, primary $PM_{2.5}$) due to EV policy implementation from 2017 to 2030. The year 2017 is chosen as the base year since this is the latest available data year for power grid emission factors (EFs). All the needed information to compute WTW emissions are summarized below and detailed in Supplementary information D.VI.

Electricity generation

To balance the electricity supply and demand in grid operation, there are daily electricity transmissions between regional grids in China—mainly from west to east and from north to south. Impacts of this inter-provincial transmission on the provincial grid carbon intensity are found to be nonnegligible (Figure D7), especially for Beijing, Chongqing, Shanghai, and Guangdong. Thus, we take electricity transmission into account when examining the climate change mitigation potentials of vehicle electrification. For the future improvement in the carbon intensity of the electricity sector, we follow the expected decarbonization rates at the regional level that were documented in Shen et al. [186] (Supplementary information D.VI.I). At the national level, the carbon intensity of the power grid would decrease from 604 to 464 gCO2/kWh.

Tang et al. [200] measured power emissions using continuous monitoring systems network and found that China's power emissions of SO2, NOx, and PM dropped substantially due to the introduction of ultra-low emissions (ULE) standards policy in 2014. Considering that Tang et al. [200] had access to an unprecedented wealth actual emission data compared to any previous estimates [201–203], we take their 2017 estimated results as the base year EFs, and project future region-level air pollutant EFs by constructing the relationship between emissions and ULE compliance rate (Supplementary information D.VI.II).

Gasoline-powered vehicles

Based on China's "Technology roadmap for energy-saving and new energy vehicles", HEVs—belonging to energy-saving vehicles—are expected to start being adopted more widely, reaching a sales market share of 40% by 2030. The average label fuel consumption rate for new ICEVs and HEVs combined will achieve 5.8 L/100 km in 2020, 4.55 L/100km in 2025, and 4.0 L/100km in 2030 [204]. The fuel consumption gaps between label and on-road values for gasoline vehicles are assumed to remain -26% out to 2030 (i.e., the corresponding real-to-lab fuel consumption ratio is 1.26) [205]. Driving conditions affect fuel consumption significantly; we apply the fuel consumption index [206] to capture the real-world differences in fuel consumption levels across provinces in our calculations. More details about on-road fuel consumption rates are provided in Supplementary information D.VI.IV.

Tailpipe air pollutant EFs of gasoline-powered vehicles are affected by vehicle technology, climate, temperature, driving condition, fuel quality (e.g., sulfur content), and so on. This study derives provincial-level on-road air pollutant EFs based on a framework developed by Tsinghua University and the Chinese Academy of Environmental Sciences [207] (Supplementary information D.V).

7.2.5 GEOS-Chem air quality model and health impact assessment

We model air quality and health impacts in each scenario following the approach described in Chossière et al. [208] and summarized hereafter. For each scenario, monthly emissions are input into the GEOS-Chem air quality model [209–212] and configured at run-time using the HEMCO module [213]. We use MERRA2 meteorology [214] to drive the simulation. The GEOS-Chem air quality model is run at a 0.5°×0.625° resolution of over East Asia (about 320200 grid cells, and 133145 over China) with 47 vertical layers up to an altitude of 80 km. The boundary conditions for this domain are obtained using a global 2°×2.5° simulation. For each scenario, the model is run over a 15-month period, and we calculate results using the final 12 months. Health impacts are estimated using surface-level $PM_{2.5}$ and ozone concentrations. This study estimates changes in mortality and morbidity impacts. Surface-level concentration of $PM_{2.5}$ and ozone are then combined with population data to estimate exposure.

The mortality impacts associated with changes in exposure to $PM_{2.5}$ across China are estimated using the Global Exposure Mortality Model [215]. The health endpoints considered include ischaemic heart disease, stroke, chronic obstructive pulmonary disease (COPD), lung cancer, and lower respiratory infection. The PM2.5-attributed morbidity impacts are estimated using the log-linear function [216]. The health endpoints considered include hospital admission due to respiratory disease, hospital admission due to cardiovascular disease, chronic bronchitis, asthma attack, and emergency room visits for respiratory disease. For mortality impacts due to changes in surface-level ozone, we apply a log-linear concentration-response function, using parameters derived from Turner et al. [217]. This function relates exposure to 8-hour maximum ozone concentration (MDA8) to premature mortality from respiratory and circulatory diseases (ICD-10 codes I00-I99 and J00-J99) using a two-pollutant model adjusted for $PM_{2.5}$. The ozone-attributed morbidity impacts are estimated using the exposure-response function given by Feng et al. [218]; the health endpoints considered include hospital admission due to respiratory disease and asthma attack.

Baseline incidence rate in China for 1) the mortality health endpoints considered for $PM_{2.5}$ and ozone are taken from the Global Burden of Disease Study 2015 [219]; 2) the PM2.5-related morbidity health endpoints are taken from Maji et al. [216]; 3) the ozone-related morbidity health endpoints are taken from Feng et al. [218]. For each health endpoint, the relative risk for each age group is related to the number of premature mortalities following the well-established method [220–222] of the population-attributable fraction in each grid cell:

$$M_{d,a} = P_a \times B_{d,a} \times \frac{RR_{d,a}-1}{RR_{d,a}} \tag{2}$$

where $M_{d,a}$ is the number of premature mortalities from endpoint *d* and age group *a* in a given grid cell, P_a is the population in the age-group in that grid cell, $B_{d,a}$ is the baseline incidence, and $RR_{d,a}$ is the relative risk obtained using the concentration-response functions described above and in Supplementary Information D.VII.

7.2.6 Monetization of CO2 emission reduction and avoided health damage benefits

The benefits of climate and health stemming from EV policies (including the introduction of tighter emission standards and the adoption of energy-saving and new energy vehicles) are quantified in terms of the economic values of CO2 emission reduction and avoided health endpoints.

The economic benefits of reduction in CO2 emission are calculated based on *social cost of carbon* (SCC), a measure of the long-term damage done by a metric ton of CO2 emissions in a given year. The SCC of CO2 emissions in this study is assumed to be $59 (in 2017 value) per ton CO2 with a discount rate of 3% [223]. The economic benefits of reduction in premature death are computed based on *value of statistical life* (VSL), an indicator of *willingness to pay* (WTP) to avoid mortality risks. The economic benefits of reduction in morbidity-related health endpoints are estimated mainly using WTP and the cost of illness (COI) method. In the absence of sufficient local empirical studies for health cost estimation in China at the provincial level, we apply a benefit-transfer approach as described in the OECD report [224]. The key assumption of this approach is that people with higher incomes are willing to pay more to reduce health risks between populations. The province-specific health costs ($HC_{2030,p}$) values are estimated using Equation (3), where HC_{base} is the base value with health cost studies. For mortality ($\mathrm{HC} = \mathrm{VSL}$), we take the most recent local VSL estimation that was provided by a contingent valuation study performed in

Chengdu, China in 2016 as the baseline; the suggested VSL is 3.85 million Yuan with the disposable income ($Income_{2016,base}$) of 36,500 Yuan [225]. For morbidity ($\mathrm{HC} = \mathrm{WTP}$ or COI), we take the estimated health costs for Beijing or a national average in China given by Maji et al. [216]. Per capita disposable income for 2030 in each province ($Income_{2030,p}$) is discussed in Section 2.2. This study used a 0.8 value of income elasticity of health cost as recommended by OECD [226].

$$HC_{2030,p} = HC_{base} \times \left(\frac{Income_{2030,p}}{Income_{2016,base}}\right)^{Elastictiy} \quad (3)$$

7.3 Results and discussion

7.3.1 Current emissions for vehicles with different powertrains

Given the technical parameters of the reference vehicles shown in Table S1, we estimate CO2 emissions per kilometer for vehicles with different powertrains based on the current (i.e., base year 2017) electricity generation and transmission in China. Figure 7.1(a) shows that EV emissions per km are approximately 71% of the emissions of comparable ICEVs. Increased emissions from battery and fuel production are offset by increased powertrain efficiency. Second, HEV emissions per km, on average, fall between ICEVs and EVs. However, the carbon footprint benefits of EVs relative to ICEVs are uncertain, mainly depending on the power grids EVs are recharging from. Errors bars for EVs represent the variation among provinces in CO2 intensity of electricity generation. Third, PHEVs and BEVs have similar carbon footprints under the current situation in China. For this analysis, we use HEV emissions as the baseline reference because in future scenarios with strong fuel-economy policies, we expect HEVs will be dominant vehicle type..

Figure 7.1(b) presents how the ratio of per-km BEV emissions to per-km HEV emissions varies across provinces, in terms of vehicle lifecycle emissions. In the northern and northeastern provinces such as Inner Mongolia, Jilin, Hebei, and Shanxi, the carbon footprints of BEVs exceed those of HEVs by more than 10%; this is due to the fact that the power grids in these regions are highly relying upon fossil fuels. On the other hand, BEVs driven in the southwestern provinces where hydropower accounts for a significant proportion in the electricity mixes, such as Yunnan, Sichuan, Hubei, Guizhou, and Qinghai, could reduce CO2 emissions by more than 30% compared to HEVs. More importantly, in the provinces that currently lead in EV sales, we find that EVs do not have noticeably greater climate benefits than HEVs. Collectively, Beijing, Shanghai,

Guangdong, Shandong, Zhejiang, and Tianjin accounted for 65% of the cumulative EV sales by the end of 2017 (with 24% of the total population in China), but the average carbon footprint of a BEV in these provinces is only 6% less than that of an HEV (the ratio ranges from 0.82 to 1.07).

Despite the advances made in understanding provincial variations in the carbon footprints of EVs, this part of the work still has its limitations that require further investigation. The embedded assumption here is that the marginal increase in electricity consumption due to plugging in an EV in a province has the same carbon footprint as the current carbon footprint of electric grid in each province. In theory, we should use the marginal grid mix instead of the average grid mix to determine the impacts of adding new loads to a utility grid owing to EV charging. However, due to the lack of needed information (e.g., electrical load profile, charging times, and charging rates) and the uncertainty in future power grid development (e.g., whether ultra-high-voltage (UHV) transmission technology can make Chinese power grid highly connected), and because identifying the current and future marginal electricity source is out of the study scope, we use the average carbon intensity of electricity generation in each province to approximate marginal displaced emissions.

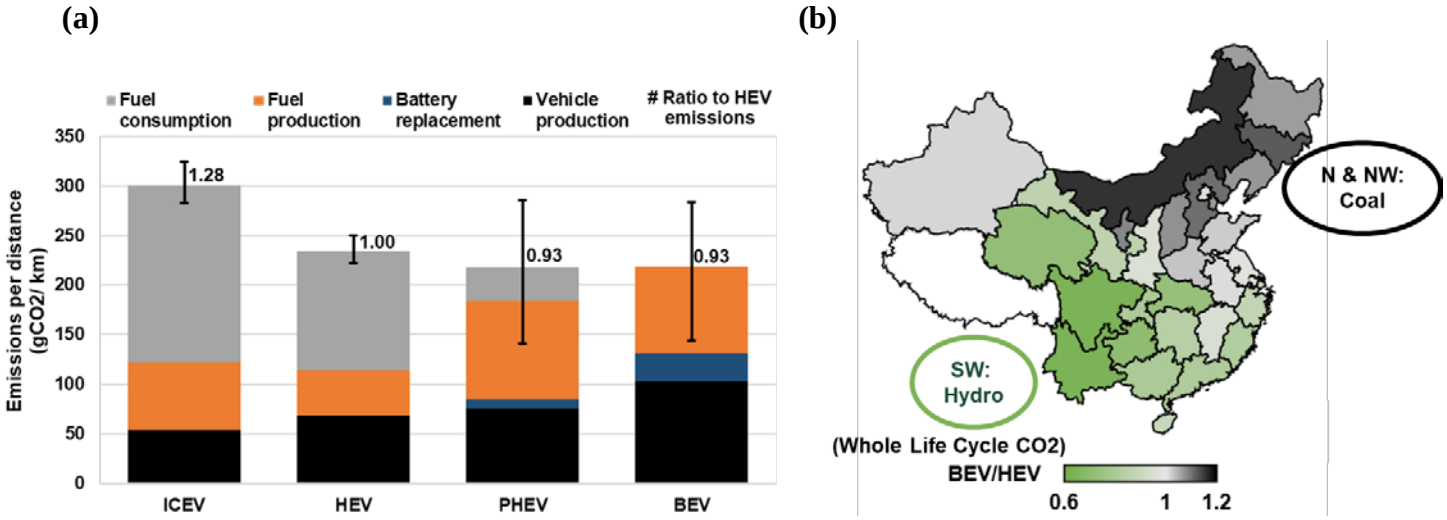

Figure 7.1. Whole life cycle CO2 emissions comparison in 2017. (a) Per-kilometer CO2 emissions for cars with different powertrains; (b) Provincial BEV-to-HEV ratios of CO2 emissions

Note: Based on 150,000-km life for all powertrains; BEV emissions are based on the average carbon-intensity of China electricity (604 gCO2/kWh) in 2017; 76% of kilometers traveled by PHEV are powered by a battery [124]*; emissions from battery replacement are derived based on 2017 situation; error bars in (a) are from provincial*

differences in on-road fuel economy and electricity mix; interprovincial electricity transmission is considered when deriving BEV carbon footprints.

Unlike climate benefits, the potential for BEVs to reduce air pollutant emissions compared to ICEVs and HEVs is very clear, as shown in Figure 7.2. Note that Figure 7.2 is comparing fuel life cycle emissions (or WTW emissions) for vehicles with model year 2017, excluding emissions from vehicle production stage due to the local data availability. However, considering the fact that BEVs are only having slightly higher aerial pollutant emissions from vehicle manufacturing stage than that of ICEVs [197], we expect the impacts of excluding vehicle manufacture emissions on the relative air pollutants reduction potentials among different types of vehicle technologies are likely to be small. WTW emissions of CO is primarily attributed to the TTW process for gasoline-powered vehicles; tailpipe exhausts contribute half of the WTW VOCs emissions of gasoline-powered cars. Vehicle electrification can significantly reduce CO and VOCs emissions, primarily due to lower emission factors for power generation relatively to fuel lifecycle of gasoline consumption. Most of the NOx, SO2, and primary PM2.5 emissions associated with gasoline are not being emitted from the tailpipe, but instead are WTT emissions, mostly from Chinese refineries, many of which burn coal for process heat. Passenger car emissions are now tightly controlled by the stringent China 5 tailpipe emission standards implemented nationwide in 2017. Tighter emissions controls on refineries are needed to reduce air pollution in nearby cities. Given substantial emission reductions found in Chinese power plants after the introduction of ultra-low emissions standards, EVs are estimated to reduce all types of criteria emissions compared to the gasoline counterparts. Note that this study considers only combustion emissions due to the lack of test data for emissions from brake and tire wear.

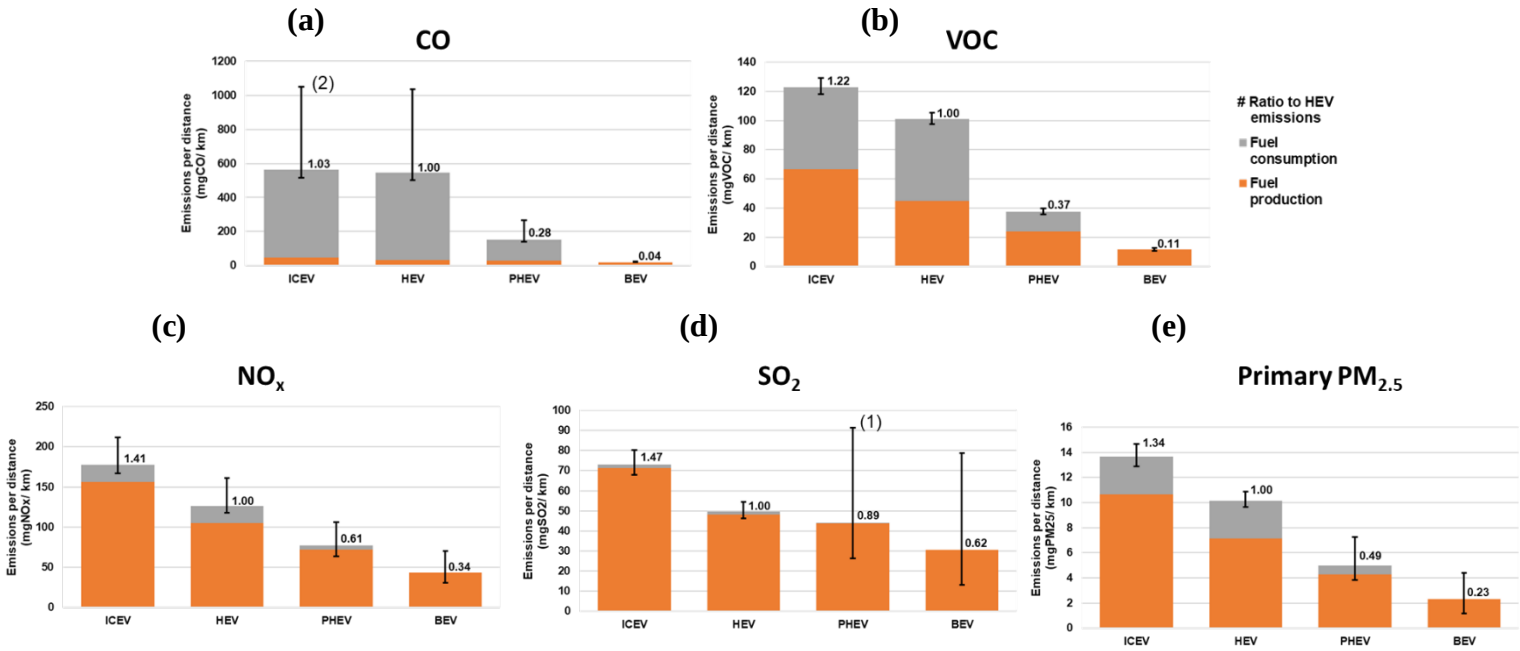

Figure 7.2. Air pollutants (a) CO (b) VOC (c) NOx (d) SO2 (e) primary PM2.5 emissions per kilometer for cars with different powertrains and with model year 2017

Note: This is well-to-wheel (WTW) emissions for vehicles; Error bars are from provincial differences in on-road emission factors (varying by temperature, altitude, and humidity) and power plant emissions (varying by compliance rate of ultra-low emissions (ULE) standards). [1]Power plants in Chongqing, Guizhou, Sichuan, and Yunnan have higher EF_{SO2}. [2] On-road CO EF in Yunnan is more than twice as much as that of regular environment condition.

7.3.2 Policy impacts on vehicle stock and electric vehicle adoption

Policies that are currently in place and would affect vehicle ownership demand include the dual-credit policy (or called EV mandates) and car ownership restriction policy. While the dual-credit policy is a nationwide mandate forcing more energy-saving and electric vehicles, car ownership restriction policy is a city-level instrument to curb the fast-growing local vehicle demand to improve the urban air quality. Figure 7.3(a) displays how these two policies reduce the motorization rate at the national level by 2030 (treemap chart): the dual-credit policy would diminish the vehicle demand by 18% from no EV policy counterfactual, and the car ownership restriction policy would further reduce the vehicle stock by 4%. We expect the private vehicle stock will reach 265 million and 302 million in 2025 and 2030 in the CPS scenario, respectively. The spatial distribution of vehicle stock across China is also presented inside the figure.

Figure 7.3(b) and (c) depict the EV adoption pattern in the CPS scenario in 2030. EV sales in Beijing, Tianjin, and Shanghai are expected to achieve about 92% (in average) market share of the local new car sales in 2030; this is comparison to the northeastern and northwestern provinces where EV market share will remain less than 10% even out to 2030 (Figure 7.3(b)). The private EV stock in China would reach 58 million in 2030, corresponding to 19% stock market share; Six provinces—Zhejiang, Henan, Sichuan, Shandong, Guangdong, and Jiangsu—would contribute 54% of the nationwide EV stock (Figure 7.3(c)). The private EV sales would achieve 11 million/year by 2030, with the top 10 contributing provinces of Zhejiang, Henan, Sichuan, Shandong, Guangdong, and Jiangsu, Hubei, Hebei, Beijing, and Shanghai; these ten provinces would contribute 74% of the nationwide EV sales per year.

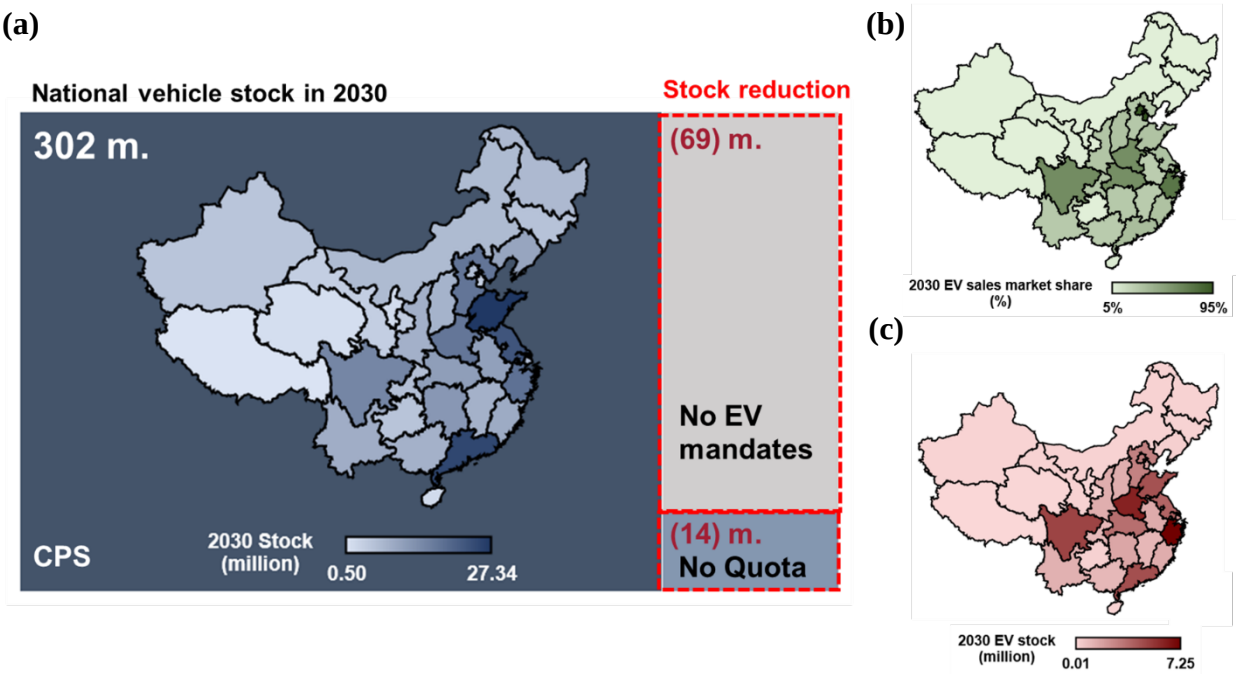

Figure 7.3. Policy impacts on vehicle market and EV adoption in 2030. (a) The stock reduction amounts due to the policy are marked in red; the inset figure presents the projected vehicle stock at the provincial level in the current policy scenario (CPS); (b) Provincial EV sales market share and (c) Provincial EV stock in 2030 in CPS.

7.3.3 Policy impacts on fuel consumption and emissions

Fast-growing motorization over the past decades has led to a significant increase in oil demand and emissions in China. In 2018, oil consumption in China amounted to nearly 13.5 million barrels

daily, contributing 13.6% of global oil demand [227]. Figure 7.4(a) depicts the oil demand trend from the private vehicle sector from 2015 to 2030, assuming 0.177 tons of gasoline are obtained from 1 ton of crude oil. In 2018, we estimate that about 19% of total China's oil consumption was from private vehicles. Moreover, the oil demand from the private vehicle sector is expected to peak in 2020; this is mainly because of the decreasing vehicle use intensity (Supplementary information D.IV) and the temporary car market contraction due to the removal of EV subsidies. Compared to no EV policy counterfactual scenario, the current policy mix would reduce nationwide oil demand by 1.3 million barrels per day in 2030 (provincial level reduction is shown in Figure 7.4(b)), which is more than 1% of the current world oil consumption. Figure 7.4(c) presents the lifecycle CO2 emissions of private car sector in China up to 2030. The overall trend of CO2 is similar to that of oil consumption, peaking around 2020 in CPS.

Figure 7.5 displays the annual nationwide WTW (i.e., fuel life-cycle) criteria air pollutant emissions of private car sector from 2015 to 2030, suggesting that under the current policy mix, annual aerial pollutant emissions would be reduced by approximately 50% nationwide relative to no EV policy scenario by 2030. CO and VOC emissions share the similar trends: the total emissions would keep decreasing, mainly driven by the continued scrapping of the older polluting vehicles and their replacement with the cleaner cars. NOx, SO2 and primary PM2.5 show a similar trajectory: the total emissions would start dropping noticeably after 2020; this is because less fuel is going to be produced and burned (i.e., oil consumption and the associated refinery emissions would peak in 2020) and the tighter tailpipe emission standards are going to be enforced (i.e., from China 5 to China 6) after 2020.

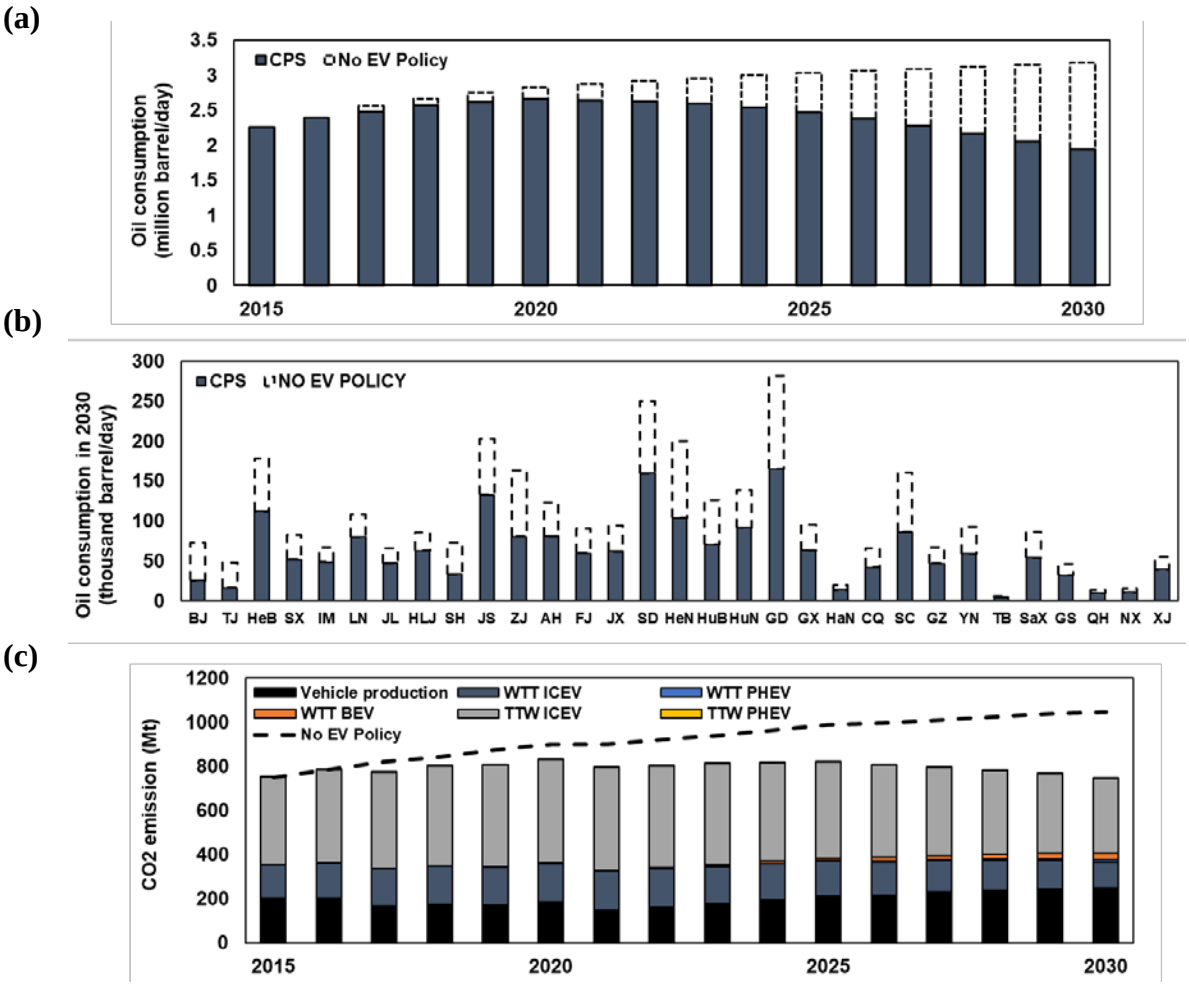

Figure 7.4. Comparison between No EV Policy scenario and Current Policy Scenario. (a) Annual nationwide amount of oil consumption in China from 2015 to 2030; (b) 2030 oil consumption from the private vehicle sector at the provincial level; (c) annual nationwide lifecycle CO2 emission in China from 2015 to 2030.

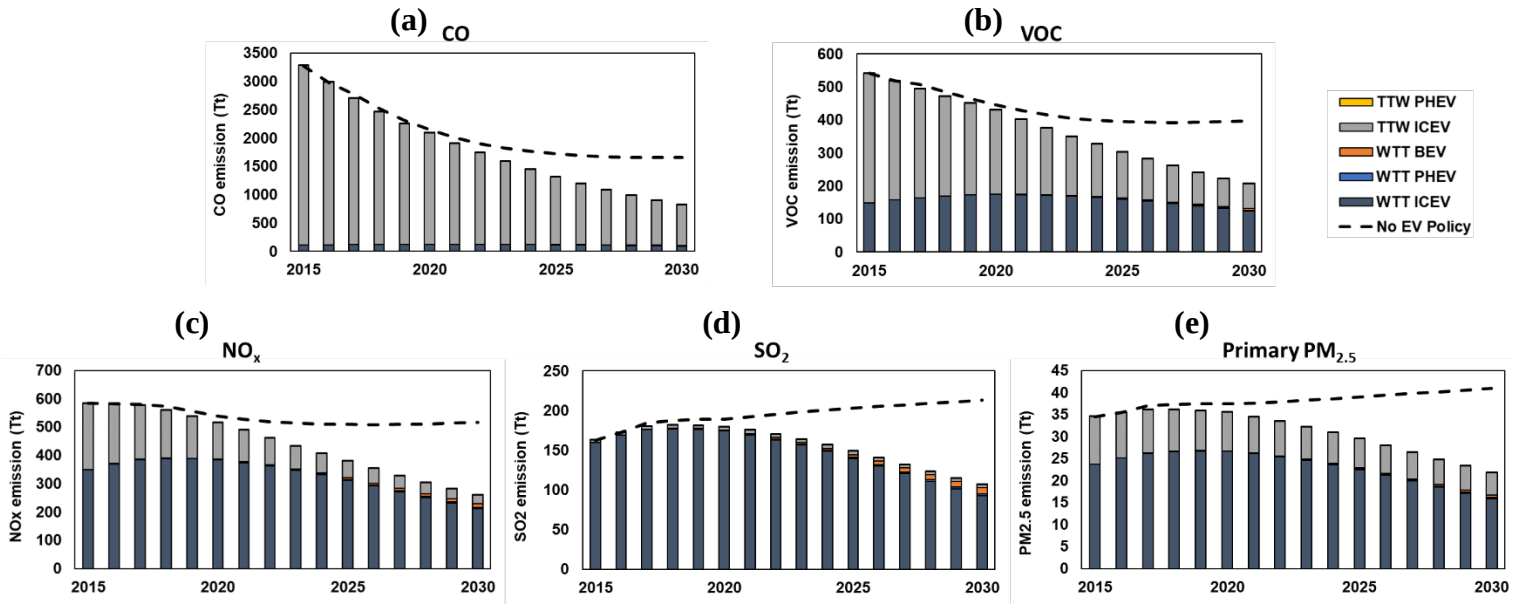

Figure 7.5. Annual amount of CO, VOC, NOx, SO2, and primary PM2.5 emissions from the WTW stage of the private cars for No EV Policy scenario and Current Policy Scenario in China from 2015 to 2030.

7.3.4 Policy impacts on air quality

Figure 7.6 depicts the changes in surface-level PM2.5 and O3 exposure in 2030. The exposure maps are in people micrograms per meter cubed[30] and people ppb per meter cubed for PM2.5 and for ozone, respectively. We estimate that by 2030, the sustainable mobility policy will lead to a consistent reduction in PM2.5 concentration nationwide, and the concentration reduction in the provinces with broader EV adoption is higher. The countrywide, population-weighted reduction in PM2.5 concentration is 0.2 μg/m3. On the other hand, relative to No EV Policy, the policy impacts on ozone concentration are more complicated: increases in O3 concentrations are observed in some urban areas. In the chemistry of O3 formation, the hydroxyl radical (OH) is the key reactive species, and there is a competition between VOC and NOx—two major O3 precursors—for the OH radical. In the low NOx limit (NOx-limited) when the rate of OH production is greater than the rate of production of NOx (generally in rural areas and suburbs downwind of center cities),

[30] That means that if the concentration in a grid cell is 100 μg/m^3 and there are 10,000 people in that grid cell, the exposure is 1,000,000.

NOx reduction reduces ambient O3. In the high NOx limit (NOx-saturated or VOC-limited) when the rate of OH production is less than the rate of production of NOx (often in urban areas with a high population concentration), NOx acts to reduce ozone, so a decrease in emissions promotes O3 production [228]. The countrywide, population-weighted increase in the annual average of the daily 8-hour maximum ozone concentration is 0.05 ppb.

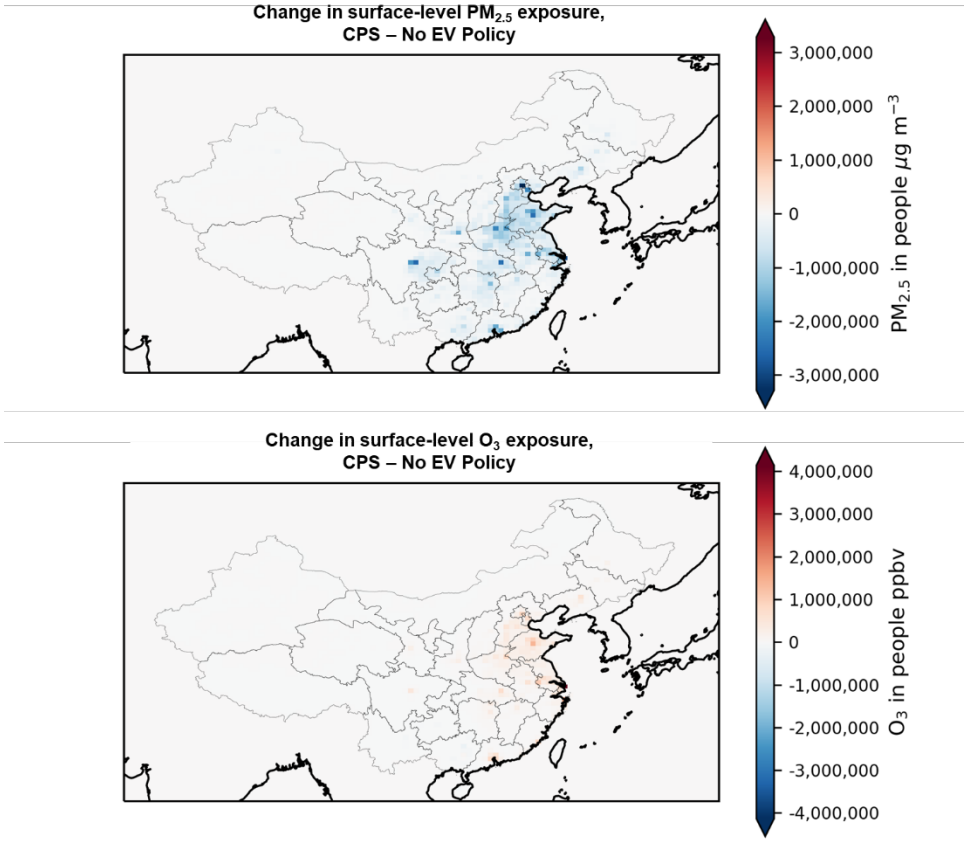

Figure 7.6. Change in surface-level (a) PM2.5 and (b) O3 exposure between No EV Policy scenario and Current Policy Scenario (CPS) in China

7.3.5 Policy impacts on public health

According to our analysis, full implementation of current government EV policies (i.e., CPS) will reduce the public's long-term exposure to air pollution, avoiding 15,536 premature deaths, 2,221 cases of hospital admission due to respiratory disease, 1,305 cases of hospital admission due to cardiovascular disease, 3,682 cases of chronic bronchitis, 3,910 cases of asthma attack, and 378

cases of emergency room visits for respiratory disease in the year of 2030. For the avoided premature deaths, the reduced health endpoint of lower respiratory infection contributes the most—nearly 53%, followed by chronic obstructive pulmonary disease (20%) and stroke (16%).

Figure 7.7 shows the total avoided number of premature deaths at the provincial level, broken down by the contributors. Nearly all the avoided premature deaths are attributable to reduction in exposure to ambient PM2.5 concentrations. The reason we don't see the avoided premature death owing to ozone is that the health concentration-response functions that are used for ozone mortality has a 35 ppb threshold; in most cases, the annual average 8-hour daily maximum ozone is below this threshold, so there is no mortality effects. At the provincial level, the largest absolute reductions in premature death will occur in Shandong, Henan, and Guangdong provinces, where more than 1,000 annual premature deaths may be avoided in 2030.

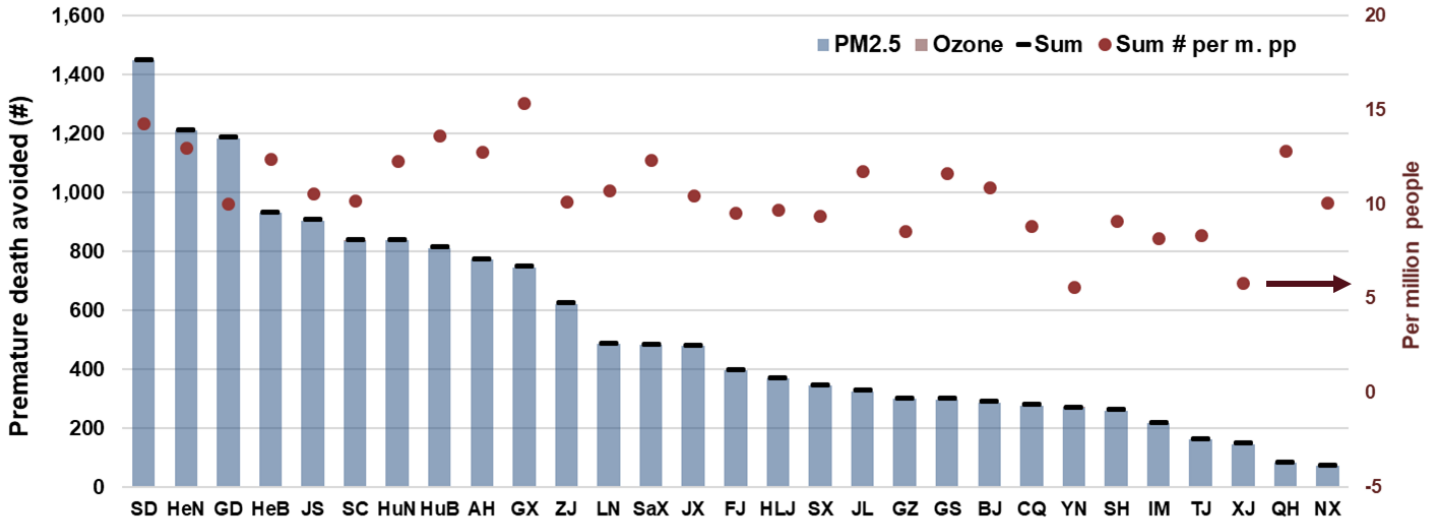

Figure 7.7. Avoided premature death in current policy scenario relative to no EV policy scenario by province in 2030

7.3.6 Economic benefits

The climate change benefits and health benefits stemming from the implementation of sustainable mobility policy (i.e., current policy scenario relative to no EV policy scenario) are quantified in terms of the economic values of avoided premature death, avoided morbidity cases, and climate

change mitigation[31]. Current policy scenario would yield tremendous economic benefits over the mid-term future (in 2030); the benefits will continue to grow up in the longer term as more energy-efficient vehicles (including HEVs and EVs) account for a greater share of vehicle activity.

The total PM2.5 and ozone-related health benefits (mostly attributable to the reduction in PM2.5-related mortality) and the total CO2-related climate change mitigation benefits from implementing sustainable mobility policy are valued at 112 billion Yuan and at 72 billion Yuan in the year 2030, respectively. Figure 7.8 presents the economic benefits at the provincial level. CO2 emissions associated with vehicle production are allocated based on the number of vehicles sold in each province in 2030 due to the lack of vehicle manufacturing data by region. On the other hand, because most of the premature mortalities are caused by the long-term exposure to PM2.5 (which is mainly due to the refineries), we allocate the air pollutants emissions associated with the upstream gasoline production phase by the capacity volume of China's oil refineries and their locations. It is shown that while Guangdong will collectively benefit the most from China's movement to sustainable mobility, Beijing will obtain larger benefits in terms of per capita economic benefits; this is because individuals in Beijing are expected to be willing to pay 56% more than that of Guangdong to avoid health-related risks.

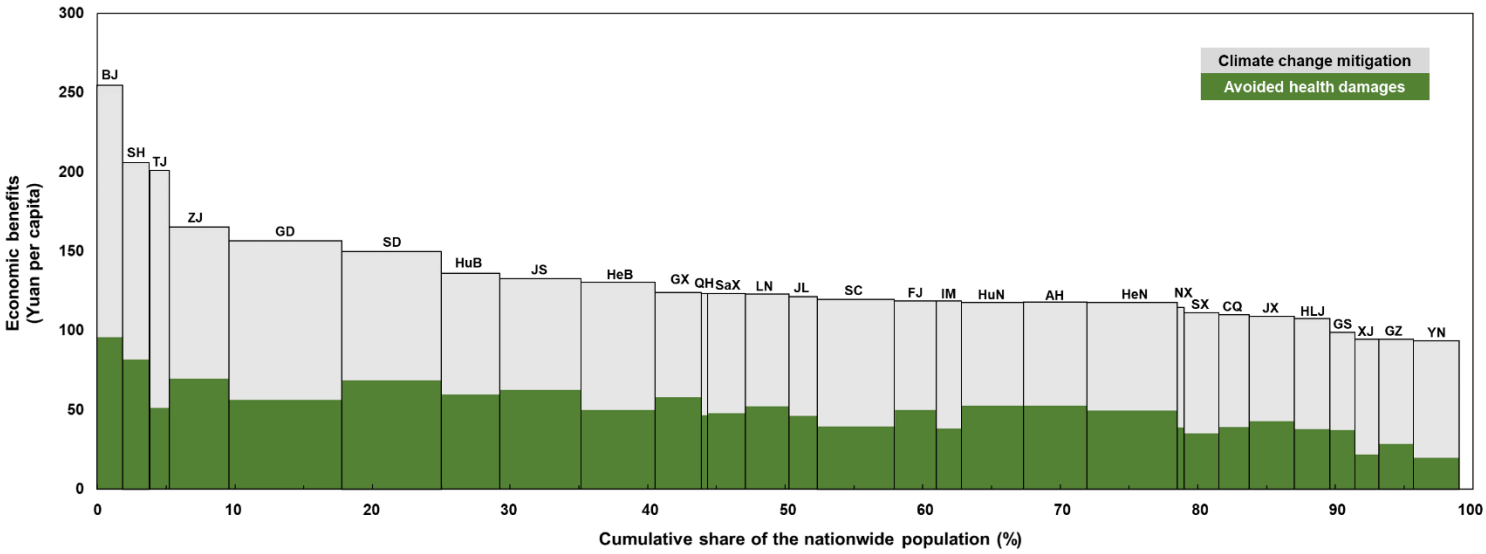

Figure 7.8. Per capita economic benefits of climate change mitigation and avoided health damages by province in 2030, in descending order. This study captures 99% of the nationwide population in China (Hainan and Tibet are not excluded).

[31] As discussed earlier, this chapter quantifies the benefits due to the changes in total lifecycle CO2 emissions and the changes in WTW air pollutants emissions under the current policy mix relative to no EV policy scenario.

7.3.7 Climate and health impact breakdown of the sustainable mobility policy

Figure 7.9 breaks down the cumulative impacts of different policies on whole lifecycle CO2 emissions from the private vehicle sector in 2030. First, the vehicle stock reduction of 83 million (Figure 7.4) would cause CO2 emissions per year to decrease by 143 million tonnes in 2030. Second, stringent fuel efficiency regulations would encourage the adoption of turbocharging/downsizing technology advances as well as HEV penetration, making the average on-road fuel consumption rate of new gasoline-powered passenger vehicles decrease to 5.0 L/100km by 2030 (compared to 7.3 L/100km in no EV policy counterfactual scenario); this fuel efficiency improvement would reduce CO2 emissions significantly by 125 million tonnes per year. Third, mandating 40% EV sales market share (accumulating 19% of the total private vehicle stock in 2030) and a reduction in grid carbon intensity combined would lower CO2 emissions by 34 million tonnes per year. We find that improved fuel efficiency of gasoline cars collectively reduces more CO2 emissions than that of vehicle electrification, mainly because most of (~81%) the vehicle stock in 2030 are powered by gasoline. However, even with the doubling of EV penetration rate relative to CPS, lifecycle CO2 emission would be reduced only by 4%; this is because greater emissions associated with EV production relative to HEV diminishes the lifecycle climate benefits of vehicle electrification.

Regarding health impact breakdown, we estimate that 3,725, 8,188, and 3,620 premature deaths would be avoided in 2030 due to reduced exposure to air pollution driven by the vehicle stock reduction, the improved fuel efficiency of gasoline vehicles, and mandating 40% EV sales market share, respectively. With the doubling of EV penetration rate relative to CPS, additional 2,135 (14%) premature death would be further avoided. The results suggest that China's benefits from electrifying private vehicle sector are more significant for public health than climate change. Besides, the uncertainties in future geographical patterns of EV population growth have little impact on the global and local benefits with the reduction of both greenhouse gas and air pollutant emissions.

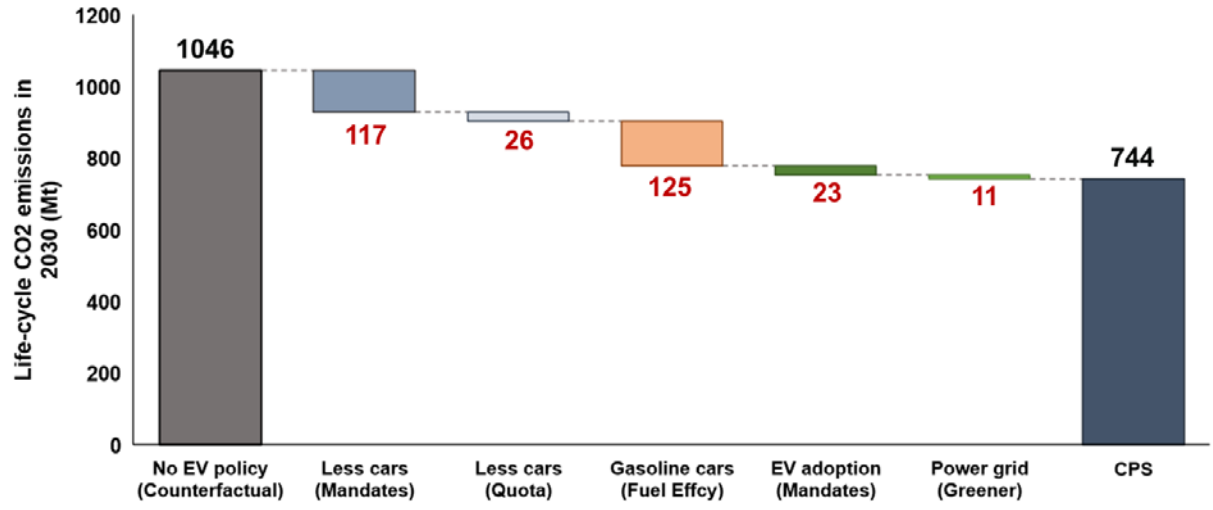

Figure 7.9. Reduction in life-cycle CO2 emissions of private vehicle sector in 2030 under different scenarios, broken down by different types of policy

7.4 Conclusion

China's fast-growing motorization has led to mounting problems regarding negative environmental externalities and national energy security, prompting a wide variety of responses from the central and local governments—EVs are considered as a solution to overcome the challenges of providing clean transportation. While the Chinese government is prioritizing and promoting EVs with the implementation of aggressive policy actions, the consequences of which, however, are still unclear. This study presents our contribution to deepen the understanding of this ongoing transition towards electrification in China's private vehicle sector.

In China today (2017), the national average CO2 emissions per km for EVs are approximately 71% of emissions for a similarly sized ICEVs. At present, EV adoption is driven by the government policies; however, the provinces that are currently leading the EV sales do not provide noticeable climate benefits for EVs compared to HEVs (the most relevant vehicle type to represent highly fuel-efficient gasoline-powered cars). For EVs, CO2 emissions are mainly from the production of electricity; accordingly, support for EV deployment needs to be accompanied by decarbonization of the electricity grid to maximize the effectiveness of climate change mitigation efforts. CO2 emissions associated with vehicle manufacture (including battery) would become more important as the electricity used to operate EVs become less carbon-intensive, so the government should also pay attention to its emission mitigation opportunities (such as battery production techniques enhancement, vehicle recycling industry development, and low-carbon

energy deployment). From the perspective of air pollution, EVs offer clear per-km emissions reductions compared to gasoline-powered counterparts thanks to the introduction of ultra-low emissions standards. For gasoline vehicles that meet China 5 emission standard, WTW NOx, SO2, and primary PM2.5 emissions are mainly from the upstream gasoline production phase; this suggests that stricter emission control should be applied in the industrial boilers (i.e., gasoline refinery) to further combat air pollution problems effectively.

Under Current Policy Scenario (CPS), private vehicle stock in China will reach 265 million and 302 million in 2025 and 2030, and its oil demand and lifecycle CO2 emissions will peak in 2020. Compared to No EV Policy counterfactual scenario, CPS will lead to a consistent reduction in PM2.5 concentration nationwide; the countrywide, population-weighted reduction in PM2.5 concentration is 0.2 μg/m3, leading to a total of nearly 15,536 premature death avoided in 2030, with the largest mortality risks reduction occurring in Shandong, Henan, and Guangdong provinces. The climate change benefits and health benefits stemming from the implementation of the current policy mix are estimated to be at 72 billion Yuan and 112 billion Yuan over the mid-term future (in 2030). At the provincial level, Guangdong will collectively benefit the most from China's movement to sustainable mobility, but in terms of per capita economic benefits, Beijing will obtain larger benefits. As more energy-efficient vehicles account for a greater share of vehicle activity in the longer term, the benefits will continue to increase.

Chapter 8. Conclusion

As world's population continues to grow and people become wealthier, the demand for personal mobility—most notably private vehicles—will increase. The benefits associated with owing a car include convenience, flexibility, and comfort. Nevertheless, vehicle ownership and use impose a variety of social costs that are not directly borne by vehicle owners, including emissions of planet-warming greenhouse gases and local air pollutants which would contribute to poor air quality. In response to these negative externalities concerns, powertrains and fuels must evolve to become more sustainable; electric vehicle (EV) offers the great potential to reduce oil dependency and achieve emissions mitigation targets.

EVs are one part of solutions to overcome the challenges of providing clean transportation; however, a range of barriers are standing in the way of wider EV adoption. To foster early market development of EVs, government supports, both financial and non-financial, are needed to remove some of the disadvantages that EVs face relative to incumbent internal combustion engine vehicles (ICEVs). Currently, China is taking a leadership position in global vehicle electrification, mostly driven by a variety of aggressive subsidies and incentives. It is likely that China will continue to dominate the EV deployment into the future. However, there are great uncertainties about the future of EVs, both in terms of their market penetration rate and in terms of the energy sources of electricity generation. To deepen our understanding of the transition towards future electric mobility systems will require methods and analytical insights that capture key uncertainties in the prospects for widespread EV deployment.

In order to have a better understanding of this complex system, this thesis has provided improved methods to characterize and project future EV battery techno-economic characteristics and China's private motor vehicle market growth; and to quantify the policy impacts of EV proliferation in China. To conclude, I review and highlight the contributions to research literatures and modeling practices (Chapter 8.1); comment on some challenges and policy implications of the findings for EV deployment (Chapter 8.2); and discuss some potential future research arising from this work (Chapter 8.3).

8.1 Summary of the research

In Chapter 2, I develop an application of the Monte Carlo method, conditioned on historical data, to sample parameters for a model projecting aspects of private car diffusion, such as the mix of new and replacement sales. I find that the uncertainty in car stock/ownership projection would continue to grow toward 2050, while the distribution of the projected share of new-growth purchases is higher in the near term than in a saturated market, with replacement sales expected to capture the car sales market after 2025. Moreover, the number of vehicles in China will continue to be fairly sensitive to car affordability from now to about 2030, whereas it will be set primarily by consumer preferences (and less sensitive to economic factors) after 2030.

In Chapter 3, I develop a two-stage learning curve model based on the battery supply chain to capture the practical limits to battery cost reduction. By incorporating floor costs set by materials, I find that the price target of $100/kWh is very unlikely to be achieved by the continued maturation of the existing NMC-based lithium-ion battery technology platform alone. The previous models based on a conventional learning curve without consideration of the floor set by materials costs would predict an unrealistically low lithium-ion battery pack price within the next decade. Chapter 3 corrects this serious mistaken assumption underlying all the previously published battery price projections, demonstrating that omitting the materials costs of batteries would lead to an over-optimistic assessment of how soon EVs will become economically competitive with conventional vehicles.

In Chapter 4, I provide up-to-date insights on China's private vehicle market in the light of the new dual-credit scheme mandate. China's EV mandate will lead to pricier battery-powered vehicles replacing ICEVs in the sales mix, and thus, increase the average car price. Significant discrepancies (~18% in 2030) in private car ownership curves are observed for projections with and without the mandate, suggesting the importance to have these policies considered when sizing the future car market in China. Besides, Chapter 4 also evaluates the battery demand driven by vehicle electrification, showing that the pressure on the global supply for lithium and cobalt will be exacerbated and a recycling-based supply chain is needed.

Chapter 5 further quantifies the impacts on societal and consumer costs of the evolving EV policies in China. The dual-credit scheme mandate is expected to maintain strong growth in the local EV market, while ostensibly transferring the burden of subsidizing the EV industry from the

government itself to the automaker. The incremental cost of EVs over counterpart ICEVs will be imposing significant transition costs throughout the society—on average consuming about 0.1% of China's growing GDP each year—and eventually to car purchasers during the transition to electric transportation; this is an economic cost to achieve the national energy security and air pollution benefits. I also investigate the temporal variation in consumer total cost of ownership (TCO) of EVs relative to ICEVs, showing that China's subsidized EVs are in TCO parity with counterpart ICEVs from 2016 to 2020. After the subsidies are removed, automakers are expected to internally subsidize EV by raising ICEV prices to achieve the mandated percentage of EV sales.

In Chapter 6, I document that while battery swapping imposes high upfront costs, cumulative costs per passenger kilometer delivered by a BEV fleet network are not higher as a consequence - this owing to the ability of swapping stations to service a higher number of BEVs compared to the conventional charging modes. Moreover, I also propose an alternative business operation where the idle time for charging could be avoided by having several extra vehicles, and always has a rotation of vehicles being charged; this allows drivers to switch to a fully charged taxi when their current vehicle battery is almost depleted. This proposed business strategy is found to dramatically improve the cost-effectiveness of double-shift BEV fleet relying on Level 2 battery chargers.

In Chapter 7, I find that EVs manufactured and charged with China-average electricity do not have much better climate benefits than ICEVs. For EVs, CO2 emissions per kilometer are highly sensitive to the carbon intensity of the power grid, and thus policies to support EV deployment should go hand-in-hand with policies to support low-carbon electricity generation for climate change mitigation effectiveness. For the current gasoline vehicles, WTW NOx, SO2, and primary PM2.5 emissions are mainly from the upstream gasoline production phase rather than tailpipe emissions; this suggests that the government needs to put more efforts to regulate emissions from gasoline refining process in order to combat air pollution problems effectively. Furthermore, I quantify the environmental impacts of sustainable mobility policy: full implementation of current government EV policies in China's private vehicle sector will make its oil demand and CO2 emissions peak around 2020, and reduce the public's long-term exposure to air pollution, avoiding approximately 15,536 premature deaths in 2030. The climate change benefits and health benefits stemming from the current policy mix are valued to be at 72 billion

Yuan and 112 billion Yuan in the year 2030. As more energy-efficient vehicles account for a greater share of vehicle activity in the longer term, the benefits will continue to increase.

8.2 Challenges and policy implications of the findings for EV deployment

8.2.1 EV cost

High upfront purchase price of an EV is the major financial barrier to EV deployment. In the absence of purchase subsidy, buying a compact BEV (with a driving range of 350 km) is about 60% more expensive than a counterpart ICEV in 2017. Out to 2030, lithium-ion NMC batteries are expected to continue dominating the passenger EV market, and passenger BEVs are very likely to remain pricier than ICEVs even with greater production volumes and improvement in manufacturing efficiency; this is mainly because the ultimate potential for battery cost reductions is bound by the base cost of input materials, particularly cobalt. EVs are not going to take over the world transportation market naturally for purely economic reasons, unless they are supported by significant government interventions such as high fuel taxes, subsidies, or mandates. Since NMC-based lithium-ion batteries are dependent on expensive metals, innovations in battery chemistry (such as lithium metal, solid state, sodium ion, multivalent-based, or lithium sulfur) are needed to lower the floor price of batteries and drive electrification of the transportation sector even in countries without pro-EV policies.

The upfront purchase price does not give the full picture of TCO for consumers; EVs have the great potential to offer fuel and maintenance savings. Currently, EV purchase subsidies are sufficient to make the TCO of EVs lower than that of ICEVs in some countries like China. Future reductions in battery costs will likely enable EVs to be TCO competitive with ICEVs in more countries even with no subsidies. However, consumers are likely to be more sensitive to higher upfront price of EVs than TCO, implying that ICEVs will continue to be regarded as the more affordable powertrain throughout 2030 and beyond. Moreover, TCO is only one of multiple factors that contribute to consumer decisions concerning vehicle purchases. Other barriers beyond cost (of ownership) have to be overcome as well to achieve mass EV adoption; barriers include limited access to charging infrastructure, range anxiety, and consumer familiarity. Policymakers should provide well-designed and adequate government incentives to support appropriate early EV market development—making EV purchase cost-attractive to consumers. Governments should help

enhance the communication and coordination among potential partners to fully leverage the efforts to promote EVs.

8.2.2 EV battery raw materials supply chain

Driven by increasing demand for consumer electronic devices and electric vehicles, the global market for lithium-ion batteries (LIBs) has grown dramatically. Growing LIBs demand has driven the essential mineral prices (including lithium, nickel, and cobalt) up over the past three years, fueling fears of a shortage. Global nickel supply is unlikely to be a limiting factor for wider battery production, but both lithium and cobalt production volumes have to be largely expanded. The supply concerns of lithium are focusing more on whether the lithium production can be speeded up in the immediate future, rather than the material quantity itself thanks to the supply diversity in terms of geographical distribution and extraction technology [102,103]. Cobalt is more likely to disrupt large-scale battery production. More than 60% of world cobalt mine production occurs in the politically unstable Democratic Republic of Congo, meaning that the political situation in that region will have a significant influence on the price and the supply security of cobalt. Besides expanding the production capacity and lessening the amount of cobalt used in batteries, the potential supply risks arising due to geo-political barriers could be ameliorated with battery recycling.

Even with continued LIB development, however, the battery recycling industry is lagging. Most of the LIBs produced in the past decade have been for use in portable electronics, and few of them are recycled—the vast majority of batteries are discarded along with the devices that contain them. The automotive sector is expected to be the fastest-growing source of spent LIBs over the next three decades, mainly due to the movement toward vehicle electrification. Since LIBs contain toxic substances, environmental concerns arise if large volumes of spent LIBs go to landfills instead of being recycled. In landfills, LIBs may catch fire and lithium can leach into groundwater [229]. Environmental regulations and a scarcity of metals for automotive applications may provide business opportunities for reclaiming spent batteries, potentially creating a global market for LIB recycling. The variety of materials used in battery cathodes (such as lithium iron phosphate, lead acid, and lithium cobalt oxide) creates a challenge for recycling; this complexity, together with low yields for individual materials, helps to explain why battery recycling has not been widely practiced. To handle mixed cathode chemistry, current recycling processes require

expensive organic reagents for solvent extraction to separate cobalt, nickel, and manganese. There is an urgent need to develop cost-effective methods for recycling batteries on an industrial scale. In addition, these methods must be capable of handling a growing volume and variety of spent LIBs. One solution that has been proposed is to develop closed-loop recycling processes in which cathode and anode materials are recovered directly from spent LIBs; this has advantages over industrialized recycling processes that are only capable of recovering secondary raw materials (such as cobalt and nickel) that need further processing to produce new cathode materials. A study has shown that recycling LIBs via a closed-loop process is feasible, regardless of cathode chemistry, with high recovery efficiencies (on the order of 90%), and a potential profit margin of $5,525 per metric ton of LIBs based on a material balance analysis [230].

Interest is also growing in potential "second-life" applications for spent batteries from EVs. While second-life batteries would have lower energy density and would continue to lose capacity, they may be a safe, adequate, and economic product for alternative uses—in grid-level energy storage devices, for example [231]. Even with second-life applications, however, EV batteries will eventually have to be recycled or disposed of. Policymakers should help integrate the entire industry chain among automakers, battery producers, used-car dealers, and scrap companies so that batteries become part of a circular economy, rather than creating a new source of hazardous waste. LIB recycling remains an important technical, economic, and policy challenge.

8.2.3 EV charging infrastructure

Cost parity alone cannot drive widespread adoption of EVs, other factors besides TCO will likely shape the adoption of EV deployment, including availability and convenience of charging infrastructure. Range anxiety (i.e., fear that a vehicle has insufficient range to reach its destination) and lack of access to charging infrastructure are the other two major barriers to mass-market adoption of EVs. EVs across the world are facing a classic "chicken-and-egg" problem: Concerned with the availability of charging stations, consumers are reluctant to switch from conventional ICEVs to EVs. Yet, building a charging infrastructure is expensive, and investors are reluctant to risk large and long-term investments in the face of great uncertainty about future demand. So what will come first: the EVs or the charging stations? Given these deployment hurdles, governments' support and effective placement of charging stations are needed to overcome externalities and system-wide inertia.

For private vehicle owners, at-home charging is the primary source of EV power; however, multi-family dwellers often have limited access to dedicated garages to install their own charging stations. Workplace charging can serve as a substitute for home charging: like the home, the workplace is a regular destination where employees spend an average of eight hours per day, long enough to replenish their EV battery. Given that reliable access to a daily charging source is critical for EV adoption, the expansion of multi-unit residential and workplace charging stations could help increase the market for EVs and decrease range anxiety. For fleet operators (like taxi), on the other hand, long EV charging times are particularly problematic because minimizing vehicle downtime is crucial to maximizing profit. To make EV taxi ecosystems more appealing to fleet owners running with multiple shifts, efficient recharging alternatives—fast charging with extra vehicles and the battery swapping—are needed. Battery swapping is one of the least costly options on a per-km basis for both single-shift and double-shift taxis, although it imposes high aggregate upfront costs for its battery inventory requirement. Its fiscal attractiveness is mainly due to a swapping station's ability to serve 10 times as many BEVs as a fast charger and 56 times as many BEVs as a Level 2 charger. Although the EV taxis ecosystem still being more costly than the business-as-usual ICEV fleet at the moment, these incremental costs will be shrinking as the battery costs drop in the future (the per-km cost competitiveness is expected to be achieved in Beijing by 2022).

8.3 Future work

Considering the endpoints of the six chapters together, some ideas for future research emerge. I give two examples here to illustrate how such extensions could further improve the understanding regarding future mobility systems.

8.3.1 Expanding the system boundary of the study scope

The thesis gives primary attention to China, private light-duty vehicles with 4 wheels, movement of people, and electrification. Focusing on private vehicles is because this sector is most rapidly and strongly impacted by fast-moving developments in advanced powertrains, alternative fuels, and environmental policies. However, the other ground transportation segments are also worth to be studied in order to thoroughly capture the performance characteristics and technological trends of all kinds of vehicle in the road transport sector.

The light- and heavy-duty vehicles fleet can be classified into four groups based on ownership (private or commercial) and purpose (passenger or freight), owing to their different growth patterns, use intensity, and potentials to be electrified or decarbonized. The groups are *1) private light-duty passenger vehicles*; *2) commercial light-duty passenger vehicles* (e.g., taxis and that are owned by companies and government entities); *3) commercial buses*; and *4) commercial trucks* (all trucks used for freight transportation); ground transportation of freight has a similar global energy demand to that of all light-duty vehicles, so analyzing its future trend will also provide great insights to help guide efficient and sustainable development of mobility. In addition to passenger and heavy-duty vehicles, two-wheeled vehicles are popular in several developing countries. Because it is unclear whether two-wheelers and light-duty vehicles are complementary, substitute or unrelated goods and information on them is lacking, the expanded model could consider two-wheelers as a separate category from the others—*5) two-wheelers*. With the model established, the integrated framework for environmental impact assessment shown in Chapter 7 in this thesis could be applied to study various alternative fuel scenario analysis, considering the latest data and energy and sustainable mobility policies with all types of vehicles in detail.

8.3.2 Extending the health impact assessment considering feedback from pollution

The thesis has attemped to quantify the economic losts of air pollution arising from its negative impact on human health, but I draw aggregate damage functions and apply them to the target air quality level in static ways, which may not be able to fully reflect the overall economic impacts because they do not identify the feedback from pollution to the supply and demand of resources and of goods and services dynamically. Matus, Kira, et al. (2012) [232] offered an estimate of long-term economic impacts caused by air pollution in China by incorporating scientific models of atmospheric chemistry with global-economy model to combine broader socio-economic aspects. Matus, Kira, et al. used a recursive dynamic computable general equilibrium (CGE) model—the MIT Economic Projection and Policy Analysis (EPPA) model—and introduced the household healthcare production sector that provided ‘pollution health services’, which allowed them to capture the health effects related to both morbidity and mortality. They used years-of-lost-life approaches to evaluate air pollution-related health impacts on the Chinese single economy and estimated the marginal welfare impact of ozone and particulate-matter concentrations above background levels. Their work focused on the benefit side of air quality control in the whole China, but they did not consider the routes and the costs to achieve target goals nor identify the regional

difference in the value of lost labor and population age structure across China. Future research could build upon Matus, Kira, et al.'s estimation method and extend from this thesis, to further investigate the long-term economic changes in pollution-health costs in China, driven by the certain transportation and energy policy, in order to capture cumulative dimensions of air pollution's impact on public health.

Appendix A. Additional Details for Vehicle Battery Outlook

A.I. Traditional and Integrated Battery Supply Chain

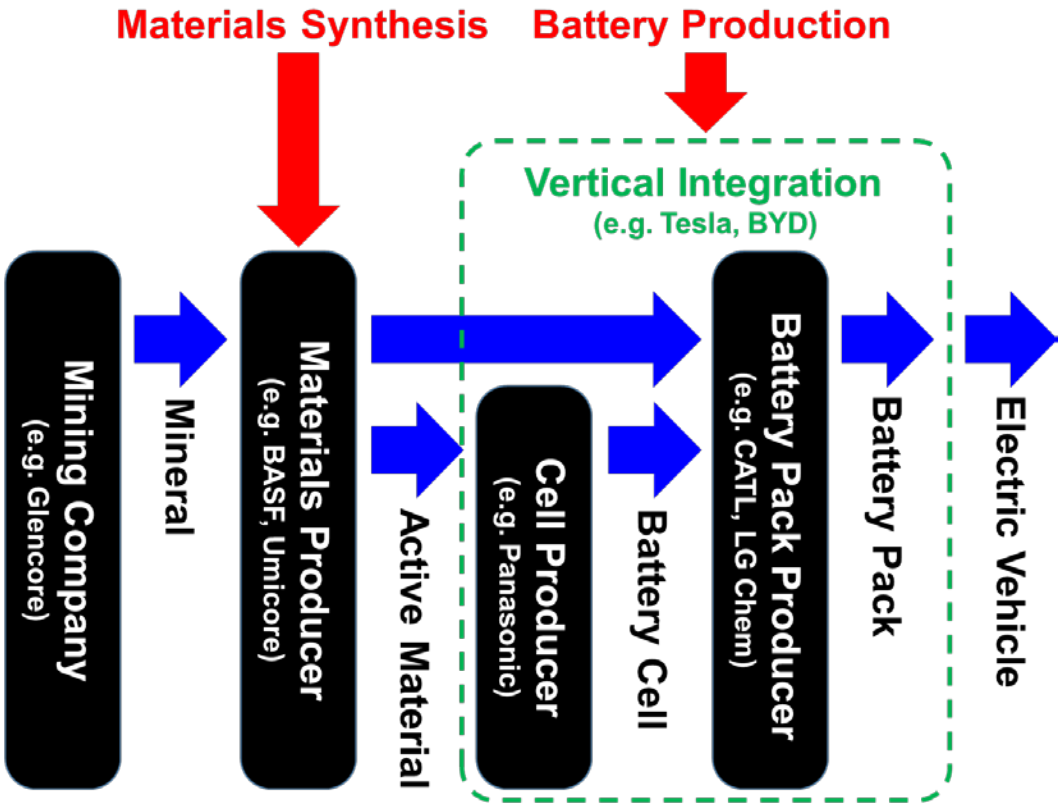

Figure A.1. Supply chain structure and recent integration in battery and EV industries

In the past few years, the supply chain of battery packs for electric vehicles (EVs) has experienced significant changes. Previously, as shown in Figure A1 with black blocks, different companies dominated each stage of battery manufacturing (and arguably still do). However, EV automakers such as Tesla and BYD have vertically integrated with battery and electrode producers to reduce battery costs in 2016, shown as green box [233,234]. These automakers can now purchase active materials and manufacture battery packs for their EVs themselves. The construction of the Gigafactory also allows Tesla to reduce reliance on outsourcing supply in batteries. Considering the fact that other automakers like GM and Volkswagen also declared their intentions to vertically integrate their manufacturing [235], we assume the future battery supply chain for EVs will consist primarily of active materials producers and integrated battery-automotive corporations. This means while the active materials costs are made up of the mineral costs and materials synthesis

costs for active materials producers, the battery pack price will only come from active materials costs (cathode and anode) and battery production costs, as shown in Figure A1.

A.II. Two-Stage Learning Curve Model: Materials Synthesis and Battery Pack Production

A.II.1. Conventional Learning Curve

Learning curves are widely applied to trace declines in production costs over long periods of time as a function of cumulative production volume of the product. The effect of learning on production costs is commonly described in the form of Eq. A1. The cost per unit (*C*) depends on the cumulative production volume (*V*), and the coefficient *b*, technology-specific experience index, which can be empirically fitted using regression analysis. The progress ratio (*PR*), defined in Eq. A2, is the ratio of the final to initial cost as cumulative production doubles. The learning rate (*LR*), presented in Eq. A3, is the proportional cost reduction as the result of doubling the cumulative output [236].

$$C_t = C_0 \left(\frac{V_t}{V_0}\right)^b \quad \text{(Eq.A1)}$$

$$PR = \frac{C_t}{C_0} = \left(\frac{2V_0}{V_0}\right)^b = 2^b \quad \text{(Eq.A2)}$$

$$LR = 1 - PR \quad \text{(Eq.A1)}$$

A.II.2. 2-Stage Learning Curve Model

Here, we present a 2-stage learning curve model, described in Eq. 3.1 and Eq. 3.2, to capture the practical limits on battery price reduction set by the costs of essential materials. Note that our mathematical model is developed based on the battery supply chain structure, shown in Figure A1.

For the first-stage learning, we subtract mineral costs (*MinC*, data taken from the USGS mineral summary report [67]) from active materials costs (*MatC*, data taken from the Avicenne report [237]) to capture the production costs during material synthesis (*MS*) that could be reduced by the greater learning or experience. Figure A2 shows the elemental costs for battery materials. The same concept is applied to the second-stage learning, in which the actual battery pack production (*BP*) cost is obtained by subtracting the active materials costs (*MatC*) from battery pack prices (*BPP*, data and sources tabulated in Table A1). Here we only include battery pack price estimates for NMC-based lithium-ion batteries (LIBs), widely considered to be the current mainstream technology, installed

in EVs. The active materials cost curve derived from the first-stage fitting is taken as a floor for battery pack production learning in the second stage; the 2-stage learning curve model has hence been given this name. As the production volume becomes large, the battery pack price predicted by the model approaches the active materials cost, and at the same time, the active materials cost approaches the mineral cost.

$$Stage\ 1: MatC_t = (MatC_0 - MinC_0)\left(\frac{V_{MS,t}}{V_{MS,0}}\right)^{b_{MS}} + MinC_t \qquad \text{(Eq.3.1)}$$

$$Stage\ 2: BPP_t = (BPP_0 - MatC_0)\left(\frac{V_{BP,t}}{V_{BP,0}}\right)^{b_{BP}} + MatC_t \qquad \text{(Eq.3.1)}$$

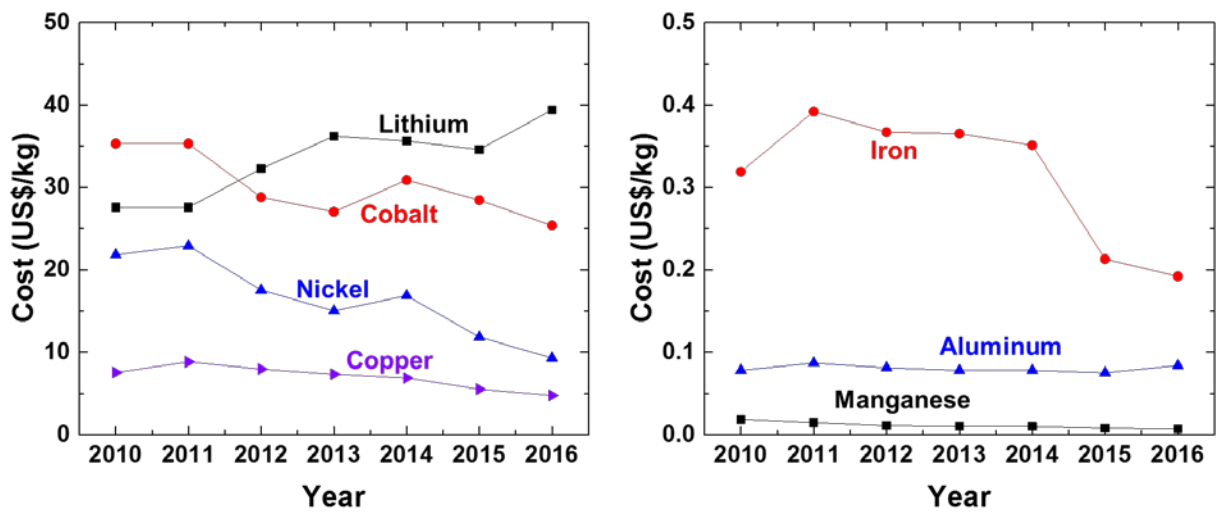

(a) (b)

Figure A.2. Elemental costs between 2010 and 2016 based on USGS Mineral Summary Reports. For more recent data on nickel and cobalt see Figure A6.

Table A. 1. Battery pack price estimates

Year	Price (2017 US$/kWh)	Source	Year	Price (2017 US$/kWh)	Source
2010	1489	[238]	2012	678	[257]
2010	968	[239]	2012	585	[258]
2010	1297	[240]	2012	516	[259]
2010	1297	[241]	2012	682	[246]
2010	1019	[242]	2012	682	[71]
2010	1119	[243]	2013	524	[260]
2010	826	[244]	2013	628	[246]
2010	1280	[245]	2013	628	[71]
2010	1119	[246]	2013	603	[261]
2010	1119	[71]	2013	629	[262]
2010	728	[247]	2014	557	[246]
2011	583	[248]	2014	557	[71]
2011	895	[249]	2014	516	[263]
2011	1282	[250]	2015	314	[63,264]
2011	814	[251]	2015	283	[247]
2011	814	[252]	2015	277	[246]
2011	868	[246]	2015	360	[71]
2011	868	[71]	2015	221	[265]
2012	478	[253]	2015	257	[266]
2012	842	[254]	2016	231	[246]
2012	1063	[255]	2016	278	[71]
2012	1010	[256]	2016	193	[267]
2012	532	[251]	2016	208	[268]

Besides price/cost estimates, production volume is the other key input in the model. In the following subsection, we will discuss how we estimate yearly installed plug-in battery capacity.

A.II.3. Estimation of Yearly Installed Plug-In Battery Capacity by Chemistry

Table A.2. Installed capacity data

	Installed Capacity (MWh)	Battery Chemistry	Cumulative Installed Capacity Ratio by Battery Chemistry (-08/2017)
2010	139	NMC	35%
2011	1,061	NCA	31%
2012	2,413	LFP	16%
2013	4,814	LMO	14%
2014	7,852	Others	4%
2015	13,609	Cumulative installed capacity in EVs to August, 2017 is 71,099 MWh.	
2016	22,386		

EV-volumes reports not only the yearly total installed plug-in battery capacity from 2010 to 2016, but also cumulative installed capacity breakdown by battery chemistry. Table A2, which tabulates the data retrieved from *EV-volumes* [57], shows that four lithium-ion intercalation cathodes dominate the EV battery market: $LiNi_xMn_yCo_{1-x-y}O_2$ (NMC), $LiNi_{0.8}Co_{0.15}Al_{0.05}O_2$ (NCA), $LiFePO_4$ (LFP) and $LiMnO_2$ (LMO). Since this chapter focuses on NMC-based LIBs, we derive yearly installed NMC battery capacity between 2010 and 2016 based on available information and some assumptions, as follows [269]:

- NCA is mainly produced by Panasonic for Tesla.

$$\text{Installed Capacity}_{NCA,t} = Sales_{Tesla\ Model\ S,t} \times Average\ Battery\ Capacity_{Tesla\ Model\ S,t}$$

- LFP is mostly produced by Chinese battery makers (such as BYD) for Chinese car makers. Therefore, we assume that China's LFP installed capacity in plug-in electric vehicles (EVs) approximates the global installed LFP capacity. The installed data for 2015 and 2016 is sourced from the Chinese lithium research institute, RealLi Research, while the installed numbers for 2010-2014 are estimated using the EV sales in China [270].

- LMO, mixed with NMC, is mostly installed in Nissan and BMW electric vehicles. These companies started with a mixing ratio of LMO-NMC 75/25 and later switched to LMO-NMC 25/75 [271].

$$Installed\ Capacity_{LMO,t} = \sum_{i=Nissan\ Leaf,BMW\ i3} LMR_{i,t} \times Sales_{i,t} \times Average\ Battery\ Capacity_{i,t}$$

where LMR_t is LMO Ratio, which is assumed to be 0.75 for the first-generation models and 0.25 for the upgraded ones.

- NMC is widely installed in the other EVs besides those mentioned above. Thus, we deduct the sum of NCA, LFP and LMO installments from the given total installed capacity to obtain NMC-based installed volume during 2010 to 2016.

A.III. Future Projection and Scenario Analysis

A.III.I. Production Volume (*V*)

Since China plays a leading role in regards to EV development, we chose China as a major driving force for global future market to explore possible outcomes of future battery pack prices. EV market penetration in China is described by fitting a Gompertz function to the historical sales market share (data taken from Global EV Outlook 2017 [63]) and the future targets set by China's government [64]. By incorporating a China-specific car ownership and sales model [65] with the derived EV penetration curve, we obtain the predicted electric private car sales in China between 2018 and 2030. To calculate the total installed capacity in China EV market and in the world, we make the assumptions as follows:

- The sales amount ratio of plug-in hybrid electric vehicle (PHEV) to pure battery electric vehicle (BEV) in China stays constant at the 2017 level, which is around 1/4 [272].
- The global average installed capacity per PHEV is assumed to be 15 kWh after 2017.
- The average installed capacity per BEV is expected to increase each year, at least until 2020, since China's new dual-credit scheme rewards longer-range models [273]. Based on the scheme, the maximum credit that BEV models can receive is 5, corresponding to 350 km for NEDC driving range or around 45 kWh battery capacity (the relationship between NEDC range and required battery capacity is derived from the table given at pushevs.com [274]). Thus, we assume that the battery capacity in BEVs in China will linearly increase from 28.34 kWh in 2017 to 45 kWh in 2020 [270], and then further linearly increase to 75 kWh by 2030 to satisfy demand for larger vehicles and longer driving ranges [92]. In the rest of the world besides China, the battery capacity per BEV is assumed to keep constant at 45 kWh from 2017 to 2020, and then also linearly increase to 75 kWh by 2030. For reference, the 2019 Chevy Bolt's battery capacity is 60 kWh.
- We assume that China's shares of the global BEV and PHEV markets will remain constant from 2018-2030, with 65% of global BEVs (and 30% of global PHEVs) being sold in China each year. For comparison, in 2017 62.3% of global BEV sales were in China, and 27.8% of PHEV sales were in China [49].

- NMC-based LIB is assumed to account for 70% of the global new EV sales market in 2017, 80% in 2018, 90% in 2019, and then eventually dominate the whole EV battery market after 2020, until 2030.

Figure 3.2 shows the resulting EV market penetration curve in China and the equivalent annual installed capacity in China and in the world.

A.III.II. Mineral Costs (*MinC*)

Growing demand for LIBs drives up the raw materials prices. Cobalt prices, in particular, have been rising sharply in the past two years, shown in Figure A5. The Democratic Republic of Congo (DRC) is the largest producer of cobalt globally, accounting for 54% of global mine production in 2016 [67]. As the supply concerns and uncertainties grow due to the unstable political situation in the DRC, as exemplified by the recent tax reform proposal, the price of cobalt spikes [275]. Since cobalt is considered the biggest source of future mineral costs uncertainties, here, we consider three different scenarios based on cobalt price projections. In Scenario 1: The cobalt price remains constant (in constant dollars) at its 2016 price. In both Scenario 2 and in the Base Case Scenario we assume that cobalt price will linearly increase with time from its 2016 price, but with different slopes in each scenario. In Scenario 2 we assume continuation of the recent very rapid price increases based on the fitted slope throughout 2016 and 2017, Figure A3. For the Base Case Scenario we assume more moderate price increases based on fitting the slope only between February to November 2017.

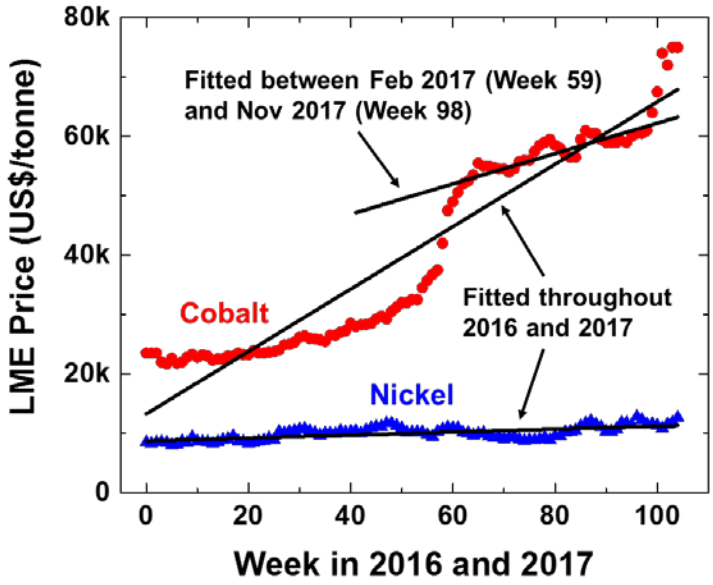

Figure A.3. Cobalt and nickel price on LME in 2016 and 2017 [68,276]

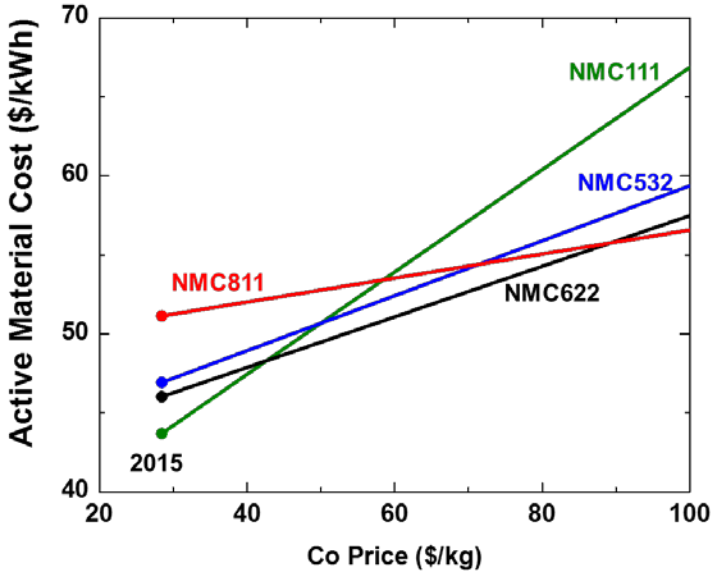

Figure A.4. Active materials cost versus cobalt price for different versions of NMC batteries. We assume the other element (Li, Ni, Mn) costs stay constant and the relative cumulative installed capacity is same across the four different NMC compositions. The cobalt price on 03/28/2018was $93.00/kg.

While the cobalt price is given by these three different projections, nickel and lithium prices are assumed to remain constant in Scenario 1 or follow the same rising trends (linear growth) as what they have done in the past several years in both Scenarios 2 and the Base Case Scenario. Manganese and graphite prices are both assumed to be constant after 2016 since their price variations are relatively negligible and insignificant. We note that the trajectory of cobalt prices will further affect our assumptions of the future NMC evolution, since the cobalt intensity differs across the four compositions of NMCs. When keeping all the other variables in the first-stage learning model constant, we find that, in terms of active materials cost, NMC622 will be the most appealing one when the cobalt price is between $43/kg to $86/kg. However, if the cobalt price rises above $86/kg, NMC811 will take over as the lowest active material cost option, as shown in Figure A4.

A.III.III. Base Case Scenario: Moderate Linear Increase in Cobalt Price after 2016

In the base case scenario, shown in Figure 3, the cobalt price is assumed to follow the same trend as that of the period between February and November 2017, giving a result of $13.3/kg increase per year. Nickel and lithium prices are also assumed to increase linearly at the same rate as their historical trends: Ni and Li prices increase by $1.3/kg and $1.9/kg annually, respectively. On the other hand, manganese and graphite prices are both assumed to be constant after 2016. The associated mineral costs for NMCs based on elemental analysis is shown in Figure A5.

The projected active materials costs, derived from the first-stage learning curve, is shown in Figure A6. It is shown that as the cobalt price increases, NMC111, NMC532, NMC622 and NMC811 take turns providing lowest synthesis cost for battery pack producers; namely, the whole industry will likely shift toward Ni-rich compounds with higher specific capacity and lower cobalt-intensity over time in this scenario. Given these conditions, our model predicts that NMC-based LIB pack prices will fall to about $124/kWh in 2030. For comparison, we also perform conventional learning curve analysis, ignoring the floor imposed by the costs of material inputs, which results in $77/kWh in 2030, i.e. the conventional approximation underestimates battery prices by about 38%, see Figure 3.5.

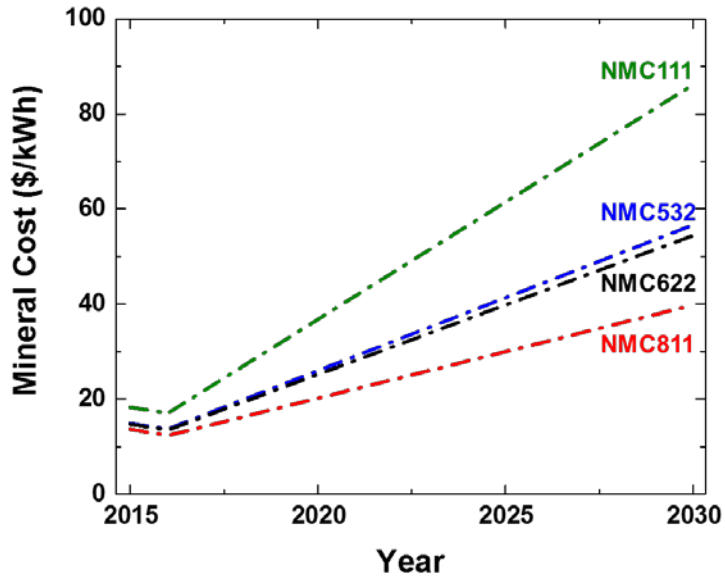

Figure A.5. Base Case projected mineral costs for 4 different compositions of NMCs

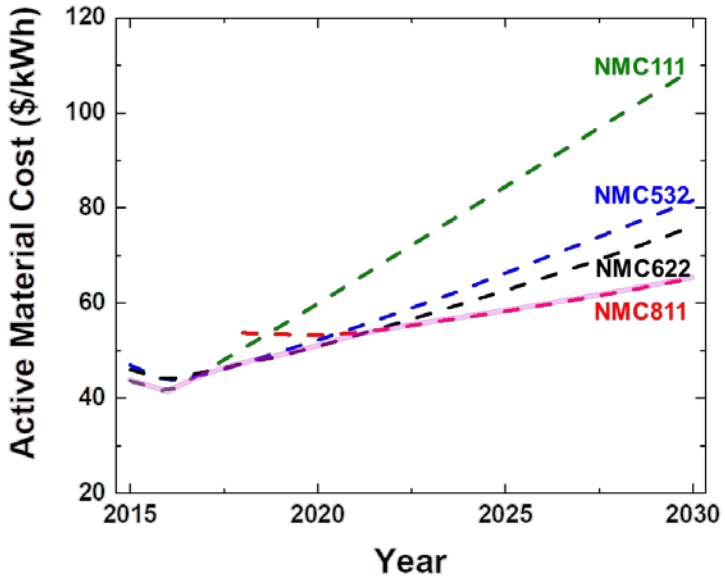

Figure A.6. Projected active materials costs for 4 different compositions of NMCs. The magenta line represents the floor price for the battery pack price learning curve.

A.III.IV. Scenarios 1 and 2: Two Extreme Scenarios

In Scenario 1, we assume that all the mineral costs for battery materials stay constant after 2016, which is unlikely for cobalt and lithium due to the growing demand of EVs. In Scenario 2, we assume that cobalt, nickel and lithium prices all follow the same trends (linear growth) as they have over the past several years: Co, Ni and Li prices increase $27.3/kg, $1.3/kg and $1.9/kg annually respectively. Since cobalt prices have been rising very rapidly recently, this leads to quite a high future price for cobalt, probably an overestimate. . Manganese and graphite prices are both assumed to be constant after 2016 in both scenarios. Figure A7 shows the mineral costs for 4 different compositions of NMCs under the two scenarios. Since the cobalt price in Scenario 1 will always be the average price during 2016 (=$25.36/kg), in Scenario 1 there will be no incentive to shift from NMC622 to NMC811. However, Scenario 2 assumes that the cobalt price will soar, and thus encouraging transition toward less cobalt-intense NMC811. As a result, in that scenario NMC811 will dominate the market. The market share evolution assumptions are presented in Figure A8 for the two scenarios. The projected annual market shares in each NMC class up to 2020 are derived from the statistics given by the report of 2017 China international annual meeting of nickel and cobalt industry, since we assume those shifts in battery type are already in the pipeline [277]. In our projections for years after 2020, we assume the market always shifts towards the most cost-effective (i.e. lowest $/kWh) NMC ratio.

The projected active materials costs and battery pack prices under these two scenarios are shown in Figs. A9 and 10. In Figure A10, the drops in mineral costs in 2019/2020 under Scenario 1 and Scenario 2 are due to projected shifts in the dominant battery types being manufactured in those years, from NMC111 to NMC622 in Scenario 1, and to NMC811 in Scenario 2. As shown in Equation (3.1), active materials cost (MatC) is determined not only by mineral cost (MinC) but also cumulative production volume (V); at present the processes used to manufacture active materials are more expensive than the minerals, but this is projected to change in some scenarios. Figure A11 shows the battery pack price breakdowns over time, suggesting that active material costs will more likely make up the major part when the cobalt price increases. Given these conditions, our model predicts that NMC-based LIB pack prices in 2030 will fall to about $93/kWh in Scenario 1 and about $140/kWh in Scenario 2. Comparing the conventional learning curve to our model, the conventional model will underestimate the price by 17% and 45% in Scenario 1 and 2, respectively. In all Scenarios the future battery price is significantly higher than predicted by the conventional

learning curve. As manufacturing improves but the elemental costs increase, the contribution to battery pack price from materials becomes more significant, and thus conventional learning curve approaches (which do not break out mineral costs) give larger errors.

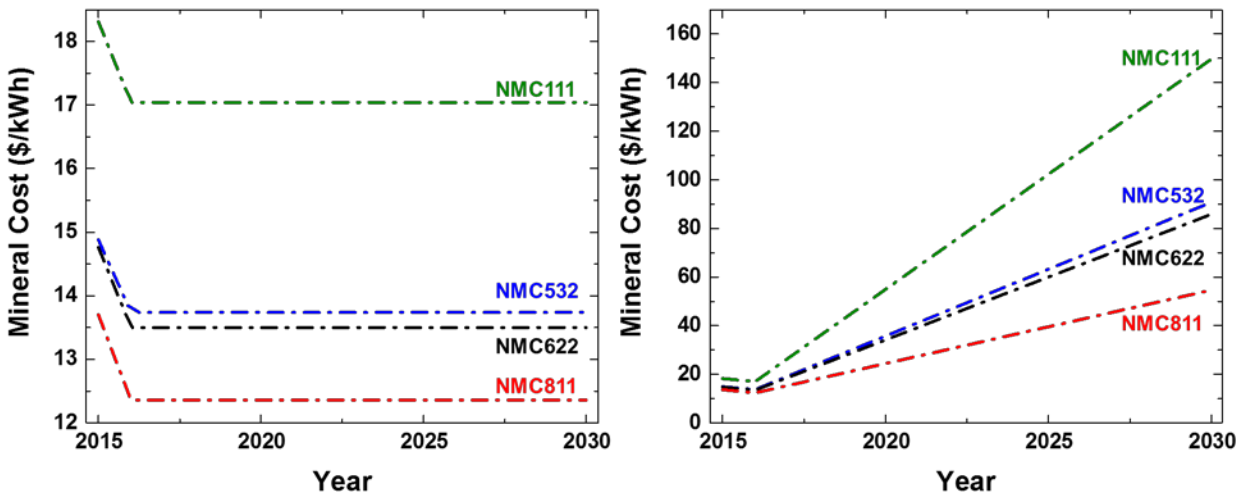

(a) (b)

Figure A.7. Mineral costs under (a) Scenario 1 and (b) Scenario 2

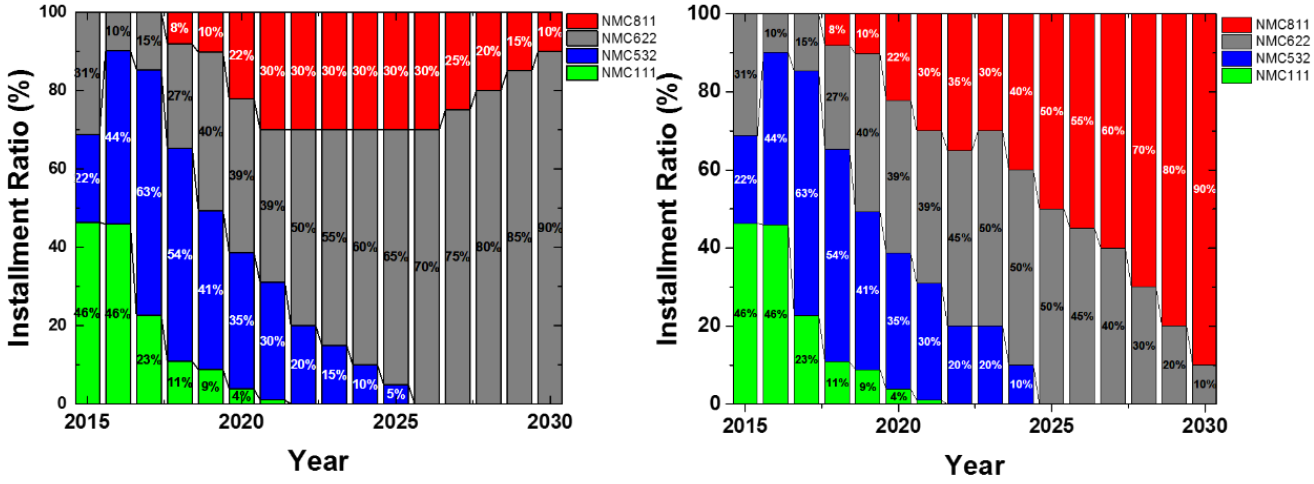

(a) (b)

Figure A.8. Projected annual market shares in the NMC class under (a) Scenario 1 and (b) Scenario 2

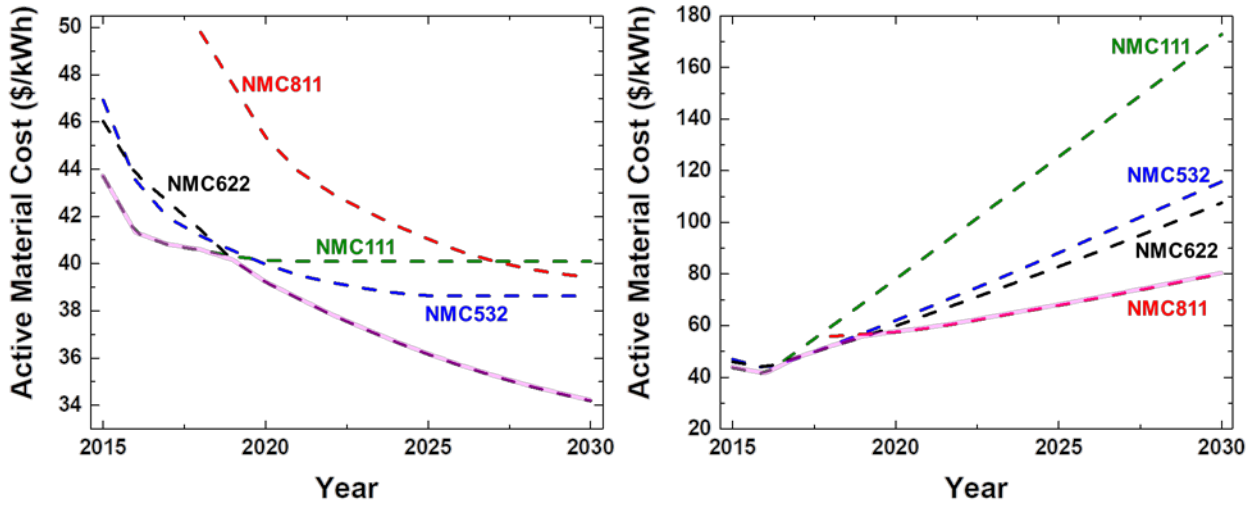

(a) (b)

Figure A.9. Projected active materials costs under Scenario 1 and 2. The magenta lines represent the floor price for the battery pack price learning curve.

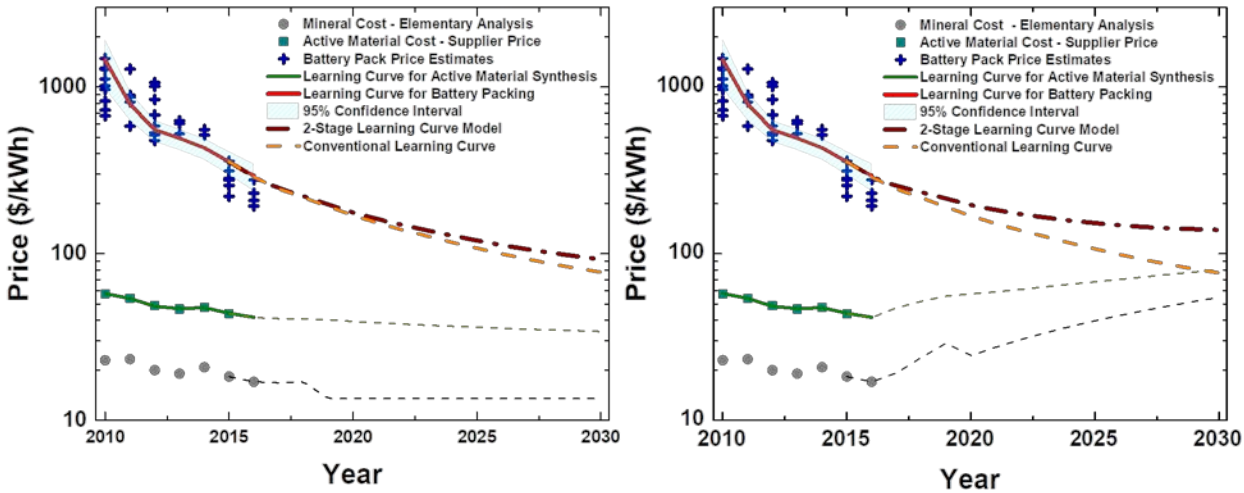

(a) (b)

Figure A.10. Price trajectory of NMC Li-ion battery pack in EV under (a) Scenarios 1 and (b) Scenario 2. Future projections from the conventional learning curve and our 2-stage learning curve model are shown, indicating that battery prices in 2030 will be

underestimated by 17% and 45% if one ignores the learning limits set by materials costs (US$77/kWh versus US$93/kWh in Scenario 1 and US$140/kWh in Scenario 2).

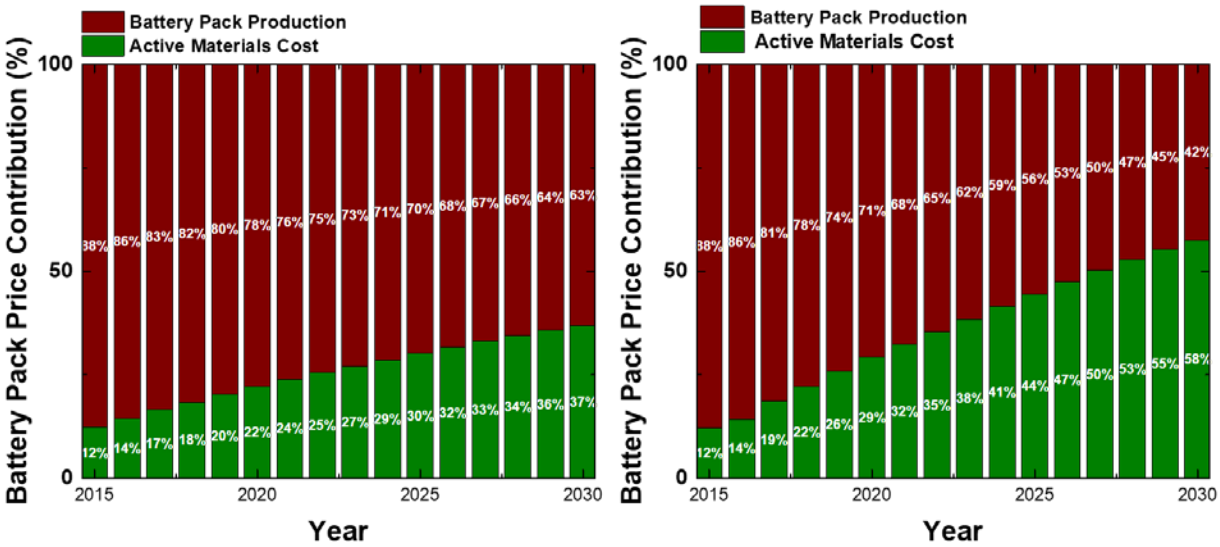

(a) (b)

Figure A.11. Battery pack price breakdowns over time under (a) Scenario 1 and (b) Scenario 2

A.IV. Chemical Cost of Storage and Chemical Specific Energy for Promising Battery Candidates for EV Applications

The chemical cost of storage (CCS) and chemical specific energy for 24 electrochemical couples promising for EV applications are listed in Table A3 and plotted in Figure 3.6. Both terms are defined here to include the costs and mass of electrochemically active materials and electrolyte. The "Year" column in Table A3 represents the filing year of the first patent, the publication year of the first paper, or the year that the electrochemical couple became technically viable. For instance, although the Li metal anode has been known since the 1980s, $LiNi_xMn_yCo_{1-x-y}O_2$ (NMC) was introduced in 1999 as a new cathode material for Li-ion batteries; therefore, the Li/NMC chemistries are listed with the year 1999. The methodology for calculating CCS and energy density was adopted and modified from Li et al. [72]. The prices and sources of electrochemically active materials are tabulated in Table A4.

$$CCS\left(\frac{US\$}{kWh}\right) = \frac{m_a\left(\frac{kg}{kAh}\right)\times P_a\left(\frac{US\$}{kg}\right)+m_c\left(\frac{kg}{kAh}\right)\times P_c\left(\frac{US\$}{kg}\right)+m_e\left(\frac{kg}{kAh}\right)\times P_e\left(\frac{US\$}{kg}\right)}{Voltage\ (V)} \quad \text{(Eq.A4)}$$

$$Chemical\ Specific\ Energy\left(\frac{kWh}{kg}\right) = \frac{Voltage(V)}{m_a\left(\frac{kg}{kAh}\right)+m_c\left(\frac{kg}{kAh}\right)+m_e\left(\frac{kg}{kAh}\right)} \quad \text{(Eq.A5)}$$

The CCS and chemical specific energy are calculated according to Eqs. A4 and A5 respectively, where m_a, m_c, and m_e are the masses of the anode, cathode, and electrolyte in a 1 kAh battery, respectively. P_a, P_c, and P_e are the unit prices of the anode, cathode, and electrolyte, respectively; and *Voltage* is the average voltage of the electrochemical couple. For the details of electrolyte to active materials ratio and how to obtain the mass of the anode, cathode, and electrolyte, please refer to Li et al. (Ref. 255). Li ion and Na ion batteries belong to Type I: Two Porous Electrodes, while Li metal, conversion cathode, and multivalent-based batteries belong to Type II: Solid Plate Electrode and Porous Electrode.

Table A.3. Year of introduction, chemical cost, and energy density for electrochemical couples

Year	Label	Cost ($ /kWh)	Energy (kWh/kg)	Anode/Cathode	Battery Type	Ref
1984	C_6/LMO	45.6	252.0	$C_6/LiMn_2O_4$	Li ion	[278]
1991	C_6/LCO	83.2	315.8	$C_6/LiCoO_2$	Li ion	[279]
1997	C_6/LFP	44.0	263.0	$C_6/LiFePO_4$	Li ion	[280]
1999	C_6/NMC_{111}	53.6	307.5	$C_6/LiNi_{0.33}Mn_{0.33}Co_{0.33}O_2$	Li ion	[281]
1999	C_6/NMC_{532}	56.1	334.4	$C_6/LiNi_{0.5}Mn_{0.3}Co_{0.2}O_2$	Li ion	[281]
1999	C_6/NMC_{622}	52.8	352.1	$C_6/LiNi_{0.6}Mn_{0.2}Co_{0.2}O_2$	Li ion	[281]
1999	C_6/NMC_{811}	57.2	363.3	$C_6/LiNi_{0.8}Mn_{0.1}Co_{0.1}O_2$	Li ion	[281]
2002	C_6/NCA	68.3	333.5	$C_6/LiNi_{0.8}Co_{0.15}Al_{0.05}O_2$	Li ion	[282]
2005	C_6/LRMO LMNO	35.6	445.7	$C_6/0.3Li_2MnO_3$ $0.7LiMn_{0.5}Ni_{0.5}O_2$	Li ion	[283]
2014	C_6/CAM-7	55.1	374.2	C_6/doped-$LiNiO_2$	Li ion	[284]
1980	Li/LCO	72.2	457.9	$Li/LiCoO_2$	Li metal	[285]
1997	Li/LFP	32.6	376.4	$Li/LiFePO_4$	Li metal	[280]
1999	Li/NMC_{111}	43.1	446.2	$Li/LiNi_{0.33}Mn_{0.33}Co_{0.33}O_2$	Li metal	[281]
1999	Li/NMC_{532}	45.8	497.0	$Li/LiNi_{0.5}Mn_{0.3}Co_{0.2}O_2$	Li metal	[281]
1999	Li/NMC_{622}	42.6	535.8	$Li/LiNi_{0.6}Mn_{0.2}Co_{0.2}O_2$	Li metal	[281]
1999	Li/NMC_{811}	46.9	561.6	$Li/LiNi_{0.8}Mn_{0.1}Co_{0.1}O_2$	Li metal	[281]
2002	Li/NCA	57.1	508.4	$Li/LiNi_{0.8}Co_{0.15}Al_{0.05}O_2$	Li metal	[282]
2005	Li/LRMO LMNO	26.3	751.1	$Li/0.3Li_2MnO_3$ $0.7LiMn_{0.5}Ni_{0.5}O_2$	Li metal	[283]
2014	Li/CAM-7	44.9	587.34	Li/doped-$LiNiO_2$	Li metal	[284]
1958	Li/S	13.7	1585.6	Li/S	Conversion	[286]

2000	Mg/Mo_6S_8	508.0	73.6	Mg/Mo_6S_8	Multivalent	[287]
2016	Mg/T_2S_4	358.7	151.4	Mg/T_2S_4	Multivalent	[288]
1992	HC/NVP	101.8	205.7	$C_6/Na_3V_2(PO_4)_3$	Na ion	[289]
2001	HC/P2-MN	52.9	301.4	$C_6/Na_{0.67}Mn_{0.67}Ni_{0.33}O_2$	Na ion	[290]
2009	HC/O3-MN	65.3	205.7	$C_6/NaMn_{0.5}Ni_{0.5}O_2$	Na ion	[291]

Table A.4. Chemical prices of active materials used in chemical costs and energy density calculations

Chemical	**Price ($/kg)**	**Source**
LCO	40.00	[292]
LFP	10.00	[293]
NMC111	20.00	[294]
NMC532	25.00	[294]
NMC622	25.00	[294]
NMC811	30.00	[294]
LMO	10.00	[293]
NCA	34.00	[292]
LRMO LNMO	20.00	[292]
CAM-7	30.00	[292]

Chemical	**Price ($/kg)**	**Source**
Graphite	12.00	[292]
Lithium metal	50.05	[293]
S	0.25	[293]
Mg	2.43	[293]
Ti_2S_4	80.00	[295]
Mo_6S_8	50.00	[296]
Hard carbon	20.00	[292]
$Na_2Mn_2NiO_6$	15.00	[292]
$NaMn_{0.5}Ni_{0.5}O_2$	15.00	[292]
$Na_3V_2(PO_4)_3$	25.00	[297,298]

A.V. Correlation between practical specific capacities of $LiNi_xMn_yCo_{1-x-y}O_2$ (NMC) and Ni content

While NMC111 and NMC532 are already commercially well-established in EV applications, NMC622 is a state-of-the-art material with room for improvement which has been introduced into the market recently. Since the Ni^{2+}/Ni^{3+} and Ni^{3+}/Ni^{4+} redox couples contribute the most to materials capacity, increasing the Ni content in NMC materials leads to higher practical capacity. However, Ni-rich NMCs still face some challenges such as side reactions with the electrolyte at high voltages and Li/Ni cation mixing in the layered oxide structure [299]. Cation mixing occurs when the transition metal ions occupy Li sites during synthesis or as a result of transition metal ion migration during upon high levels of delithiation during charging. Such cation mixing can give raise to high overpotential by impeding Li-ion transport or form electrochemically inactive phases, both of which cause capacity fading under fixed voltage cutoff condition. Despite these challenges, LG Chem has announced that they will start producing NMC811 batteries for EV applications in 2019 [300]. In an attempt to quantify the capacity gains from Ni-rich NMC, we collected the practical specific capacity of NMCs of widely studied compositions. Data reported for industrial practice and research results under conditions projected for real world applications are included and tabulated in Table A5. Specifically, the NMC532 and NMC622 capacities are for cycling between 3.0 – 4.5 V and 2.5 – 4.6 V versus Li/Li^+, respectively, as reported at DOE Vehicle Technologies Office review [301]. The CAM-7 data, supplied by TIAX LLC, are obtained from an Army Research Laboratory evaluation report, in which the cell was discharged from ~4.3 V to 3.0 V [302]. Data for the remaining three materials are obtained from publications describing current industrial practices or outlooks.

To illustrate the effect of increasing Ni content, Figure A12 shows the specific capacity and calculated extractable Li per $LiNi_xMn_yCo_{1-x-y}O_2$ formula in black circles and blue squares, respectively. The specific capacity for $LiCoO_2$ (LCO) and CAM-7 are also included for comparison. CAM-7, announced by CAMX Power, is an example of the continuing trend toward even more Ni-rich intercalation compounds beyond NMC811 [284]. Although the exact chemistry remains undisclosed, CAM-7 is believed to be composed of $LiNiO_2$ with a few percent dopants. The clear upward trend in NMC capacity with respect to Ni content also allows us to predict the maximum capacity that is achievable with Ni-rich NMC. The black line in Figure A12 represents

a linear regression from the capacities of NMC materials, and the blue line for extractable Li per formula. The linear extrapolation predicts a specific capacity of ~140 mAh/g at 0% Ni and ~230 mAh/g at 100% Ni. Interestingly, in the early development of Li-ion batteries, LCO had a typical specific capacity of 140 mAh/g in commercial batteries, in agreement with the linear extrapolation [303]. The reported 155 mAh/g of LCO was enabled more recently by discoveries in new electrolytes that can sustain higher voltages [304]. On the other end of the spectrum, the 220 mAh/g of CAM-7 agrees reasonably with the prediction at 100% Ni, and the practical capacity may increase slightly with additional development of $LiNiO_2$-based cathode materials.

Table A.5. Practical specific capacity of lithium nickel manganese cobalt oxide ($LiNi_xMn_yCo_{1-x-y}$, NMC) and other representative cathode materials

Abbreviation	Materials	Ni Content (%)	Capacity (mAh/g)	Source
NMC111	$LiNi_{1/3}Mn_{1/3}Co_{1/3}O_2$	33.3	170	[303]
NMC532	$LiNi_{0.5}Mn_{0.3}Co_{0.2}O_2$	50	185	[301]
NMC622	$LiNi_{0.6}Mn_{0.2}Co_{0.2}O_2$	60	200	[301]
NMC811	$LiNi_{0.8}Mn_{0.1}Co_{0.1}O_2$	80	210	[305]
LCO	$LiCoO_2$	0	155	[306]
CAM-7	Doped-$LiNiO_2$	~100	220	[302]

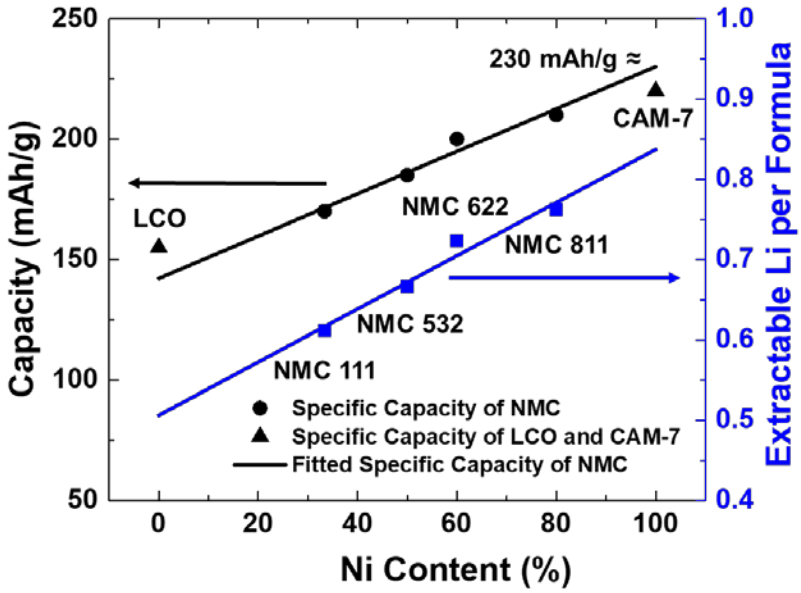

Figure A.12. Enhanced practical specific capacity and extractable Li per $LiNi_xMn_yCo_{1-x-y}O_2$ formula and other representative cathode materials with increasing Ni content

A.VI. Specific capacity enhancement of $LiCoO_2$ between 1995 and 2017

Table A.6. Representative lithium cobalt oxide ($LiCoO_2$, LCO) practical specific capacity in historical journal publications

Year	Capacity (mAh/g)	Source
2017	201	[307]
2017	196	[308]
2017	203	[309]
2017	187	[310]
2016	176	[311]
2015	198	[312]
2015	177	[313]
2015	178	[314]
2014	174	[315]
2014	189	[316]
2012	182	[317]
2012	179	[318]
2011	176	[319]
2010	177	[320]
2009	190	[321]
2009	180	[322]
2009	176	[323]
2008	177	[324]
2007	190	[325]
2007	179	[326]
Year	**Capacity (mAh/g)**	**Source**
2006	185	[327]
2006	171	[328]
2005	174	[329]
2005	175	[330]
2005	178	[331]
2005	176	[332]
2004	186	[333]
2004	179	[334]
2003	188	[335]
2003	192	[336]
2003	169	[337]
2002	179	[338]
2001	161	[339]
2000	151	[340]
2000	168	[341]
1999	152	[342]
1998	132	[343]
1997	135	[344]
1997	132	[345]
1995	129	[346]

As mentioned earlier, the typical specific capacity of $LiCoO_2$ (LCO) in commercial batteries has increased from 140 to 155 mAh/g due to discoveries of new electrolyte compositions that can sustain higher charge voltage [304]. To gauge the evolution of practical LCO capacity and illustrate the capacity enhancement for Li intercalation compounds, we collected reversible capacity data from scientific publications between 1995 and 2017. The data were obtained using Google Scholar with the search term "$LiCoO_2$ Cathode," then portioning the results according to year. Only discharge capacities obtained after 20 or more cycles are included. Thus results under unrealistic test conditions such as where a high charge voltage resulted in rapid initial capacity fade were not included. The exception to these rules occurs for data before 1998, in which cycling results for 20 cycles or more are rare. Using this procedure, the year of publication and the reversible specific capacity of LCO are tabulated in Table A6 and plotted in Figure A13.

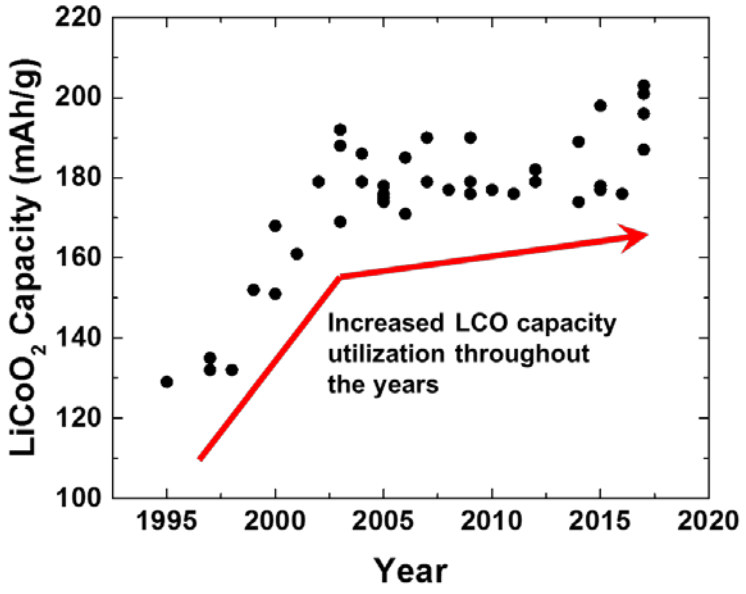

Figure A.13. Specific capacity of $LiCoO_2$ between 1995 and 2017

The reported reversible capacity of LCO increased over time as shown in Figure A13. Initially, the capacity rapidly increased from ~130 mAh/g in 1995 to ~180 mAh/g in 2002. After 2002, however, the rate of enhancement slowed down significantly with reversible capacity reaching ~195 mAh/g in 2017. We believe that most battery electrode compounds will follow a similar trajectory of capacity improvement over time to the results obtained for LCO. Therefore, the newer or less developed chemistries, presented in Figure 3.6 and Appendix. A.IV, will likely experience

chemical cost reductions and energy density improvements in the coming years as a result of electrode capacity enhancement. At the same time, the economics of scale will also decrease the active materials costs, and thus chemical costs of storage for these chemistries. However, the mineral costs are unlikely to drop significantly, since mining technology is well-established, and typically the richest resources are exploited first.

Appendix B. Additional Details for Implications for Private Motorization Rate

B.I. Sensitivity Analysis

The private passenger vehicle market presented in Chapter 4.4.1 relies on several parameters (Table B1). We use a tornado diagram (Figure B1) to illustrate how the private car market is conditioned by the EV-related assumptions. The major EV-related parameters here are EV adoption rate, battery pack price, and the ratio of PHEVs to BEVs sold. The sensitivity range for each variable is based on the low and high values provided in Table B1. The governing parametric values described in Chapter 4.2 are used to calculate the base case of the tornado diagram (ratio of 1 in Figure B1). We found that EV penetration rate is the most important parameter; however, all of them have a mild impact of less than 5% on the private passenger vehicle stock in 2030.

Table B.1. Parametric values for sensitivity analysis

Variable	Low value	Base value	High value
EV sales market share in 2030 (%) [a]	19	37	75
Battery pack price ($/kWh) [b]	93	124	140
Ratio of PHEVs to BEVs sold (-) [c]	0.14	0.3	0.91

Note: [a] To examine what if EV penetration rate doubles or reduces by half scenario; [b] ranges for BEV battery prices are taken from our previous study that considered the impacts of materials cost [81]*; [c] the lower value of 0.14 is the ratio of PHEVs to BEVs sold in Korean in 2018, while the higher value of 0.91 is the average ratio of the European market in 2018* [2].

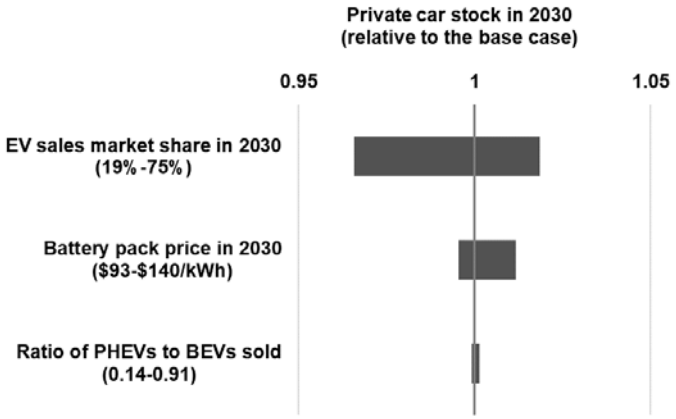

Figure B.1. Sensitivity of the projected private car stock in 2030 to the major EV-related assumptions.

Appendix C. Additional Details for Battery Swapping Deployment

C.I. Equations for per-km cost evaluations

Abbreviations shown in Table C1 are defined as follows (all the right-hand side parameters are defined in Table 6.1):

- Aggregate Vehicle Procurement Cost (**AVPC**) ($) = MSRP ($) - Battery Capacity (kWh) × Battery Cost ($/kWh)
- Aggregate Battery Cost (**ABC**) ($) = Battery Capacity (kWh) × Battery Cost ($/kWh)
- Battery Inventory for battery swapping mode (**BI**) ($) = 28 (#) × Battery Capacity (kWh) × Battery Cost ($/kWh)
- Aggregate Land Cost (**ALC**) ($/Year) = Land Use ($m^2$) × Unit Land Use Cost ($/m^2)
- Annual Number of Vehicles Served (**ANVS**) (#/Year) = Annual Productivity (Days/Year) × 24 (Hours/Day) / Recharging Time for 208 km (Hours)
- Annual Number of Trips Served (**ANTS**) (#/Year) = Annual Productivity (Days/Year) × 24 (Hours/Day) / (Recharging Time for 208 km + Active Hours of Taxi Time for 208 km) (Hours)
- Vehicle Lifespan ($\mathbf{N_V}$) (Year); Recharging System Lifespan ($\mathbf{N_R}$) (Year); Land Lifespan ($\mathbf{N_L}$) (Year)
- Hourly Operating Revenue (**HOR**) ($/Hour) = Operating Revenue ($/km) × Distance Driven per Active Hour of Taxi Time (km/Hour)
- Capital Recovery Factor ($\mathbf{CRF_i}$) (1/Year) = $\mathbf{r}\times(1+\mathbf{r})^{\mathbf{Ni}}/((1+\mathbf{r})^{\mathbf{Ni}}-1)$; Annual discount rate ($\mathbf{r}$) = 5% , $\mathbf{N_i} = \mathbf{N_V}$ for vehicle procurement and battery in extra vehicles; $\mathbf{N_i} = \mathbf{N_R}$ for refueling system and battery inventory in swap stations; $\mathbf{N_i} = \mathbf{N_L}$ for land cost.
- Scale up factor (**SF**) is applied in BEV charging w/ extra vehicles scenarios to capture the increased vehicle capital costs (see Chapter 6.2.1 for more details).
- Utilization factor for vehicle usage ($\mathbf{UF_v}$) =

  1) Single-shift taxis: [12 (Hours) + (Recharging Time for 208 km (Hours) × 285 (km) / 208 (km))] / 24 (Hours)

  2) Double-shift taxis:
    - BEV charging with extra vehicles scenarios: $\mathbf{UF_v} = \mathbf{SF}$ because increasing vehicle fleet size would increase the vehicle capital utilization at the same times.

- Conventional BEV charging and battery swapping scenarios: $\mathbf{UF_v} = 1$.

- Utilization factor for recharging facility (including recharging system, land, and maintenance) ($\mathbf{UF_{RF}}$): see Chapter 6.2.3 for more details.
- The derived values for **SF** and **UF** are listed in Table C2.

Table C.1. Governing equations for per-km cost calculations in BEV/ICEV fleet ecosystems

Per-km Cost	Generalized Equations for BEV Fleet Ecosystem
Vehicle Procurement	$\frac{\text{SF} \times \text{AVPC (\$)} \times \text{CRF}_\text{V}\ (1/\text{Year})}{\text{UF}_\text{V} \times \text{ANTS (\#/Year)} \times 208\ \text{(km)}}$
Battery	$\frac{\text{ABC (\$)}}{\text{Battery Cycle Life (\# Cycle Life)}} \times \frac{1\ \text{(\# Cycle Life)}}{260\ \text{(km)}}$
Extra Battery	For BEV Charging w/ Extra Vehicles: $\frac{\text{(SF-1)} \times \text{ABC (\$)} \times \text{CRF}_\text{V}\ (1/\text{Year})}{\text{UF}_\text{V} \times \text{ANTS (\#/Year)} \times 208\ \text{(km)}}$ For Battery Swapping: $\frac{\text{BI (\$)} \times \text{CRF}_\text{R}\ (1/\text{Year})}{\text{UF}_\text{RF} \times \text{ANVS (\#/Year)} \times 208\ \text{(km)}}$
Electricity	Electricity cost (\$/kWh) $\times \frac{\text{Battery Capacity (kWh)}}{\text{Driving Range per Full Charge (km)}}$
Refueling System	For BEV Charging: $\frac{\text{Recharging System Cost (\$)} \times \text{CRF}_\text{R}\ (1/\text{Year})}{\text{UF}_\text{RF} \times \text{ANVS (\#/Year)} \times 208\ \text{(km)}}$ For Battery Swapping: $\frac{\text{(Swap Station Cost-BI) (\$)} \times \text{CRF}_\text{R}\ (1/\text{Year})}{\text{UF}_\text{RF} \times \text{ANVS (\#/Year)} \times 208\ \text{(km)}}$
Land	$\frac{\text{ALC (\$)} \times \text{CRF}_\text{L}\ (1/\text{Year})}{\text{UF}_\text{RF} \times \text{ANVS (\#/Year)} \times 208\ \text{(km)}}$
Maintenance	For BEV Charging: $\frac{10\% \times \text{Recharging System Cost (\$)}}{1\ \text{(Year)} \times \text{UF}_\text{RF} \times \text{ANVS (\#/Year)} \times 208\ \text{(km)}}$ For Battery Swapping: $\frac{10\% \times \text{(Swap Station Cost-BI) (\$))}}{1\ \text{(Year)} \times \text{UF}_\text{RF} \times \text{ANVS (\#/Year)} \times 208\ \text{(km)}}$

Labor	Labor Cost ($/km)
Opportunity	For BEV Charging (single shift): HOR ($/Hour) $\times \frac{\text{Recharging Time for 77 km (Hour)}}{\text{285 (km)}}$ For BEV Charging (double shifts): HOR ($/Hour) $\times \frac{\text{Recharging Time for 208 km (Hour)}}{\text{208 (km)}}$ For BEV Charging w/ Extra Vehicles & Battery Swapping: HOR ($/Hour) $\times \frac{\text{4 (Minute/Swap)}}{\text{60 (Minute/Hour)}} \times \frac{\text{1 (Swap)}}{\text{208 (km)}}$
Per-km Cost	**ICE (Gasoline)**
Vehicle Procurement	$\frac{\text{ICEV MSRP (\$)} \times \text{CRF}_\text{V}\ \text{(1/Year)}}{\text{UF}_\text{V} \times \text{ANTS (\#/Year)} \times \text{208 (km)}}$
Gasoline Refueling	Fuel Economy (L/100km) $\times$ Retail Gasoline Price ($/L) $\times \frac{\text{1 (km)}}{\text{100 (km)}}$
Labor	Labor Cost ($/km)
Opportunity	For single − shift taxis: 0 For double − shift taxis: HOR ($/Hour) $\times \frac{\text{4 (Minute/Refuel)}}{\text{60 (Minute/Hour)}} \times \frac{\text{1 (Refuel)}}{\text{536 (km)}}$

Table C.2. Scale up factor (SF) and utilization factor (UF) for cost calculations

Number of shifts (12 hours) per day	Business model	Scale up factor (SF)	Utilization factor$_{vehicle}$ (UF_V)	Utilization factor$_{recharging\ facility}$ (UF_{RF})
Single shift	Conventional Level 2	1.00	0.77	0.27
	Conventional Fast	1.00	0.55	0.39
	Swapping	1.00	0.50	0.35
	ICE	-	0.50	-
Double shifts	Conventional Level 2	1.00	1.00	0.90
	Level 2 w/ Extra Vehicle	1.55	1.55	0.80
	Conventional Fast	1.00	1.00	0.90
	Fast w/ Extra Vehicle	1.10	1.10	0.80
	Swapping	1.00	1.00	0.80
	ICE	-	1.00	-

C.II. Sensitivity analysis

The ranges of values used in the sensitivity analysis are provided in Table C3.

Table C.3. Parametric values for sensitivity analysis

Variable	Low value	Base value	High value
Non-swappable battery cost ($/kWh)	144[a]	288	288
Swappable battery cost ($/kWh)	192[a]	383	383
Equipment life (years)	6	8	10
Electricity (¢/kWh)	6.85[b]	13.5	16.03[c]
Gasoline ($/L)	0.77[d]	1.14	1.91[e]
Maintenance (%)	5	10	15
Discount rate (%)	4	5	6

Note: [a] To examine what if battery cost drops by half scenarios; [b] average industrial electricity price in U.S. for October 2019 (U.S. EIA, 2019); [c] average industrial electricity price in Japan for 2018 (U.K. BEIS, 2019); [d] average regular gasoline in U.S. for week of January 13, 2020 (GlobalPetrolPrices.com, 2019); [e] average regular gasoline in Norway for week of January 13, 2020 (GlobalPetrolPrices.com, 2019).

C.III. BEV purchase subsidy policy

The representative BEV model (EU260, range = 260 km) could receive $10,450 (=66,000 Yuan) as a general purchase subsidy from the central and municipal governments. With the first-stage subsidy, the purchase cost differential between BEV and ICEV would be reduced to $6,810 (= $MSRP_{BEV}$ - $MSRP_{ICEV}$ - $10,450). And this remaining cost gap of $6,810 could be entirely covered by the second-stage subsidy for BEV taxi procurement. This suggests that the subsidies for the BEV taxi (EU260) purchased in Beijing in 2017 amounted to $17,260 (= $10,450 + $6,810), making its purchase cost on par with the counterpart ICEV to fleet owners.

Table C.4. Cumulative costs per kilometer (¢/km) with and without the purchase subsidies in Beijing's BEV taxi ecosystems in 2017

Number of shifts (12 hours) per day	Business model	Without subsidies (1)	With subsidies (2)	Difference = |(2)-(1)|
Single shift	Conventional Level 2	43.7	40.3	3.4
	Conventional Fast	35.0	31.6	3.4
	Swapping	36.2	32.8	3.4
Double shifts	Conventional Level 2	51.8	49.1	2.6
	Level 2 w/ Extra Vehicle	34.0	31.3	2.6
	Conventional Fast	35.2	33.3	1.9
	Fast w/ Extra Vehicle	32.2	30.3	1.9
	Swapping	32.7	30.9	1.7

Appendix D. Additional Details for Environmental Impact Assessment

D.I. Integrative framework for environmental impact assessment

One of the major novelties in this work is the linkage between policy scenario construction, private vehicle fleet modeling, air quality modeling, and climate change and health impact assessment. Fleet size estimation is integrated into policy scenario analysis for subsequent climate and health impact quantification. This linkage allows us to capture the environmental impacts of diminished/avoided motorization due to electric vehicle policies, which has been ignored in the existing studies for air quality impact assessment of vehicle electrification. The integrative framework for understanding how sustainable mobility policy alters the vehicle ownership demand and the corresponding environmental externalities is presented in Figure D1. Another major novelty is in the fleet model development which would be described in more detailed below (*).

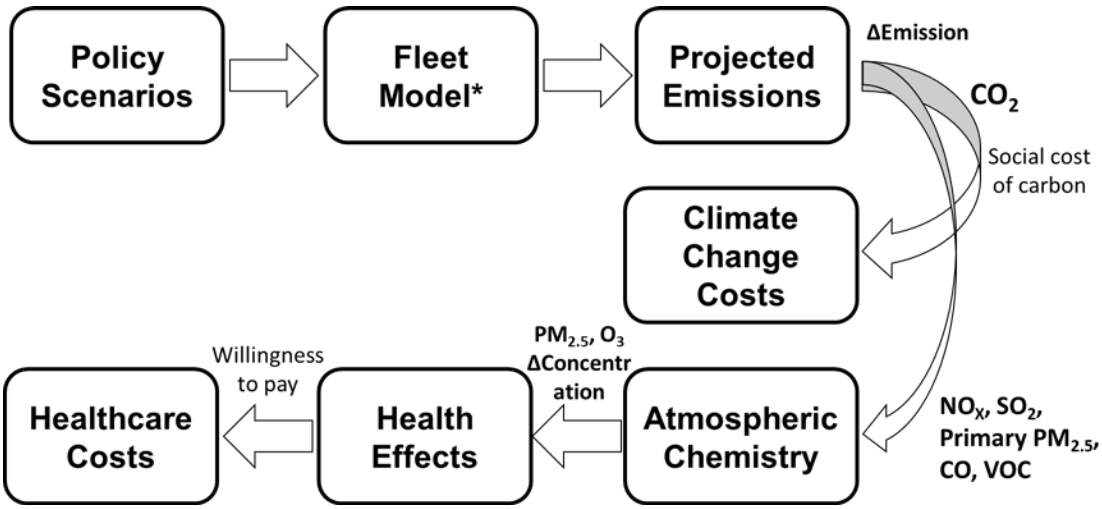

Figure D.1. Integrated assessment framework of emissions, air quality, climate and health impact assessment

*We make contributions to modeling practices in the following three aspects:

1) Vehicle market size estimation (Supplementary information D.IV):

- The developed fleet model is able to perform nationwide as well as detailed subnational level analysis on oil demand, CO2 emissions, and air pollutants of the private vehicle

sector, considering provincial differences in economic development, vehicle market maturity, and vehicle use intensity.

- Interprovincial migration model is built and incorporated into the fleet model to capture people flows across provinces.
- Impact of city-level car ownership restriction policy on the provincial car fleet is investigated and incorporated into the fleet size estimation.

2) Well-to-tank stage emissions (Supplementary information D.VI):

- Interprovincial electricity transmission is taken into account when calculating provincial grid carbon intensity.
- The most up-to-date air pollutant emission factors (i.e., 2017) of regional electricity generation are used in the air pollutant calculation.

3) Tank-to-wheel stage emissions (Supplementary information D.VI):

- Provincial heterogeneity in real-world fuel consumption (varying by weather, traffic, driver behavior, and fuel quality) is considered when computing oil demand and carbon footprint.
- Provincial-level on-road air pollutant emission factors of gasoline-powered cars (varying by vehicle technology, climate, temperature, altitude, fuel quality and so on) are derived and applied in this work.

D.II. Technical parameters of the reference vehicles

CO2 emissions from vehicle manufacturing are derived from multiple sources [197,347–350] and adjusted based on the reference cars weights and battery capacity. Since there was a very limited number of conventional hybrid electric vehicles (HEVs) being sold in China, the fuel consumption rate and manufacturing emissions of HEV are assumed to be 33% less and 27% more than that of the counterpart ICEV [351]. Parameters for ICEV, HEV, PHEV, and BEV are summarized in Table S1 (more details about vehicle specifications car be found in [182]).

Table D.1. Summary of the reference vehicle technical parameters

Vehicle Technology	ICEV	HEV	PHEV	BEV
Fuel consumption	7.6 L/100 km	5.1 L/100 km	6.0 L/100km 18.6 kWh/100km	14.4 kWh/100 km
Curb weight and battery capacity	1,280 kg	--	1,623 kg; 11.9 kWh NMC	1,619 kg; 50.5 kWh NMC
Emissions from vehicle manufacture (tons CO2)	8.1	10.3	11.3 (including battery 1.4 tons CO2)	15.5 (including battery 4.1 tons CO2)

D.III. EV penetration pattern in current policy scenario (CPS)

"Open market index of new energy vehicle" was used to describe the differences in EV brand/model variety and EV market penetration rate across provinces in China [199]. Provinces with a higher open market index are considered more acceptable to this new vehicle technology and with fewer EV adoption barriers (such as charging convenience, EV purchase price, and familiarity). We categorize 31 provinces into four groups based on their open market index documented in the iCET report [199], as shown in Table D2.

Table D.2. Group categorization for new energy vehicle (NEV) open market index and their contribution to the national cumulative EV sales in the end of 2017

NEV open market index	Province	Cumulative EV sales share in 2017 (%)
Group 1 (k=1)	Tianjin, Beijing, Zhejiang, Hubei, Shanghai, Sichuan, Henan	50
Group 2 (k=2)	Fujian, Jiangsu, Shaanxi, Guangdong, Shandong, Hebei, Hunan, Shanxi	37
Group 3 (k=3)	Chongqing, Yunnan, Anhui, Guangxi, Jiangxi	10
Group 4 (k=4)	Inner Mongolia, Liaoning, Jilin, Heilongjiang, Hainan, Guizhou, Tibet, Gansu, Qinghai, Ningxia, Xinjiang	3

Projecting future EV sales at province level is uncertain. In the CPS, we assume that the provincial EV sales growth would follow Equation D1, meaning that the incremental increase in EV sales in group *k* would be proportional to its contribution to the nationwide EV cumulative sales by 2017 (see Table D2 for the contribution percentage); the incremental increase in EV sales in province *p* in group *k* would be proportional to its contribution to the group vehicle sales in year *i*.

$$\mathbf{Sales_{p,i,EV}} = \mathbf{Sales_{p,i\text{-}1,EV}} + \Delta\mathbf{Sales_{N,i,EV}} \times \frac{\sum_{p\in k}\mathbf{CumSales_{p,2017,EV}}}{\mathbf{CumSales_{N,2017,EV}}} \times \frac{\mathbf{Sales_{p,i}}}{\sum_{p\in k}\mathbf{Sales_{p,i}}} \quad \text{(D1)}$$

where $Sales_{p,i,EV}$ is EV sales in province *p* in year *i*; $\Delta Sales_{N,i,EV}$ (=$Sales_{N,i,EV}$-$Sales_{N,i\text{-}1,EV}$) is the national increase in EV sales in year *i*; $\sum_{(p\in k)} CumSales_{p,2017,EV}$ is the provincial sum of the

cumulative EV sales in NEV market open index group k in 2017; $CumSales_{N,2017,EV}$ is the national cumulative EV sales in 2017; $Sales_{p,i}$ is private car sales in province *p* in year *i*; $\sum_{(p \in k)} Sales_{p,i}$ is the provincial sum of the private car sales in NEV market open index group k in year *i*.

It is noted that the national EV sales are expected to keep growing owing to the dual-credit mandate. EV sales projection at national level is detailed in our previous study [132]: we estimate that EVs will account for 21% and 37% of the total private passenger vehicle market share in 2025 and 2030.

D.IV. Private vehicle fleet size projection

Here we explain how we disaggregate the national-level fleet model by provinces and how we evaluate the impacts of city-level car ownership restriction policy on provincial car fleet.

D.IV.I Disaggregating the national model by province (no car ownership restriction policy counterfactual):

The car ownership function, g(x, pi)

Much of the uncertainty in China's future private car stock stems from data limitations for estimating the γ parameter for the Gompertz function, which represents the eventual probability of possessing a car when people have high purchasing power. Gompertz function curves (g) are expected to be varied across provinces depending on the urban population density, auto dependency, mobility levels across all modes, road infrastructure investment, consumer preference, and so on. Figure D2(a) shows the historical relationship (2013-2016) between car ownership level (i.e., cars per 100 people) versus per-capita disposable income at a provincial level. Shanghai was an early adopter of license auctioning, putting the policy in place in 1994 before motorization had really picked up. Beijing, on the other hand, did not implement its own car restriction system until 2011 when its private car had hit to 4 million.

Thus, when we compute the saturation parameters of the Gompertz function (γ) at a provincial level, we exclude Shanghai because the license plate quota policy has obscured the underlying relationship between the probability of owning a car and car affordability. Figure D2(b) depicts the resulting mean Gompertz curves that are obtained from 300 samples of γ with the associated probability distribution from Monte Carlo simulation. For Shanghai, we assume its γ is the same as that of the city cluster 1 (discussed below).

(a) **(b)**

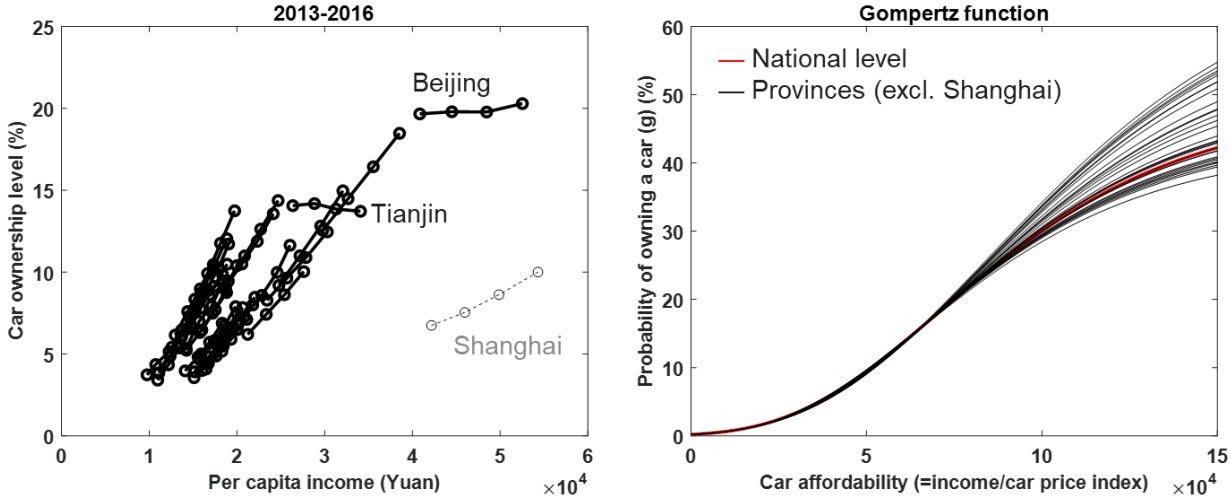

Figure D.2. (a) Private car ownership level versus per capita disposable income at the provincial level; (b) the computed Gompertz function curves that describe the probability of owning a car versus car affordability at both national and provincial level in China; Shanghai is excluded because its early adoption of license plate quota policy had obscured the underlying relationship.

Shanghai: Mapping Provinces to City Cluster 1

Four city types were previously established in the literature, derived from trends in urbanization and motorization patterns for 287 Chinese municipal administrative areas for the period from 2001-2014 [352]:

1. Large, wealthy cities with metro rail systems (N = 23, including *Shanghai*, Beijing, Guangzhou, Shenzhen, Tianjin, and Hangzhou),
2. Low-density, wealthy cities with auto-oriented mobility patterns (N = 41, including Haikou and Sanya in Hainan Province),
3. Low-density, medium-wealth cities with moderate mobility (N = 134), and
4. High-density, low-wealth cities with lower mobility levels (N = 89).

The most disaggregate form of easily available data for our fleet model is at the provincial level. So we begin by estimating the saturation parameters (γ_p) of car ownership function (i.e., $g(x, p_i)$) for each of the 30 provinces in China, excluding Shanghai (Figure D2(b)). Next we map the province-level models to the four city clusters using a method presumably similar to that used by Gan et al. (2019) [353]. While Gan et al. (2019) used car stock as the weighting factor, we use GDP. GDP is often used for projecting vehicle ownership [30,354] and is therefore the best proxy available for car purchasing characteristics in the absence of information on income and car price before 1994 in Shanghai. It is noted that here we only focus on city cluster 1 to which Shanghai province belongs.

We calculate γ_{c1} for cluster 1 by taking the average of the provincial parameters weighted by the proportion of cluster GDP contributed by each province (w_p):

$$\gamma_{c1} = \sum_{p=1}^{30} w_p \gamma_p = \sum_{p=1}^{30} \frac{GDP_{p,c1}}{GDP_{c1}} (\gamma_p) = \gamma_{SH} \tag{D2}$$

where $w_p = \frac{GDP_{p,c}}{GDP_c}$, GDP_c is the total GDP of all cities in cluster *c1* and $GDP_{p,c1}$ is the total GDP of the cities in province *p* that are assigned to cluster *c1*, such that $\sum_{p=1}^{30} w_p = 1$. α_{c1} and β_{c1} are then determined by regression to historical data at a given γ_{c1}. We assume the saturation parameter of Shanghai (γ_{SH}) and the other two shape parameters (α_{SH} and β_{SH}) are the same as that of city cluster 1.

Population: Interprovincial migration model, P_i

Migrants are defined as individuals who changed their province of permanent residence during each five-year period. Gravity model has been widely applied and expanded to include factors like economic well-being to simulate migration flows. Similar to X. Luo et al. (2016) [355], we model interprovincial migration flows based on population numbers and per capita GDP levels of both the origin and destination provinces, as well as the past migration patterns. Including past migration as an independent variable is to reflect structural factors (such as distance and transport linkages) that might affect migration decisions. Data include migration flows between each pair of 31 provinces for the four-time period (1995–2000, 2005–2010, and 2010-2015 from the national

census; 2000-2005 derived from the X. Luo et al. (2016)). The log-log migration model is created using Poisson distribution[32] and linear regression; the resulting model is presented below:

$$\ln(M_{io,t}) = -0.33115 + 0.02873 \ln(pop_{i,t-1}) + 0.11987 \ln(pop_{o,t-1})$$
$$+ 0.11526 \ln(GDPcap_{i,t-1}) - 0.17861 \ln(GDPcap_{o,t-1}) + 0.86724 \ln(M_{io,t-1}) \quad \text{(D3)}$$

where the dependent variable $M_{io,t}$ represents the number of migrants moving from province o to province i, time t; the independent variables include population of the destination and the origin province, time t-1, GDP per capita of the destination and the origin province, time t-1, and the number of migrants moving from province o to province i, time t-1.

The model reveals that 1) the projected migration would primarily reflect the past migration; 2) the effect of GDP is more significant than that of population. Figure D3 shows the historical and projected number of migrants, suggesting that the migration volume will be stabilizing around 60 million people per each time period; this is due to a decline in economic well-being differences between in- and out-migration provinces. Figure D4 presents the net migration flows at provincial level projected in the period of 2025-2030.

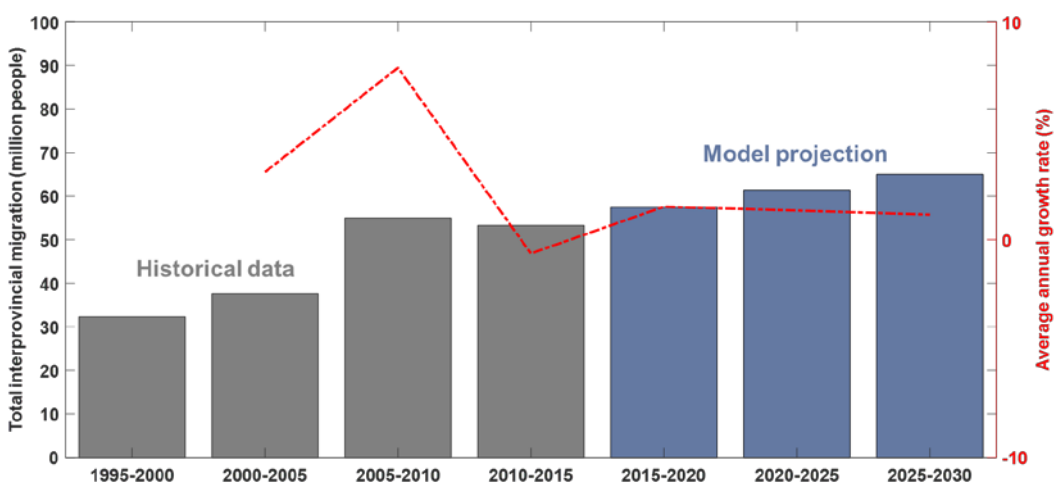

Figure D.3. Total historical and projected migration volume (shown in bar chart; left ordinate) and annual migration growth rate (shown in dashed red line; right ordinate)

[32] A discrete probability distribution for the counts of events that occur randomly in a given interval of time or space.

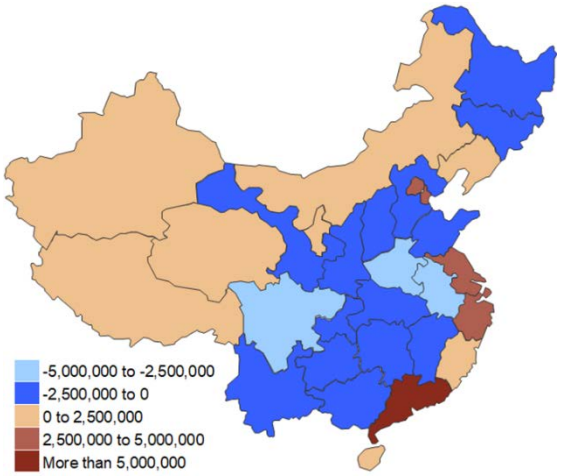

Figure D.4. Net interprovincial migration flow map during 2025-2030: The colors describe the net interprovincial migration. Blue indicates net emigration provinces, and red indicates the net immigration provinces.

D.IV.II Incorporating municipal car ownership restriction policies

Background

Continuing motorization, accompanied by trends of urbanization and sprawl, is putting pressure on China's cities in the form of rising congestion and local air pollution [356,357]. To combat these issues some of China's megacities are adopting car ownership restrictions, which limit growth in new-purchase vehicle sales by rationing the number of new license plates in a city and allocating these licenses through lottery or auction [358]. To date, six cities and one province have adopted stringent car ownership restriction policies (Table D3). Shanghai was the first to adopt such a policy in 1994 using an auction mechanism to allocate new vehicle licenses to those with the highest bid. In 2011, Beijing became the second city to adopt a car ownership restriction, opting for a pure lottery process. In 2012, Guangzhou adopted a hybrid policy that allows residents seeking vehicle licenses to opt-in to either an auction or a lottery. Other cities followed suit, with Tianjin and Hangzhou adopting hybrid policies in 2014 and Shenzhen in 2015. In late 2018, the island province of Hainan also adopted an ownership restriction.

Table D.3. Car Ownership Restriction Policies (as of Sept 2019)

City/Province	Adoption year	Policy type
Shanghai	1994	Auction

Beijing	2010	Lottery
Guangzhou	2012	Hybrid
Shenzhen	2014	Hybrid
Tianjin	2014	Hybrid
Hangzhou	2014	Hybrid
Hainan	2018	Hybrid

Notes: The cities of Guiyang and Shijiazhuang adopted less stringent restrictions on car sales in 2011 and 2013, respectively. Guiyang's policy uses a lottery to allocate a special kind of license plate to enter specific districts with serious congestion (generally, in the inner city). Shijiazhuang's policy does not allow households to purchase a third car.

Fearing the impact of additional city-level ownership restrictions on China's domestic car manufacturing industry—particularly with vehicle sales falling in 2018 for the first time since the 1990s—China's national government announced a new policy to temporarily stop local governments from implementing new restrictions on car purchases for 2019-2020 [137]. The policy also encouraged cities with existing car ownership restrictions to consider removing the vehicle quotas all together. Guangzhou and Shenzhen have responded by increasing the number of ICEV licenses that they will allocate in 2019 [359], while other cities with existing policies have yet to take any action to respond to this mandate.

Assumptions on status quo car ownership restriction policy

There remains significant uncertainty surrounding the long-term continuity and stringency of car restriction policy. In this study with the base model year of 2017, we consider the effects of status quo policy adoption – representing a future in which no additional cities adopt car ownership restriction policies, but the 6 municipal policies that do exist continue to be enforced through 2030.

We assume cities that adopt a car ownership restriction policy would cap first-time purchase vehicle sales at certain levels of economically driven counterfactual demand. The cap values are various across cities, derived from the average ratio of the actual number of vehicles sold via quota to counterfactual first-time purchase vehicle sales for 2016 and 2017 in the 6 cities that currently have car ownership restrictions (Table D4).

Table D.4. Cap values derived from the comparison of demand to vehicles allocated (both in million vehicles) in 6 Chinese cities in 2016 and 2017

City	Demand: projected first-time purchase sales without quota policy		Quota: total vehicles actually allocated		Q/D		
	2016	**2017**	**2016**	**2017**	**2016**	**2017**	**Avg**
Shanghai	0.507	0.488	0.132	0.133	0.26	0.27	**0.27**
Beijing	0.533	0.567	0.082	0.083	0.15	0.15	**0.15**
Guangzhou*	0.571	0.588	0.089	0.107	0.16	0.18	**0.17**
Hangzhou*	0.547	0.563	0.070	0.065	0.13	0.12	**0.12**
Tianjin	0.340	0.352	0.073	0.072	0.21	0.20	**0.21**
Shenzhen*	0.263	0.250	0.056	0.057	0.21	0.23	**0.22**

* We first project the no-car-ownership-restriction demand for first-time purchase sales for Guangdong and Zhenjiang provinces, then we disaggregate the demand of these two provinces by city based on the GDP contribution of each city to the province GDP. Guangzhou city contributed about 25% of Guangdong province GDP; Hangzhou city contributed about 23% of Zhenjiang province GDP; Shenzhen city contributed about 24% of Guangdong province GDP.

In our defined status quo policy adoption, the six megacities in China that had car ownership restriction policies in 2017 (i.e., the base year in this study) continue to enforce these policies out to 2030, but no additional cities adopt the policy. Shanghai, Beijing, and Tianjin are province-level cities, so we apply the derived cap values (0.27, 0.15, and 0.21, respectively) to 100% of the projected economically-driven demand for first-time purchase sales in these three provinces. On the other hand, for the city-level quota policy's impacts on Guangdong and Zhenjiang provinces, we apply the cap values to only about 49% and 23% of each no-quota-policy first-time purchase projections; details are described as below:

- Guangdong: Guangzhou city and Shenzhen city represent 25% and 24% of Guangdong GDP, respectively, so we apply the cap values of 0.17 and 0.22 to 25% and 24% of the projected economically driven first-time purchases for Guangdong. And we allow the other 51% (=100%-25%-24%) of demand (representing the demand from the cities that

currently do not have car ownership restriction policies in Guangdong) to remain uncapped through 2030.

- Zhenjiang: Hangzhou city represents 23% of Zhenjiang GDP, so we apply the cap value of 0.12 to 23% of the projected economically driven first-time purchases for Zhenjiang. We allow the other 77% (=100%-23%) of demand to remain uncapped through 2030.

The effect of car ownership restriction policy (starting from late 2018) on Hainan's fleet is expected to be mild; this is because the number of quotas allocated in 2019 in Hainan is found to be approximately equal to the province's economically driven first-time car purchase demand. As a result, we ignore the quota policy in the modeled Hainan's fleet projection and the potential bias to 2030 is likely to be small.

D.V. Vehicle kilometers traveled (VKT)

Based on the historical nationwide gasoline consumption (assuming 88% of which is consumed by private gasoline-powered car [360]), on-road fuel consumption (Figure D5(a)), and vehicle fleet breakdown by vehicle age in China (Figure D5(b)), the relationship is determined and shown in Figure D5(c). Note that we fit a power law to the estimated VKT only from 2013 to 2016 (shown in a red line) because those VKT estimations before 2013 are very uncertain due to the limited and sparse data on fuel consumption and vehicle sales in the earlier years. The results show that the annual VKT of private cars would decrease gradually toward the future when the car ownership level is increasing, which is consistent with other national and city VKT survey studies [121,122,361,362].

(a)

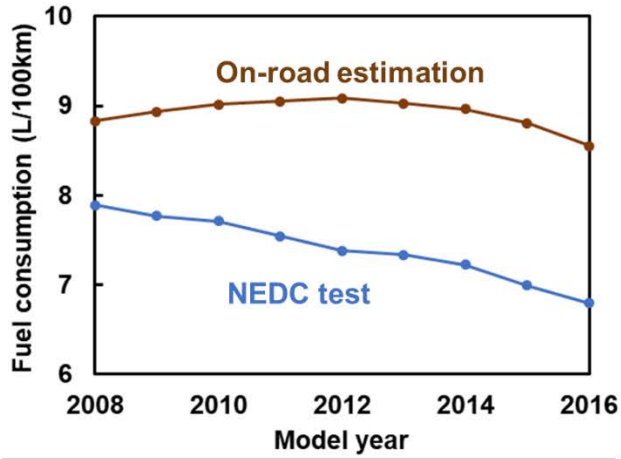

(b)

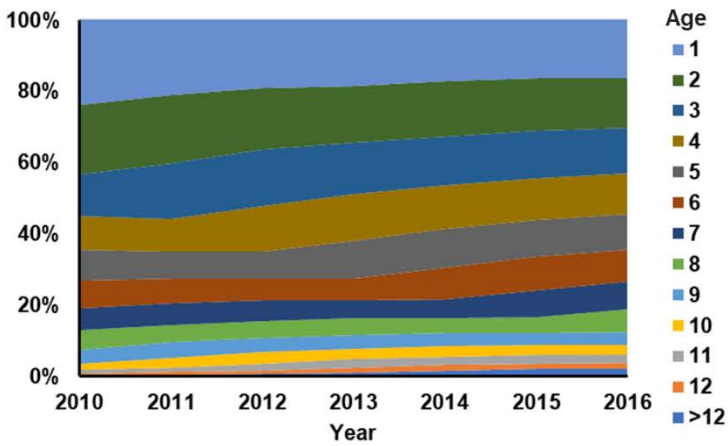

(c)

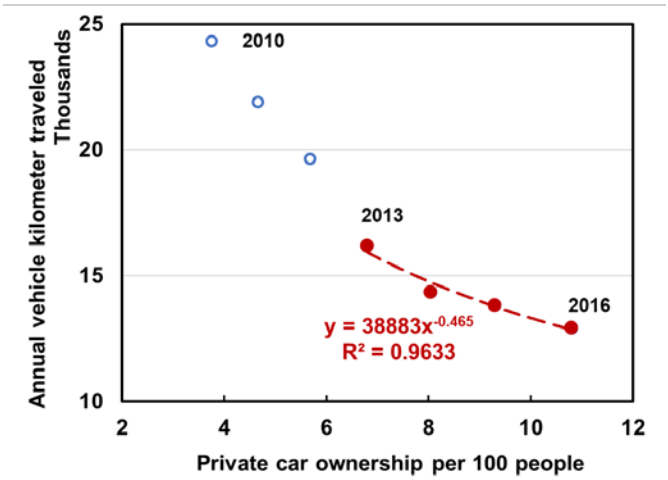

Figure D.5. (a) Labeled and real-world fuel consumption rates for private vehicles in China with different model year; (b) private vehicle fleet breakdown by vehicle age; (c) estimated annual vehicle kilometer traveled (VKT) and the derived relationship between VKT and vehicle ownership level (in red line).

Based on the obtained equation (shown in Figure D5(c)), we further estimate the VKT at the provincial level based on the provincial vehicle ownership level, as shown in Figure D6.

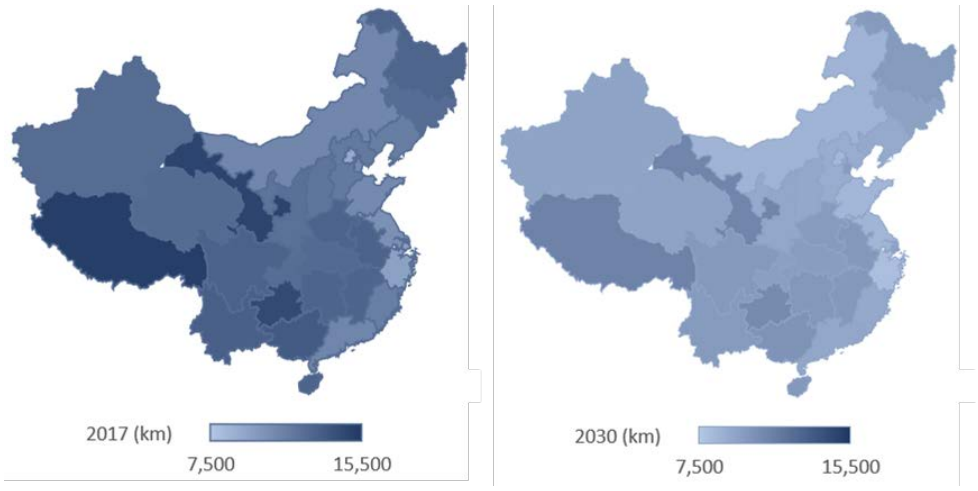

Figure D.6. Provincial annual vehicle kilometer traveled in 2017 and 2030.

D.VI. Emission factors

D.VI.I Well to tank (WTT): Electricity generation carbon emission factor

The scale of China's power grids has been expanded from small urban power grids, provincial power grids, and regional power grids to interconnected national power grids. Energy resource distribution in China is geographically unbalanced: ~85% of coal reserves are in the seven provinces (north and northwest) [363]; ~70% of exploitable hydropower are concentrated in the southwest [364].

Figure D7 presents the impacts of this inter-provincial transmission on the provincial grid carbon emission factor in 2017, categorized by the regional power grids. Carbon intensities of grids are found to be noticeably different in Beijing, Chongqing, Shanghai, and Guangdong between ones with and without considering the transmission. Collectively, Beijing, Shanghai, and Guangdong accounted for 46% and 33% of China's EV sales in 2016 and 2017. This implies that ignoring the electricity transmission might result in the wrong conclusions when examining the benefits of EVs in terms of climate change mitigation.

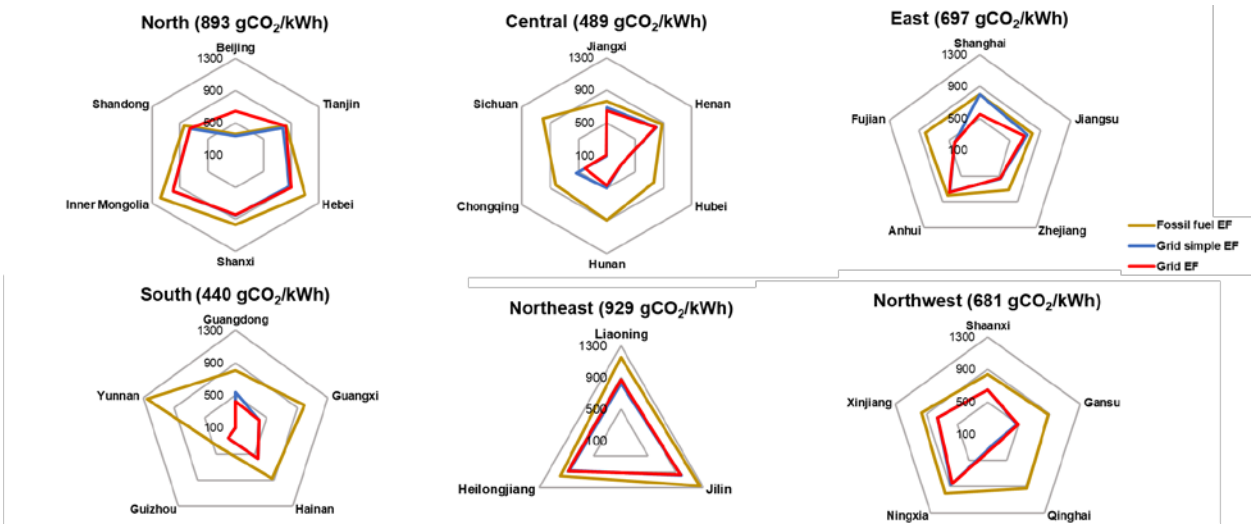

Figure D.7. Carbon dioxide emission factors (EFs) for Chinese province electricity generation in 2017, categorized by regional power grids; red lines represent CO_2 EFs considering inter-provincial power flows while blue lines denote simple CO_2 EFs; EFs of local fossil fuel power plants are also presented (in yellow) here for reference.

For the future carbon intensity of the electricity sector, we follow the expected decarbonization rates at regional level that were documented in Shen et al. [186]. Shen et al. provided a projection of 2030 energy structure transformation of regional power grids based on China's ongoing large-scale construction of non-fossil electricity capacity and the released five-year and long-term plans; the inter-regional transmission capacity was also considered in Shen et al. The expected CO2 reduction rates that are applied in this study are shown in Table D5.

Table D.5. Improvement rates of power grid's carbon emission factor by region applied in this study based on Shen et al. [186]

Province	2030/2017 EF_{CO2} ratio
Beijing, Tianjin, Hebei, Shanxi, Inner Mongolia, Shandong	0.684
Liaoning, Jilin, Heilongjiang	0.667
Shanghai, Jiangsu, Zhejiang, Anhui, Fujian	0.761
Jiangxi, Henan, Hubei, Hunan, Chongqing, Sichuan	0.869
Shaanxi, Gansu, Qinghai, Ningxia, Xinjiang	0.880
Guangdong, Guangxi, Hainan, Guizhou, Yunnan	0.820

D.VI.II WTT: Electricity generation air pollutant emission factor

In a recent study by Tang et al. [200], researchers found that between 2014 and 2017 China's annual power emissions of SO2, NOx, and PM dropped substantially thanks to the introduction of ultra-low emissions (ULE) standards policy in 2014. The researchers estimated emissions using continuous monitoring systems network, which covered most of the Chinese thermal power capacity, to be up to 92% below other recent estimates. The most disaggregated data Tang et al. [200] provided are at regional level, and since we do not have their study's full dataset, here we assume that every province belonging to the same region has the same emission factors.

Based on the historical data given in Tang et al. [200], we construct the relationship between emissions and the ULE compliance rate, as shown in Figure D8 (points are historical data). Since the eastern, northern, central and southern regions (collectively account for 74.4% of the total national power capacity in 2017) faced the most considerable pressure for emission reductions, the ULE policy prioritized them over the other regions in terms of timelines. And these

regions also face the toughest policy stringency, we expect and assume that they will 100% meet the ULE standards by 2030. For the rest three regions (northeast, southwest, and northwest), we assume the compliance rates will achieve 60% so that the nationwide target of 90% compliance can be achieved in 2030. Table S6 summarizes the region-level air pollutant emission factors in 2017 and 2030 used in this study; we convert PM to $PM_{2.5}$ based on the satellite-based observation that PM contains about a 46% mass fraction of primary PM2.5 in China's power plant emissions [365].

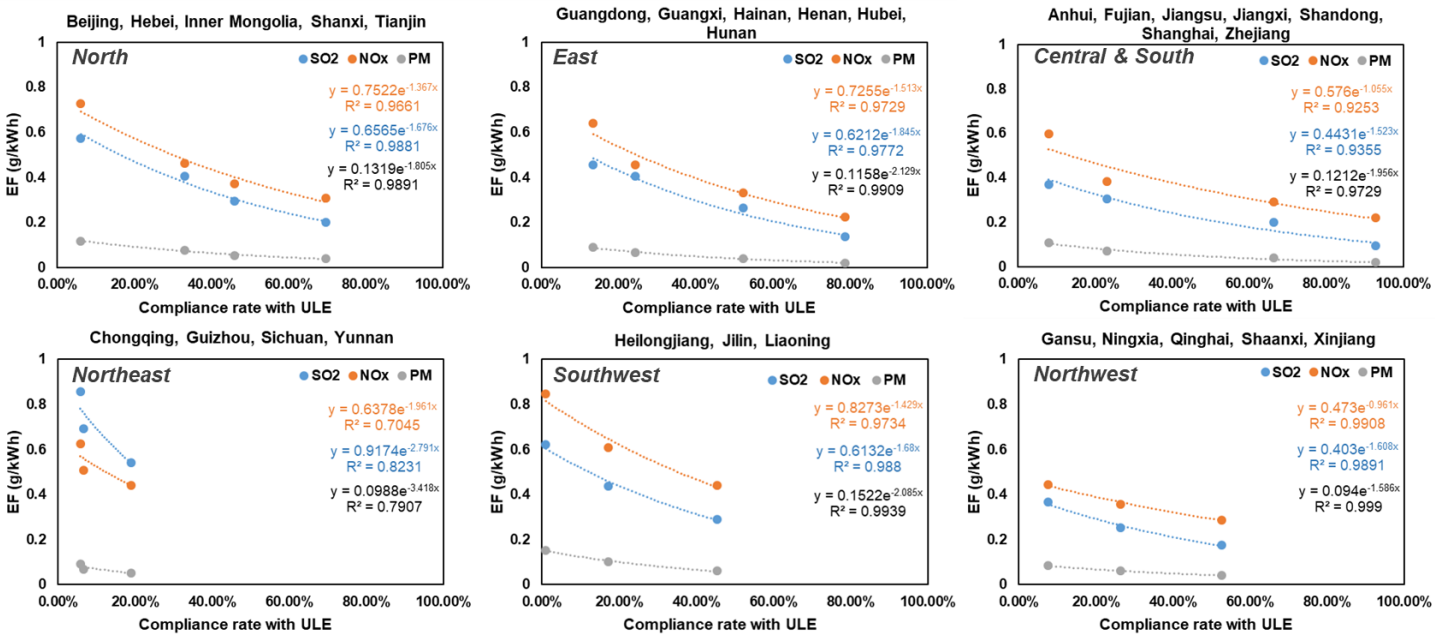

Figure D.8. The relationship between air pollutant emission factors and ultra-low emissions standard (ULE) compliance rate by regions.

Table D.6. Regional power air pollutant emission factors in China used in the study

	SO_2 (g/KWh)	NO_X (g/KWh)	$PM_{2.5}$ (g/KWh)
	2017		
North	0.201	0.309	0.018
East	0.093	0.219	0.008
Central & South	0.136	0.223	0.010
Northeast	0.291	0.442	0.028

Southwest	0.543	0.442	0.024
Northwest	0.176	0.288	0.019
	2030		
North	0.123	0.192	0.010
East	0.093	0.201	0.008
Central & South	0.098	0.160	0.006
Northeast	0.224	0.351	0.020
Southwest	0.172	0.197	0.006
Northwest	0.154	0.266	0.017

D.VI.III. WTT: Emissions to produce gasoline

The emissions factors of CO_2, VOC, NO_x, SO_2, $PM_{2.5}$ applied in this study are derived from Zheng et al. [198,366], as summarized in Table D7. Due to the lack of data, all provinces are assumed to have the same upstream WTT emissions for a liter of gasoline production.

Table D.7. Emission to produce gasoline in China, i.e., upstream well-to-tank stage

g/L	CO2	CO	VOC	NOx	SO2	PM2.5
2017	899	0.630	1.02	2.06	0.94	0.14
2030	817		1.00	1.46	0.64	0.11

D.VI.IV. Tank to whale (TTW): On-road energy consumption

Due to a lack of local car sales data by vehicle size, we assume that the average label fuel consumption in each province is the same as the national sales-average level. The historical sales-average label fuel consumption of ICEVs and BEVs in China are taken from multiple sources [88,367]. In 2017, the average label value of ICEVs is 6.7 L/100 km and that of BEVs is 15 kWh/100km. For BEV fuel consumption improvement, we take the projection from MIT On the Road Toward 2050 [351], suggesting that there will be a ~17% reduction in BEV fuel consumption from 2017 to 2030. We estimate sales-average PHEVs fuel consumption based on the reference vehicles' fuel consumption ratios (Table S1) between PHEV and ICEV (gasoline-powered PHEV fuel consumption is 21% lower than ICEV) and between PHEV and BEV (battery-powered PHEV fuel consumption is 29% higher than BEV).

The New European Driving Cycle (NEDC), the currently-used type approval cycle, is inconsistence with the characteristics of the actual driving condition in China, causing the fuel consumption gaps between lab and on-road values to become larger—the real-to-lab divergence for gasoline vehicles has increased from 12% in 2008 to 26% in 2016 [205]. Considering the more realistic testing cycle, the Worldwide harmonized Light vehicles Test Procedures (WLTP), will be implemented soon [368], we expect and assume the real-to-lab gap for gasoline cars would not increase further, and would instead remain 26% out to 2030. For battery-powered vehicles fuel consumption, we estimate the real-to-lab gap based on the difference in electric driving range between WLTP test and NEDC test for the same car model (i.e., Tesla Model 3 is chosen here), which is found to be 19%.

Driving conditions—such as weather, traffic, driver behavior, and fuel quality—affect fuel consumption significantly. Fuel consumption index was proposed to describe the real-world fuel consumption levels across provinces [206], showing that Heilongjiang and Jilin have the highest fuel consumption (~10% higher than the national average), while Yunnan has the lowest fuel consumption (~7% lower than the national average). Figure D9 shows the on-road fuel consumption of ICEV and HEV combined used in this study at provincial level in 2017 and 2030.

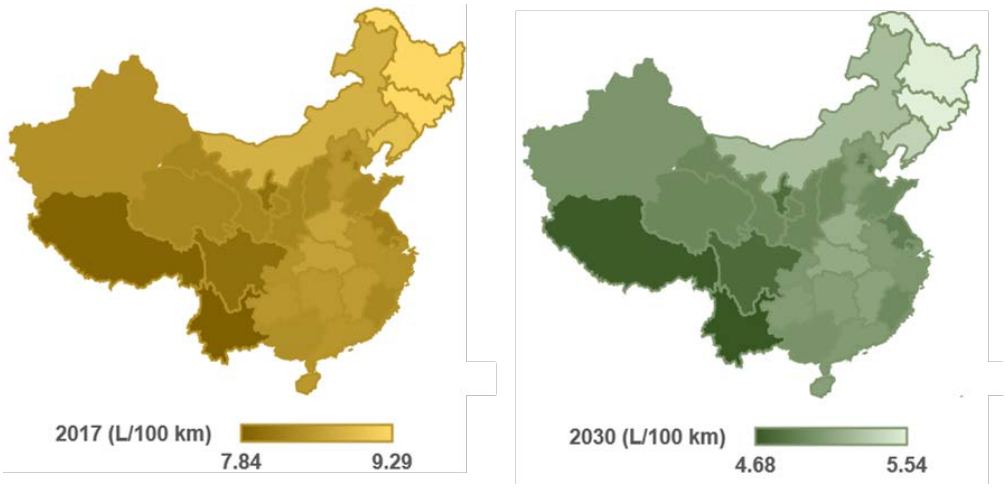

Figure D.9. Provincial on-road fuel consumption of gasoline vehicle (ICEV and HEV combined) in 2017 and 2030

D.VI.V. TTW: On-road emissions from using gasoline

Carbon emission from using gasoline is assumed to be 75 gCO_2/MJ, derived from Yang et al. [369]. With the given on-road fuel consumption, we can compute the carbon emission per km driven at the provincial level. It is noted that the low heating value of gasoline is used in this study.

We derive provincial-level on-road air pollutant EFs based on a framework developed by Tsinghua University and the Chinese Academy of Environmental Sciences [207], as represented in Equation D4.

$$EF_{i,j} = BEF_i \times \delta_{i,j} \tag{D4}$$

$EF_{i,j}$ is the emission factor of air pollutant *i* in region *j*; BEF_i is the integrated base emission factor of air pollutant *i*; $\delta_{i,j}$ is the correction factor of temperature, humidity, altitude, driving speed, and oil quality in region *j*. All factors are summarized in Table S8. Unlike the previous fuel standards in China, China 6 does not only follow the basic European regulation system, but also goes beyond it in terms of emission stringency. It was expected that many automakers would be producing vehicles meeting California's LEV III light-duty vehicle emission standards for California market and thus could produce them much quicker than the China 6 in China [370]. EFs under China 6 are obtained from Ke et al. [196].

Table D.8. Values of base emission factor (BEF), correction factor (δ), and on-road emission factor for different fuel standards, air pollutants, provinces for the gasoline vehicles

Fuel standard	**BEF (g/km)**				**Implementation year**
	CO	**VOC**	**NOx**	**$PM_{2.5}$×10**	(BJ:Beijing; SH: Shanghai; GD: Guangdong)
China Pre 1	32.15	3.23	2.05	0.28	
China 1	11.61	0.91	0.41	0.26	BJ 1999; SH 2000; Nationwide 2001
China 2	2.6	0.48	0.43	0.11	BJ, SH 2003; Nationwide 2006
China 3	1.58	0.22	0.15	0.07	BJ 2006; SH, GD 2007; Nationwide 2009
China 4	0.69	0.08	0.03	0.03	BJ 2009; SH 2010; GD 2011; Nationwide 2012
China 5	0.46	0.06	0.02	0.03	BJ 2013; SH 2015; GD 2016; Nationwide 2017
Province	**δ**				**Causes for correction**
	CO	**VOC**	**NOx**	**$PM_{2.5}$×10**	

Yunnan	2.15	3.62	3.62	--	Average temperature <10 ºC & altitude>1500 m
Heilongjiang, Hainan, Chongqing	1.36	1.47	1.15		Average temperature <10 ºC
Qinghai	1.58	2.46	3.34		Average humidity <50 % & altitude>1500 m
Xinjiang	1	1	1.06		Average humidity <50 %
Tibet	1.58	2.46	3.15		Average altitude>1500 m
The rest	1	1	1		
Fuel standard	**EF (g/km)**				**Implementation year**
	CO	**VOC**	**NOx**	**$PM_{2.5}$×10**	
China 6	0.23	0.02	0.01	0.02	BJ, SH 2018; GD 2019; Nationwide 2020

D.VI.VI. Cradle to gate: CO2 emissions from vehicle and battery production

Several research studies analyzed the CO2 emissions related to vehicle and battery production in China [197,347–350]. Based on the vehicle weights and battery capacity, we derive the reference vehicle-specific CO2 emissions from vehicle and battery manufacturing process in 2017 (Table D1). For the future improvement (throughout 2030), we follow the CO2 emission reduction rate given by Elgowainy, Amgad, et al. (2018) [371]: 12% for ICEV, 13% for HEV, 52% for EV battery, and 15% for EV components except for battery.

D.VII. Air quality modeling and health concentration-response functions

China's gasoline refining process is using coal as the main process fuel, and in the absence of strict emission standards, substantial emissions are expected to be produced. Hence, this study accounts for the changes in upstream emissions from gasoline production when computing air quality (in addition to the emissions from electricity generation and gasoline consumption). For spatial allocation of WTT emissions from gasoline vehicles, we first calculate total fuel demand from the private vehicle sector in each scenario, and then multiplied it by the emission factor (g/L) shown in Table S7 to get the nationwide WTT emissions from gasoline production; we than reallocate the total national emissions based on the location (latitude/longitude) and the capacity volumes of the gasoline refineries [372].

For each of the scenarios described above, projected annual power generation and passenger car emissions of CO, NO_x, VOC, SO_2, and $PM_{2.5}$ in 2030 are estimated at the province-level. For each province, these sectoral totals are disaggregated by month following the temporal pattern observed in the 2016 MEIC inventory [373]. This assumes that the temporal profile of power and road transportation emissions will remain constant by 2030. We further disaggregate VOC emissions by species (considering formaldehyde, ethane, propane, alkanes with 4 or more carbon atoms, acetone, acetaldehyde, methyl ethyl ketone, and alkenes with 3 or more carbon atoms) according to their respective share in the total VOC emissions in the 2016 MEIC inventory.

Anthropogenic emissions other than passenger car emissions and power emissions related to the deployment of EVs are taken from the MEIC inventory [373] and scaled up from 2016 to 2030 on a monthly basis according to the projections by pollutant and province obtained from the GAINS China model [374,375] with the World Energy Outlook (WEO) New Policies Scenario [375] which assumes the full implementation of current legislation.

Surface-level concentration of $PM_{2.5}$ and ozone are then combined with population data to estimate exposure. Total population by province for the base year 2017 is taken from the China Statistical Yearbook [376]. Population growth by 2030 is from the UN World Population Prospects [377], and inter-provincial migration flows are estimated following the method described in Supplementary information D.IV.I. The spatial distribution of population within each province is taken from the Global Human Settlement Layer developed by the EU Commission's Joint Research Center [378] and is assumed to remain constant between 2015 and 2030. The population

age structure in 2017 is taken from WHO data [379] and also assumed to remain constant by 2030. Mortality impacts are calculated for the fraction of population aged 30 and above.

The mortality impacts associated with changes in exposure to $PM_{2.5}$ across China are estimated using the Global Exposure Mortality Model [215]. The model relates the relative risk (RR) to the $PM_{2.5}$ concentration according to the following relation:

$$RR(z) = \exp[\theta \log(z/(\alpha + 1)/\exp(-(z - \mu)/\upsilon], \textit{ where z=max(0, c-2.4)} \quad \text{(D5)}$$

with c the concentration of $PM_{2.5}$ in $g.m^{-3}$ in each grid cell. The parameters θ, α, μ, υ are defined for each 5-year age bracket between 30 and 85 years and for each of the following health endpoints: ischaemic heart disease, stroke, chronic obstructive pulmonary disease (COPD), lung cancer, and lower respiratory infection. Using the distributions for each of these parameters provided in Burnett et al. [215], we generate 10,000 independent samples of the health impacts related to changes in concentrations of $PM_{2.5}$.

For mortality impacts due to changes in surface-level ozone, we apply a log-linear concentration-response function, using parameters derived from Turner et al. [217]. This function relates exposure to 8-hour maximum ozone concentration (MDA8) to premature mortality from respiratory and circulatory diseases. The reported central relative risk for circulatory diseases is 1.03 (95% CI: 1.01 to 1.05) and the central relative risk for respiratory diseases is 1.12 (95% CI: 1.08 to 1.16) for a 10 ppb increase in ozone MDA8. We generate 10,000 independent samples of each of these parameters using a triangular distribution fitted to the reported modes and values. Each of these samples translates to a sample of the parameter and we estimate the relative risk under each scenario in each grid cell using the following formula:

$$RR(z) = \exp(\beta z), \textit{ where z=max(0, c-35)} \quad \text{(D6)}$$

with c the ozone MDA8 in ppb, and 35 ppbv the threshold suggested by Turner et al. [217]. Based on the data reported in the original study, we estimate central a value of 0.00296 for β for circulatory diseases, and 0.0113 for respiratory diseases.

In addition to premature death, for each scenario, we also quantify the morbidities caused by PM2.5 and ozone exposure in 2030. Five PM2.5-related morbidity health impacts (including hospital admission due to respiratory disease (RHA), hospital admission due to cardiovascular disease (CHA), chronic bronchitis (CB), asthma attack (AA) and emergency room visits (ERV) for respiratory disease) and two ozone-related morbidity health impacts (including RHA and AA)

among all ages are calculated using Equation S7; exposure-response coefficients (ER) coefficients and the threshold (i.e., c_0=10 μg/m^3 for PM2.5 and 35 ppb for ozone) are taken from Maji, Kamal Jyoti, et al and Feng, Zhaozhong, et al studies [216,218].

$$RR(z) = \exp[ER \times (c - c_0)] \quad \text{(D7)}$$

References

[1] U.S. Department of Energy. All-Electric Vehicles n.d. http://www.fueleconomy.gov/feg/evtech.shtml (accessed February 27, 2020).

[2] IEA. Global EV Outlook 2019. Paris: IEA; 2019.

[3] Phase-out of fossil fuel vehicles. Wikipedia 2020.

[4] Ipsos. What Will it Take to Put Consumers in the Driver's Seat of Battery Electric Vehicles? Ipsos 2020. https://www.ipsos.com/en-us/news-polls/Battery-Electric-Vehicles (accessed February 28, 2020).

[5] Singer MR. The Barriers to Acceptance of Plug-in Electric Vehicles: 2017 Update. National Renewable Energy Lab.(NREL), Golden, CO (United States); 2017.

[6] Gardner G. Tesla, GM Lose Bid To Raise Ceiling For Federal EV Tax Credit. Forbes n.d. https://www.forbes.com/sites/greggardner/2019/12/17/tesla-gm-lose-bid-to-raise-ceiling-for-federal-ev-tax-credit/ (accessed February 28, 2020).

[7] European Alternative Fuels Observatory. Compare the Market - Electric Vehicle Incentives across Europe n.d. https://www.comparethemarket.com/car-insurance/content/electric-vehicle-incentives/ (accessed February 28, 2020).

[8] Zhang X, Liang Y, Yu E, Rao R, Xie J. Review of electric vehicle policies in China: Content summary and effect analysis. Renewable and Sustainable Energy Reviews 2017;70:698–714. https://doi.org/10.1016/j.rser.2016.11.250.

[9] Center for Climate and Energy Solutions. U.S. State Clean Vehicle Policies and Incentives. Center for Climate and Energy Solutions 2019. https://www.c2es.org/document/us-state-clean-vehicle-policies-and-incentives/ (accessed February 28, 2020).

[10] Bill 28 – 2019: Zero-Emission Vehicles Act n.d. https://www.leg.bc.ca:443/parliamentary-business/legislation-debates-proceedings/41st-parliament/4th-session/bills/first-reading/gov28-1 (accessed February 28, 2020).

[11] Rokadiya S, Yang Z. Overview of global zero-emission vehicle mandate programs. International Council on Clean Transportation (ICCT) 2019.

[12] Ou S, Lin Z, Qi L, Li J, He X, Przesmitzki S. The dual-credit policy: Quantifying the policy impact on plug-in electric vehicle sales and industry profits in China. Energy Policy 2018;121:597–610. https://doi.org/10.1016/j.enpol.2018.06.017.

[13] Ou S, Hao X, Lin Z, Wang H, Bouchard J, He X, et al. Light-duty plug-in electric vehicles in China: An overview on the market and its comparisons to the United States. Renewable and Sustainable Energy Reviews 2019;112:747–61.

[14] International Organization of Motor Vehicle Manufacturers. 2005-2018 Sales Statistics n.d. http://www.oica.net/category/sales-statistics/ (accessed February 28, 2020).

[15] OICA [Organisation Internationale des Constructeurs d'Automobiles]. World Motor Vehicle Sales, by country and type 2005-2017. Sales Statistics 2017. http://www.oica.net/category/sales-statistics/ (accessed February 22, 2018).

[16] Davis SC, Williams SE, Boundy RG. Transportation Energy Data Book, Edition 33. Oak Ridge National Lab., TN (US); 2014. https://doi.org/10.2172/1240517.

[17] Hamilton W. Price and price policies. McGraw-Hill Book Company, New York; 1938.

[18] Jong GD, Fox J, Daly A, Pieters M, Smit R. Comparison of car ownership models. Transport Reviews 2004;24:379–408. https://doi.org/ 10.1080/0144164032000138733.

[19] Zachariadis T, Samaras Z, Zierock K-H. Dynamic modeling of vehicle populations: an engineering approach for emissions calculations. Technological Forecasting and Social Change 1995;50:135–49.
[20] Wu T, Zhao H, Ou X. Vehicle ownership analysis based on GDP per capita in China: 1963–2050. Sustainability 2014;6:4877–99.
[21] Dargay J, Gately D, Sommer M. Vehicle ownership and income growth, worldwide: 1960-2030. The Energy Journal 2007;28.
[22] Huo H, Wang M. Modeling future vehicle sales and stock in China. Energy Policy 2012;43:17–29.
[23] United Nations. Department of Economic. World population prospects: The 2015 revision. United Nations Econ Soc Aff 2015;33:1–66.
[24] Hao H, Wang H, Ouyang M, Cheng F. Vehicle survival patterns in China. Science China Technological Sciences 2011;54:625–9.
[25] Huo H, Wang M. Modeling future vehicle sales and stock in China. Energy Policy 2012;43:17–29.
[26] Dargay JM. The effect of income on car ownership: evidence of asymmetry. Transportation Research Part A: Policy and Practice 2001;35:807–21.
[27] National Development and Reform Commission. Consumer Price Index n.d. http://en.ndrc.gov.cn/.
[28] China Industry Information Network Website n.d. http:// www.chyxx.com.
[29] Davis SC, Williams SE, Boundy RG. Transportation Energy Data Book, Edition 35. Oak Ridge National Lab., TN (US); 2016. https://doi.org/10.2172/1240517.
[30] Dargay J, Gately D. Income's effect on car and vehicle ownership, worldwide: 1960–2015. Transportation Research Part A: Policy and Practice 1999;33:101–38.
[31] National Bureau of Statistics of China. China Statistical Yearbook 2016. 2017.
[32] Kishimoto PN. Applying Advanced Uncertainty Methods to Improve Forecasts of Vehicle Ownership and Passenger Travel in China. 31st USAEE/IAEE North American Conference. Austin, TX, USA, 2012.
[33] Steyn HS. A model for the distribution of incomes. South African Journal of Economics 1959;27:149–56.
[34] McDonald JB, Ransom MR. Functional forms, estimation techniques and the distribution of income. Econometrica: Journal of the Econometric Society 1979:1513–25.
[35] Chen J, Fang F, Hou W, Li F, Pu M, Song M. Chinese Gini coefficient from 2005 to 2012, based on 20 grouped income data sets of urban and rural residents. Journal of Applied Mathematics 2015;2015.
[36] OECD. Long-Term Baseline Projections, No. 95 (Edition 2014). 2017.
[37] Hu J, Luo Y, Yang X. Forecast and Policy Suggestions of Gini Coefficient in China in the Future Decade: Analysis Based on Grey Forecasting Model (In Chinese). West Forum on Economy and Management 2015;26:44–9.
[38] Beijing Times. Experts: 2030 China's Vehicles Per 1000 People Will Maintain the Amount of 300 (in Chinese) 2016.
[39] United States Department of Transportation. National Transportation Statistics n.d.
[40] Wang X, Woo WT. The size and distribution of hidden household income in China. Asian Economic Papers 2011;10:1–26.
[41] Ward K. The world in 2050: Quantifying the shift in the global economy. HSBC London; 2011.

[42] Daily C. Per Capita Income to Rise by up to 50% by 2030. 2011.
[43] Curran E. China Will Avoid a Bank Crisis, Reach High Income Status: Morgan Stanley. 2017.
[44] Wang X, Chen KZ, Robinson S, Huang Z. Will China's demographic transition exacerbate its income inequality?–CGE modeling with top-down microsimulation. Journal of the Asia Pacific Economy 2017;22:227–52.
[45] Xue L. Lessons from Beijing and Shanghai Show How China's Cities Can Curb Car Congestion. World Resources Institute Apr 4;10:2015.
[46] Sivak M, Schoettle B. What do current owners of hybrids and non-hybrids think about hybrids? University of Michigan, Ann Arbor, Transportation Research Institute; 2014.
[47] Knittel CR. Automobiles on steroids: Product attribute trade-offs and technological progress in the automobile sector. American Economic Review 2011;101:3368–99.
[48] Ross J. China's Five Year Plan to achieve a "moderately prosperous society" - China.org.cn 2015. http://www.china.org.cn/opinion/2015-10/30/content_36935303_2.htm (accessed March 3, 2020).
[49] Neufville R de, Scholtes S. Flexibility in Engineering Design | The MIT Press. Cambridge: MIT Press; 2011.
[50] Chu S, Cui Y, Liu N. The path towards sustainable energy. Nature Materials 2017;16:16–22. https://doi.org/10.1038/nmat4834.
[51] Dodge E. The Case for Electric Vehicles, Part 2: EV Costs. Breaking Energy n.d. https://breakingenergy.com/2014/10/02/the-case-for-electric-vehicles-part-2-ev-costs/ (accessed February 1, 2018).
[52] Knupfer SM, Hensley R, Hertzke P, Schaufuss P, Laverty N, Kramer N. Electrifying insights: How automakers can drive electrified vehicle sales and profitability. McKinsey & Company 2017.
[53] China's GEM Locks Up Large Share of Hot Commodity: Cobalt. Electronic Design 2018. http://www.electronicdesign.com/automotive/china-s-gem-locks-large-share-hot-commodity-cobalt (accessed March 30, 2018).
[54] Cremer A. VW assigns 20 billion euros in battery orders in electric car drive. Reuters 2018. https://uk.reuters.com/article/uk-volkswagen-results/vw-assigns-20-billion-euros-in-battery-orders-speeds-ev-push-idUKKCN1GP12L (accessed April 2, 2018).
[55] Nykvist B, Nilsson M. Rapidly falling costs of battery packs for electric vehicles. Nature Climate Change 2015;5:329.
[56] Consumer Price Index (CPI) Tables : U.S. Bureau of Labor Statistics n.d. https://www.bls.gov/cpi/tables/home.htm (accessed February 7, 2018).
[57] Irle R, Pontes J, Irle V. EV-Volumes - Global plug-in vehicle sales for 2017 H1 + July, August update (2017) n.d. http://www.ev-volumes.com/country/total-world-plug-in-vehicle-volumes/ (accessed December 10, 2017).
[58] Schmidt O, Hawkes A, Gambhir A, Staffell I. The future cost of electrical energy storage based on experience rates. Nature Energy 2017;2:17110.
[59] Kittner N, Lill F, Kammen DM. Energy storage deployment and innovation for the clean energy transition. Nature Energy 2017;2:17125.
[60] Zhang X, Liang Y, Yu E, Rao R, Xie J. Review of electric vehicle policies in China: Content summary and effect analysis. Renewable and Sustainable Energy Reviews 2017;70:698–714.
[61] IEA. Global EV Outlook 2018. International Energy Agency; 2018.

[62] UPDATE-China NEV sales quota system takes effect on April 1, 2018. Gasgoo n.d. http://autonews.gasgoo.com/70010270.html (accessed February 2, 2018).
[63] Global EV outlook 2017. International Energy Agency; 2017.
[64] Li F. Road map outlined for new energy industry - Business - Chinadaily.com.cn 2016. http://www.chinadaily.com.cn/business/motoring/2016-10/31/content_27226277.htm (accessed February 5, 2018).
[65] Hsieh I-YL, Kishimoto PN, Green WH. Incorporating multiple uncertainties into projections of Chinese private car sales and stock. Transportation Research Record 2018.
[66] Starting from next year, all BYD's passenger cars will use NMC batteries 2017. http://k.sina.com.cn/article_5454155336_14517ce48001001o5v.html?from=auto&subch=iauto (accessed February 3, 2018).
[67] Ober JA. Mineral commodity summaries 2017. U.S. Geological Survey; 2017. https://doi.org/10.3133/70180197.
[68] London Metal Exchange: LME Cobalt 2018. https://www.lme.com/Metals/Minor-metals/Cobalt#tabIndex=2 (accessed March 30, 2018).
[69] Howell D. Electrochemical Energy Storage R&D Overview 2017.
[70] Berckmans G, Messagie M, Smekens J, Omar N, Vanhaverbeke L, Van Mierlo J. Cost Projection of State of the Art Lithium-Ion Batteries for Electric Vehicles Up to 2030. Energies 2017;10:1314. https://doi.org/10.3390/en10091314.
[71] Curry C. Lithium-ion Battery Costs and Market 2017.
[72] Li Z, Pan MS, Su L, Tsai P-C, Badel AF, Valle JM, et al. Air-breathing aqueous sulfur flow battery for ultralow-cost long-duration electrical storage. Joule 2017;1:306–27.
[73] Hsieh I-YL, Kishimoto PN, Green WH. Incorporating Multiple Uncertainties into Projections of Chinese Private Car Sales and Stock. Transportation Research Record 2018. https://doi.org/10.1177/0361198118791361.
[74] Chagnes A, Pospiech B. A brief review on hydrometallurgical technologies for recycling spent lithium-ion batteries. Journal of Chemical Technology & Biotechnology 2013;88:1191–9. https://doi.org/10.1002/jctb.4053.
[75] Lv W, Wang Z, Cao H, Sun Y, Zhang Y, Sun Z. A critical review and analysis on the recycling of spent lithium-ion batteries. ACS Sustainable Chemistry & Engineering 2018;6:1504–21. https://doi.org/10.1021/acssuschemeng.7b03811.
[76] LME. London Metal Exchange: Home 2019. https://www.lme.com/ (accessed January 11, 2019).
[77] Natarajan S, Aravindan V. Recycling Strategies for Spent Li-Ion Battery Mixed Cathodes. ACS Energy Letters 2018;3:2101–3. https://doi.org/10.1021/acsenergylett.8b01233.
[78] Li F. Road map outlined for new energy industry. ChinadailyComCn 2016. http://www.chinadaily.com.cn/business/motoring/2016-10/31/content_27226277.htm (accessed February 5, 2018).
[79] DRC. New energy vehicles will account for 25% in 2025 (2025年新能源汽车占比将达25%) 2019. http://www.drc.gov.cn/xscg/20191209/182-473-2899924.htm (accessed February 16, 2020).
[80] Liang X, Zhang S, Wu Y, Xing J, He X, Zhang KM, et al. Air quality and health benefits from fleet electrification in China. Nature Sustainability 2019;2:962–71.
[81] Hsieh I-YL, Pan MS, Chiang Y-M, Green WH. Learning only buys you so much: practical limits on battery price reduction. Applied Energy 2019;239:218–24. https://doi.org/10.1016/j.apenergy.2019.01.138.

[82] National Research Council. Transitions to alternative vehicles and fuels. National Academies Press; 2013.
[83] Hummel P, Lesne D, Radlinger J, Golbaz C, Langan C, Takahashi K, et al. UBS Evidence Lab Electric Car Teardown—Disruption Ahead. Basel: UBS Evidence Lab; 2017.
[84] German J. Hybrid vehicles: Technology development and cost reduction. ICCT Technical Brief 2015.
[85] Cui H, Minjares R, Posada F, Blumberg K, Jin L, He H, et al. Cost-benefit assessment of proposed China 6 emission standard for new light-duty vehicles. International Council on Clean Transportation; 2017.
[86] Perkowski J. Will 2018 Be An Inflection Point For China's Auto Sales? Forbes 2018. https://www.forbes.com/sites/jackperkowski/2018/11/27/will-2018-be-an-inflection-point-for-chinas-auto-sales/ (accessed July 12, 2019).
[87] Zhang D, Rausch S, Karplus VJ, Zhang X. Quantifying regional economic impacts of CO2 intensity targets in China. Energy Economics 2013;40:687–701. https://doi.org/10.1016/j.eneco.2013.08.018.
[88] CATRC. 2017 Report on the Development of China Energy-saving and New Energy Vehicle (2017 中国节能与新能源汽车发展研究报告). China Automotive Technology & Research Center; 2017.
[89] Cui H. China's new energy vehicle mandate policy (Final Rule). Policy Update ICCT Report 2018.
[90] JMedia. Demand for lithium and cobalt resources from the development of electric passenger car and the corresponding lithium battery industry (电动乘用车及对应锂电产业发展对锂钴资源的需求) 2017. https://www.jiemian.com/article/1244469.html (accessed July 13, 2019).
[91] Lima P. Electric car range and efficiency table (NEDC). PushEVs 2017. https://pushevs.com/2017/05/23/electric-car-range-efficiency-table-nedc/ (accessed July 13, 2019).
[92] Cazzola P, Gorner M, Schuitmaker R, Paoli L, Scheffer S, Teter J, et al. Global Electric Vehicles Outlook - 2018. 2018. https://doi.org/10.1787/9789264302365-en.
[93] RealLi Research. Market development forecast of lithium-ion battery and electric vehicle (锂电及电动汽车市场发展预测). RealLi Research; 2016.
[94] Sun X, Hao H, Zhao F, Liu Z. Tracing global lithium flow: A trade-linked material flow analysis. Resources, Conservation and Recycling 2017;124:50–61. https://doi.org/10.1016/j.resconrec.2017.04.012.
[95] Harvey J. Cobalt cannot be eradicated from electric car batteries - Umicore. Reuters 2018.
[96] US Geological Survey. Mineral commodity summaries 2018. US Geological Survey; 2018.
[97] INSG. The World Nickel Factbook 2018. International Nickel Study Group; 2019.
[98] Global Energy Metals Corp. Cobalt's end market. Global Energy Metals Corp 2016. https://www.globalenergymetals.com/cobalt/cobalt-demand/ (accessed July 23, 2019).
[99] Statista. Lithium end usage in the global market share 2018. Statista 2018. https://www.statista.com/statistics/268787/lithium-usage-in-the-world-market/ (accessed July 23, 2019).
[100] Milewski A. Cobalt, the Electric Vehicle, and Ways to Profit from Both 2019.
[101] Brown TJ, Idoine NE, Raycraft ER, Shaw RA, Deady EA, Hobbs SF, et al. World mineral production 2013-2017. British Geological Survey; 2019.

[102] Kushnir D, Sandén BA. The time dimension and lithium resource constraints for electric vehicles. Resources Policy 2012;37:93–103. https://doi.org/10.1016/j.resourpol.2011.11.003.
[103] Olivetti EA, Ceder G, Gaustad GG, Fu X. Lithium-ion battery supply chain considerations: analysis of potential bottlenecks in critical metals. Joule 2017;1:229–43. https://doi.org/10.1016/j.joule.2017.08.019.
[104] US Geological Survey. Mineral commodity summaries 2019 2019. https://doi.org/10.3133/70202434.
[105] Andrews J, Jelley N. Energy science: principles, technologies, and impacts. Oxford university press; 2017.
[106] Zhuang L, Sun C, Zhou T, Li H, Dai A. Recovery of valuable metals from LiNi0. 5Co0. 2Mn0. 3O2 cathode materials of spent Li-ion batteries using mild mixed acid as leachant. Waste Management 2019;85:175–85. https://doi.org/10.1016/j.wasman.2018.12.034.
[107] Ziemann S, Müller DB, Schebek L, Weil M. Modeling the potential impact of lithium recycling from EV batteries on lithium demand: a dynamic MFA approach. Resources, Conservation and Recycling 2018;133:76–85. https://doi.org/10.1016/j.resconrec.2018.01.031.
[108] Battery University. Battery Recycling as a Business 2019. https://batteryuniversity.com/learn/article/battery_recycling_as_a_business (accessed July 24, 2019).
[109] Zheng X, Zhu Z, Lin X, Zhang Y, He Y, Cao H, et al. A mini-review on metal recycling from spent lithium ion batteries. Engineering 2018;4:361–70. https://doi.org/10.1016/j.eng.2018.05.018.
[110] Li L, Fan E, Guan Y, Zhang X, Xue Q, Wei L, et al. Sustainable recovery of cathode materials from spent lithium-ion batteries using lactic acid leaching system. ACS Sustainable Chemistry & Engineering 2017;5:5224–33. https://doi.org/10.1021/acssuschemeng.7b00571.
[111] Zou H, Gratz E, Apelian D, Wang Y. A novel method to recycle mixed cathode materials for lithium ion batteries. Green Chemistry 2013;15:1183–91. https://doi.org/10.1039/C3GC40182K.
[112] King S, Boxall NJ. Lithium battery recycling in Australia: Defining the status and identifying opportunities for the development of a new industry. Journal of Cleaner Production 2019;215:1279–87. https://doi.org/10.1016/j.jclepro.2019.01.178.
[113] De Clerck Q, van Lier T, Messagie M, Macharis C, Van Mierlo J, Vanhaverbeke L. Total Cost for Society: A persona-based analysis of electric and conventional vehicles. Transportation Research Part D: Transport and Environment 2018. https://doi.org/10.1016/j.trd.2018.02.017.
[114] Letmathe P, Suares M. A consumer-oriented total cost of ownership model for different vehicle types in Germany. Transportation Research Part D: Transport and Environment 2017;57:314–35. https://doi.org/10.1016/j.trd.2017.09.007.
[115] Hao H, Ou X, Du J, Wang H, Ouyang M. China's electric vehicle subsidy scheme: Rationale and impacts. Energy Policy 2014;73:722–32.
[116] autoobserver.net. Market analysis of new energy vehicle industry (新能源汽车行业市场分析现状) 2019. https://baijiahao.baidu.com/s?id=1644337111396325010&wfr=spider&for=pc (accessed February 17, 2020).

[117] Ren D. China's drive to become world's most powerful electric car maker. South China Morning Post 2018. https://www.scmp.com/business/china-business/article/2169698/made-china-2025-worlds-biggest-auto-market-wants-be-most (accessed February 18, 2020).
[118] Schoettle B, Sivak M. Resale Values of Electric and Conventional Vehicles: Recent Trends and Influence on the Decision to Purchase a New Vehicle. The University of Michigan 2018.
[119] Wolfram P, Lutsey N. Electric vehicles: Literature review of technology costs and carbon emissions. The International Council on Clean Transportation: Washington, DC, USA 2016:1–23.
[120] Dezan Shira & Associates. VAT Rates in China Lowered - 2019 Work Report Announcement. China Briefing News 2019. https://www.china-briefing.com/news/vat-rates-china-lowered-2019/ (accessed May 15, 2019).
[121] Huo H, Zhang Q, He K, Yao Z, Wang M. Vehicle-use intensity in China: Current status and future trend. Energy Policy 2012;43:6–16. https://doi.org/10.1016/j.enpol.2011.09.019.
[122] Lu Z, Zhou Y, Cai H, Wang M, He X, Przesmitzki S. China Vehicle Fleet Model: Estimation of Vehicle Stocks, Usage, Emissions, and Energy Use-Model Description, Technical Documentation, and User Guide. Argonne National Lab.(ANL), Argonne, IL (United States); 2018.
[123] PBC. People's Bank of China (PBC) central bank base interest rate 2018. https://www.global-rates.com/interest-rates/central-banks/central-bank-china/pbc-interest-rate.aspx (accessed February 8, 2019).
[124] Wang N, Gong Z, Ma J, Zhao J. Consumer total ownership cost model of plug-in hybrid vehicle in China. Proceedings of the Institution of Mechanical Engineers, Part D: Journal of Automobile Engineering 2012;226:591–602. https://doi.org/10.1177/0954407011421859.
[125] j.autohome.com.cn. Quote for a new car purchase. Autohome 2019. https://j.autohome.com.cn/pcplatform/staticpage/quankuan/index.html#pvareaid=2023633 (accessed February 7, 2019).
[126] Guo C. Low maintenance cost is the reason why electric cars will be the future. 12365auto.com 2016. http://www.12365auto.com/dcbg/20160919/249462-all.shtml (accessed May 1, 2018).
[127] car.autohome.com.cn. Maintenance cost -- 1.5L CVT Senova D50 2018. https://car.autohome.com.cn/mtn/spec/cycle/30263 (accessed June 20, 2018).
[128] Lin B, Wu W. Why people want to buy electric vehicle: An empirical study in first-tier cities of China. Energy Policy 2018;112:233–41.
[129] yunpaiwang.net. License plate price in Shanghai (上海车牌价格走势) 2020. http://www.yunpaiwang.net/jiagezoushi/ (accessed February 20, 2020).
[130] https://www.bjhjyd.gov.cn/. Beijing passenger car index management information system (北京市小客车指标管理信息系统) 2020. https://www.bjhjyd.gov.cn/ (accessed February 20, 2020).
[131] diandong.com. Charging rate in Beijing's public charging stations (北京充电桩如何收费) 2018. http://www.diandong.com/zixun/86729.html (accessed February 14, 2019).
[132] Hsieh I-YL, Pan MS, Green WH. Transition to electric vehicles in China: Implications for private motorization rate and battery market (submitted) n.d.

[133] NBS. National Data 2019. http://data.stats.gov.cn/english/index.htm (accessed August 26, 2019).
[134] Wang N, Tang L, Pan H. Effectiveness of policy incentives on electric vehicle acceptance in China: A discrete choice analysis. Transportation Research Part A: Policy and Practice 2017;105:210–8. https://doi.org/10.1016/j.tra.2017.08.009.
[135] Evergrande Research Institute. 2019 China New Energy Vehicle Development Report (2019 中国新能源汽车发展报告) 2019. https://baijiahao.baidu.com/s?id=1645547007075849033&wfr=spider&for=pc (accessed February 18, 2020).
[136] Davis LW, Knittel CR. Are fuel economy standards regressive? Journal of the Association of Environmental and Resource Economists 2019;6:S37–63.
[137] National Development and Reform Commission. Notice of the National Development and Reform Commission, the Ministry of Ecology and Environment, and the Ministry of Commerce on Issuing the Implementation Plan for Promoting the Upgrading of Key Consumer Goods and the Recycling of Resources (2019-2020). 2019.
[138] OECD. The Cost of Air Pollution: Health Impacts of Road Transport. OECD Publishing Paris; 2014.
[139] Saikawa E, Kurokawa J, Takigawa M, Borken-Kleefeld J, Mauzerall DL, Horowitz LW, et al. The impact of China's vehicle emissions on regional air quality in 2000 and 2020: a scenario analysis. Atmospheric Chemistry and Physics 2011;11:9465–84. https://doi.org/10.5194/acp-11-9465-2011.
[140] Merchant EF. The Next Big Obstacle for Electric Vehicles? Charging Infrastructure 2017. https://www.greentechmedia.com/articles/read/the-next-big-obstacle-for-electric-vehicles-charging-infrastructure (accessed February 23, 2018).
[141] Guinn S. Level 1 vs Level 2 Electric Vehicle Charging Stations. ClipperCreek 2018. https://www.clippercreek.com/level-1-level-2-charging-stations/ (accessed April 5, 2019).
[142] Rosa LP, Abdalla K. Modernizing and greening taxi fleets in Latin American cities 2011.
[143] Beijing Transport Institute. Beijing Transport Institute Annual Report (2011 年北京交通发展年报). Beijing: Beijing Transport Institute; 2011.
[144] Rezvanizaniani SM, Liu Z, Chen Y, Lee J. Review and recent advances in battery health monitoring and prognostics technologies for electric vehicle (EV) safety and mobility. Journal of Power Sources 2014;256:110–24. https://doi.org/10.1016/j.jpowsour.2014.01.085.
[145] Bullis K. Israel to Get Electric Car Battery Swap Stations - MIT Technology Review 2011. https://www.technologyreview.com/s/424587/israel-to-get-electric-car-battery-swap-stations/ (accessed June 11, 2018).
[146] BJEV B. World's Largest Network of EV Battery Charging and Switching Stations Commences Operation in Beijing 2016. https://www.prnewswire.com/news-releases/worlds-largest-network-of-ev-battery-charging-and-switching-stations-commences-operation-in-beijing-300355823.html (accessed March 6, 2018).
[147] Li D. China's BAIC Group Launches EV Battery-Swap Station Network In Beijing. China Money Network 2016. https://www.chinamoneynetwork.com/2016/11/03/chinas-baic-group-launches-ev-battery-swap-station-network-in-beijing (accessed March 6, 2018).
[148] Mak H-Y, Rong Y, Shen Z-JM. Infrastructure planning for electric vehicles with battery swapping. Management Science 2013;59:1557–75. https://doi.org/10.1287/mnsc.1120.1672.

[149] Rao R, Zhang X, Xie J, Ju L. Optimizing electric vehicle users' charging behavior in battery swapping mode. Applied Energy 2015;155:547–59. https://doi.org/10.1016/j.apenergy.2015.05.125.
[150] Sarker MR, Pandžić H, Ortega-Vazquez MA. Optimal operation and services scheduling for an electric vehicle battery swapping station. IEEE Transactions on Power Systems 2015;30:901–10. https://doi.org/10.1109/TPWRS.2014.2331560.
[151] Wang Y, Huang L, Wei H, Zheng W, Gu T, Liu H. Planning battery swapping stations for urban electrical taxis. 2015 IEEE 35th International Conference on Distributed Computing Systems, IEEE; 2015, p. 742–3. https://doi.org/10.1109/ICDCS.2015.87.
[152] Tu W, Li Q, Fang Z, Shaw S, Zhou B, Chang X. Optimizing the locations of electric taxi charging stations: A spatial–temporal demand coverage approach. Transportation Research Part C: Emerging Technologies 2016;65:172–89. https://doi.org/10.1016/j.trc.2015.10.004.
[153] Z. Tian, T. Jung, Y. Wang, F. Zhang, L. Tu, C. Xu, et al. Real-Time Charging Station Recommendation System for Electric-Vehicle Taxis. IEEE Transactions on Intelligent Transportation Systems 2016;17:3098–109. https://doi.org/10.1109/TITS.2016.2539201.
[154] Liang Y, Zhang X. Battery swap pricing and charging strategy for electric taxis in China. Energy 2018;147:561–77. https://doi.org/10.1016/j.energy.2018.01.082.
[155] Wang N, Liu Y, Fu G, Li Y. Cost–benefit assessment and implications for service pricing of electric taxies in China. Energy for Sustainable Development 2015;27:137–46. https://doi.org/10.1016/j.esd.2015.05.008.
[156] Cai H, Xu M. Greenhouse gas implications of fleet electrification based on big data-informed individual travel patterns. Environmental Science & Technology 2013;47:9035–43. https://doi-org.libproxy.mit.edu/10.1021/es401008f.
[157] Shi X, Wang X, Yang J, Sun Z. Electric vehicle transformation in Beijing and the comparative eco-environmental impacts: A case study of electric and gasoline powered taxis. Journal of Cleaner Production 2016;137:449–60. https://doi.org/10.1016/j.jclepro.2016.07.096.
[158] Rao R, Cai H, Xu M. Modeling electric taxis' charging behavior using real-world data. International Journal of Sustainable Transportation 2018;12:452–60. https://doi.org/10.1080/15568318.2017.1388887.
[159] Zou Y, Wei S, Sun F, Hu X, Shiao Y. Large-scale deployment of electric taxis in Beijing: A real-world analysis. Energy 2016;100:25–39. https://doi.org/10.1016/j.energy.2016.01.062.
[160] Liu X, Wang N, Dong D. A cost-oriented optimal model of electric vehicle taxi systems. Sustainability 2018;10:1557. https://doi.org/10.3390/su10051557.
[161] Wang X. It takes 6 years to recoup the costs of building public EV charging station (充电桩网点 6 年才能收回成本 投资人称补贴落地迟缓). people.cn 2016. http://auto.people.com.cn/n1/2016/0705/c1005-28524666.html (accessed March 10, 2018).
[162] Lee H. Taxi Fare Adjustment and Improvement of Dynamic Adjustment Mechanism of Fuel Surcharge in Beijing (北京市出租汽车租价调整和完善燃油附加费动态调整机制方案). Beijing: Beijing Municipal Commission of Reform and Development; 2013.
[163] BBTNews. BAIC BJEV invests billion RMB on battery swapping (北汽新能源百亿豪赌换电模式) 2017. http://www.bbtnews.com.cn/2017/1106/216930.shtml (accessed April 7, 2019).

[164] Zhou Y. BAIC, Aulton, and Dianba are working together on commercializing battery swapping technology and service (北汽新能源 奥动 电巴三方的强强联手合作) 2016. http://www.12365auto.com/news/20160810/243984.shtml (accessed March 7, 2018).
[165] d1ev.com. Beijing six ring has formed an average of 5 km service radius of the public charging network (北京形成六环内 5 公里公用充电桩网络) 2017. https://www.d1ev.com/news/shichang/54718 (accessed March 7, 2018).
[166] Autohome.com. Autohome.com.cn: Vehicle Models Search 2018. https://car.autohome.com.cn/ (accessed February 28, 2018).
[167] Kearney MJ. Electric vehicle charging infrastructure deployment: policy analysis using a dynamic behavioral spatial model. Massachusetts Institute of Technology, 2011.
[168] Chang D, Erstad D, Lin E, Rice AF, Goh CT, Tsao AA, et al. Financial viability of non-residential electric vehicle charging stations. Luskin Center for Innovation: Los Angeles, CA, USA 2012.
[169] chemcp.com. Today's Beijing gasoline price 2018. http://youjia.chemcp.com/beijing/ (accessed May 26, 2018).
[170] MOT. Beijing: Taxis now have to be retired in 6 years (北京：出租车报废年限从 8 年降至 6 年) 2015. http://www.chinahighway.com/news/2015/921727.php (accessed February 27, 2018).
[171] Beijing Jiaotong University. Beijing Taxi Operation Survey (北京出租车运营调查(含专车)). Beijing: 2012 MBA of Beijing Jiaotong University; 2016.
[172] Yang Y. 2016 Beijing Land Market Review and 2017 Outlook (2016 年北京土地市场回顾及 2017 年展望) 2017. http://www.doc88.com/p-8901319993703.html (accessed May 26, 2018).
[173] Beijing Municipal Commission of Development and Reform. Beijing's multi-step electricity price standard (关于合理调整电价结构有关事项的通知) 2018.
[174] Aulton.com. Aulton New Energy 2019. http://www.aulton.com/aulton.html (accessed February 28, 2019).
[175] Chlebis P, Tvrdon M, Havel A, Baresova K. Comparison of standard and fast charging methods for electric vehicles. Advances in Electrical and Electronic Engineering 2014;12:111–6. https://doi.org/10.15598/aeee.v12i2.975.
[176] bjev.com.cn. BJEV's battery swapping services 2019. http://www.bjev.com.cn/html/charge-transfer.html (accessed May 6, 2019).
[177] China Energy Storage Alliance. BAIC BJEV Announces "Optimus Prime Plan" Combining Battery Swapping, Energy Storage, and Solar Models 2017. http://en.cnesa.org/featured-stories/2017/12/11/baic-bjev-announces-optimus-prime-plan-combing-battery-swapping-energy-storage-and-solar-models (accessed February 25, 2018).
[178] Beijing Municipal Government. Notice on the implementation of relevant incentives for the early retirement or renewal of taxis (北京鼓励出租汽车更新为纯电动：最高 5 万补贴) 2015. www.sohu.com/a/271409255_100282316 (accessed March 4, 2019).
[179] Kaplowitz SA, McCright AM. Effects of policy characteristics and justifications on acceptance of a gasoline tax increase. Energy Policy 2015;87:370–81.
[180] Shih X. Nearly 50% of the gasoline price at the pump are taxes (100 块汽油近 50 块税你知道都是哪些税吗). www.ce.cn 2015.

http://www.ce.cn/cysc/ny/gdxw/201501/16/t20150116_4355412.shtml (accessed February 10, 2019).
[181] Zhang C. Chinese coal town embraces electric vehicles 2018. https://www.chinadialogue.net/article/show/single/en/10335-Chinese-coal-town-embraces-electric-vehicles (accessed May 4, 2019).
[182] Hsieh I-YL, Green WH. Transition to electric vehicles in China: Implications for total cost of ownership and cost to society (submitted) n.d.
[183] Wang M, Elgowainy A, Benavides PT, Burnham A, Cai H, Dai Q, et al. Summary of Expansions and Updates in GREET® 2018. Argonne National Lab.(ANL), Argonne, IL (United States); 2018.
[184] Nordelöf A, Messagie M, Tillman A-M, Söderman ML, Van Mierlo J. Environmental impacts of hybrid, plug-in hybrid, and battery electric vehicles—what can we learn from life cycle assessment? The International Journal of Life Cycle Assessment 2014;19:1866–90.
[185] Onat NC, Kucukvar M, Tatari O. Conventional, hybrid, plug-in hybrid or electric vehicles? State-based comparative carbon and energy footprint analysis in the United States. Applied Energy 2015;150:36–49.
[186] Shen W, Han W, Wallington TJ, Winkler S. China Electricity Generation Greenhouse Gas Emission Intensity in 2030: Implications for Electric Vehicles. Environmental Science & Technology 2019.
[187] Wang H, Ou X, Zhang X. Mode, technology, energy consumption, and resulting CO2 emissions in China's transport sector up to 2050. Energy Policy 2017;109:719–33. https://doi.org/10.1016/j.enpol.2017.07.010.
[188] Hao H, Liu Z, Zhao F, Li W, Hang W. Scenario analysis of energy consumption and greenhouse gas emissions from China's passenger vehicles. Energy 2015;91:151–9. https://doi.org/10.1016/j.energy.2015.08.054.
[189] Gambhir A, Lawrence KC, Tong D, Martinez-Botas R. Reducing China's road transport sector CO2 emissions to 2050: Technologies, costs and decomposition analysis. Applied Energy 2015;157:905–17. https://doi.org/10.1016/j.apenergy.2015.01.018.
[190] Zheng B, Zhang Q, Borken-Kleefeld J, Huo H, Guan D, Klimont Z, et al. How will greenhouse gas emissions from motor vehicles be constrained in China around 2030? Applied Energy 2015;156:230–40. https://doi.org/10.1016/j.apenergy.2015.07.018.
[191] Xu B, Lin B. Differences in regional emissions in China's transport sector: determinants and reduction strategies. Energy 2016;95:459–70. https://doi.org/10.1016/j.energy.2015.12.016.
[192] Hao H, Geng Y, Wang H, Ouyang M. Regional disparity of urban passenger transport associated GHG (greenhouse gas) emissions in China: a review. Energy 2014;68:783–93. https://doi.org/10.1016/j.energy.2014.01.008.
[193] Peng T, Ou X, Yuan Z, Yan X, Zhang X. Development and application of China provincial road transport energy demand and GHG emissions analysis model. Applied Energy 2018;222:313–28. https://doi.org/10.1016/j.apenergy.2018.03.139.
[194] Huo H, Cai H, Zhang Q, Liu F, He K. Life-cycle assessment of greenhouse gas and air emissions of electric vehicles: A comparison between China and the US. Atmospheric Environment 2015;108:107–16. https://doi.org/10.1016/j.atmosenv.2015.02.073.
[195] Wang R, Wu Y, Ke W, Zhang S, Zhou B, Hao J. Can propulsion and fuel diversity for the bus fleet achieve the win–win strategy of energy conservation and environmental

protection? Applied Energy 2015;147:92–103. https://doi.org/10.1016/j.apenergy.2015.01.107.
[196] Ke W, Zhang S, He X, Wu Y, Hao J. Well-to-wheels energy consumption and emissions of electric vehicles: Mid-term implications from real-world features and air pollution control progress. Applied Energy 2017;188:367–77.
[197] Shi S, Zhang H, Yang W, Zhang Q, Wang X. A life-cycle assessment of battery electric and internal combustion engine vehicles: A case in Hebei Province, China. Journal of Cleaner Production 2019;228:606–18.
[198] Zheng Y, He X, Wang H, Wang M, Zhang S, Ma D, et al. Well-to-wheels greenhouse gas and air pollutant emissions from battery electric vehicles in China. Mitigation and Adaptation Strategies for Global Change 2019:1–16.
[199] iCET. Report on the open market index of China new energy vehicle (新能源汽车市场开放指数报告). Beijing: Innovation center for energy and transformation (能源与交通创新中心); 2018.
[200] Tang L, Qu J, Mi Z, Bo X, Chang X, Anadon LD, et al. Substantial emission reductions from Chinese power plants after the introduction of ultra-low emissions standards. Nature Energy 2019:1–10.
[201] Cai W, Wang C, Jin Z, Chen J. Quantifying Baseline Emission Factors of Air Pollutants in China's Regional Power Grids. Environ Sci Technol 2013;47:3590–7. https://doi.org/10.1021/es304915q.
[202] Shen S, Wang C. Decomposition analysis on the air pollutant baseline emission factors in China's power sector. Energy Procedia 2017;105:3355–62.
[203] Yang J, Song D, Wu F. Regional variations of environmental co-benefits of wind power generation in China. Applied Energy 2017;206:1267–81.
[204] iCET. A study on China's timetable for phasing-out traditional ICE-vehicles (中国传统燃油汽车退出时间表研究). Innovation center for energy and transformation (能源与交通创新中心); 2019.
[205] iCET. 2018 New Data Analysis on Real-world Driving and Fuel Consumption for Passenger Cars in China (2018 中国乘用车实际道路行驶与油耗分析年度报告). Innovation center for energy and transformation (能源与交通创新中心); 2018.
[206] xiaoxiongyouhao. Fuel consumption index in China (中国油耗指数地图) n.d. https://www.xiaoxiongyouhao.com/dashboard/FCImap.php (accessed November 1, 2019).
[207] Zhang S. Technical Guide for the Compilation of Emission Inventory for Road Vehicle Air Pollutants (Trial) (道路机动车大气污染物排放清单编制技术指南（试行）). Chinese Academy of Environmental Sciences; 2015.
[208] Chossiere GP, Eastham SD, Jenn, Allroggen F, Barrett SR. Air quality trade-offs of a rapid expansion of personal electric vehicles in China n.d.
[209] GEOS-Chem n.d. https://doi.org/10.5281/zenodo.1553349.
[210] Bey I, Jacob DJ, Yantosca RM, Logan JA, Field BD, Fiore AM, et al. Global modeling of tropospheric chemistry with assimilated meteorology: Model description and evaluation. Journal of Geophysical Research: Atmospheres 2001;106:23073–95.
[211] Park RJ, Jacob DJ, Field BD, Yantosca RM, Chin M. Natural and transboundary pollution influences on sulfate-nitrate-ammonium aerosols in the United States: Implications for policy. Journal of Geophysical Research: Atmospheres 2004;109.

[212] Li M, Zhang Q, Streets DG, He KB, Cheng YF, Emmons LK, et al. Mapping Asian anthropogenic emissions of non-methane volatile organic compounds to multiple chemical mechanisms. Atmos Chem Phys 2014;14:5617–38.
[213] Keller CA, Long MS, Yantosca RM, Da Silva AM, Pawson S, Jacob DJ. HEMCO v1. 0: a versatile, ESMF-compliant component for calculating emissions in atmospheric models. Geosci Model Dev 2014.
[214] Gelaro R, McCarty W, Suárez MJ, Todling R, Molod A, Takacs L, et al. The modern-era retrospective analysis for research and applications, version 2 (MERRA-2). Journal of Climate 2017;30:5419–54.
[215] Burnett R, Chen H, Szyszkowicz M, Fann N, Hubbell B, Pope CA, et al. Global estimates of mortality associated with long-term exposure to outdoor fine particulate matter. Proceedings of the National Academy of Sciences 2018;115:9592–7.
[216] Maji KJ, Ye W-F, Arora M, Nagendra SS. PM2. 5-related health and economic loss assessment for 338 Chinese cities. Environment International 2018;121:392–403. https://doi.org/10.1016/j.envint.2018.09.024.
[217] Turner MC, Jerrett M, Pope III CA, Krewski D, Gapstur SM, Diver WR, et al. Long-term ozone exposure and mortality in a large prospective study. American Journal of Respiratory and Critical Care Medicine 2016;193:1134–42.
[218] Feng Z, De Marco A, Anav A, Gualtieri M, Sicard P, Tian H, et al. Economic losses due to ozone impacts on human health, forest productivity and crop yield across China. Environment International 2019;131:104966. https://doi.org/10.1016/j.envint.2019.104966.
[219] Forouzanfar MH, Afshin A, Alexander LT, Anderson HR, Bhutta ZA, Biryukov S, et al. Global, regional, and national comparative risk assessment of 79 behavioural, environmental and occupational, and metabolic risks or clusters of risks, 1990–2015: a systematic analysis for the Global Burden of Disease Study 2015. The Lancet 2016;388:1659–724.
[220] Di Q, Wang Y, Zanobetti A, Wang Y, Koutrakis P, Choirat C, et al. Air pollution and mortality in the Medicare population. New England Journal of Medicine 2017;376:2513–22.
[221] Ostro B, Organization WH. Outdoor air pollution: assessing the environmental burden of disease at national and local levels. World Health Organization; 2004.
[222] Chossière GP, Malina R, Allroggen F, Eastham SD, Speth RL, Barrett SR. Country-and manufacturer-level attribution of air quality impacts due to excess NOx emissions from diesel passenger vehicles in Europe. Atmospheric Environment 2018;189:89–97.
[223] US EPA O. The Social Cost of Carbon n.d. /climatechange/social-cost-carbon (accessed December 10, 2018).
[224] OECD. Valuing Mortality Risk Reductions in Regulatory Analysis of Environmental, Health and Transport Policies: Policy Implications. Paris: OECD; 2011.
[225] Hammitt JK, Geng F, Guo X, Nielsen CP. Valuing mortality risk in China: Comparing stated-preference estimates from 2005 and 2016. Journal of Risk and Uncertainty 2019;58:167–86.
[226] OECD. The Economic Consequences of Outdoor Air Pollution. 2016.
[227] Statista. Oil consumption in China in barrels per day 2018. Statista 2019. https://www.statista.com/statistics/265235/oil-consumption-in-china-in-thousand-barrels-per-day/ (accessed March 30, 2020).

[228] Seinfeld JH, Pandis SN. Atmospheric chemistry and physics: from air pollution to climate change. John Wiley & Sons; 2016.
[229] Heelan J, Gratz E, Zheng Z, Wang Q, Chen M, Apelian D, et al. Current and prospective Li-ion battery recycling and recovery processes. Jom 2016;68:2632–2638.
[230] Gratz E, Sa Q, Apelian D, Wang Y. A closed loop process for recycling spent lithium ion batteries. Journal of Power Sources 2014;262:255–62.
[231] Olsson L, Fallahi S, Schnurr M, Diener D, van Loon P. Circular Business Models for Extended EV Battery Life. Batteries 2018;4:57.
[232] Matus K, Nam K-M, Selin NE, Lamsal LN, Reilly JM, Paltsev S. Health damages from air pollution in China. Global Environmental Change 2012;22:55–66.
[233] Gorzelany J. Why Tesla's Vertical Manufacturing Move Could Prove Essential To Its Success. Forbes n.d. https://www.forbes.com/sites/jimgorzelany/2014/02/27/why-teslas-vertical-manufacturing-move-is-manifest-destiny/ (accessed February 6, 2018).
[234] Masiero G, Ogasavara MH, Jussani AC, Risso ML. Electric vehicles in China: BYD strategies and government subsidies. RAI Revista de Administração e Inovação 2016;13:3–11. https://doi.org/10.1016/j.rai.2016.01.001.
[235] Min-hee J. Automakers' Production of EV Battery Gives Huge Pressure on Battery Producers. BusinessKorea 2017. http://www.businesskorea.co.kr/english/news/industry/18066-vertical-integration-automakers%E2%80%99-production-ev-battery-gives-huge-pressure (accessed February 6, 2018).
[236] Argote L, Epple D. Learning curves in manufacturing. Science 1990;247:920–4.
[237] Pillot C. Avicenne Energy Profile 2017 2017.
[238] Van Vliet O, Brouwer AS, Kuramochi T, van Den Broek M, Faaij A. Energy use, cost and CO 2 emissions of electric cars. Journal of Power Sources 2011;196:2298–310.
[239] Gerssen-Gondelach SJ, Faaij AP. Performance of batteries for electric vehicles on short and longer term. Journal of Power Sources 2012;212:111–29.
[240] McKinsey A. Portfolio of power-trains for europe: A fact-based analysis. McKinsey & Company, Tech Rep 2010.
[241] Mayer T, Kreyenberg D, Wind J, Braun F. Feasibility study of 2020 target costs for PEM fuel cells and lithium-ion batteries: A two-factor experience curve approach. International Journal of Hydrogen Energy 2012;37:14463–74.
[242] Miller JF. Analysis of current and projected battery manufacturing costs for electric, hybrid, and plug-in hybrid electric vehicles. World Electric Vehicle Journal 2010;4:347–50.
[243] Offer GJ, Howey D, Contestabile M, Clague R, Brandon NP. Comparative analysis of battery electric, hydrogen fuel cell and hybrid vehicles in a future sustainable road transport system. Energy Policy 2010;38:24–9.
[244] How Much And How Fast Will Electric-Car Battery Costs Fall? Green Car Reports n.d. https://www.greencarreports.com/news/1074183_how-much-and-how-fast-will-electric-car-battery-costs-fall.
[245] Propfe B, Redelbach M, Santini DJ, Friedrich H. Cost analysis of plug-in hybrid electric vehicles including maintenance & repair costs and resale values 2012.
[246] Lambert F. Electric vehicle battery cost dropped 80% in 6 years down to $227/kWh – Tesla claims to be below $190/kWh | Electrek 2017.

https://electrek.co/2017/01/30/electric-vehicle-battery-cost-dropped-80-6-years-227kwh-tesla-190kwh/ (accessed January 26, 2018).
[247] Ghosn overruling electric engineers - Press Room - TBC n.d. https://www.totalbatteryconsulting.com/press/Ghosn-overruling-electric-engineers-makes-Lutz-see-losing-bet.html (accessed January 26, 2018).
[248] Lee H, Lovellette G. Will electric cars transform the US vehicle market?: An analysis of the key determinants. Harvard Kennedy School, Belfer Center for Science and International Affairs; 2011.
[249] Shulock C, Pike E, Lloyd A, Rose R. Vehicle electrification policy study, task 1 report: technology status. Washington DC, US: The International Council on Clean Transportation 2011.
[250] Weiss M, Patel MK, Junginger M, Perujo A, Bonnel P, van Grootveld G. On the electrification of road transport-Learning rates and price forecasts for hybrid-electric and battery-electric vehicles. Energy Policy 2012;48:374–93.
[251] Wråke M, Breen K, Burnard K, Cheung K, Chiavari J. Energy Technology Perspectives 2012 excerpt as IEA input to the Clean Energy Ministerial. Paris: OECD/IEA; 2012.
[252] Catenacci M, Verdolini E, Bosetti V, Fiorese G. Going electric: Expert survey on the future of battery technologies for electric vehicles. Energy Policy 2013;61:403–13.
[253] Lache R, Galves D, Nolan P. Vehicle Electrification: More rapid growth; steeper price declines for batteries. Deutsche Bank Industry Update 2010.
[254] Cluzel C, Douglas C. Cost and performance of EV batteries. Element Energy, Final Report for the Committee on Climate Change 2012.
[255] Tran M, Banister D, Bishop JD, McCulloch MD. Realizing the electric-vehicle revolution. Nature Climate Change 2012;2:328–33.
[256] Cheung A. Bloomberg New Energy Finance Summit 2012.
[257] Liebreich M. Bloomberg New Energy Finance Summit 2013.
[258] Hensley R, Newman J, Rogers M. Battery technology charges ahead | McKinsey & Company n.d. https://www.mckinsey.com/business-functions/sustainability-and-resource-productivity/our-insights/battery-technology-charges-ahead (accessed January 26, 2018).
[259] Trigg T, Telleen P, Boyd R, Cuenot F, D'Ambrosio D, Gaghen R, et al. Global EV outlook: understanding the electric vehicle landscape to 2020. Int Energy Agency 2013:1–40.
[260] Howell D. The EV Everywhere Challenge. US Department of Energy, Washington DC; 2014.
[261] Ramsey M. GM Developing Car to Rival Tesla. Wall Street Journal 2013.
[262] Dumaine B. Electric vehicles aren't out of juice just yet. Fortune n.d. http://fortune.com/2013/11/04/electric-vehicles-arent-out-of-juice-just-yet/ (accessed January 26, 2018).
[263] Van Noorden R. A better battery. Nature 2014;507:26.
[264] Wolfram P, Lutsey N. Electric vehicles: Literature review of technology costs and carbon emissions. Working Paper 2016.
[265] Lambert F. Tesla confirms base Model 3 will have less than 60 kWh battery pack option, cost is below $190/kWh and falling. Electrek 2016. https://electrek.co/2016/04/26/tesla-model-3-battery-pack-cost-kwh/.

[266] Beene R. Audi's A3 e-tron to pave way for electrified vehicle push 2 plug-in hybrids and 2 battery EVs to join lineup in coming years 2015. http://www.autonews.com/article/20151101/OEM05/311029960/&template=print.
[267] Lambert F. Tesla is now claiming 35% battery cost reduction at 'Gigafactory 1' – hinting at breakthrough cost below $125/kWh. Electrek 2017. https://electrek.co/2017/02/18/tesla-battery-cost-gigafactory-model-3/.
[268] UBS Evidence Lab Electric Car Teardown – Disruption Ahead? UBS Evidence Lab; 2017.
[269] Buchmann I. Types of Lithium-ion Batteries – Battery University. Battery University n.d. http://batteryuniversity.com/learn/article/types_of_lithium_ion (accessed February 4, 2018).
[270] Mo K. Electric Passenger Cars and Lithium-ion battery industry devlopment 2017.
[271] Pillot C. The rechargeable battery market and main trends 2016–2025. 33rd International Battery Seminar & Exhibit, 2017.
[272] Irle R, Pontes J, Irle V. EV-Volumes - China Plug-in Sales for 2017-Q4 and Full Year – Update n.d. http://www.ev-volumes.com/country/china/ (accessed February 5, 2018).
[273] Zhang Y, Tian Y. China Revises EV Credit Points to Reward Longer-Range Models - Bloomberg 2017. https://www.bloomberg.com/news/articles/2017-06-13/china-tweaks-proposed-ev-formula-to-reward-longer-range-models-j3v68b09 (accessed February 5, 2018).
[274] Lima P. Electric car range and efficiency table (NEDC). Push EVs 2017. https://pushevs.com/2017/05/23/electric-car-range-efficiency-table-nedc/ (accessed February 5, 2018).
[275] Clowes W, Wilson T. Congo May More Than Double Tax on Critical Cobalt Supply. BloombergCom 2018.
[276] London Metal Exchange: LME Nickel 2018. https://www.lme.com/Metals/Non-ferrous/Nickel#tabIndex=0 (accessed February 5, 2018).
[277] He J-C. Coremax Group Investor Conference, 2017 Q3. 2017.
[278] Thackeray MM, Johnson PJ, de Picciotto LA, Bruce PG, Goodenough JB. Electrochemical extraction of lithium from LiMn2O4. Materials Research Bulletin 1984;19:179–87. https://doi.org/10.1016/0025-5408(84)90088-6.
[279] Whittingham MS. Lithium Batteries and Cathode Materials. Chem Rev 2004;104:4271–302. https://doi.org/10.1021/cr020731c.
[280] Padhi AK, Nanjundaswamy KS, Goodenough JB. Phospho-olivines as Positive-Electrode Materials for Rechargeable Lithium Batteries. J Electrochem Soc 1997;144:1188–94. https://doi.org/10.1149/1.1837571.
[281] Liu Z, Yu A, Lee KY. Synthesis and characterization of LiNi1−x−yCoxMnyO2 as the cathode materials of secondary lithium batteries. Journal of Power Sources 1999;81–82:416–9. https://doi.org/10.1016/S0378-7753(99)00221-9.
[282] Lee KK, Yoon WS, Kim KB, Lee KY, Hong ST. Characterization of LiNi0.85Co0.10M0.05O2 (M = Al, Fe) as a cathode material for lithium secondary batteries. Journal of Power Sources 2001;97–98:308–12. https://doi.org/10.1016/S0378-7753(01)00516-X.
[283] Thackeray MM, Johnson CS, Vaughey JT, Li N, Hackney SA. Advances in manganese-oxide 'composite' electrodes for lithium-ion batteries. J Mater Chem 2005;15:2257–67. https://doi.org/10.1039/B417616M.

[284] CAMX Power Announces CAM-7.2™ - Its Breakthrough Lithium-Ion Battery Cathode Material n.d. https://www.prnewswire.com/news-releases/camx-power-announces-cam-72---its-breakthrough-lithium-ion-battery-cathode-material-264640441.html (accessed February 1, 2018).
[285] Mizushima K, Jones PC, Wiseman PJ, Goodenough JB. LixCoO2 (0<x<-1): A new cathode material for batteries of high energy density. Materials Research Bulletin 1980;15:783–9. https://doi.org/10.1016/0025-5408(80)90012-4.
[286] Danuta H, Juliusz U. Electric dry cells and storage batteries. US3043896 A, 1962.
[287] Aurbach D, Lu Z, Schechter A, Gofer Y, Gizbar H, Turgeman R, et al. Prototype systems for rechargeable magnesium batteries. Nature 2000;407:724. https://doi.org/10.1038/35037553.
[288] Sun X, Bonnick P, Duffort V, Liu M, Rong Z, Persson KA, et al. A high capacity thiospinel cathode for Mg batteries. Energy Environ Sci 2016;9:2273–7. https://doi.org/10.1039/C6EE00724D.
[289] Gopalakrishnan J, Rangan KK. Vanadium phosphate (V2(PO4)3): a novel NASICO N-type vanadium phosphate synthesized by oxidative deintercalation of sodium from sodium vanadium phosphate (Na3V2(PO4)3). Chem Mater 1992;4:745–7. https://doi.org/10.1021/cm00022a001.
[290] Lu Z, Dahn JR. In Situ X-Ray Diffraction Study of P 2 - Na2 / 3 [Ni1 / 3Mn2 / 3] O 2. J Electrochem Soc 2001;148:A1225–9. https://doi.org/10.1149/1.1407247.
[291] Komaba S, Nakayama T, Ogata A, Shimizu T, Takei C, Takada S, et al. Electrochemically Reversible Sodium Intercalation of Layered NaNi0.5Mn0.5O2 and NaCrO2. ECS Trans 2009;16:43–55. https://doi.org/10.1149/1.3112727.
[292] Estimate based on quotes from multiple undisclosed vendors. n.d.
[293] Gold supplier with high transaction level from www.alibaba.com. Available at: https://www.alibaba.com. (Accessed: 14th May 2017) n.d.
[294] Pillot C. Avicenne Energy Profile 2017 2017.
[295] This price is estimated based on price of Titanium powder (US$30+/kg) and its sensitivity to O2 & moisture. n.d.
[296] This price is estimated based on price of Molybdenum disulfide powder (US$25+/kg) and assumed processing costs. n.d.
[297] This price is estimated based on price of Na2CO3 (US$0.2/kg), Vanadium (US$20/kg), and NH4H2PO4 (US$0.4/kg). n.d.
[298] Darling RM, Gallagher KG, Kowalski JA, Ha S, Brushett FR. Pathways to low-cost electrochemical energy storage: a comparison of aqueous and nonaqueous flow batteries. Energy Environ Sci 2014;7:3459–77. https://doi.org/10.1039/C4EE02158D.
[299] Schipper F, Erickson EM, Erk C, Shin J-Y, Chesneau FF, Aurbach D. Review—Recent Advances and Remaining Challenges for Lithium Ion Battery Cathodes I. Nickel-Rich, LiNixCoyMnzO2. J Electrochem Soc 2017;164:A6220–8. https://doi.org/10.1149/2.0351701jes.
[300] Lima P. LG Chem will introduce NCM 811 battery cells for EVs next year. Push EVs 2017. https://pushevs.com/2017/09/08/lg-chem-will-introduce-ncm-811-battery-cells-evs-next-year/ (accessed February 4, 2018).
[301] Vaughey J. High Energy - High Voltage Program: Materials 2016.

[302] Allen JL, Allen JL, Delp SA, Jow TR. Evaluation of TIAX High Energy CAM-7/Graphite Lithium-Ion Batteries at High and Low Temperatures. Sensors and Electron Devices Directorate, Army Research Laboratory; 2014.
[303] Doeff MM. Battery Cathodes. Encyclopedia of Sustainability Science and Technology, Springer, New York, NY; 2012, p. 708–39. https://doi.org/10.1007/978-1-4419-0851-3_497.
[304] Petibon R, Xia J, Ma L, Bauer MKG, Nelson KJ, Dahn JR. Electrolyte System for High Voltage Li-Ion Cells. J Electrochem Soc 2016;163:A2571–8. https://doi.org/10.1149/2.0321613jes.
[305] Andre D, Kim S-J, Lamp P, Lux SF, Maglia F, Paschos O, et al. Future generations of cathode materials: an automotive industry perspective. J Mater Chem A 2015;3:6709–32. https://doi.org/10.1039/C5TA00361J.
[306] Blomgren GE. The Development and Future of Lithium Ion Batteries. J Electrochem Soc 2017;164:A5019–25. https://doi.org/10.1149/2.0251701jes.
[307] Kalluri S, Yoon M, Jo M, Park S, Myeong S, Kim J, et al. Surface Engineering Strategies of Layered LiCoO2 Cathode Material to Realize High-Energy and High-Voltage Li-Ion Cells. Adv Energy Mater 2017;7:1601507. https://doi.org/10.1002/aenm.201601507.
[308] Liu A, Li J, Shunmugasundaram R, Dahn JR. Synthesis of Mg and Mn Doped LiCoO2 and Effects on High Voltage Cycling. J Electrochem Soc 2017;164:A1655–64. https://doi.org/10.1149/2.1381707jes.
[309] Yano A, Shikano M, Ueda A, Sakaebe H, Ogumi Z. LiCoO2 Degradation Behavior in the High-Voltage Phase Transition Region and Improved Reversibility with Surface Coating. J Electrochem Soc 2017;164:A6116–22. https://doi.org/10.1149/2.0181701jes.
[310] Park JS, Mane AU, Elam JW, Croy JR. Atomic Layer Deposition of Al–W–Fluoride on LiCoO2 Cathodes: Comparison of Particle- and Electrode-Level Coatings. ACS Omega 2017;2:3724–9. https://doi.org/10.1021/acsomega.7b00605.
[311] Wu N, Zhang Y, Guo Y, Liu S, Liu H, Wu H. Flakelike LiCoO2 with Exposed {010} Facets As a Stable Cathode Material for Highly Reversible Lithium Storage. ACS Appl Mater Interfaces 2016;8:2723–31. https://doi.org/10.1021/acsami.5b10977.
[312] Quinlan RA, Lu Y-C, Kwabi D, Shao-Horn Y, Mansour AN. XPS Investigation of the Electrolyte Induced Stabilization of LiCoO2 and “AlPO4”-Coated LiCoO2 Composite Electrodes. J Electrochem Soc 2016;163:A300–8. https://doi.org/10.1149/2.0851602jes.
[313] Dai X, Zhou A, Xu J, Lu Y, Wang L, Fan C, et al. Extending the High-Voltage Capacity of LiCoO2 Cathode by Direct Coating of the Composite Electrode with Li2CO3 via Magnetron Sputtering. J Phys Chem C 2016;120:422–30. https://doi.org/10.1021/acs.jpcc.5b10677.
[314] Yabuuchi N, Kinoshita Y, Misaki K, Matsuyama T, Komaba S. Electrochemical Properties of LiCoO2 Electrodes with Latex Binders on High-Voltage Exposure. J Electrochem Soc 2015;162:A538–44. https://doi.org/10.1149/2.0151504jes.
[315] Li X, Liu J, Meng X, Tang Y, Banis MN, Yang J, et al. Significant impact on cathode performance of lithium-ion batteries by precisely controlled metal oxide nanocoatings via atomic layer deposition. Journal of Power Sources 2014;247:57–69. https://doi.org/10.1016/j.jpowsour.2013.08.042.
[316] Dai X, Wang L, Xu J, Wang Y, Zhou A, Li J. Improved Electrochemical Performance of LiCoO2 Electrodes with ZnO Coating by Radio Frequency Magnetron Sputtering. ACS Appl Mater Interfaces 2014;6:15853–9. https://doi.org/10.1021/am503260s.

[317] Zuo X, Fan C, Xiao X, Liu J, Nan J. High-voltage performance of LiCoO2/graphite batteries with methylene methanedisulfonate as electrolyte additive. Journal of Power Sources 2012;219:94–9. https://doi.org/10.1016/j.jpowsour.2012.07.026.
[318] Cheng H-M, Wang F-M, Chu JP, Santhanam R, Rick J, Lo S-C. Enhanced Cycleabity in Lithium Ion Batteries: Resulting from Atomic Layer Depostion of Al2O3 or TiO2 on LiCoO2 Electrodes. J Phys Chem C 2012;116:7629–37. https://doi.org/10.1021/jp210551r.
[319] Scott ID, Jung YS, Cavanagh AS, Yan Y, Dillon AC, George SM, et al. Ultrathin Coatings on Nano-LiCoO2 for Li-Ion Vehicular Applications. Nano Lett 2011;11:414–8. https://doi.org/10.1021/nl1030198.
[320] Kitagawa T, Azuma K, Koh M, Yamauchi A, Kagawa M, Sakata H, et al. Application of Fluorine-containing Solvents to LiCoO2 Cathode in High Voltage Operation. Electrochemistry 2010;78:345–8. https://doi.org/10.5796/electrochemistry.78.345.
[321] Sun Y-K, Yoon CS, Myung S-T, Belharouak I, Amine K. Role of AlF3 Coating on LiCoO2 Particles during Cycling to Cutoff Voltage above 4.5 V. J Electrochem Soc 2009;156:A1005–10. https://doi.org/10.1149/1.3236501.
[322] Jo M, Hong Y-S, Choo J, Cho J. Effect of LiCoO2 Cathode Nanoparticle Size on High Rate Performance for Li-Ion Batteries. J Electrochem Soc 2009;156:A430–4. https://doi.org/10.1149/1.3111031.
[323] Lu Y-C, Mansour AN, Yabuuchi N, Shao-Horn Y. Probing the Origin of Enhanced Stability of “AlPO4” Nanoparticle Coated LiCoO2 during Cycling to High Voltages: Combined XRD and XPS Studies. Chem Mater 2009;21:4408–24. https://doi.org/10.1021/cm900862v.
[324] Takahashi Y, Tode S, Kinoshita A, Fujimoto H, Nakane I, Fujitani S. Development of Lithium-Ion Batteries with a LiCoO2 Cathode Toward High Capacity by Elevating Charging Potential. J Electrochem Soc 2008;155:A537–41. https://doi.org/10.1149/1.2916685.
[325] Appapillai AT, Mansour AN, Cho J, Shao-Horn Y. Microstructure of LiCoO2 with and without “AlPO4” Nanoparticle Coating: Combined STEM and XPS Studies. Chem Mater 2007;19:5748–57. https://doi.org/10.1021/cm0715390.
[326] Liu J, Liu N, Liu D, Bai Y, Shi L, Wang Z, et al. Improving the Performances of LiCoO2 Cathode Materials by Soaking Nano-Alumina in Commercial Electrolyte. J Electrochem Soc 2007;154:A55–63. https://doi.org/10.1149/1.2388731.
[327] Miyashiro H, Yamanaka A, Tabuchi M, Seki S, Nakayama M, Ohno Y, et al. Improvement of Degradation at Elevated Temperature and at High State-of-Charge Storage by ZrO2 Coating on LiCoO2. J Electrochem Soc 2006;153:A348–53. https://doi.org/10.1149/1.2149306.
[328] Jin Y, Li N, Chen CH, Wei SQ. Electrochemical Characterizations of Commercial LiCoO2 Powders with Surface Modified by Li3PO4 Nanoparticles. Electrochem Solid-State Lett 2006;9:A273–6. https://doi.org/10.1149/1.2188081.
[329] Li X, Cheng F, Guo B, Chen J. Template-Synthesized LiCoO2, LiMn2O4, and LiNi0.8Co0.2O2 Nanotubes as the Cathode Materials of Lithium Ion Batteries. J Phys Chem B 2005;109:14017–24. https://doi.org/10.1021/jp051900a.
[330] Cho J, Kim B, Lee J-G, Kim Y-W, Park B. Annealing-Temperature Effect on Various Cutoff-Voltage Electrochemical Performances in AlPO4-Nanoparticle-Coated LiCoO2. J Electrochem Soc 2005;152:A32–6. https://doi.org/10.1149/1.1825387.

[331] Kim J, Noh M, Cho J, Kim H, Kim K-B. Controlled Nanoparticle Metal Phosphates (Metal = Al , Fe, Ce, and Sr) Coatings on LiCoO2 Cathode Materials. J Electrochem Soc 2005;152:A1142–8. https://doi.org/10.1149/1.1896526.
[332] Fang T, Duh J-G, Sheen S-R. Improving the Electrochemical Performance of LiCoO2 Cathode by Nanocrystalline ZnO Coating. J Electrochem Soc 2005;152:A1701–6. https://doi.org/10.1149/1.1952707.
[333] Chen Z, Dahn JR. Improving the Capacity Retention of LiCoO2 Cycled to 4.5 V by Heat-Treatment. Electrochem Solid-State Lett 2004;7:A11–4. https://doi.org/10.1149/1.1628871.
[334] Lee J-G, Kim B, Cho J, Kim Y-W, Park B. Effect of AlPO4-Nanoparticle Coating Concentration on High-Cutoff-Voltage Electrochemical Performances in LiCoO2. J Electrochem Soc 2004;151:A801–5. https://doi.org/10.1149/1.1723495.
[335] Chen Z, Dahn JR. Studies of LiCoO2 Coated with Metal Oxides. Electrochem Solid-State Lett 2003;6:A221–4. https://doi.org/10.1149/1.1611731.
[336] Kannan AM, Rabenberg L, Manthiram A. High Capacity Surface-Modified LiCoO2 Cathodes for Lithium-Ion Batteries. Electrochem Solid-State Lett 2003;6:A16–8. https://doi.org/10.1149/1.1526782.
[337] Kim YJ, Cho J, Kim T-J, Park B. Suppression of Cobalt Dissolution from the LiCoO2 Cathodes with Various Metal-Oxide Coatings. J Electrochem Soc 2003;150:A1723–5. https://doi.org/10.1149/1.1627347.
[338] Wang Z, Wu C, Liu L, Wu F, Chen L, Huang X. Electrochemical Evaluation and Structural Characterization of Commercial LiCoO2 Surfaces Modified with MgO for Lithium-Ion Batteries. J Electrochem Soc 2002;149:A466–71. https://doi.org/10.1149/1.1456919.
[339] Cho J, Kim YJ, Park B. LiCoO2 Cathode Material That Does Not Show a Phase Transition from Hexagonal to Monoclinic Phase. J Electrochem Soc 2001;148:A1110–5. https://doi.org/10.1149/1.1397772.
[340] Cho J, Kim C-S, Yoo S-I. Improvement of Structural Stability of LiCoO2 Cathode during Electrochemical Cycling by Sol-Gel Coating of SnO2. Electrochem Solid-State Lett 2000;3:362–5. https://doi.org/10.1149/1.1391149.
[341] Cho J, Kim YJ, Park B. Novel LiCoO2 Cathode Material with Al2O3 Coating for a Li Ion Cell. Chem Mater 2000;12:3788–91. https://doi.org/10.1021/cm000511k.
[342] Wang H, Jang Y-I, Huang B, Sadoway DR, Chiang Y-M. TEM Study of Electrochemical Cycling-Induced Damage and Disorder in LiCoO2 Cathodes for Rechargeable Lithium Batteries. J Electrochem Soc 1999;146:473–80. https://doi.org/10.1149/1.1391631.
[343] Chiang Y-M, Jang Y-I, Wang H, Huang B, Sadoway DR, Ye P. Synthesis of LiCoO2 by Decomposition and Intercalation of Hydroxides. J Electrochem Soc 1998;145:887–91. https://doi.org/10.1149/1.1838362.
[344] Tukamoto H, West AR. Electronic Conductivity of LiCoO2 and Its Enhancement by Magnesium Doping. J Electrochem Soc 1997;144:3164–8. https://doi.org/10.1149/1.1837976.
[345] Yan H, Huang X, Lu Z, Huang H, Zue R, Chen L. Microwave synthesis of LiCoO2 cathode materials. Journal of Power Sources 1997;68:530–2. https://doi.org/10.1016/S0378-7753(96)02565-7.
[346] Rabou LPLM, Roskam A. Cycleilife improvement of Li/LiCoO2 batteries. Journal of Power Sources 1995;54:316–8.

[347] Xiong S, Ji J, Ma X. Comparative life cycle energy and GHG emission analysis for BEVs and PHEVs: A case study in China. Energies 2019;12:834.
[348] Qiao Q, Zhao F, Liu Z, Jiang S, Hao H. Cradle-to-gate greenhouse gas emissions of battery electric and internal combustion engine vehicles in China. Applied Energy 2017;204:1399–1411.
[349] Yu A, Wei Y, Chen W, Peng N, Peng L. Life cycle environmental impacts and carbon emissions: A case study of electric and gasoline vehicles in China. Transportation Research Part D: Transport and Environment 2018;65:409–20.
[350] Hao H, Mu Z, Jiang S, Liu Z, Zhao F. GHG Emissions from the production of lithium-ion batteries for electric vehicles in China. Sustainability 2017;9:504.
[351] Heywood J, MacKenzie D, Akerlind IB, Bastani P, Berry I, Bhatt K, et al. On the Road toward 2050 Potential for Substantial Reductions in Light-Duty Vehicle Energy Use and Greenhouse Gas Emissions. MIT: Cambridge, MA; 2015.
[352] Moody J, Wang S, Chun J, Ni X, Zhao J. Transportation policy profiles of chinese city clusters: A mixed methods approach. Transportation Research Interdisciplinary Perspectives 2019;2:100053.
[353] Gan Y, Lu Z, Cai H, Wang M, He X, Przesmitzki S. Future private car stock in China: current growth pattern and effects of car sales restriction. Mitigation and Adaptation Strategies for Global Change 2019:1–18. https://doi.org/10.1007/s11027-019-09868-3.
[354] Dargay JM. The effect of income on car ownership: evidence of asymmetry. Transportation Research Part A: Policy and Practice 2001;35:807–21.
[355] Luo X, Caron J, Karplus VJ, Zhang D, Zhang X. Interprovincial migration and the stringency of energy policy in China. Energy Economics 2016;58:164–73. https://doi.org/10.1016/j.eneco.2016.05.017.
[356] Sun B, Zhang T, He Z, Wang R. Urban spatial structure and motorization in China. Journal of Regional Science 2017;57:470–86.
[357] Ma S-C, Fan Y, Feng L. An evaluation of government incentives for new energy vehicles in China focusing on vehicle purchasing restrictions. Energy Policy 2017;110:609–18.
[358] Wang S, Zhao J. Adoption of Car Restriction Policies Across 287 Chinese Municipalities, Washington, D.C.: 2018.
[359] China Automotive Supplier Network. Guangzhou and Shenzhen Relax Vehicle Ownership Restriction (广州和深圳放宽汽车摇号和竞拍指标) 2019. http://www.chinaautosupplier.com/newslast-75338.html (accessed November 7, 2019).
[360] cebm.caixin.com. Research on China's oil refining industry: IMO2020 is approaching and the we are optimistic about the future of diesel market (石油行业中国炼油行业研究（下）：IMO2020 将至，看好柴油基本面) 2018. http://www.huaon.com/story/415321 (accessed September 10, 2019).
[361] Hao H, Wang H, Ouyang M. Fuel conservation and GHG (Greenhouse gas) emissions mitigation scenarios for China's passenger vehicle fleet. Energy 2011;36:6520–8.
[362] Liu H, Man H, Cui H, Wang Y, Deng F, Wang Y, et al. An updated emission inventory of vehicular VOCs and IVOCs in China. Atmospheric Chemistry and Physics 2017;17:12709.
[363] Wang Q. Coal Industry in China: Evolvement and Prospects. Nautilus Institute; 2011.
[364] Hou B, Li X, Ma X, Du C, Zhang D, Zheng M, et al. The cost of corrosion in China. Npj Materials Degradation 2017;1:4.

[365] Zheng B, Tong D, Li M, Liu F, Hong C, Geng G, et al. Trends in China's anthropogenic emissions since 2010 as the consequence of clean air actions. Atmospheric Chemistry and Physics 2018;18:14095–111.
[366] Wang R. Fuel-cycle assessment of energy and environmental impacts from elctric vehicles and natural gas vehicles (电动车和天然气车能源环境影响的燃料生命周期评价研究). Tsinghua University, 2015.
[367] China SAE. Life cycle assessment report for greenhouse gases and air pollants emissions of automobiles 2018 (汽车生命周期温室气体及大气污染物排放评价报告 2018). China Society of Automotive Engineers; 2018.
[368] xiaoxiongyouhao. WLTP test procedure on fuel consumption estimation will be adopted by MIIT (工信部油耗将迎来 WLTP 时代) 2019. https://chejiahao.autohome.com.cn/info/3287986/ (accessed November 1, 2019).
[369] Yang Z, Yang L. Evaluation of real-world fuel consumption of light-duty vehicles in China. Retrieved from International Council on Clean Transportation https://www …; 2018.
[370] Wu Y, Zhang S, Hao J, Liu H, Wu X, Hu J, et al. On-road vehicle emissions and their control in China: A review and outlook. Science of the Total Environment 2017;574:332–49.
[371] Elgowainy A, Han J, Ward J, Joseck F, Gohlke D, Lindauer A, et al. Current and future United States light-duty vehicle pathways: Cradle-to-grave lifecycle greenhouse gas emissions and economic assessment. Environmental Science & Technology 2018;52:2392–9.
[372] wenku.baidu.com. Distribution of major refineries in China (全国主要炼厂分布图) 2020. https://wenku.baidu.com/view/5a4327c05222aaea998fcc22bcd126fff6055d5e.html (accessed March 30, 2020).
[373] Li M, Zhang Q, Kurokawa J, Woo J-H, He K, Lu Z, et al. MIX: a mosaic Asian anthropogenic emission inventory under the international collaboration framework of the MICS-Asia and HTAP. Atmospheric Chemistry and Physics (Online) 2017;17.
[374] Amann M. Integrated assessment tools. The greenhouse and air pollution interactions and synergies (GAINS) model. Pollution Atmospherique 2009:73–6.
[375] International Energy Agency. World energy outlook 2016. Int Energy Agency 2016. https://doi.org/10.1787/weo-2016-en.
[376] National Bureau of Statistics of China. China Statistical Yearbook 2018. 2018.
[377] United Nations Department of Economic and Social A. World population prospects: The 2015 revision. United Nations Econ Soc Aff 2015;33:1–66.
[378] Schiavina M, Freire S, MacManus K. GHS population grid multitemporal (1975, 1990, 2000, 2015) R2019A. Eur Comm JRC 2019.
[379] Health Nutrition and Population Statistics | DataBank n.d. https://databank.worldbank.org/reports.aspx?source=health-nutrition-and-population-statistics (accessed January 29, 2020).